Flood damage assessment
in two western Mediterranean regions

Present conditions and future scenarios

Maria Cortès Simó

Flood damage assessment in two western Mediterranean regions

Present conditions and future scenarios

Maria Cortès Simó

PhD Thesis

UNIVERSITAT DE BARCELONA

Flood damage assessment in two western Mediterranean regions

Present conditions and future scenarios

UNIVERSITAT DE BARCELONA

Maria Cortès Simó

Department of Applied Physics

University of Barcelona

Director :   Dr. Mª Carmen LLasat   —   University of Barcelona

Co-Director :   Dr. Marco Turco   —   University of Murcia / BSC

Tutor: Dr. Joan Bech   —   University of Barcelona

A thesis submitted for the degree of

Doctor of Philosophy in Physics

Agraïments

Aquesta tesis no l'hauria pogut escriure sense el suport de moltes persones que durant aquests anys han estat al meu costat fent molt més fàcil la seva elaboració. És per això que m'agradaria dedicar unes paraules d'agraïment a totes les persones que d'alguna manera o altra m'han ajudat.

En primer lloc, m'agradaria agrair a la Dra Carme Llasat i al Dr Marco Turco per haver-me dirigit i codirigit, respectivament, aquesta tesis. Moltes gràcies Carme per ajudar-me des del primer moment que vaig entrar al grup GAMA i descobrir-me el món de la investigació. Gràcies per guiar-me donant-me bons consells i fent que tot es veiés més fàcil. *Grazie mille Marco per tutto quello che mi hai insegnato e per farmi amare ancora di più la ricerca e la voglia di continuare ad imparare.*

Vull agrair al *Ministerio de Ciencia, Innovación y Universidades* per finançar aquesta tesis a través dels projectes HOPE (CGL2014-52571-R) i M-CostAdapt (CTM2017-83655-C2-R). *I would like to thank Philip for giving me a warm welcome in Amsterdam and helping me to give the final push to conclude this thesis. Merci beaucoup Freddy de m'accueillir à Lourdes et de me laisser participer à une campagne sur le terrain.* Unes línes també per Josep Sánchez, per trobar sempre moments per ajudar-me en tot el que em fes falta.

No em vull deixar cap dels meus companys i companyes de feina amb els quals fem una gran pinya i creem un ambient de treball insuperable. Gràcies a totes i tots vosaltres per està sempre allà quan us necessitava, per compartir bons moments junts, molts riures, anècdotes i, sobretot, menjars. Gràcies per fer-me tenir ganes de venir a treballar només perquè sé que quan arribi vosaltres hi sereu i que en algun moment del dia, o més aviat varis, compartirem una estona junts. Us heu convertit amb la meva família i us trobaré molt a faltar.

Vull fer una menció especial al meu grup de recerca GAMA. A la Montse, que ha dedicat moltes hores del seu temps en ajudar-me fins i tot quan no les tenia. Al Joan, aportant bon ambient al grup i ajudant-me sempre que li he demanat. *A Marina, que aunque no hayamos tenido mucho tiempo para conocernos y compartir más cervezas juntas, cada vez hemos conectado más y ha estado siempre a mi lado ayudándome en todo momento. A Isabel, por su positivismo y manera de ser que hace que parezca que llevemos mucho tiempo trabajando juntas. Además, quiero darte las gracias por dedicar tu tiempo en corregir la tesis.* Al Raül, per totes les tardes de llargues xerrades que m'han ajudat a tirar endavant.

Si hi ha una persona que li dec moltíssim, o més ben dit, tot, és l'Anna. Aquí em quedaré curta amb qualsevol cosa que pugui dir. Anna, sense tu directament aquesta tesis no l'hagués

pogut fer. Si l'he tirat endavant és perquè t'he tingut al meu costat. Et vull agrair tota la paciència que has tingut en ensenyar-me, escoltar-me, ajudar-me en tot els problemes que m'anava trobant... Però, sobretot, et vull agrair que t'hagis convertit en una de les meves millors amigues que no vull perdre mai.

Una menció especial per la Yolanda, que tothom estarà d'acord que és la persona més bona que et puguis trobar i que mai tindrà un no per ningú. Yolanda, és un privilegi tenir una companya i amiga com tu. Unes línies pels meus MeteoFreaks Oriol i Enric, per aportar bon ambient al grup, passió pel nostre camp i compartir el mateix sentit d'humor fent que les tonteries estiguin assegurades cada cop que ens ajuntem. A la Mireia Udina, la Mireia Mateu, la Míriam, la Chloé, la Froila, el Javi, el Richard, l'Àngela, el Carrasco, Joan Bech, per formar part d'aquesta gran família que dia rere dia compartim molt més que el dinar. Als informàtics Jordi, Gabi, Dani, Joan, que mai m'han negat l'ajuda encara que no els hi pertoqués, i amb els qui he compartit molts esmorzars, dinars, riures i sobretot, xocolata. I en especial al Jordi, que sempre procura que no falti de res, bon humor, converses... però per damunt de tot bon menjar i beure!

Al JR i a la Rosa que encara que ens separessin de departament sempre han estat allà per ajudar-nos i cuidar-nos en tot moment. A la Cristina, la Maite i la Cristina per compartir xerrades i per facilitar-nos la feina.

Per una altra banda, vull dedicar unes línies als meus amics de Sant Just, que encara que cadascú hagi fet el seu camí mai ens hem separat. Al Carles, que m'ha ajudat amb molts dubtes estadístics i amb correccions, però sobretot li vull agrair el seu suport i ànims com a amic. A la Mireia, que sempre ha vingut al meu rescat amb una birra (bé, amb vàries) per aguantar i escoltar tots els meus problemes. A la Blanca que encara que sempre l'he tingut lluny l'he sentit ben a prop estant al meu costat amb tots els alts i baixos pels que he passat. Al Marc, per escoltar-me i fer-me riure quan ho necessitava. A la Marta, per està sempre allà i fer-me saber que sempre que ho necessiti hi estarà. Al Damià i a la Laia per continuar tirant del grup i no deixar que ens separem.

No em vull deixar d'agrair a la meva companya de pis, però sobretot amiga Montse, que m'ha fet sentir com a casa des del primer moment que vaig anar a viure amb ella.

A les meves companyes i companys de Touch, a tota la família TRB en general i en concret als lokitos: a la Marta, la Míriam, la Vero, el Nico, el Campre, el Jornet i el Guayasen. En especial vull agrair a l'Anna Blanco per ajudar-me amb el disseny de la tesis però sobretot per la seva manera de ser amb el seu positivisme i ganes de viure que s'encomanen. I al Guayasen, per estar al meu costat quan més ho necessitava i fer-me veure quin era el camí.

Finalment, vull donar les gràcies a la meva família, que encara que no sabien ben bé el que estava fent, m'han donat sempre suport i han estat al meu costat. En especial als meus pares, Anna i Albert, a la meva germana, Carla, a la Maria i a la meva tieta Imma.

Resum

Les inundacions són un dels principals desastres naturals al món ja que causen molts impactes econòmics i humans. L'avaluació dels danys de les inundacions a l'àrea Mediterrània és essencial, principalment degut a la seva gran susceptibilitat al canvi climàtic. La majoria d'inundacions que afecten l'oest del Mediterrani són inundacions d'aigua superficial que poden produir danys catastròfics. Aquest tipus d'inundacions estan causades per episodis de precipitació intensa, per tant, l'anàlisi de les relacions entre la precipitació i els danys produïts per les inundacions esdevé de vital importància per poder entendre aquest tipus d'episodis.

L'objectiu general d'aquesta tesis és analitzar els danys per inundacions que es produeixen a dues regions Mediterrànies: Catalunya i la Comunitat Valenciana, les quals es veuen freqüentment afectades per episodis de precipitació intensa, així com estimar els canvis en aquests danys tenint en compte tant les projeccions futures de canvi climàtic com diferents escenaris socioeconòmics. Per assolir aquest propòsit, el treball s'ha dividit en els següents objectius específics:

- Identificar els episodis d'inundacions que han afectat les regions d'estudi

- Estimar la relació entre la precipitació i els danys de les inundacions en el clima present

- Analitzar els canvis en els extrems de precipitació considerant diferents projeccions de canvi climàtic

- Avaluar els canvis en l'exposició a les regions d'estudi

- Estimar les variacions en els danys de les inundacions degut al canvi climàtic i a diferents projeccions climàtiques i escenaris socioeconòmics

En primer lloc, s'ha analitzat la relació entre la precipitació intensa i els danys per inundacions estimats a partir de dades d'asseguradores, subministrades pel consorci de compensacions d'assegurances (Consorcio de Compensación de Seguros, CCS). A més de les dues regions d'estudi mencionades anteriorment, també s'ha realitzat l'anàlisi en una àrea urbana altament vulnerable com és l'Àrea Metropolitana de Barcelona (MAB). L'estudi comprèn el període 1996-2015. S'han provat diferents models de regressió logística que estimen la probabilitat que tinguin lloc episodis d'inundacions amb grans danys donada una quantitat de precipitació determinada i considerant altres variables relacionades amb l'exposició del territori. El diagrama ROC (Relative Operating Characteristic), concretament l'indicador de l'àrea sota la corba ROC (RA),

s'ha utilitzat per validar els models generats. Després de realitzar anàlisis de correlacions i desenvolupar diferents models de regressió logística simple i múltiple, els resultats han demostrat que els models lineals mixtes generalitzats (Generalized Linear Mixed Models, GLMM) són la metodologia més apropiada per estudiar la relació entre la precipitació i els danys causats per les inundacions. La probabilitat de que tingui lloc un episodi d'inundacions amb grans danys augmenta amb la precipitació i la població de la conca. Per les dues regions d'estudi, els valors RA indiquen que el nostre model té un bon rendiment, amb valors propers a 1 en tots els casos. A més a més, s'ha demostrat que la precipitació enregistrada en 30 minuts és un millor predictor de la probabilitat de danys importants produïts per inundacions que la precipitació diària, tot i que aquest tipus d'informació no sempre està disponible. Aquests resultats justifiquen la importància dels episodis curts de precipitacions intenses en la generació d'inundacions urbanes i sobtades (flash floods) a les regions d'estudi, que constitueixen un exemple paradigmàtic del nord-oest del Mediterrani. En general, els nostres resultats sobre la relació entre els danys d'inundacions i les seves causes en el clima actual, han confirmat la hipòtesi que la precipitació és un factor clau per explicar els danys causats per episodis d'inundacions en regions on les inundacions d'aigua superficial són el principal tipus, com és el cas de les dues regions d'estudi Mediterrànies. A més a més, els resultats demostren la importància d'incorporar variables que proporcionen informació sobre l'exposició del territori (és a dir, la població) a l'hora d'explicar els danys produïts per les inundacions.

Per una altra banda, s'han analitzat els canvis projectats en els extrems de precipitació per la península Ibèrica considerant l'escenari RCP (Representative Concentration Pathway) 8.5 i un conjunt de set simulacions del projecte EURO-CORDEX que comprenen el període 1976-2100. S'han calculat diferents índexs climàtics per estimar els canvis en la precipitació quan s'assumeix un escalfament global de 1,5, 2 i 3 °C per sobre dels nivells preindustrials. Els resultats mostren una disminució general de la precipitació total anual i un augment del número de dies sense pluja a la majoria de la Península. Aquest augment s'accentua quan es consideren nivells d'escalfament més alts i durant els mesos d'estiu. En el cas de la precipitació extrema, s'han observat augments, amb l'escalfament global, de la precipitació màxima diària i de l'enregistrada en 5 dies consecutius, així com del nombre de dies amb precipitació diària per sobre dels 40 mm, principalment durant els mesos de tardor i hivern i al nord i nord-est de la península Ibèrica.

Finalment, s'han avaluat els canvis en la probabilitat que es produeixin episodis d'inundacions amb grans danys a les dues regions d'estudi quan es considera un escalfament global d'1,5, 2 i 3 °C i es tenen en compte diferents projeccions climàtiques i escenaris socioeconòmics. Per dur-ho a terme, s'ha utilitzat el model estadístic climàtic anteriorment desenvolupat que relaciona la precipitació, la població i els danys produïts per les inundacions, per avaluar les condicions climàtiques futures. S'han incorporat en el model les dades de precipitació diàries dels set models climàtics prèviament utilitzades i les dades de projeccions de població basades en cinc escenaris socioeconòmics diferents (Shared Socioeconomic Pathways, SSPs). Els resultats han mostrat que hi ha un augment general de la probabilitat de que es produeixin inundacions amb

danys grans a la majoria de casos i per ambdues regions d'estudi, sent més accentuada en el cas de Catalunya. Aquest canvi és major quan es considera un nivell d'escalfament superior i per percentils de danys més alts. A més a més, la probabilitat augmenta quan es tenen en compte tant els canvis en la precipitació com en la població.

Els nostres resultats ressalten que, quan es tracta d'analitzar els danys de les inundacions, és molt important tenir en compte tant el canvi climàtic com també les condicions socioeconòmiques. A més a més, els resultats mostren que limitar l'escalfament global esdevé una necessitat per minimitzar les conseqüències dels episodis d'inundacions a la zona d'estudi.

Abstract

Flooding is one of the main natural hazard in the world causing huge economic and human impacts. Assessing the flood damage in the Mediterranean region is of great importance, mainly due to its pronounced sensitivity to climate change. A large number of floods affecting the western Mediterranean region of study are surface water floods that can cause catastrophic damage. These floods are caused by intense precipitation events, thus, in order to understand properly these type of events, the analysis of the relationship between precipitation and flood damage is crucial.

The overall objective of this thesis is to analyse flood damages in two Mediterranean regions, namely Catalonia and the Valencian Community, frequently affected by intense precipitation events, as well as to estimate their changes when future climate change projections and different socioeconomic scenarios are considered. To achieve this goal, this work has been divided in the following sub-objectives:

- Identify the flood events that have affected the regions of study

- Estimate the relationship between precipitation and flood damage for the present climate

- Analyse changes in precipitation extremes considering different climate change projections

- Assess the changes in the exposure of the regions of study

- Estimate flood damage variations due to global warming and considering different climate projections and socioeconomic scenarios

To do this, the relationship between heavy precipitation and flood damage estimates from insurance datasets, provided by the Spanish Insurance Compensation Consortium (Consorcio de Compensación de Seguros, CCS), have been analysed. Other than for the above mentioned two areas of study, this analysis was performed for the Metropolitan Area of Barcelona (MAB), a highly vulnerable urban area. The study period covers 1996-2015. Several regression models have been tested in order to gauge the probability of large damaging events occurring given a certain precipitation amount and taking into account other variables related to the exposure of the territory. The Relative Operating Characteristic (ROC) diagram has been used to validate the models, specifically the area under the ROC curve (RA) indicator. After testing correlation analyses and simple and multiple logistic regression models, results have shown that Generalized Llinear Mixed Models (GLMM) are the most appropriate tool for studying the relationship

between precipitation and flood damage. The probability of a damaging flood event increases with precipitation and population of the basin. For both regions of study, the RA values indicate that our model has a good performance, with values close to 1 in all cases. Moreover, 30-min precipitation data proved to be a better predictor of the probability of large damages than daily precipitation, however, this type of information is not always available. These results justify the importance of short and intense precipitation events in flash and urban floods in the regions of study, which constitute a paradigmatic example of the north-western Mediterranean region. Overall, our results regarding the relationship between flood damage and their causes in the present climate have confirmed the hypothesis that precipitation is a key factor in explaining the damage caused by flood events in regions in which surface water floods are the main type of flood, as is the case of both Mediterranean regions of study. Furthermore, when it comes to explaining flood damage, the results point towards the benefit of incorporating variables that provide information about the exposure of the territory (i.e. population).

On the other hand, we have analysed the projected changes in precipitation extremes in the Iberian Peninsula considering the Representative Concentration Pathway (RCP) 8.5 scenario and an ensemble of seven EURO-CORDEX simulations spanning the period 1976-2100. In order to do this, different climate indices were calculated to estimate the changes in precipitation assuming global warming scenarios of 1.5, 2 and 3 °C above preindustrial levels. Results show a general decrease of the total annual precipitation and an increase in the length of dry spell in most of the Peninsula. This increase accentuates with higher levels of global warming and during summer months. In terms of heavy precipitation, we have found increases with global warming in the maximum 1-day and consecutive 5-day precipitation indices as well as in the number of days with precipitation exceeding 40 mm, especially during the months of autumn and winter and in the north and north-east of the Iberian Peninsula.

Finally, changes in the probability of occurrence of damaging flood events have been assessed for both regions when considering a global warming of 1.5, 2 and 3 °C and taking into account different climate projections and socioeconomic scenarios. To do this, the previously developed statistical climate model that links precipitation, population and flood damage estimates, has been used to assess future climate conditions. The daily precipitation data from the seven climate models used previously and population projections based on five different socioeconomic scenarios (Shared Socioeconomic Pathways, SSPs) were incorporated into the model. Results have shown a general increase in the probability of a damaging event for most of the cases and in both regions of study, being higher in the case of Catalonia. This change is usually larger when greater warming is considered and for higher percentiles of damage. Moreover, the increase in probability is larger when both climate and population changes are included.

Our findings highlight that, when it comes to flood damage analysis, it is crucial not only to account for climate change but also consider socioeconomic conditions. Furthermore, results show that limiting global warming is a must in order to minimise the consequences of flood events in the study area.

Contents

Acronyms

AEMET Agencia Estatal de Meteorología.

BT Best Threshold.

CCS Consorcio de Compensación de Seguros.

D Total damage.

DPC Damage Per Capita.

DPW Damage Per unit of Wealth.

F False alarm rate.

GLMM Generalized Linear Mixed Model.

H Hit rate.

MAB Metropolitan Area of Barcelona.

RA Area under the ROC curve.

RCP Representative Concentration Pathways.

ROC Relative Operating Characteristic.

SMC Servei Meteorològic de Catalunya.

SSP Shared Socioeconomic Pathways.

SWF Surface Water Floods.

List of Figures

List of Tables

Chapter 1

Introduction

1.1 Motivation

Floods are one of the most damaging natural hazards that account for the majority of all economic losses due to natural hazards worldwide (UNISDR, 2015). On average, between 2001 and 2010, floods and other hydrological events accounted for more than 50 % of all disasters (Guha-Sapir et al., 2012). Between 2005 and 2014 more than 85 million people were directly affected annually by flood and around 6,000 people lost their lives due to these events (UNISDR, 2015). Therefore, the knowledge of the flood phenomenon and its consequences is crucial for the development of flood control, risk reduction, improvement of resilience, and flood management in general. The main purpose of risk analysis is to understand and measure the possible consequences associated with the occurrence of flooding in areas occupied by vulnerable systems (Elmer et al., 2010).

In Spain, floods represent a 69.4 % of the total compensation paid by the Spanish public reinsurer, Consorcio de Compensación de Seguros (CCS), for extraordinary risks in Spain. CCS is a public institution that compensates homeowners for damage caused by floods, playing a role similar to that of a reinsurance company (Barredo et al., 2012). Between 1987 and 2017 the CCS paid around 5,000 M Euro in compensation due to these events (CCS, 2018). Catalonia and the Valencian Community, both in the western Mediterranean, are frequently affected by highly localised convective rainfall events that cause highly damaging floods (Llasat et al., 2016b). The most catastrophic flood event that took place in Catalonia (and in Spain) was the flash flood occurred in September 1962, which recorded more than 200 mm in less than 3 h and caused 815 deaths (Llasat et al., 2005; Martín-Vide and Llasat, 2018). In the Valencian Community, more than 40 people lost their lives in the flood event of October 1982 (EM-DAT, 2018) when the Tous damn, on Jucar river, collapsed producing a major flood of 10,000 m^3 s^{-1} of water (Serra-Llobet et al., 2013). Table 1.1 shows the three most catastrophic events recorded in each of these regions over the last 50 years based on the total insurance compensation received according to CCS (CCS, 2018).

Not all damages are caused by the same type of flood. There are different types of flooding and several classifications exist. According to Pitt et al. (2008) 4 main types can be found.

Date	Region	Total compensation
October 1982	Valencian Community	226
November 1982	Catalonia	60
November 1987	Valencian Community	289
October 1994	Catalonia	80
September 2006	Catalonia	68
October 2007	Valencian Community	98

Table 1.1: Most catastrophic flood events according to CCS for Catalonia and the Valencian Community (1971-2018) with the total compensation paid by CCS (M Euro)

River or fluvial floods are the most known type, which occur as a result of water overflowing from river channels. In contrast, pluvial floods are caused by intense rainfall that cannot be drained by natural or artificial drainage systems and is directed towards a watercourse, but does not originate from it nor has reached it (Bernet et al., 2017). Several authors distinguish between pluvial and Surface Water Floods (SWF). SWF can be regarded as coming under the most general definition of rainfall-related floods (Bernet et al., 2017), including pluvial floods but also flooding from sewer systems, small open channels, diverted watercourses or groundwater springs (Falconer et al., 2009). Coastal floods occur when the sea level rises above the level of coastal land (Pitt et al., 2008). Finally, groundwater floods result when the level of water underground rises and water emerges above the natural surface (Pitt et al., 2008). Nevertheless, other types of floods related to one or more of the main types described above can be found. For example, the term "flash flood" refers to both fluvial and SWF triggered by intense, short, and local precipitation events in small and torrential catchments. The type of flooding depends on the meteorological, topographical, and geological features of the region.

In the Mediterranean, most of the floods are flash floods (Llasat et al., 2014a). This is a consequence of the presence of small and medium-sized torrential catchments, and the characteristics of the Mediterranean region that favour the development of very heavy precipitation. The Mediterranean region currently lies in a transition zone between mid-latitude and sub-tropical atmospheric circulation regimes. It is characterised by a complex morphology of mountain chains and strong land-sea contrasts, a dense and growing human population and various environmental pressures (Cramer et al., 2018). This results in interactions and feedback between ocean-atmosphere-land processes that play a prominent role in the climate and hydrological cycle, including in the high-impact weather events that frequently affect the region (Ducrocq et al., 2016). In the region, intense precipitation events constitute a real danger to the population. Heavy precipitation, sometimes associated with strong winds, can cause floods with dire consequences for people and the environment (Fourrie et al., 2016) particularly during the autumn season. The relief surrounding the Mediterranean Sea forces the convergence of low-level atmospheric flows and the uplift of warm wet air masses that drift from the Mediterranean Sea to the coasts, thereby creating active convection. In addition, population growth is particularly high along the Mediterranean coasts, leading to a rapid increase in urban settlements and populations exposed to flooding (Gaume et al., 2016). A large number of floods affecting the western Mediterranean region of study are SWF that can cause catastrophic damage (Llasat

et al., 2014a, 2016b; Cortès et al., 2018). The majority of these flood events are caused by intense and short-lived rainfall rather than river overflow (Llasat et al., 2016b). River floods that affect great distances are, nowadays, very rare in the region, and are only related to catastrophic and extended floods. Nevertheless, these are usually absorbed by reservoirs. SWF have received increasing attention in the recent years, however there is still few studies that deal with it, mainly due to the limitation in the availability of data. Spekkers (2015) mentioned the lack of data and the impact on small spatial scales as possible explanations of why relatively little scientific research has been dedicated to SWF in comparison to fluvial floods.

Over the past 60 years, the frequency and intensity of heavy rainfall events has increased in many parts of the world (Hartmann et al., 2013) and it is likely that it will continue to grow in the next decades as a consequence of climate change (Kirtman et al., 2013). In the last years, much research has focused on the study of climate change in the Mediterranean region, an area that is identified as highly vulnerable to climate change according to the Fifth Assessment Report of the Intergovernmental Panel on Climate Change (Pachauri et al., 2014). This is the case of The Hydrological cycle in the Mediterranean Experiment (HyMeX) (Drobinski et al., 2014), which is a 10-year international programme in which the present doctoral thesis has been partially developed. This project aims for a better understanding and quantification of the hydrological cycle and related processes in the Mediterranean Sea. It focuses on high-impact weather events, inter-annual to decennial variability of the Mediterranean coupled system, and associated trends in the context of global climate change (for more information see http://www.hymex.org). Some studies framed within the HyMeX project have found an increase in precipitation extremes with global warming in the Mediterranean region (Colmet-Daage et al., 2018; Drobinski et al., 2018), although a general decrease in the annual precipitation is projected (Jacob et al., 2014; Cramer et al., 2018; Sillmann et al., 2013; Rajczak and Schär, 2017). Cramer et al. (2018) state that future warming in the Mediterranean region is expected to exceed global mean rates by 25 %, with peaks of 40 % in summer. Furthermore, flood risk associated with extreme precipitation events is expected to increase not only due to climate change in this area, but also due to non-climatic factors such as increasingly sealed surfaces in urban areas and ill-conceived storm-water management systems (Cramer et al., 2018). Flood disasters are the result of both societal and climatological factors, hence several other drivers other than climate must be considered for the assessment of flood-damage trends (Barredo, 2009). Several studies show the need to include exposure and vulnerability changes in future risk projections, which clearly contribute substantially to changing risks (Bouwer, 2011). For instance, Barredo et al. (2012) find no significant trend in adjusted insured flood losses between 1971 and 2008, pointing towards increasing concentrations and values of assets as the principle cause of the increasing damages and losses from natural disasters. A large number of researchers are making efforts to create methodologies that are able to analyse the impacts of floods, due to the significant consequences of this phenomenon (Messner and Meyer, 2006; Garcia et al., 2014). Indeed, progress is being made on incorporating impact and vulnerability analyses in flood risk assessment, although the limitations of the impact data (availability and quality)

make it challenging (Elmer et al., 2010; Petrucci, 2013; Jongman et al., 2014; Papagiannaki et al., 2015; Thieken et al., 2016; Kreibich et al., 2017).

In this context, the question of how climate change will affect damages caused by floods arises. This was the aim of the Spanish Project HOPE (CGL2014-52571-R), to which this pre-doctoral fellowship and thesis are associated. This thesis has also contributed to the M-CostAdapt project (CTM2017-83655-C2-R) providing the databases on floods and damages, the methodology to estimate impacts from precipitation and exposure, and part of the future scenarios. To answer this question the first step is to solve the problem of the estimation of flood damage. The economic evaluation of flood damage plays an important role in decision-making processes. There are different data sources that can potentially be used for the analysis of flood damage, being insurance data a good proxy (Gradeci et al., 2019; Barredo et al., 2012). These data often contain many claim records that have been collected continuously in time. Several recent works have used this type of data to explore the causes and impacts of floods. For instance, in some European regions researchers have noted that precipitation has a significant influence on flood insurance data (see, for instance, Spekkers et al., 2013, 2015 for the Netherlands; Zhou et al., 2013 for Denmark; Sampson et al., 2014 for Ireland; Moncoulon et al., 2014; Bihan et al., 2017 for France; Torgersen et al., 2015 for Norway; Bernet et al., 2017; Zischg et al., 2018 for Switzerland). These data are very valuable for establishing causal relationships between precipitation extremes and the costs of flood damage, for the development of risk maps, and to be used as a validation tool for damage models (Zhou et al., 2013). These studies note the potential of insurance data for describing economic damages caused by SWF and urban floods. However, there are still few studies that relate flooding with insurance data, mainly due to the reluctance of the insurance companies to share their data, in some cases due to confidentiality restrictions (André et al., 2013; Leal et al., 2019). However, in the Mediterranean region 20 years of flood-related insurance damage claims are available from the Spanish public reinsurer (CCS), for the Spanish regions of Catalonia and the Valencian Community. This means that an assessment of the links between precipitation and impacts is possible.

Taking into account that the most common flood events that affect the regions of study are caused by intense precipitation events, it is expected that flood insurance data will correlate strongly with precipitation and SWF. For this reason, in this thesis, insurance data are used as a proxy for flood damage.

Considering the above points, this work is based on three main hypotheses.

1. Precipitation is the main hazard driver of the damage produced by surface water floods.

2. Insurance data provide a good proxy for describing flood damage.

3. The relationship between precipitation and insurance data assessed in the present climate can be applied to estimate the probability of flood damage in the future.

1.2 Objectives

1.2.1 Open questions

In spite of several advances, the analysis of flood damage remains a major challenge due to its complexity which depends on several factors and data availability. To overcome these challenges, some questions arise that are to be addressed in this thesis:

- Is it possible to explain flood damages from precipitation?

- What other variables can predict damages caused by surface water floods?

- What is the best methodology to assess the relationship between these variables and flood damage?

- What are the projected changes in extreme precipitation with global warming scenarios?

- Will changes in precipitation and exposure increase flood damage in the regions of study?

1.2.2 Objectives of the thesis

According to the previous discussion, the overall objective of this thesis is to analyse flood damages in two Mediterranean regions frequently affected by intense precipitation events and to estimate their changes when future climate change projections and different socioeconomic scenarios are considered. To achieve this goal, this work has been divided in 5 different sub-objectives:

1. **Identify the flood events that have affected the regions of study (Catalonia and the Valencian Community)**. First of all, a characterisation of the flood events that comprise the flood database is needed. This requires an analysis of their spatial distribution considering the basins affected and the collection of the information related to hazard, exposure, vulnerability, and damage of each flood event.

2. **Estimate the relationship between precipitation and flood damage for the present climate**. The final goal of this sub-objective is to develop a robust model that is able to estimate the probability of flood damage given a certain precipitation amount and other variables related to the exposure of the region.

3. **Analyse changes in precipitation extremes considering different climate change projections**. We will estimate the changes in several extreme precipitation indices assuming a global warming of 1.5, 2 and 3 °C above preindustrial levels and using a multi-model ensemble of EURO-CORDEX simulations.

4. **Assess the changes in the exposure of the regions of study**. We will estimate the changes in the exposure (i.e. population) considering five different narratives that describe possible alternative socio-economic developments in the future.

5. **Estimate flood damage variations due to global warming and considering different climate projections and socioeconomic scenarios**. This last sub-objective of the thesis brings together all findings obtained in objectives 1-4, considering that the final goal is to estimate changes in the probability of flood damage with global warming of 1.5, 2 and 3 °C above preindustrial levels while considering different socioeconomic scenarios, by using the relationships found in the damage model developed for the present climate.

1.3   Methodological framework and outline of the thesis

Figure 1.1 summarises the general methodology of the thesis (further details of the specific methodology are given in each of the following chapters). After the introduction, the state-of-the-art (Chapter 2) provides a review in the field of flood risk assessment. Chapter 3 describes the regions of study and the data used. The analysis of the flood events that have affected the regions of study as well as the relationships between precipitation and damage produced studied by using different regression models, are described in Chapters 4, 5 and 6. In Chapter 7, the changes in the extremes of precipitation based on an ensemble of future climate change simulations of the EURO-CORDEX project (Jacob et al., 2014) are analysed for the entire Iberian Peninsula. The regression models developed in Chapters 4, 5 and 6 for the present climate (in particular those developed in Chapter 6) allow to estimate the probability of future flood damage, taking into account not only future precipitation data (analysed in Chapter 7), but also different socioeconomic projections (described in Chapter 8). Finally, the doctoral thesis ends with a last chapter summarising the conclusions drawn from the different chapters of the study and suggesting possible lines of future research (Chapter 9).

```
                    ┌─────────────────┐          ┌──────────────────────┐
                    │ 1. Introduction │ ------→   │ Objectives of the    │
                    └─────────────────┘          │ thesis               │
                            ⇓                     └──────────────────────┘
                    ┌─────────────────┐
                    │ 2. State-of-the-Art │
                    └─────────────────┘
                            ⇓
                    ┌─────────────────┐
                    │ 3. Region of study │
                    │ and data sources   │
                    └─────────────────┘
                            ⇓
```

Present climate (4-5-6)

Precipitation – flood damage relationship

| 4. Metropolitan Area of Barcelona | → | Simple linear regression / Simple logistic regression | ----→ | *Llasat et al. 2016b / Cortès et al. 2017 / Cortès et al. 2018a* |

| 5. Catalonia | → | Simple linear regression / Simple logistic regression / Multiple logistic regression | ----→ | *Cortès et al. 2018a / Cortès et al. 2018b* |

| 6. Western Mediterranean | → | Generalized linear mixed model | ----→ | *Cortès et al. 2019* |

Future climate (7-8)

| 7. Precipitation future projections | ----→ | *Turco et al. 2018* |

| 8. Flood damage future scenarios | ----→ | *Cortès et al. 2019* |

9. Conclusions and future research lines

Figure 1.1: Thesis scheme

Chapter 2

State-of-the-Art review of flood risk analysis

Abstract

This chapter provides a review of the field of flood risk research. The chapter has been divided into three main sections. The first part is a review of the main methodologies applied in the study of the impact of floods. In addition, a compilation of the most commonly used indicators to assess the risk of these events and to estimate their damage is presented in table format. The second part includes a synthesis of the trends in extreme precipitation events and floods at global, regional and local scale. Finally, the last section of the chapter summarises the main ideas extracted from this review.

2.1 Analysis of flood impacts

2.1.1 Holistic approach to flood study

The main factors involved in flood risk analysis are the **hazard**, or *the likelihood of a natural phenomenon causing damage*, and the **vulnerability**, that is, *the characteristics and circumstances of a community/system that make it susceptible to potential flood damage* (UNISDR, 2009). Some studies such as Field et al. (2012) differentiate between **exposure**, *the presence of people; livelihoods; environmental services and resources; infrastructure; or economic, social, or cultural assets in places that could be adversely affected* and **vulnerability**, *the propensity or predisposition to be adversely affected. The vulnerability comprises a variety of concepts and elements that include sensitivity or susceptibility to damage and lack of response capacity and adaptation.* The **resilience** is *the ability of a system and its component parts to anticipate, absorb, accommodate, or recover from the effects of a hazardous event in a timely and efficient manner, including through ensuring the preservation, restoration, or improvement of its essential basic structures and functions* (Field et al., 2012).

The analysis of flood risk is very complex and needs to be addressed from a holistic per-

spective using techniques that take into account all the factors involved, those related to the dangerous nature of the phenomenon, those related to vulnerability and exposure and those related to the impacts. Most studies analyse the risk of flooding from a top-down perspective, that is, from the nature of the phenomenon while leaving aside other factors. Currently, progress is being made in incorporating the analysis of impacts, vulnerability and exposure in the studies, although the lack of these data makes this challenging. The approach based on the study of floods from impacts is called bottom-up (Garcia et al., 2014). An example is the research carried out in relation to the recent catastrophic flood event that took place in 2013 and affected a large part of central Europe, which led to studies that, on the one hand, analyse the determinant hydrometeorological factors that caused the episode and, on the other hand, investigate the impacts that were produced (e.g. Schröter et al., 2015; Thieken et al., 2016). Nevertheless, according to Merz et al. (2010), the analysis of flood risk continues to be very unbalanced since, in comparison, much more attention is paid to the dangerousness of the phenomenon than to its impacts.

2.1.2 Impact classification analysis

Types of damages

The damages can be classified as **direct** and **indirect**. Direct damages are those that occur with the physical contact of the flood water with people, properties or other objects. On the other hand, indirect damages take place, both in space and time, outside the flood event (Merz et al., 2010). The two types of damages can, in turn, be classified into **tangible** and **non-tangible**, depending on whether they can be valued in monetary terms. Most studies are based on direct and tangible damages, but non-tangible and indirect ones are crucial for a complete evaluation of the impacts caused by natural disasters (Petrucci, 2013). Indirect damages are more difficult to estimate and only a few studies consider them (Elmer et al., 2010). For instance, some studies apply a coefficient to the direct damages in order to estimate the indirect ones. Other example are those that have developed indirect damage estimates considering several variables such as the business cycle (Pfurtscheller and Schwarze, 2010), the loss of work hours (Thieken et al., 2016) or the number of fire service operations done in flooded properties (Papagiannaki et al., 2015). Tables 2.1-2.5 show the most commonly used damage indicators and some references of studies that have used them. Table 2.1 presents those used for describing the hazard level of the flood event, such as the maximum precipitation intensity recorded during the event. Tables 2.2 and 2.3 show examples of indicators applied for quantifying the tangible and non-tangible direct damages, respectively. The most common indicators used for describing tangible and non-tangible indirect damages are shown in tables 2.4 and 2.5, respectively.

Indicator	Threshold/definition	Unit	Reference
Precipitation	Maximum precipitation in 24 h, peak precipitation of the event, return period of the precipitation; precipitation per basin; % of precipitation higher than the monthly mean, etc.	mm; years; %	Nasiri and Shahmohammadi-Kalalagh (2013); Barbería et al. (2014); Amaro et al. (2010); Petrucci et al. (2012)
Precipitation intensity	Accumulated precipitation over 30 min (i.e.), return period of the precipitation for different accumulation intervals	mm h^{-1}; years	Nasiri and Shahmohammadi-Kalalagh (2013); Barbería et al. (2014); Petrucci et al. (2012)
Affected area	IDA=affected area/total area; Number of affected municipalities	N$^{\text{o}}$	Petrucci (2013)
Event duration	Number of days of the meteorological event	Days	Barbería et al. (2014); Amaro et al. (2010)
flood duration	Number of days or hours that the area remains flooded	Hours; days	Schröter et al. (2014); Merz et al. (2013); Thieken et al. (2005); Elmer et al. (2010)
Wind	Coincidence of the flood event with strong wind	Days	Barbería et al. (2014); Amaro et al. (2010)
Depth of water	Water level	cm	Dottori et al. (2016); Schröter et al. (2014); Escuder-Bueno et al. (2012); Thieken et al. (2005); Elmer et al. (2010)
Flooded surface	Flooded area, or percentage related to the total	km^2; %	Petrucci et al. (2012)
Flow	Peak flow, unitary flow, peak flow/mean flow	m^3 s^{-1}; m^3 s^{-1} km^2	Dottori et al. (2016); Schröter et al. (2014); Escuder-Bueno et al. (2012); Thieken et al. (2005)
Contamination indicator	From 0=no contamination to 6=high contamination	-	Schröter et al. (2014); Merz et al. (2013); Thieken et al. (2005)
Return period and occurrence probability	Precipitation, flow, flood volume	Years	Schröter et al. (2014); Merz et al. (2013); Petrucci et al. (2012)
Wetness index	Number of consecutive precipitation days before the flood event	-	Schröter et al. (2015)

Table 2.1: Hazard indicators

Indicator	Threshold/definition	Unit	Reference
Public buildings	Hospitals, schools, city councils, etc.	Nº; €; damage level	Cortès et al. (2017); Petrucci and Pasqua (2009); Petrucci (2013)
Private buildings	Private houses with one or more floors	Nº; €; damage level	Cortès et al. (2017); Petrucci and Pasqua (2009)
Immovable property affected	Affected buildings; bridges; km of roads; hectares of agriculture affected	Nº; km; Ha	Petrucci (2013)
Loss rate	Loss in buildings rate	-	Schröter et al. (2014); Merz et al. (2013)
Bridges	Bridges and footbridges affected by the event	Nº; €; damage level	Cortès et al. (2017); Petrucci and Pasqua (2009); Petrucci (2013)
Hydraulic infrastructures	Windmills, irrigation channels, km of affected dykes	Nº; km; €; damage level	Cortès et al. (2017); Petrucci and Pasqua (2009); Petrucci (2013)
Communication routes	Roads, highways, railways	Nº; €; km; damage level	Cortès et al. (2017); Petrucci and Pasqua (2009); Petrucci (2013)
Vehicle	Vehicles washed away or damaged by water	Nº; €; damage level	Cortès et al. (2017); Petrucci and Pasqua (2009); Petrucci (2013)
Productive activities	Industry, agriculture and livestock, commerce, tourist infrastructures	Nº; €; damage level	Cortès et al. (2017); Petrucci and Pasqua (2009); Petrucci (2013)
Emergency management	Hour of emergency tasks; Nº of calls to 112; Nº of fire service operations	Hours; Nº; €	Cortès et al. (2017); Petrucci (2013); Gain et al. (2015); Papagiannaki et al. (2015)
Requests received in meteorological services	Number of reports that the population requests from the meteorological service	Nº	Barbería et al. (2014)
Cleaning	Cleaning tasks	€	Gain et al. (2015)
Damages by type of land use	Damage in agriculture, infrastructure, residences, commercial sector, industries	Ha; €	Gain et al. (2015), INUN-CAT, ACA

Table 2.2: Direct and tangible damage indicators

Indicator	Threshold/definition	Unit	Reference
Deaths	Number	Nº	Llasat et al. (2013); Petrucci (2013), EM-DAT
Injured	Serious and slightly injured	Nº	Cortès et al. (2017); Petrucci (2013)
Evacuees	Number of evacuees due to flooding	Nº	Cortès et al. (2017); Petrucci (2013)
Affected population	Population or population density for a given precipitation value; population with a runoff value greater than a given value; population in impermeable soil; density of population or total population in an affected region, etc.	Nº; Nº km^{-1}	Barbería et al. (2014); Amaro et al. (2010); Petrucci et al. (2012), EM-DAT

Table 2.3: Direct and non-tangible damage indicators

Indicator	Threshold/definition	Unit	Reference
Productive activities	Agriculture, business, tourism, etc. (e.g. lack of an essential product for the activity)	Nº; Ha	Cortès et al. (2017); Petrucci (2013); Gain et al. (2015)
Services cuts	Gas, electricity, telephone lines, water	Hours	Cortès et al. (2017); Petrucci (2013)
Transit	Losses due to traffic interruptions; loss of working hours, etc.	€	Cortès et al. (2017); Petrucci (2013)
Public transport	Transport cuts	€; Hours	Cortès et al. (2017); Petrucci (2013)
Accommodation of the affected population	According to the period of accommodation and the number of people accommodated	€	Petrucci (2013)
Restoration of initial conditions	Construction and restoration of affected buildings, retaining walls, opening of alternative routes, cleaning of affected roads	Nº; €	Petrucci (2013)
Job losses	Number of people without job due to flooding	Nº	Cortès et al. (2017); Petrucci et al. (2012)
GDP	Variation rate	%	Neumayer and Barthel (2011)

Table 2.4: Indirect and tangible damage indicators

Indicator	Threshold/definition	Unit	Reference
Psychological effects	Due to: loss of a family member, injury of a family member, prolonged condition of displaced people, temporary condition of displaced people, loss of personal belongings, use of alternative roads, public services inefficiency, temporary traffic delay	-	Petrucci (2013)
Illness	Propagation of diseases, contaminated water	Nº of affected people	Gain et al. (2015)
Loss of trust in authorities	-	-	Merz et al. (2010)
Nº of news	Number of news related to the event	Nº	Llasat et al. (2009)

Table 2.5: Indirect and non-tangible damage indicators

Scales of analysis

The spatial scale of a study based on impacts has to be defined from the start, since different methods will be applied depending on it (Messner and Meyer, 2006). There are three main spatial scales: **micro-scale** (local, based on the individual elements at risk), **meso-scale** (regional, spatial aggregations such as different land-use zones) or **macro-scale** (large scales, regions, countries, etc). The Flood-site guide carried out by Messner et al. (2007) provides good guidelines for choosing the most convenient scale. For instance, the spatial scale used in the FLEMOps model developed by Thieken et al. (2008) is the micro-scale, since the most relevant factors contributing to flood damage caused to buildings are analysed. In contrast, most of the administration works in meso-scale and namely at municipality level, but disaggregating the economic damages by type of soil, as for example the Civil Protection of Catalonia and the Catalan Water Agency (ACA). In macro-scale, the studies generally use indicators of economic

value such as the Gross Domestic Product (Balbi et al., 2015). Table 2.6 summarises the 3 types of spatial scale used in flood damage assessments, with examples of studies in which they have been applied.

Scale	Definition	Methodology	Reference
Micro-scale	Based on single elements at risk (e.g. buildings)	FLEMOps, FLEMOcs	Elmer et al. (2010); Thieken et al. (2005); Kreibich et al. (2010)
Meso-scale	Based on spatial aggregations such as types of land use	INUNCAT, ACA, vulnerability and/or impacts indices	Gain et al. (2015); Petrucci (2013); Zhou et al. (2013); Balica et al. (2012)
Macro-scale	Damages in regions, countries, etc.	GDP, inflation, per capita income, input-output models	Merz et al. (2010); Barredo et al. (2012); Balbi et al. (2015); Gain et al. (2015)

Table 2.6: Spatial scales used for flood damage assessments

Databases, criteria and thresholds

There are different global databases that collect information of natural disasters, including information related to the damage caused (Barredo, 2009). The most extensively used databases are: **Emergency Events Database (EM-DAT, 2018)**, from the Centre of Research on Epidemiology of Disasters (CRED) and the **Natural Hazards Assessment Network (NATHAN, 2018)**, from the Munich Re insurance company.

In the case of the EM-DAT, at least one of the following criteria must be met to register an event in the database: a) 10 or more human deaths; b) 100 or more people affected/injured/homeless; c) declaration of state of emergency; d) need for international assistance. In the NATHAN database, the events recorded are those considered by the Munich Re as *major natural catastrophes*, which according to the United Nations occurs when the capacity of the affected region to manage the event independently is clearly overcome and supra-regional or international assistance is needed (Barredo, 2009; Llasat et al., 2009, 2013).

In Spain, the Insurance Compensation Consortium (*Consorcio de Compensación de Seguros*, CCS), is responsible for compensating homeowners for damage caused by floods. CCS recompenses for damages to people and properties caused by different natural disasters and other occurrences derived from certain events of political or social incidence, subject to having a policy subscribed (UTE, 2013). CCS covers the economic losses produced by natural catastrophes when the market does not assume them, as for example in the case of flood events, since most private insurance companies do not cover this hazard (Barredo et al., 2012).

Some studies classify flood events according to the level of impact they have caused (Barriendos et al., 2003; Llasat et al., 2016b). Llasat et al. (2016b) distinguish between three categories based on the impacts produced and the categories established in the European project SPHERE (Barriendos et al., 2003). From lower to higher impact, flood events are classified as: (i) ordinary, (ii) extraordinary, and (iii) catastrophic (see Chapter 4 for more information about the impact classification of flood events applied in this thesis). For instance, INUNGAMA is a

database that uses these categories to classify the flood events recorded from 1900 to 2015 in Catalonia according to their impacts. Another example is the FLOODHYMEX database which follows the same methodology to classify the flood events that affected different Mediterranean regions for the period 1980-2015 (further information about INUNGAMA and FLOODHYMEX databases will be given in Chapter 3).

Other classifications are based on the top-down approach using precipitation thresholds. One example is Amaro et al. (2010), in which a severe hydrometeorological episode is considered when the daily precipitation exceeds 60 mm, following the methodology developed in the MEDEX project (Jansa et al., 2014). Torgersen et al. (2015) also apply a precipitation threshold in Norway. In this case, a precipitation episode will be considered a flood event when the daily precipitation accumulates more than 25 mm in at least 3 stations and, at the same time, the number of insurance claims is equal to or greater than 4.

2.1.3 Methodology for the evaluation of damages

When analysing the risk of flood events, one must first distinguish between two types of studies: those that refer to the **damage assessment or damage caused by floods** and those related to **risk assessment** (Thieken et al., 2005). The first studies use indicators that depend on the type and magnitude of the flood and the impact they produce, whereas the second ones depend on the characteristics of the elements located in the flood zones (Merz et al., 2010). Examples of impact indicators are the velocity of the flow or the inundation depth, while risk factors include indicators (also called resistance parameters) such as the type of buildings, protection measures, existence of warning systems, among others. For this reason, this section has been divided into **damage assessment or methods used to analyse the damage caused by floods** and **flood risk estimation methods**.

Damage assessment

The assessment of flood damage is necessary to analyse flood vulnerability (elements at risk), develop flood risk maps (European Comission, 2007), optimise decisions on mitigation measures, perform comparative risk analyses and conduct financial appraisals for insurers and for compensation when an event occurs (Merz et al., 2010). In this thesis we will be mainly focused on economic damages. Given its critical importance there are a large number of studies focusing on the estimation of flood damages and trying to improve their predictive capacity. There are different methods used depending on both the scale and the type of damage considered. Two main approaches can be distinguished for flood damage models: empirical approaches, which use damage data collected after flood events (Kreibich et al., 2005; Thieken et al., 2008); and synthetic approaches, which use damage data collected via what-if-questions (Merz et al., 2010). In the latter, the expected damage in case of flood event occurrence is analysed. An example of this synthetic approach is the INUNCAT flood risk plan (*Pla especial d'emergències per inundacions de Catalunya*), developed by the Civil Protection of Catalonia (Protecció Civil

de Catalunya, 2017), which estimates the economic losses and people that would be affected by different water levels.

The following sections describe the main methods used to estimate direct and tangible damages. The last part of this section summarises the principal methodologies used to assess the indirect damages caused by floods.

Stage-damage curves   The most commonly used method to estimate losses caused by floods is the *stage-damage curves*, in which the degree of damage or absolute damage is usually calculated based on the depth of the flood or water level (Elmer et al., 2010). This approach is used in the well-known *Multi-Colored Manual* released by the Flood Hazard Research Center (FHRC) of the Middlesex University (Penning-Rowsell et al., 2005), as well as in many other studies such as the curves developed by the Emergency Management Australia (EMA, 2002), or those from the Federal Emergency Management Agency (FEMA, Scawthorn et al., 2006). FEMA stage-damage curves are used in Civil Protection plans as well as by the Catalan Water Agency (*Agència Catalana de l'Aigua*, ACA, 2018), and they are defined as the flood damage that would occur at specific water depths per land-use class (expressed as price per unit of area). The Valencian Community also applies stage-damage curves in the *Territorial Action Plan for Flood Risk Prevention in the Valencian Community* (Generalitat Valenciana, 2015). Another example of application of this methodology is the study carried out by Dottori et al. (2016) in which an index called *The Flood Intensity Index* was developed to quantify the flood hazard. This index is mainly based on the water depth, which then relates to the flood impact by applying depth-damage curves in different flood scenarios.

Multi-parametric damage models   Multi-parametric statistical models are widely applied in empirical analyses (Merz et al., 2013; Thieken et al., 2005, 2008, 2016; Elmer et al., 2010; Kreibich et al., 2010). Thieken et al. (2008) developed a model to assess the flood losses for the residential sector (FLood LOss EStimation MODel for the PRivate Sector, FLEMOps) while Kreibich et al. (2010) developed one for the commercial sector (FLood LOss EStimation MODel for the Comercial Sector, FLEMOcs). Both models include information about the objects at risk and consider water level, flood water contamination and precautionary measures as impact factors (Elmer et al., 2010). These studies gather a large number of indicators from post-event surveys done to the population affected by one or several flood events. In particular, the FLEMOps and FLEMOcs models were developed based on the results obtained after the 2002 flood event that affected Danube and Elbe basins, as well as after the events of 2005 and 2006 that affected Germany, in the case of FLEMOcs.

The survey questions are grouped into 5 different catregories according to the topic, from which, different indicators are obtained. The categories are: flow, contamination, warning system, emergency measures, experience in previous floods and socioeconomic variables. Then, the relationships between these variables and 4 parameters of damage produced in buildings (total and ratio loss in the content of the building, and total and ratio loss in the structure of the building) are studied. Different multivariate techniques are used to carry out the statistical

analysis of this large number of variables. Merz et al. (2013) applied *Regression trees* to study the impact of flooding on buildings. Other statistical techniques commonly used are the *Bagging decision tree* and the *Random Forest*, which are extensions regression trees aiming to reduce the uncertainty and improve the predictive results when working with a large number of variables (Wagenaar et al., 2017).

Schröter et al. (2014) performed a comparative study of the techniques used for assessing flood damage from 8 different models: two with models based on regression trees, one with depth-damage curves, one based on multifactor analysis of the FLEMOps project and four using Bayesian techniques. The results showed that the increase in the complexity of the model improves its predictive capacity both spatially and temporally, although only the direct damages to buildings obtained from telephone surveys were taken into account.

Impact indices Impact indices are an alternative methodology used to evaluate the damages produced by flood events. An example is the study of Amaro et al. (2010), in which a social impact index was developed within the MEDEX project (Jansa et al., 2014). In a second study, Barbería et al. (2014) improved the index by modifying some variables and introducing new ones. This index takes into account hazard indicators such as the maximum rainfall recorded in 24 h or the precipitation intensity, as well as damage indicators such as the population affected by the event.

Petrucci (2013) developed a complex index for assessing the damage (direct and indirect) caused by past landslide events. The index estimates the damage per municipality by giving a loss degree and a value for each of the elements considered.

In Boudou (2015), an index was developed for classifying flood events based on the intensity (e.g. return period, duration of the flood), the severity (e.g. fatalities, economic damages) as well as the spatial extension of the event (e.g. number of administrations affected). Each of these sections is subdivided into other ones composed by different indicators, each one with different value. The total score of the index (from 8 to 34) is an indicator of the importance of the event.

Insurance data Insurance data are becoming an important source of information to estimate flood damage. These data are very valuable for assessing causal relationships between hazard data such as precipitation and economic damages (Zhou et al., 2013; Torgersen et al., 2015; Spekkers et al., 2013, 2015), as well as a validation method for impact flood models (Zhou et al., 2013; Bihan et al., 2017; Zischg et al., 2018). Insurance data are commonly used in pluvial flood studies and only when direct and tangible damages are considerd (Torgersen et al., 2015; Bernet et al., 2017; Van Ootegem et al., 2018). For instance, Zhou et al. (2013) and Torgersen et al. (2015) applied regression models to assess the association between precipitation and compensation paid by insurance companies due to pluvial flood events. In both studies, a good correlation between these two variables was found and, therefore, it was proved that it is feasible to build models that explain the costs of damage as a simple function of precipitation (Zhou et al., 2013). Other studies use these data as a tool to differentiate between different types of

floods. This is the case of Bernet et al. (2017), which proposed a methodology to distinguish between river and surface water flooding using insurance data.

An adjustment is needed when working with economic data using different periods of time. The most common methodology applied is the one established by Pielke Jr and Landsea (1998), in which the damages are adjusted by the population, wealth and inflation of the region or country. Nevertheless, studies such as Barredo (2009) and Neumayer and Barthel (2011) developed other methods that allow a better comparison between different regions. The application of a normalization process to economic damage data allows to know whether the observed trends in damages are related to climatic factors or to changes in vulnerability and exposure (Neumayer and Barthel, 2011).

Indirect damage assessment Indirect damages are difficult to assess, and are specially challenging when regional scale is considered (Przyluski and Hallegatte, 2011). There are several techniques to analyse this type of damages. The most commonly used is the collection of a great amount of indicators regarding past events. For example, Petrucci (2013) developed a complex index that takes into account both direct and indirect damages. For indirect ones, it uses indicators related to tangible damages such as the cost to allocate affected people, as well as non-tangible ones such as the psychological effect of losing a family member or personal belongings.

Econometric approaches are another method used to estimate indirect losses from natural disasters although they focus on the average indirect costs of a series of events, such as the long-term impact on economic growth rather than single event losses (Przyluski and Hallegatte, 2011). For instance, Strobl (2011) analysed the impact of hurricanes on economic growth in the United States at a county level. Other techniques applied are the *input-output* models, developed by Wassily Leontief and recognised by Nobel Prize in economics which consist on analysing the interdependences between industries in an economy. The model is based on the requirement of a fixed amount of all inputs for the production of an output unit. For example, in Gain et al. (2015) tables *input-output* were used for estimating the losses in agriculture due to flood events.

Flood risk indices

A large number of studies focus on the development of complex **vulnerability or risk indices** for analysing flood events and allow to discern zones, goods or people more susceptible to suffer damages. An example is the elaborate index developed in Balica et al. (2012), in which a big number of indicators related to hydrogeological (e.g. maximum flow for the last 10 years), socioeconomic (e.g. recovery time after an event) and political-administrative factors (e.g. existence of structural prevention measures) were used to study the vulnerability of coastal cities. These indicators, depending on the type of variables they represent, that is, exposure, resilience or susceptibility, will have a different weight in the final index. Mclaughlin and Cooper (2010) applied a similar methodology but taking into account different spatial scales

(local, regional and national). These indices are commonly used for analysing floods in urban areas, as for instance the one developed in Nasiri and Shahmohammadi-Kalalagh (2013).

Tables 2.7, 2.8 and 2.9 summarise the most common indicators applied for estimating flood risk separately by type: hazard, vulnerability-exposure and resilience, respectively.

Definition	Unit	Reference
Maximum flow in the last 10 years	$m^3 \, s^{-1}$	Balica et al. (2012)
Sea level rise (coastal zones)	mm year^{-1}	Balica et al. (2012)
Increase in precipitation	mm; %	Nasiri and Shahmohammadi-Kalalagh (2013)
Increase in precipitation intensity	mm h^{-1}; %	Nasiri and Shahmohammadi-Kalalagh (2013)
Evaporation rate	mm	Nasiri and Shahmohammadi-Kalalagh (2013)
Time of concentration of the basin	Hours	Petrucci et al. (2012)
Basin slope	%	Zhou et al. (2017)

Table 2.7: Hazard indicators

Definition	Unit	Reference
Number of historic buildings, museums, etc. (cultural heritage)	Nº; absence-presence	Balica et al. (2012); Mclaughlin and Cooper (2010)
Population, population density	Nº inhab.; inhab. km^{-2}	Balica et al. (2012); Mclaughlin and Cooper (2010); Nasiri and Shahmohammadi-Kalalagh (2013)
Population or population density increase rate	%	Nasiri and Shahmohammadi-Kalalagh (2013)
Population or population density during the night	Nº hab.; inhab. km^{-2}	Zhou et al. (2017)
Proximity to the river	m; km	Nasiri and Shahmohammadi-Kalalagh (2013)
Number of industries	Nº	Nasiri and Shahmohammadi-Kalalagh (2013)
Topography	-	Nasiri and Shahmohammadi-Kalalagh (2013)
Communication routes	Absence-presence	Mclaughlin and Cooper (2010); Nasiri and Shahmohammadi-Kalalagh (2013)
Land use types	-	Mclaughlin and Cooper (2010); Nasiri and Shahmohammadi-Kalalagh (2013)
GDP, per capita income	€	Pielke Jr and Landsea (1998); Barredo et al. (2012)
Age	Years	Schröter et al. (2014); Merz et al. (2013); Thieken et al. (2005)
Number of people in the building or house	Nº	Schröter et al. (2014); Merz et al. (2013); Thieken et al. (2005)
Number of kids (<14 years) and elderly people (>65 years)	Nº	Schröter et al. (2014); Merz et al. (2013); Thieken et al. (2005)
Monthly net salary	€	Schröter et al. (2014); Merz et al. (2013); Thieken et al. (2005)
Socioeconomic status	-	Schröter et al. (2014); Merz et al. (2013); Thieken et al. (2005)
Literacy and dependency rate	%	Gain et al. (2015)
Percentage of population with some disability	%	Balica et al. (2012); Nasiri and Shahmohammadi-Kalalagh (2013)
Designation of protected areas or regions (natural, biodiversity, etc.), existence of local biodiversity or adaptation plans	Absence-presence	Mclaughlin and Cooper (2010)
Unemployed people	%	Nasiri and Shahmohammadi-Kalalagh (2013)
Human development Index (HDI) (expected years of life, years of schooling, GDP, etc.)	-	Nasiri and Shahmohammadi-Kalalagh (2013)
Type of building	€	Schröter et al. (2014); Merz et al. (2013)
Building age: number of buildings > 30 years	Nº	Gain et al. (2015)
Number of floors of the buildings	Nº	Schröter et al. (2014); Merz et al. (2013); Thieken et al. (2005)
Total surface of the building	m^2	Schröter et al. (2014); Merz et al. (2013); Thieken et al. (2005)
Building quality	-	Schröter et al. (2014); Merz et al. (2013); Thieken et al. (2005)
Building value	€	Schröter et al. (2014); Merz et al. (2013); Thieken et al. (2005)

Table 2.8: Vulnerability-exposure indicators

Definition	Unit	Reference
Number of shelters per km²	Nº km⁻²	Balica et al. (2012)
Experience of flood events in the last 10 years ; 0 = no experience to 9 = recent experience; number of flood events experienced, time from the last event, experience of events with damages greater than specific amount	Nº; Absence-presence; Days	Balica et al. (2012); Nasiri and Shahmohammadi-Kalalagh (2013); Schröter et al. (2014); Merz et al. (2013); Thieken et al. (2005)
Recovery time of an event	Days	Balica et al. (2012)
Km of canalization in the city	Km	Balica et al. (2012)
Existence of international organizations, Nº of civil protection volunteers, Nº of organisations	Absence-presence; Nº	Balica et al. (2012); Schröter et al. (2014)
Existence of protection measures against floods; existence or number of rainwater tanks	Absence-presence; Nº	Balica et al. (2012); Schröter et al. (2014); Merz et al. (2013); Thieken et al. (2005)
People taking their own protective measures (move furniture, put some protection, etc.	Absence-presence	Merz et al. (2013); Thieken et al. (2005)
Warning system, system quality (degree of awareness of the alert), hours in advance	Absence-presence; hours	Nasiri and Shahmohammadi-Kalalagh (2013); Schröter et al. (2014); Escuder-Bueno et al. (2012); Thieken et al. (2005); Elmer et al. (2010)
Lead time period elapsed without using emergency measures	Days	Schröter et al. (2014); Merz et al. (2013)
Emergency systems	Absence-presence	Nasiri and Shahmohammadi-Kalalagh (2013); Schröter et al. (2014); Escuder-Bueno et al. (2012); Thieken et al. (2005)
Work recovery time	Hours	Elmer et al. (2010)
Time passed from the alert to the application of the mitigation measure	Hours	Elmer et al. (2010)
Storage capacity of the dams	m³	Nasiri and Shahmohammadi-Kalalagh (2013)
Insurance compensation for floods	Absence-presence	Nasiri and Shahmohammadi-Kalalagh (2013)
Amount of investment	€	Nasiri and Shahmohammadi-Kalalagh (2013)
Flood risk awareness	Absence-presence	Schröter et al. (2014); Merz et al. (2013)
Existence of flood risk maps	Absence-presence	Balica et al. (2012); Escuder-Bueno et al. (2012)

Table 2.9: Resilience indicators

2.2 Trends in extreme precipitation and flood events

The study of changes in extreme precipitation and flood events has become a very active research area, and in recent years numerous studies have been published analysing the historical trends of those events (Madsen et al., 2014; Brázdil et al., 2014; Herget et al., 2014; Barriendos Valve et al., 2014; Llasat et al., 2013; Barrera-Escoda and Llasat Botija, 2015; Llasat et al., 2016b).

There are different criteria to define an extreme event. According to the Fifth Assessment Report of the Intergovernmental Panel on Climate Change (IPCC, Pachauri et al., 2014) an extreme event is defined as being *exceptional* on specific place and/or time of year. The definitions of *exceptional* vary, but an extreme climatic event would normally be as equal or more extreme

than the 10th or 90th percentile of a probability density function estimated from the empirical data. For some climatic extreme events as droughts, floods and heat waves, several factors such as duration and intensity must be combined to produce an extreme event (Seneviratne et al., 2012).

2.2.1 Extreme precipitation

The Fifth Assessment Report of the IPCC (Pachauri et al., 2014) concludes that it is likely that, since the mid-20th century, the number of extreme precipitation events (e.g. above the 95th percentile) has increased in more regions of the world than it has decreased, as already has shown in the results of the Fourth report (IPCC, 2007) and the report related to extreme events and disasters (Field et al., 2012). Nonetheless, there are strong regional and subregional variations in trends. In particular, many regions show null or negative trends in extremes and also important differences between the seasons of the year. In general, the most consistent trends towards more intense precipitation events are found in the center of North America (very likely increase) and in Europe, where there have been very likely trends of increase in both frequency and intensity of precipitation extremes. However, for Europe and especially the Mediterranean region, these results show a wide seasonal and/or regional variability.

Several studies have analysed the trends in precipitation extremes in Europe. Ye et al. (2017) distinguished between three types of precipitation (convective, non-convective and mixed) and showed that the total annual precipitation due to convective episodes in Eurasia between 1966-2000 had increased, whereas the precipitation due to non-convective and mixed episodes had decreased. Van den Besselaar et al. (2013) also found an increase in precipitation extremes in the north and south of Europe for the 1951-2000 period, showing a decrease of 21 % in the return period of the extreme events. These results align with those shown in Cioffi et al. (2015), in which a statistically significant trend in the increase in the number of days exceeding the 90th and 95th percentiles of precipitation was found in the north and west of Europe from October to March between 1901 and 2006. Madsen et al. (2014) summarised the results found in different studies on trends in precipitation extremes based on observations as well as future climate projections. The main finding was the general increase in precipitation extremes while no clear trend was detected in flow data. In terms of projections, most studies show an increase in precipitation extremes with global warming, while in the case of flows, both increase and decrease can be expected (see also Chapter 7 for more information about precipitation projections).

In spite of this evidence, negative trends in total and extreme precipitation have also been observed in the Mediterranean region, as is the case of Turco and Llasat (2011), in which the indices of the Expert Team on Climate Change Detection and Indices (ETCCDI, Karl et al., 1999; Peterson et al., 2001) for Catalonia region and for the period 1951-2003 were estimated. The results showed that although most of the indices of high precipitation did not show any trend, a significant negative trend in total precipitation and in the maximum accumulated in 5 days were found in the Ebro Observatory (Turco and Llasat, 2011). Lemus-

Canovas et al. (2019) also observed a statistically significant negative trend in the annual precipitation recorded between 1960 and 2010 in some parts of the Catalan Pyrenees. In terms of projections in Catalonia, the results of the Third Report on Climate Change in Catalonia (TICC, 2016), although with large uncertainty, point towards a general reduction of the total annual precipitation with global warming. Nonetheless, Barrera-Escoda et al. (2014) found an increase of the frequency of heavy precipitation events (>200 mm in 24 h) during the 2021-2050 period in this region. In a part of Catalonia, the Metropolitan Area of Barcelona, an increase in the number of days with precipitation over 100 mm in 24 h is also expected, according to Altava-Ortiz et al. (2016).

In Portugal, the majority of the ETCDDI indices did not show any significant trend between 1941-2007 (de Lima et al., 2014). However, for the period 1976-2007, there was an increasing trend of extreme events, specifically an increase in the maximum 1-day precipitation index (Rx1day) and in the daily precipitation amount on wet days (R99pTOT), especially in the south of Portugal.

2.2.2 Flood events

As mentioned in the introduction, the study of floods is crucial since they are the most important natural risk around the world (Field et al., 2012) that may be exacerbated in the future with increased precipitation events linked to climate change (Pachauri et al., 2014) in some regions of the world, including Europe (see Chapter 7). According to Field et al. (2012), a flood is the overflowing of the normal confines of a stream or another body of water, or the accumulation of water over areas that are not normally submerged. The main causes of floods are intense and / or prolonged precipitation, snow / ice melting, a combination of these causes, the breakdown of a dam (for example, glacial lakes), reduced transport due to ice jams or landslides, or an intense local storm (Smith and Ward, 1998).

Trends in flood events are not as clear as those found in extreme precipitation events. There is a large uncertainty on their magnitude and frequency. For example, Madsen et al. (2014) showed that there is evidence of a general increase in the extremes of precipitation in most studies analysed, while there is no clear indication of significant trends of increase in the flows. Hall et al. (2014) state that it is difficult to establish a general conclusion about changes in floods in Europe due to the diversity of processes, the periods of study and the variety of methodologies applied.

Several methods to study flood trends have been used. Most methods use different hydrological variables to analyse flood trends (Petrow and Merz, 2009). For instance, Douglas et al. (2000) applied the annual mean in the maximum daily flow to study flood trends in the United States. Svensson et al. (2005) used the same indicator for time series worldwide and compared it with the series of peaks-over-threshold (POT), a method commonly applied to estimate extreme values. Mediero et al. (2014) studied flood trends in Spain using a total of 9 indicators obtained from series of the average in maximum daily flow, maximum seasonal flow and POT. A similar methodology was followed by Petrow and Merz (2009), in which 8

indicators from hydrological variables were used to analyse flood trends in Germany. Wilson et al. (2010) and Blöschl et al. (2012) are other examples for analysing flood trends based on hydrological thresholds in the Nordic countries and in Austria, respectively.

The variability in results of flood trends analyses can be observed in different studies at regional scale. For example, Mediero et al. (2014) found a general decrease in the frequency and magnitude of flood events in Spain for three different time periods 1942-2009, 1949-2009, 1956-2009, with more notable evidence in the last one. These results could be related to an increase in evapotranspiration in the area that increase water losses in soils and a decrease in soil moisture content before the occurrence of floods. On the contrary, Llasat et al. (2016b) found an increase of flood events between 1900 and 2011 in Catalonia, however, there is no evidence in the precipitation extremes, showing that this growth could be related to a rise in vulnerability and exposure of the region. Sun et al. (2015) also observed a significant increase in flood events in Germany for a long period of more than 80 years (1934-2005). On the other hand, Glaser et al. (2010) found 4 periods from 1500 where the frequency on river flood events in Europe increased: 1540-1600, 1640-1700, 1730-1790 and 1790-1840. However, from 1950 until now, there are no consistent patterns, a fact that could be related to modern flood protection systems.

2.3   Discussion framework

In the first part of this chapter a summary of the methodologies and indicators most commonly applied to study the impact of floods has been made. As noted, although there are many studies that use different techniques to estimate the damage caused by these events, a large body of literature still focuses on the dangerousness of the event rather than on the impacts it produces, usually due to the lack of damage data. In this context, insurance databases represent a potential and valuable source of flood damage data. Consequently, research has been conducted in recent years to use insurance data as a proxy in the analysis of the impact of flooding events.

Secondly, as shown in the second part of this chapter, there is great uncertainty regarding trends in floods and precipitation extremes. However, increases in these episodes, especially those regarding extreme precipitation, have been found in Europe. Moreover, an increase in extreme precipitation events (potentially enhanced by global warming), would lead into an increase in the number of surface water flood events. Considering the risks associated to this type of events in the area of study, it is crucial to keep on the research to fully understand the consequences in terms of potential damage.

Considering all the above-mentioned, this work has followed the next considerations. First, as already mentioned in the introduction, insurance data have been used as a proxy of flood damage. In addition, flood events have been classified according to the impact they produce following the methodology described in Chapter 4. As explained above, given that most of floods are SWF, precipitation has been used as the main hazard driver of flood risk. The precipitation

produced in each of the flood events and affected basins as well as the changes in precipitation extremes with global warming have been calculated. In addition, in order to account for variables other than the dangerousness of the event, indicators related to the exposure and vulnerability of the territory have also been analysed. Specifically, population, gross domestic product, proportion of urban zone, land use and slope have been used as indicators. Finally, several regression models have been fitted to find the most appropriate method for describing flood damage.

Chapter 3

Region of study and data sources

3.1 Region of study

This thesis is composed by two regions of study: Catalonia and the Valencian Community. Other than these two areas, a flood risk analysis has also been carried out in the Metropolitan Area of Barcelona (MAB), a highly vulnerable urban area which is part of Catalonia region. In this chapter, the three regions are presented separately.

3.1.1 Metropolitan Area of Barcelona
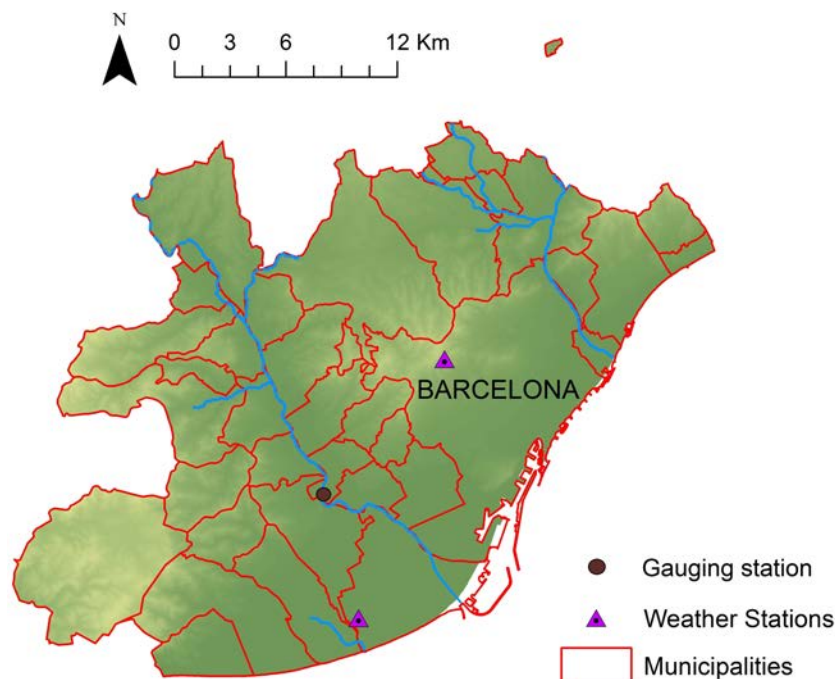
Figure 3.1: Map of the Metropolitan Area of Barcelona (MAB), showing its municipalities, the gauging station in the Llobregat River (brown circle) and the two main weather stations (purple triangle). The Besòs River (east of Barcelona) and the Llobregat River (west of Barcelona) are also shown (in blue colour)

The first analysis (Chapter 4) is referred to the Metropolitan Area of Barcelona (MAB), composed of Barcelona and 35 adjacent municipalities around the city. This urban and peri-urban area has a surface of 534.7 km^2 and a population larger than 3.3 million of residents. The larger part of the population is concentrated in the municipality of Barcelona (1,620,343 people in 101.6 km^2, IDESCAT, 2018), located between the Besòs River and the Llobregat River, the Littoral Range and the Mediterranean Sea (Figure 3.1). Although both rivers have experienced catastrophic flood events (e.g. September 1971) with return periods higher than 100 years, minor flood events occur frequently (with an average of 3 flood events per year, Cortès et al., 2017) as a consequence of convective and local precipitation mainly recorded in late summer and autumn (Llasat et al. 2013; del Moral et al. 2016). A total of 109 flood events have been recorded in the MAB for the 1981-2015 period (61 between 1996 and 2015), eight of them causing catastrophic impacts in the region.

The city of Barcelona is crossed by 20 streams, most of them are covered by part of the Barcelona drainage system, managed by the Barcelona Water Cycle (*Barcelona Cicle de l'Aigua* or BCASA). The United Nations International Strategy for Disaster Reduction (UNISDR) recognised Barcelona as a resilient city and a model city for dealing with floods (Nakamura and Llasat, 2017), as it has a permanent surveillance and warning system running on hydraulic modelling that includes 15 rainwater tanks that allow for better flood prevention. As a result, the number of flood events recorded in the city as well as the damages associated to them have decreased over time (Barrera et al., 2006; Llasat et al., 2016a; Cortès et al., 2017).

3.1.2 Catalonia
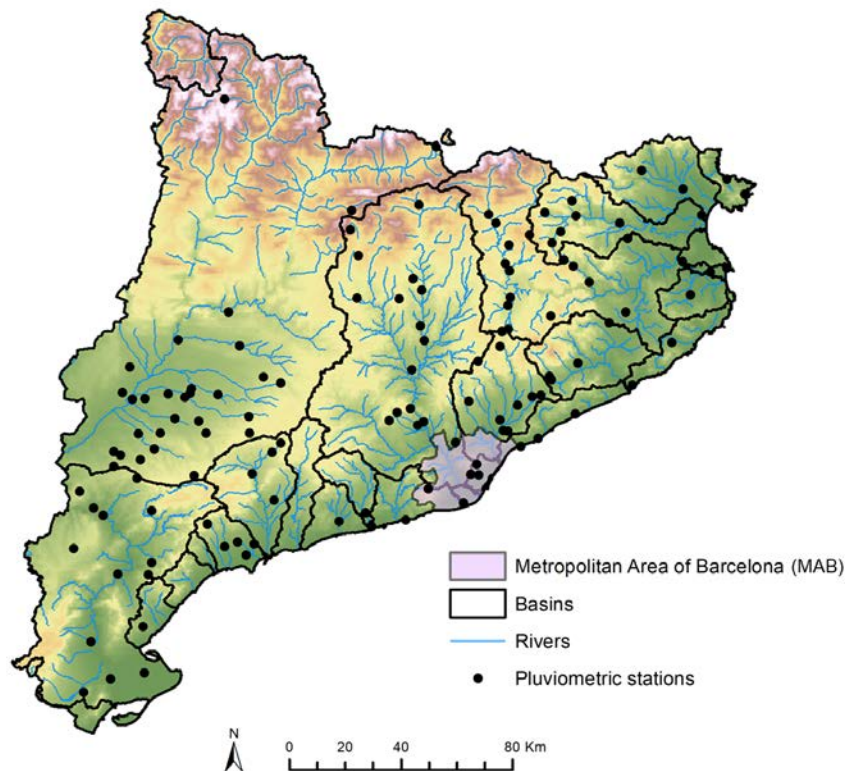
Figure 3.2: Map of Catalonia showing the aggregated basins (black lines), the Metropolitan Area of Barcelona (MAB), the main rivers (blue lines) and the 24 h pluviometric stations used (black points)

The second area of study is Catalonia, a region of 32,108 km^2 in the north-east Iberian Peninsula where more than 7.5 million people live (IDESCAT, 2018). The region is characterised by three mountain ranges (Figure 3.2): the Pyrenees in the north (maximum altitude above 3,000 m a.s.l.) and parallel to the Mediterranean coast (SW-NE) between the Catalan Pre-Coastal Range (maximum altitude around 1,800 m a.s.l.) and the Catalan Coastal Range (maximum altitude around 600 m a.s.l.). This marked orography is the key reason for the development of floods, both from a hydrological point of view (small torrential catchments) and meteorological factors (the orography forces water vapour to rise from the Mediterranean, triggering instability, Llasat et al., 2016b). The impact of the Pyrenees can also produce remarkable effects in the mesoscale pressure distribution, giving place to convergence lines, orographic dipoles, etc. One example was the flood event of October 1987, when more than 400 mm of rainfall were recorded in 24 h near Barcelona favoured by the convergence forced for a mesohigh created at the south of Pyrenees (Ramis et al., 1994).

During the 1996-2015 period a total of 166 flood events were recorded in Catalonia, 13 of them caused catastrophic impacts, 87 extraordinary and 66 ordinary impacts (Cortès et al., 2018).

3.1.3 Valencian Community
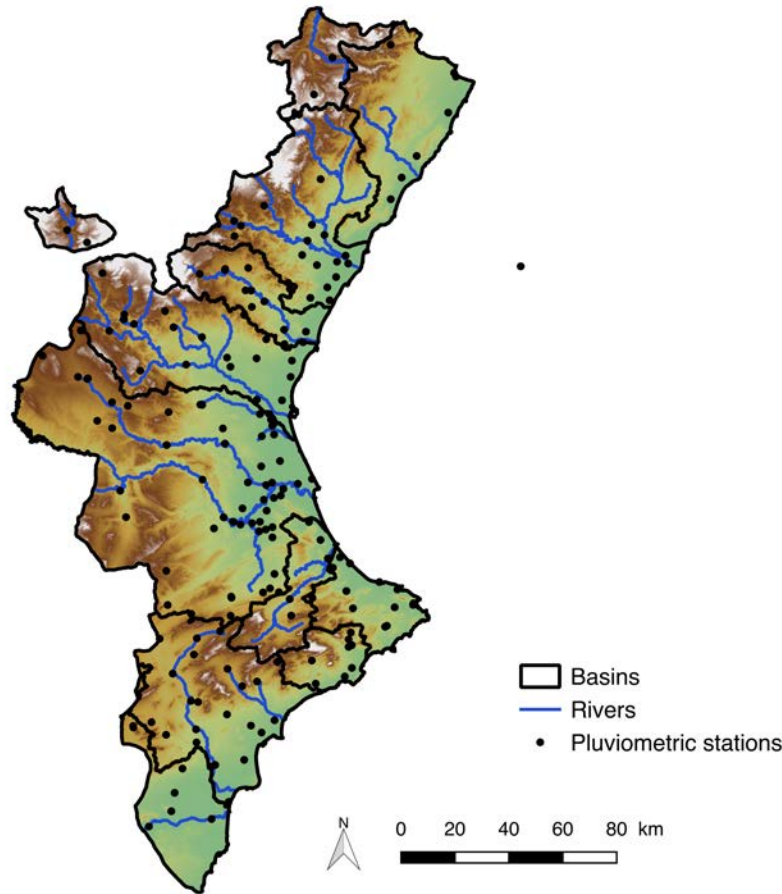
Figure 3.3: Map of the Valencian Community, showing its basins (black lines), main rivers (blue lines) and the 24 h pluviometric stations (black points)

Chapter 6 and 8 are focused on two areas of the western Mediterranean: Catalonia and the Valencian Community. In this latter region (Figure 3.3), around 5 million people live in a total surface of 23,255 km² (INE, 2018). As in the case of the Catalonia region, coastal plains are crossed by torrential non-permanent streams surrounded by intensively urbanised areas. In the South of the region, mountains reach almost the coast line (maximum altitude around 1,560 m.a.s.l.) favouring heavy precipitations that can exceed 700 mm in less than 24 h. This was the case in November 1987, when more than 800 mm of rainfall were recorded in 24 hours in the municipality of Oliva (Valencia) (Ramis et al., 2013).

The Valencian Community has recorded a total of 69 flood events during the 1996-2015 period, 11 of which were catastrophic, 26 extraordinary and 32 ordinary (Cortès et al., 2018; Cortès et al., 2019).

3.2   Data

This section summarises all the data used for the execution of this thesis, divided into different parts according to the type of data.

3.2.1   Flood events databases

In order to select the flood events that have affected the regions of study of the thesis (MAB, Catalonia and Valencian Community), three different databases have been used: INUNGAMA (Barnolas and Llasat, 2007; Llasat et al., 2016b), PRESSGAMA (Llasat et al., 2009) and FLOODHYMEX (Llasat et al., 2013). The INUNGAMA is a database sourced by GAMA (*Grup d'Anàlisi de situacions Meteorològiques Adverses*) that reports the flood events occurred in Catalonia from 1900 to 2015 on a municipal, county and basin level. Information contained in the database includes hydrometeorological data, impacts caused, and the affected areas for each of the events. The major part of this information is provided by PRESSGAMA, a database formed from press data and other data sources such as official reports. This database, which includes more than 15,000 news items, systematically collects information on natural risks and climate change in the newspaper *La Vanguardia* from 1981. Finally, as per the flood events recorded in the Valencian Community, the FLOODHYMEX database has been used, which contains both hydrometeorological and impacts information as a consequence of flood events that affected different Mediterranean regions during the period 1980-2015. The data used in this thesis are from 1996 to 2015.

3.2.2   Meteorological data

The precipitation data used in this thesis come from different sources, depending on the accumulation time interval used. We have used daily precipitation data provided by the Spanish State Meteorological Agency (*Agencia Estatal de Meteorología*, AEMET), which has an extensive network of automatic meteorological stations spread throughout the entire region of study collecting the accumulated daily precipitation between 7 UTC and 7 UTC of the following day. Figures 3.4 and 3.5 show the effectiveness of AEMET weather stations for the period 1996-2015 for Catalonia and the Valencian Community, respectively. Only the stations with an effectiveness value higher than 90 % between 1996 and 2015 have been taken into account in the study, in order to guarantee the use of well-functioning stations that cover the entire study period. That represents the significant number of 127 stations for Catalonia and 183 for the Valencian Community.
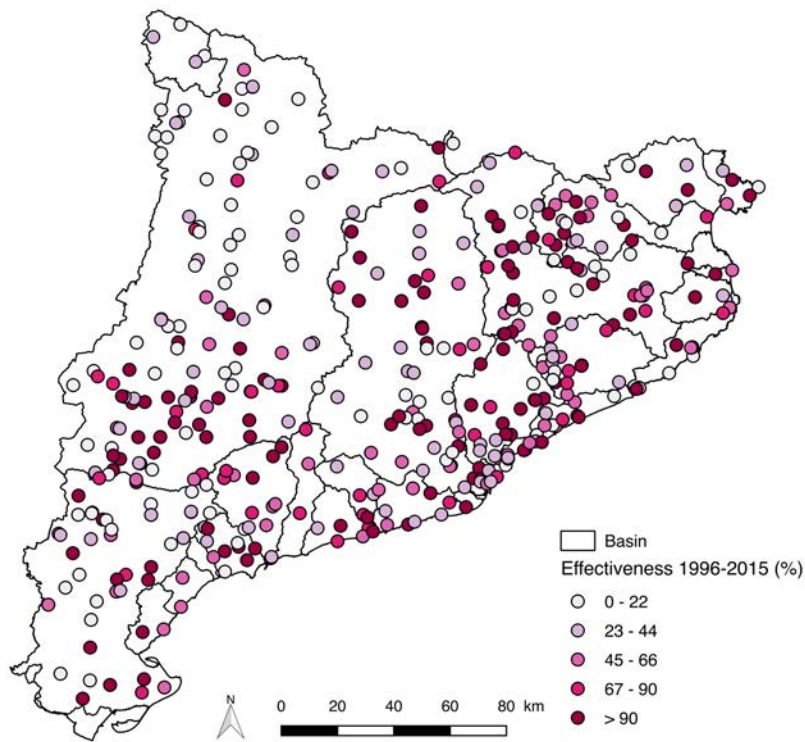
Figure 3.4: AEMET weather stations effectiveness for the period 1996-2015 for Catalonia
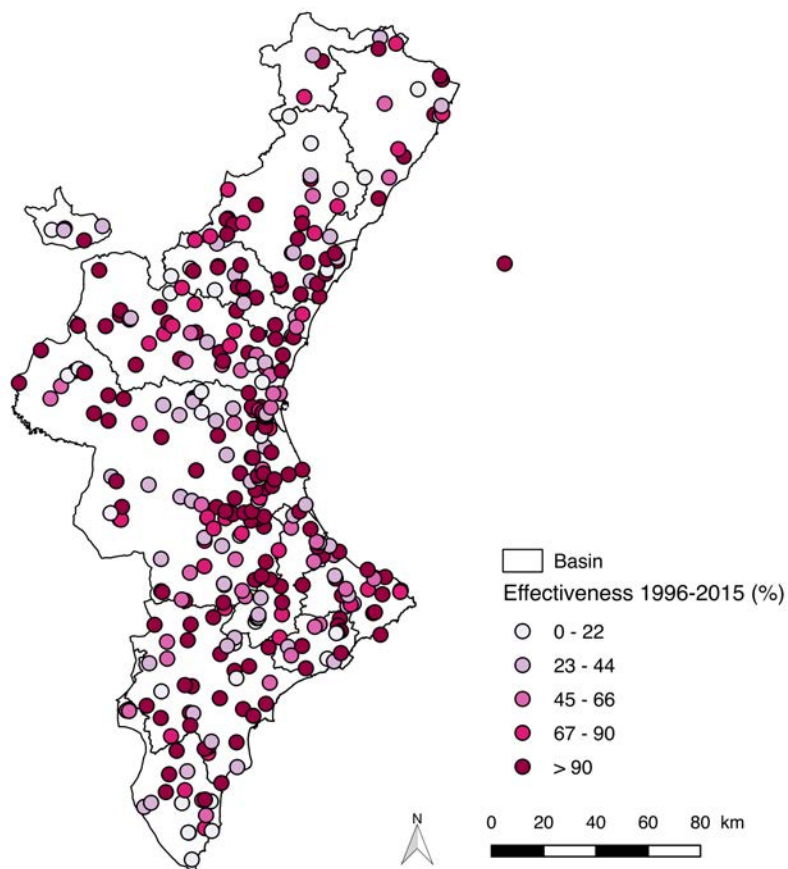
Figure 3.5: AEMET weather stations effectiveness for the period 1996-2015 for the Valencian Community

The 30-minute precipitation data for the entire Catalonia have been obtained from the network of automatic meteorological stations (*Xarxa d'Estacions Meteorològiques Automàtiques*, XEMA) belonging to the Meteorological Service of Catalonia (*Servei Meteorològic de Catalunya*, SMC). In the case of the Valencian Community, 5-minute precipitation data provided by the Hydrographic Confederation of Júcar (*Confederación Hidrográfica del Júcar*, CHJ) have been used. These data have been accumulated into 30 minutes time steps for consistency with the data provided by the SMC.

Figure 3.6 shows the two types of weather stations used for the precipitation data for the MAB region: 30-min rainfall stations from the SMC and the daily precipitation stations from the AEMET (effectiveness > 90 %).
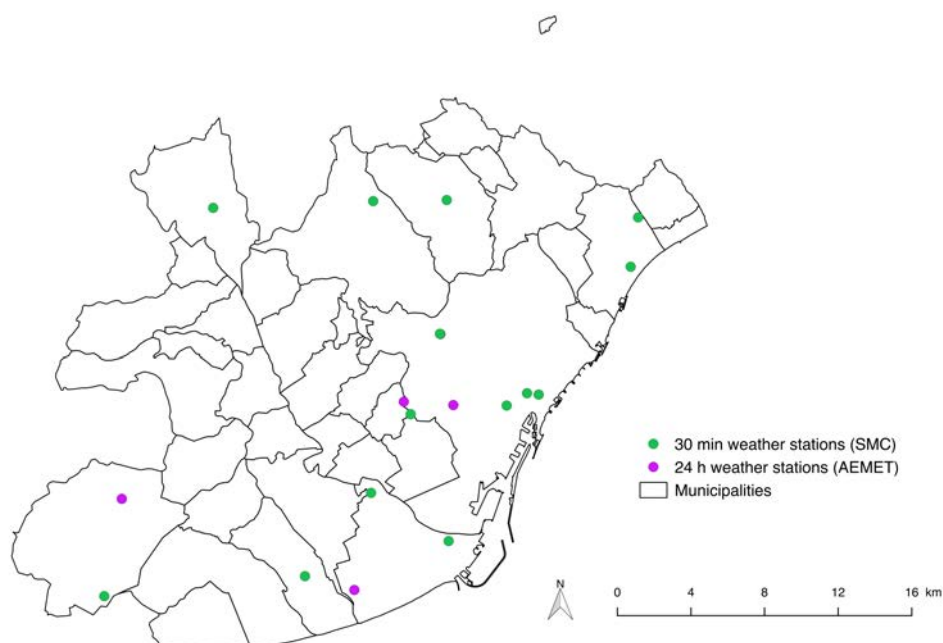
Figure 3.6: Metropolitan Area of Barcelona with the weather stations used in the study. Green points indicate the SMC stations (30 minute) and the purple ones the AEMET stations (daily). The black lines represent the delimitation of each of the 36 municipalities that constitute the MAB

3.2.3   Vulnerability and exposure data

Vulnerability and exposure data used in the thesis come from different sources. Population and Gross Domestic Product (GDP) data for Catalonia region were obtained from the Statistical Institute of Catalonia (*Institut d'Estadística de Catalunya*, IDESCAT, 2018). In the case of the Valencian Community, the data were provided by the Spanish National Statistics Institute (*Instituto Nacional de Estadística*, INE, 2018). The population and GDP data used correspond to the year when the flood event took place. GDP data were adjusted to the value of the Euro in 2015, in order not to take into account the inflation effect. This has been done following the methodology defined by the Spanish National Statistics Institute (INE, 2018), which consists on using the exchange rate in the consumer price index (CPI) between the specific year of the event and the reference one (2015).

The urban area for these two regions has been obtained from the maps of 2005 and 2011 of the Land Use Information System of Spain (*Sistema de Información sobre Ocupación del Suelo de España*, SIOSE, 2018), for which a treatment with Geographical Information Systems tools has been made (ArcGIS and QGIS) to obtain the proportion of urban area per each basin. In the case of the MAB region, changes in land cover were analysed through the Land Use Maps of Catalonia, drawn up by the Ecological and Forestry Applications Research Centre (*Centre de Recerca Ecològica i Aplicacions Forestals*, CREAF, 2018) for the available editions (1993, 2000-2002, 2005-2007 and 2009). Table 3.1 summarises the main characteristics for each edition. Runoff coefficients for different land uses were taken from Chow et al. (1988). The methodology used to obtain the average runoff value for each municipality of the MAB region is explained in detail in Chapter 4.

Edition	LCLU-I	LCLU-II	LCLU-III	LCLU-IV
Year	1993	2000-2002	2005-2007	2009
Orthophotos scale	1:25,000	1:5,000	1:5,000	1:2,500
Resolution (pixel)	2.5 m	0.5 m	0.5 m	0.25 m
Working scale	1:3,000	1:1,500	1:1,500	1:1,000
Categories	24	61	241	241

Table 3.1: Features of the LCLU (land cover and land use maps of Catalonia) for each edition used for the MAB region

The average slope of the basin has been produced using the Digital Elevation Map provided by the Spanish National Geographic Institute (*Instituto Geográfico Nacional*, IGN, 2018) and doing a subsequent treatment with Geographical Information Systems tools (ArcGIS and QGIS).

3.2.4   Damage flood data

Flood damage data were obtained from the insurance compensation due to floods paid by the Spanish Insurance Compensation Consortium (*Consorcio de Compensación de Seguros*, CCS). The CCS compensates for damage caused to people and property by floods and other adverse weather events covered by an insurance policy. These data are provided at postcode level and with a daily temporal resolution. The CCS database includes around 58,000 flood claims paid recorded in Catalonia and over 100,000 in the Valencian Community for the 1996-2015 period (no previous information is available with this level of detail).

In order to be able to compare these data with other variables, we aggregated the damage in each postcode to the municipality level and then calculated the total amount paid per flood event and basin affected. This process was carried out taking into account the claims made for the days on which the event occurred (according to INUNGAMA and FLOODHYMEX databases), and the following seven days after the event took place. We used this 7-day window as this is the period of time that the CCS allows insurance claims to be made. When the time difference between two events is less than 7 days, damages are associated with the first event, if the date of the claim was before the first day of the second event. Finally, damage data were

adjusted to 2015 values, following the methodology defined by the Spanish National Statistics Institute (INE, 2018), in the same way that was done in the case of the GDP (Section 3.2.3).

In addition to insurance data, the INUNGAMA and FLOODHYMEX databases, described in Section 3.2.1, also contain a qualitative information on the impacts that each flood event has produced as well as a categorisation of these according to various impact indicators (Barriendos et al., 2003; Llasat et al., 2005; Barrera et al., 2006; Llasat et al., 2014a). This methodology for classifying flood events based on the impacts is explained in more detail in Chapter 4 and in Cortès et al. (2017) (see Appendix, Section B).

3.2.5   Climate change projections data

Daily precipitation data for seven climate projections have been obtained from an ensemble of simulations developed within the EURO-CORDEX project (Jacob et al., 2014), which covers the whole Europe with a spatial resolution of 0.11 degrees in latitude and longitude (around 12 km). These are the models (see Table 3.2) that had the necessary variables at the moment of the design of our study, and they have been extensively validated in previous studies (see, e.g., Jacob et al., 2014; Alfieri et al., 2018) and the ones used by the Joint Research Centre from the European Commission (e.g. Alfieri et al., 2015b). The Representative Concentration Pathway 8.5 (RCP8.5) from the Intergovernmental Panel on Climate Change (Pachauri et al., 2014) is the scenario used from 2006 to 2100. For the historical simulations (or reference period) the 1976-2005 period has been used. Chapter 7 describes in more detail the data and the methodology used.

Model	Institute	GCM	RCM	Authors (examples of application)
1	KNMI	EC-EARTH	RACMO22E	Cardell et al. (2018); Alfieri et al. (2015b)
2	SMHI	HadGEM2-ES	RCA4	Cardell et al. (2018); Alfieri et al. (2015b)
3	SMHI	EC-EARTH	RCA4	Cardell et al. (2018); Alfieri et al. (2015b)
4	MPI-CSC	MPI-ESM-LR	REMO2009	Brönnimann et al. (2018); Alfieri et al. (2015b)
5	CLMcom	MPI-ESM-LR	CCLM4-8-17	Brönnimann et al. (2018); Alfieri et al. (2015b)
6	SMHI	MPI-ESM-LR	RCA4	Cardell et al. (2018); Alfieri et al. (2015b)
7	CLMcom	EC-EARTH	CCLM4-8-17	Cardell et al. (2018); Alfieri et al. (2015b)

Table 3.2: EURO-CORDEX climate models used in this study and their characteristics

3.2.6   Population projections data

In order to account for vulnerability and exposure in future flood risk analysis, data of population projections are required. These data, together with future precipitation projections data, are used to estimate the future probability of flood damage in Chapter 8. The five Shared Socioeconomic Pathways (SSP) have been applied for the estimation of the population change in the future. The SSP projections (Riahi et al., 2017) have been developed by the research community to facilitate integrated assessments of climate impacts, vulnerabilities, adaptation and mitigation. These socioeconomic pathways include projections for population, urbanisation and GDP at global and national scales. In order to obtain this information in the spatial

resolution required for the study (basin level), the 2UP (Towards an Urban Preview) model, developed by the Netherlands Environmental Assessment Agency (PBL, abbreviation in Dutch), has been used. The core of the 2UP model and its primary objective is to disaggregate the scenario-based projected national-level urban population to 30 arcseconds (approximately 1 km near the earth's equator) and simulate urban expansion for 194 countries and territories. This high spatial resolution grid has been used to calculate the future total population in each basin of the regions of study of the thesis and for the different SSP's. Figure 3.7 shows these data aggregated at regional scale for both areas of study. Further details about the treatment carried out with the population projections is explained in Chapter 8.
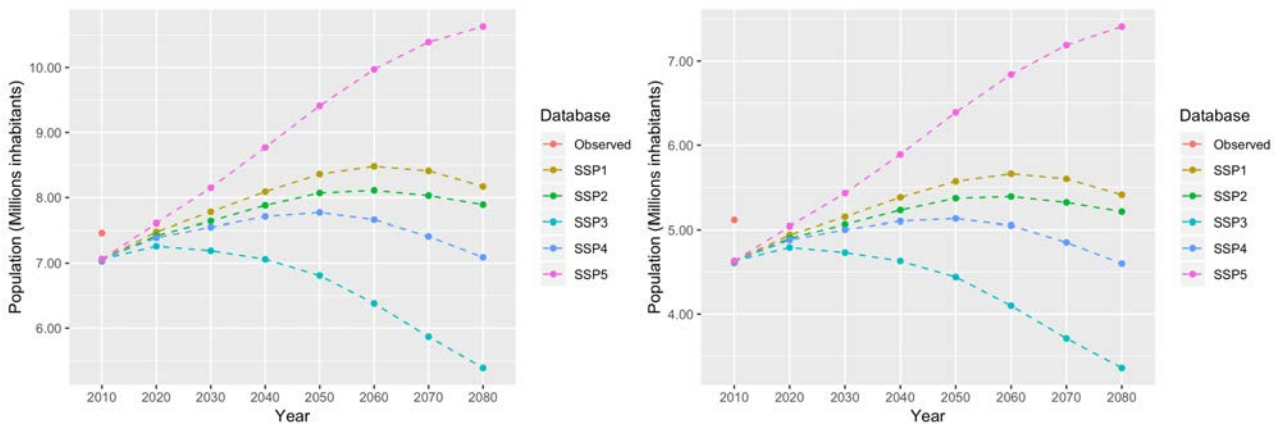
Figure 3.7: Population projections for the whole regions of Catalonia (left) and Valencian Community (right) using the 2UP model and the 5 SSP scenarios. The red point (observed) indicates the total population of each region for the 2010 year. The method used to correct the differences in the population of the year 2010 between observations and projections is explained in Chapter 8

Chapter 4

Flood risk analysis at local level: the case of the Metropolitan Area of Barcelona

Abstract

In this chapter[1], the relationships between flood damages and their causes in the Metropolitan Area of Barcelona is analysed. This region is affected by an average of more than three flood events per year, some of them with catastrophic effects. Most floods that have affected the region of study are surface water floods, which are produced by short, local and heavy precipitation events. Therefore, it is expected that precipitation will be the main contributing factor in the damages produced by these events. For this reason, different statistical models have been developed in order to study the relationship between precipitation and flood damage. Variables related to the vulnerability and exposure of the studied area have been taken into account. The results confirm the hypothesis that precipitation is a key factor in explaining the damage caused by flood events in regions in which surface water floods are the main type of flood.

4.1 Introduction

More than 250 events causing floods, flash floods and urban floods were recorded in Catalonia (north-east Spain) between 1981 and 2015 (Cortès et al., 2017). The coastal zone has the highest number of episodes (70 %) caused by highly localised convective rainfall events (Llasat et al., 2016b; Gascón et al., 2016). Approximately one-third of the episodes affected the regions of Maresme, Barcelonès and Baix Llobregat, which belong, totally or partially, to the Metropolitan Area of Barcelona (MAB). This is an area with significant exposure and vulnerability due to the high population density and concentration of infrastructures (Llasat et al., 2014a), as has been shown in Chapter 3. The problem is expected to worsen, considering that 70 % of the population will be concentrated in coastal cities by 2050, according to Benoit and Comeau (2005). In other words, the MAB constitutes a good example of a Mediterranean coastal

---

[1]This Chapter has been partially published in Cortès et al. (2017)

region, with significant urbanisation of flood-prone areas and a high population density in an area crossed by numerous streams.

Several studies have analysed extreme climate and weather events affecting the region of Barcelona (Turco et al., 2014; Llasat et al., 2014b) and the evolution of floods in Catalonia, also considering the evolution of floods over the last six centuries (Barrera-Escoda and Llasat Botija, 2015) and over the recent period of 1981-2010 (Llasat et al., 2014a, 2016b). For both periods, the extraordinary flood events (flood classification is explained in Section 4.2.1 of this chapter) show a positive trend, probably linked to land use changes and an increase in assets and dwellings in flood-prone areas, leading to an increased flood risk. However, there is still little known about flood evolution in Mediterranean urban areas, combining drivers and consequences (Faccini et al., 2015). That is, the analysis of flood risk is very complex and needs to be dealt with from a holistic perspective using techniques that take into account all the factors involved, both those related to the dangerous nature of the phenomenon, those related to vulnerability and exposure and those related to the impacts (Llasat et al., 2009; Blöschl et al., 2013; Nakamura and Llasat, 2017).

In this chapter, we study the flood risk in the MAB, by doing an holistic approach and taking into account the different factors related to the hazard, vulnerability and exposure involved, as well as the damages caused. To this end, we analyse the changes in land use, runoff, population and precipitation extremes in the MAB and their potential relationship with floods. Also, we analyse the link between damages and precipitation over 1996-2015 period. To this aim, we have developed and evaluated a methodology to estimate surface water flood damage from heavy precipitation in the MAB. The relationship between precipitation and insurance data has been assessed, using logistic regression models, to ascertain the probability of large monetary damages in relation to heavy precipitation events. To sum up, the results of this study can help better understand flood risk in urban Mediterranean areas by analysing flood causes and impacts, as well as assisting with accurate estimations of flood damage under high levels of rainfall.

4.2   Methods

The available data as well as the description of the region of study are explained in Chapter 3. An extensive and detailed methodology used for this chapter is described below. Part of the methodology will also be applied in the following chapters (Chapter 5 and 6), so it will not be repeated and will always be referred to this section.

4.2.1   Classification of flood events according to their impact

Flood events that have affected the MAB between 1996 and 2015 have been classified according to their impact (Barriendos et al., 2003; Llasat et al., 2005; Barrera et al., 2006; Llasat et al., 2014a; Cortès et al., 2017). In order to be more specific, we have suggested some indicators shown in Table 4.1. This classification allows us to distinguish between three categories: (a)

ordinary flood events (rivers or streams not overflowing; floods in restricted areas; minor damages, damage to hydraulic infrastructure or cars parked in the temporary flow of the torrential channel; flooded car parks, basements or ground floors; disturbances to daily activities); (b) extraordinary flood events (overflowing rivers or streams; some streets or other urban places flooded; damages or partial destruction of structures near the stream or river, damage to street furniture or cars; inconveniences in the daily life of the population); and (c) catastrophic flood events (overflowing riverbanks; extensive flooded areas; total destruction or serious damage to hydraulic infrastructures –e.g. bridges–, buildings, crops, road infrastructures and private assets). As mentioned before, the classification was applied according to the impact (following the criteria described in Table 4.1) in the MAB region exclusively, not for the whole region of Catalonia as is the usual case in the literature.

Indicator	Definition	Catastrophic event	Extraordinary event	Ordinary event
Public buildings	City hall, hospital, school, church, emergency centres, police station, etc.	Total destruction or collapse	Partial destruction or structural damage	Flooded, habitable
Private houses	Houses with one or more floors, basements, etc.	Total destruction or collapse	Partial destruction or structural damage	Flooded, habitable
Bridges	Bridges, footbridges	Destroyed, unusable	Structural damage, unusable bridges or damage to footbridges	Usable
Hydraulic infrastructures	Mills, irrigation channels	Destroyed	Medium damage	Minor damage
Roads	Railway, highway, state road, country road, regional road, municipal road	Partially destroyed, one or more stretches of the road damaged	Flooded, closed for > 12 h	Flooded, closed between 0 and 12 h or not closed
Services	Gas, electricity, telephone lines, water	Destruction and/or closure of infrastructures for > 24 h	Closed between 6 and 24 h	Closed for < 6 h
Productive activities	Industry, agriculture and livestock, commerce, touristic infrastructures	Interruption of production and loss of the production system	Interruption of production and loss of products	Loss of products
Cars	Cars washed away or damaged by water	20 or more washed away	Between 5 and 19 washed away	Between 1 and 4 damaged and/or washed away
Deaths	No. of people dead	10 or more	Between 5 and 9	Between 1 and 4

Table 4.1: Indicators to determine the impact of each flood event

4.2.2 Precipitation, runoff and flood damage correlations

Information regarding the economic damage caused by floods was provided by the state insurance company *Consorcio de Compensacion de Seguros* or CCS. These data have the advantage that is possible to transform them to the spatial resolution of municipal level, as has been explained in Chapter 3, spanning the period from 1996 to 2015. We considered the compensation paid by the CCS during the flooding episodes, as well as during the following 7 days after their

conclusion (see further information in Section 3.2.4, Chapter 3). The variables used were: total damages, the ratio of total damages/population density and the ratio between total damages and population. The temporal evolution of the compensation paid by CCS was also analysed, along with the correlation between damages/precipitation and damages/runoff for 13 specific cases.

For the precipitation data, 30-min rainfall stations from the SMC and the daily precipitation stations from the AEMET have been used (see Chapter 3 for further details).

For estimating the runoff, 4 different editions of Land Cover and Land Use maps (LCLU) for Catalonia have been used (see Table 3.1 of Chapter 3). In order to obtain the average runoff value for each municipality of the MAB region, the available maps have been homogenised following the characteristics of the first edition of the Land Cover and Land Use map (LCLU-I). The oldest edition of the LCLU was based on American flight photographs made in 1956 over the Barcelona Province. It was recently processed and for this reason includes 241 categories, as many as the later editions. LCLU-1956, LCLU-III and LCLU-IV use a hierarchical legend with 5 levels of categories. In order to compare the different time editions and analyse the evolution of land use, all maps have been homogenised in a common resolution of 2.5 m x 2.5 m and have been classified using 24 categories as used in LCLU-I. Taking into account the heterogeneity of the region and its hydraulic features, a streamlined method has been applied to estimate the runoff, based on the application of the runoff coefficients proposed by Chow et al. (1988) for different return periods. Taking into account that the average slope in the MAB is between 2 and 7 %, we considered that runoff coefficients only depend on the return period (Table 4.2). The 24 initial categories of the LCLU have been merged into 7 categories according to land permeability, in order to avoid the dispersal that excess categories would cause.

Permeability categories	Return Period							LCLU categories
	2	5	10	25	50	100	500	
Lakes	0	0	0	0	0	0	0	Wetlands, beaches, water, canals and ponds, urban ponds
High perviousness	0.31	0.34	0.36	0.40	0.43	0.47	0.57	Forest (dense, not dense, riverside)
Moderate perviousness	0.33	0.36	0.38	0.42	0.45	0.49	0.58	Meadows, bushes
Low perviousness	0.35	0.38	0.41	0.44	0.48	0.51	0.60	Crops, populus and platanus plantations
Low imperviousness	0.35	0.39	0.41	0.45	0.48	0.52	0.58	Recent reforestation, burned areas, forest tracks and firebreaks
Moderate imperviousness	0.40	0.43	0.45	0.49	0.52	0.55	0.62	Vacant lots, sport and recreational areas
High imperviousness	0.74	0.78	0.82	0.87	0.91	0.96	1.00	Scree slopes, snowdrifts and glaciers, urban areas, roads and train tracks, mines

Table 4.2: Runoff coefficients for each category and return period (Chow et al., 1988)

Each layer has been classified in a category with an assigned runoff coefficient. All this information has been aggregated on a municipal scale as the average of all the pixels. Consequently, each municipality is characterised by the previously selected return periods and a runoff coefficient, calculated using the average of all the pixels included in it. Although it only

provides an approximate runoff, this approach is typical used in urban public works and helps improve estimates for running or accumulated water that can affect exposed assets and the population in general. The advantage is that it can be used in regional analysis.

The return periods for rainfall have also been obtained on a municipal scale from the maps of maximum daily precipitation expected in Catalonia for different return periods (Casas-Castillo et al., 2005).

In this section (results in Section 4.3.2), we analyse the possible correlation between flood damage, precipitation and runoff for the extraordinary and catastrophic flood episodes that affected the MAB between 1996 and 2015. We selected 10 extraordinary and 3 catastrophic flood episodes, considering their individual impact in each one of the 36 municipalities. That means, our minimum unit of study in this section is the municipality. Table 4.3 shows the episodes studied along with their start/end dates and their category (according to their impact).

Start date	End date	Event category
02/12/1998	02/12/1998	Extraordinary
03/09/1999	04/09/1999	Extraordinary
13/09/1999	15/09/1999	Extraordinary
10/06/2000	12/06/2000	Extraordinary
31/07/2002	02/08/2002	Extraordinary
10/08/2002	11/08/2002	Extraordinary
12/09/2002	14/09/2002	Extraordinary
08/10/2002	11/10/2002	Catastrophic
05/09/2005	09/09/2005	Catastrophic
12/09/2006	15/09/2006	Catastrophic
22/10/2009	23/10/2009	Extraordinary
30/07/2011	31/07/2011	Extraordinary
28/09/2014	01/10/2014	Extraordinary

Table 4.3: Flood events recorded in the MAB when CCS data are available (1996-2015)

For each episode, the average precipitation values on a municipal level were obtained through ordinary Kriging with ArcGIS. In order to obtain the daily runoff values, the runoff coefficient on a municipal level (the average from the runoff categories for the different pixels) was multiplied by the accumulated daily precipitation. We consider the following variables: precipitation over 24 h, accumulated precipitation for the entire duration of the episode, runoff, total damage, damage relative to population density and damage relative to total population of the municipality. Correlation with damages was carried out for all the events, for the events in which precipitation in 24 h exceeded the return period of 2 years and for events in which accumulated precipitation surpassed 100 mm. The correlation analysis was achieved using the Spearman test.

Finally, in the last part of this section, we also analyse the distribution of the precipitation accumulated in 30-min, 24 h and for the full event, as well as the damage produced, according to the flood impact category. The results are discussed in Section 4.3.2.

4.2.3 Simple logistic regression model

In the case of the simple logistic regression model, the minimal unit of study is the entire MAB region, which means each flood event corresponds to a single flood case. After gathering together a list of all the floods that affected MAB between 1996 and 2015, we filtered them based on specific rainfall thresholds (P_0). A previous study shows that with precipitation over 20 mm 30 min^{-1}, extraordinary and catastrophic flood events can occur (Cortès et al., 2017) in the region. Since the sample size is small, a 10 mm threshold was also used. In the case of the damages, we considered three categories: (i) total damage (D), (ii) Damage Per Capita (DPC) and (iii) Damage Per unit of Wealth (DPW), that means damage per unit of GDP. This allows the estimation of the impact of socioeconomic factors on damage, while taking into account population and wealth (Zhou et al., 2017).

Figure 4.1 shows the relationship between total damages (D) and precipitation (24 h and 30-min) in the MAB. Even if a linear regression indicates a significant link (p value $<$ 0.01), the explanatory power of the model for D and 24 h precipitation is rather low ($r^2 = 0.22$). Better results are obtained for 30 min precipitation ($r^2 = 0.54$), underlying the importance of considering finer temporal resolutions of precipitation data in the case of urban zones.

The large spread of Fig. 4.1 indicates that modelling insurance compensation is a complex issue, due to the limitations in observational data and the concurrence of a variety of relevant factors. For instance, monetary data could be affected by limitations, as the value of the assets exposed and insurance coverage may change over time (Barredo et al., 2012). Unfortunately, exact data on the value and location of assets exposed were not available at the time of analysis.
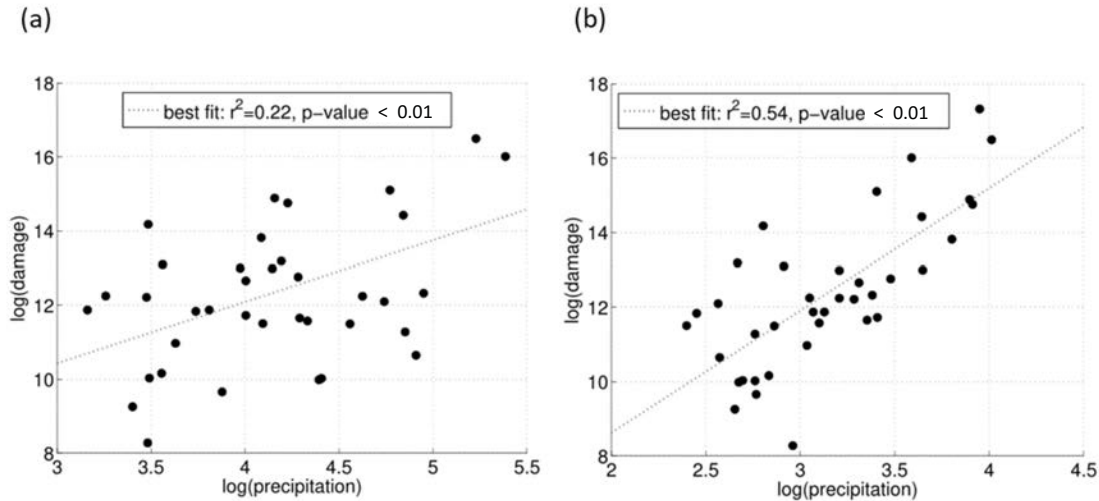
Figure 4.1: Scatter plot (a) damages (D) versus 24 h precipitation and (b) damages (D) versus 30 min precipitation in units of log(mm) for flood events recorded in the MAB between 1996 and 2015. Each point represents the total insurance compensation paid and the maximum 24 h precipitation and 30 min for each flood event in the MAB. The dashed line indicates the fit based on a linear regression model

However, the significant correlation between insurance compensation and precipitation suggests that rainfall data can be used to extract information on damage in the MAB. To do this, we applied a logistic regression model to gauge the probability of large damaging events occurring given a certain precipitation amount (an approach that is frequently used for this kind of modelling study: Kim et al., 2012; Wobus et al., 2014). That is, our aim is not to estimate the precise amount of the monetary compensation, but to estimate when a 'large' damaging event will occur given a certain precipitation amount. Since there is not a standard definition of a large damaging event, we tested several cases: insurance compensation exceeding the 50th, 60th, 70th, 80th and 90th percentile of the total sample. The response variable has been transformed in binary variable, taking the value "1" when the specific damage percentile is exceeded and "0" if it is not. This methodology is repeated for both precipitation thresholds (10 and 20 mm in 30 min) and for the three damage indicators (D, DPC, DPW) for the whole MAB, meaning we made a total of 30 models. Finally, the logistic model is calculated following Eq. 5.1:

$$\log(\frac{\pi}{1-\pi}) = \beta_0 + \beta_1 P \tag{4.1}$$

where π is the response variable (i.e. the probability above a certain percentile) and P is the predictor (precipitation in 30 min in our case). The value of the β coefficient is determined using Generalized Linear Models (GLMs). The Wald χ^2 statistic is used to assess the statistical significance of individual regression coefficients (Harrell Jr, 2015).

4.2.4   Validation method for the logistic model

The Relative Operating Characteristic (ROC) diagram was used as logistic prediction diagnostic, which shows the hit rate (i.e. the relative number of times a forecasted event actually occurred) against the false alarm rate (i.e. the relative number of times an event had been forecasted but did not actually happen) for different potential decision thresholds (Mason and Graham, 2002). Thus, for each insurance compensation percentile and for each precipitation threshold, the forecast probabilities for that event was first calculated, and then grouped the probability forecasts into batches (here 100 with a width of 0.01) to count the observed occurrences/non-occurrences. That is, the observed and forecasted series, expressed as continuous amounts, were converted into exceedance categories (yes/no statements indicating whether the data equal or exceed a selected probability). Then, the resulting elements were plotted on a standard contingency table (see Table 4.4). The ROC diagram shows the hit rate (H) against the false alarm rate (F). These indices are defined as

$$H = \frac{a}{a+c}; 0 \leq H \leq 1 \tag{4.2}$$

$$F = \frac{b}{b+d}; 0 \leq F \leq 1 \tag{4.3}$$

| | Observed | |
	Yes	No
Forecast Yes	a	b
No	c	d

Table 4.4: Contingency table to support eq.4.2 and eq.4.3

4.3 Results

4.3.1 Spatial distribution

Flood events in the MAB

A total of 61 flood events were recorded in the Metropolitan Area of Barcelona (Figure 4.2) for the 1996-2015 period, which means an average of more than three events per year. The summer and autumn months have the highest number of flood events, with September having the most (31 %), followed by October (16 %). The municipality of Barcelona recorded a total of 37 events between 1996 and 2015, all due to in situ precipitation and drainage problems in the city (Llasat et al., 2016a).
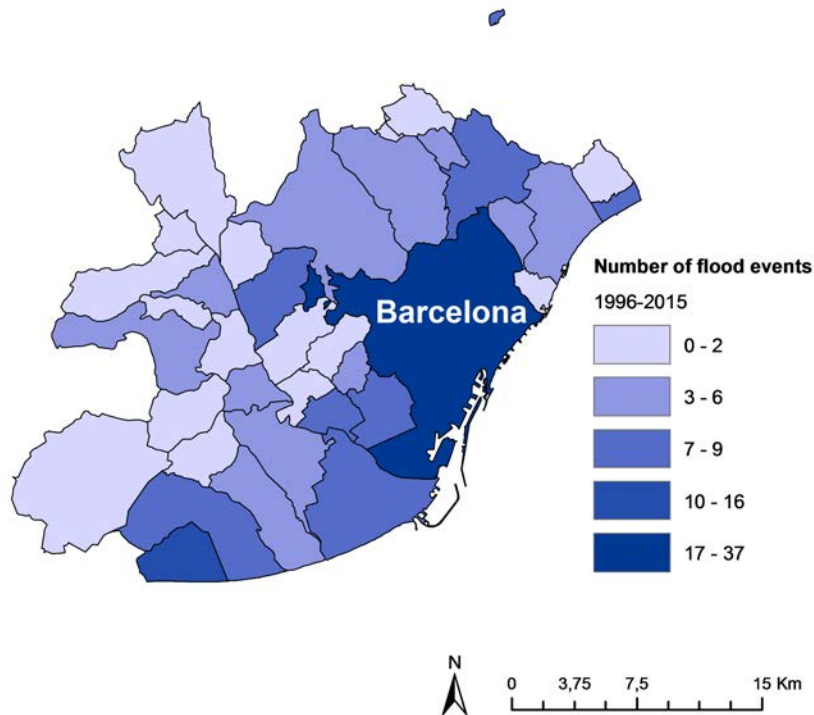
Figure 4.2: Flood events in the MAB municipalities for the period 1996-2015

Precipitation in the MAB

Figure 4.3 shows the average annual rainfall of the AEMET's weather stations used. As can be observed, these values are around 530 and 650 mm per year, with the westernmost station presenting the highest values.
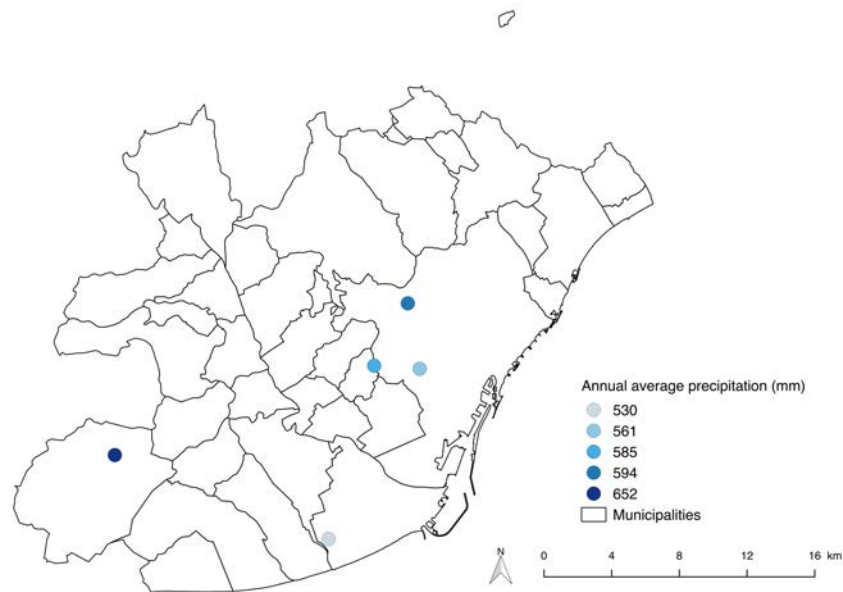
Figure 4.3: Annual average rainfall (mm) of the AEMET stations with more than 90 % valid data over the period 1996-2015. The black lines represent the delimitation of each of the 36 municipalities that constitute the MAB

Insurance compensation paid due to flood events in the MAB

The insurance compensation paid by the CCS for floods amounted to 86.30 M Euro, which represents 20 % of the total compensation paid by the CCS in Catalonia. The city of Barcelona also receives the most compensation for floods (around 24 M Euro).
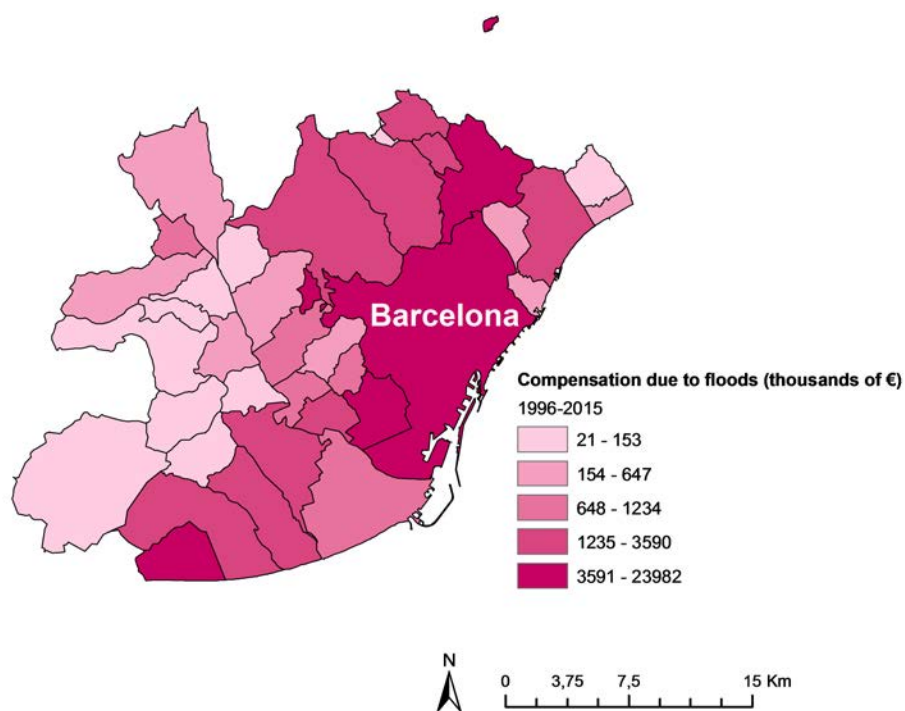
Figure 4.4: Insurance compensation paid by CCS due to flood events at municipal level for the period 1996-2015 (thousand Euro)

4.3.2 Relationship between precipitation and flood damage

Precipitation, runoff and flood damage correlations

In order to estimate the correlations between precipitation, runoff and damages, first of all, we only considered cases that caused catastrophic impacts in the MAB, before looking at all the extraordinary and catastrophic events documented in the region. Table 4.5 summarises the results obtained for catastrophic cases, highlighting the larger correlation values. In all cases, the correlations were significant at 95 % using the Spearman test. As can be observed, correlations between damages and runoff are stronger than the former with precipitation. This result may be explained by the stream's impact in flood damages and suggests the importance of the type of soil cover as a determining factor in the analysis of flood risk.

	Total damage (M Euro)	Damage/population density (Euro/inhab km^2)	Damage/population (Euro/inhab)
Precipitation 24 h (mm)	0.19**	0.22**	**0.26****
Precipitation 24 h (mm) with T>2 years	0.33**	0.36**	**0.46****
Accumulated precipitation	0.23**	0.23**	**0.29****
Accumulated precipitation >100 mm (mm)	0.35**	0.40**	**0.50****
Runoff 24 h (mm)	0.29*	**0.32****	0.27**
Runoff 24 h (mm) for precipitation in 24 h with T>2 years	**0.57***	0.38**	0.50**
Estimated runoff (mm) for accumulated precipitation	**0.41***	0.27**	0.35**
Estimated runoff (mm) for accumulated precipitation>100 mm	**0.60***	0.44**	0.55**

Table 4.5: Correlation values between damage (CCS), precipitation and runoff for catastrophic flood events for the 1996-2015 period (with available CCS data). The best results are in bold. *p value <0.1; **p value <0.05

Figure 4.5 shows the best correlation results and the histograms for each variable (precipitation and accumulated runoff) for all of the flood cases (extraordinary and catastrophic) when the accumulated total rainfall was greater than 100 mm. As in catastrophic episodes, precipitation is more closely related (a correlation of 0.51) to the density of damages (damages per inhabitant), whereas runoff relates slightly better to total damage (0.60). This behaviour might be a consequence of the fact that the runoff already takes into account land use through the runoff coefficient. A larger population is associated with a larger impermeable surface and thus with a higher mean runoff value. Nevertheless, it must be taken into account that the drainage network is not considered.
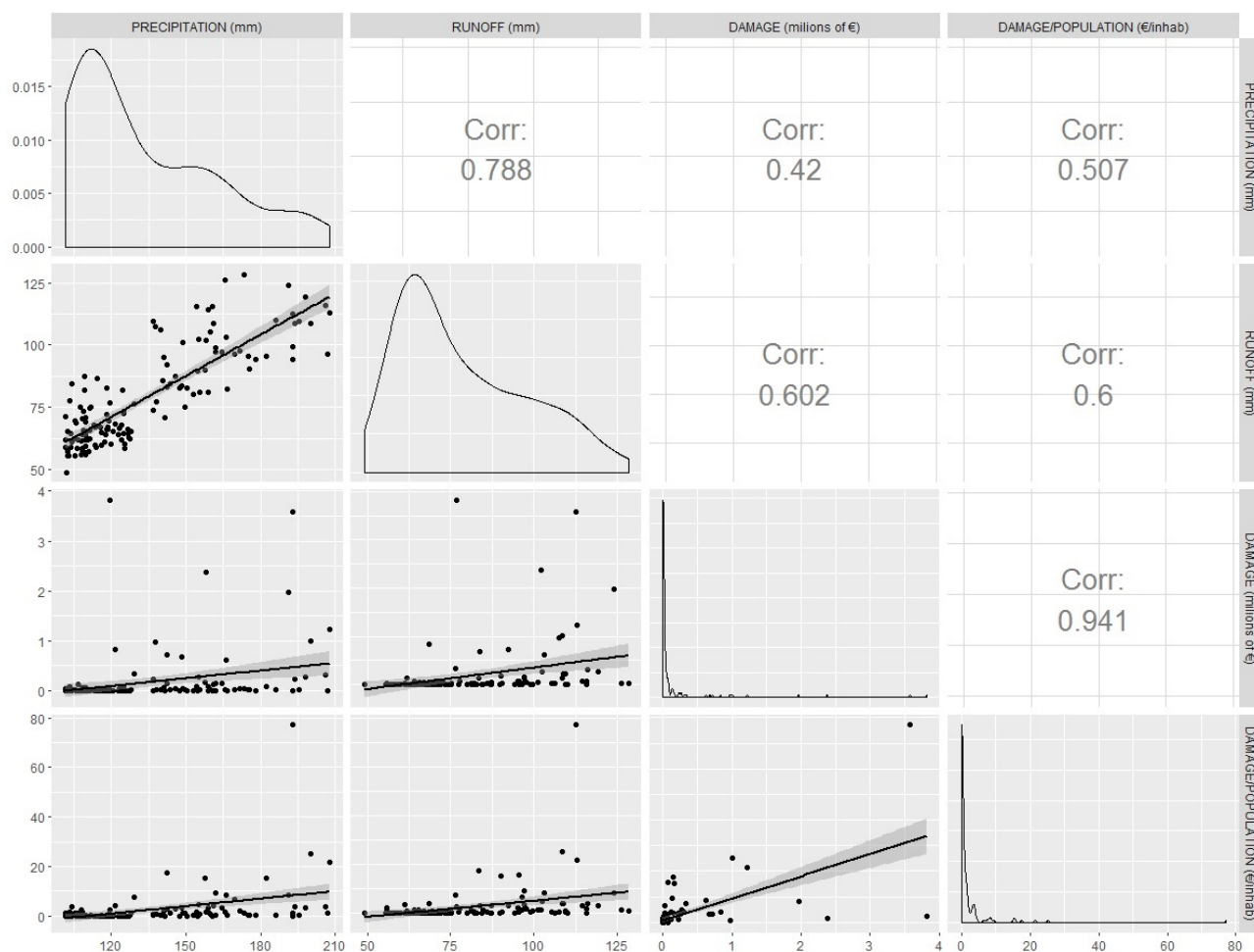
Figure 4.5: Correlation results for extraordinary and catastrophic flood events where the total accumulated precipitation recorded was more than 100 mm, over the 1996-2015 period (for which CCS data are available)

Finally, we analysed the distribution of precipitation over 24-h, 30-min rainfall intensity, accumulated precipitation and damage according to the flood category (1: extraordinary, 2: catastrophic) for the full event (Fig. 4.6; Table 4.6). As could be expected, accumulated precipitation and damages are higher for catastrophic floods than for extraordinary ones. The extraordinary episodes have a mean maximum 24-h precipitation of 68 mm, whereas catastrophic episodes have a mean maximum of 118 mm. Furthermore, 75 % of the former have a maximum 24-h value higher than 55 mm. The maximum precipitation intensity values of the two categories are very high, at around 29 and 50 mm in 30 min for extraordinary and catastrophic episodes, respectively. These results confirm that the most common type of floods in this region, flash floods, are consequence of intense and short precipitation events (Llasat et al., 2016b).
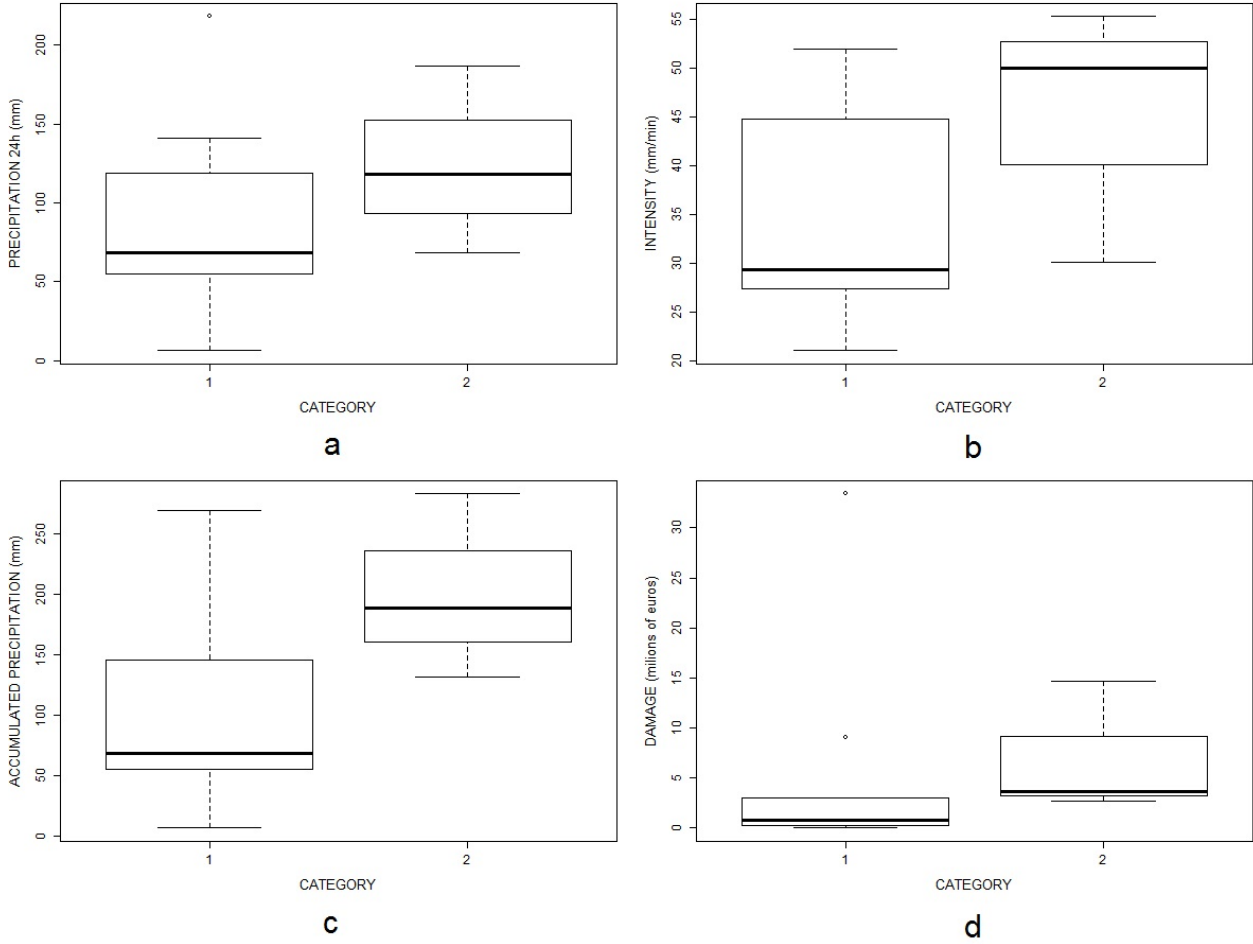
Figure 4.6: Boxplots showing the distribution according to the flood category (1 extraordinary, 2 catastrophic): precipitation in 24 h (a); precipitation in 30 min (intensity) (b); accumulated precipitation (c); and damage (d)

	Extraordinary			Catastrophic		
	Q1	Q2	Q3	Q1	Q2	Q3
Precipitation in 24 h (mm)	56	68	115	93	118	152
Intensity (mm min^{-1})	28	29	43	40	50	53
Accumulated precipitation (mm)	56	68	139	160	189	236
Damage (M Euro)	0.21	0.71	2.67	3.14	3.63	9.12

Table 4.6: Quartiles (Q1 = 25th percentile; Q2 = median; Q3 = 75th percentile) distribution for precipitation and damage variables according to flood category

The greatest differences in precipitation come from the total amount per episode, where the median for catastrophic floods was more than 175 % larger than for extraordinary events. In fact, the latter have mean cumulative precipitation values equal to those of 24-h precipitation, indicating that the majority of episodes that produce extraordinary impacts have a duration of 1 day or less, as proposed in Llasat et al. (2016a). In terms of damages, catastrophic events produce median losses in the MAB that exceed 3 M Euro per episode, while in the case of extraordinary episodes these values are generally below 1 M Euro. This result is interesting because it allows to associate an objective criteria based on total insured losses paid by the CCS to distinguish between extraordinary and catastrophic events.

Simple logistic regression in the MAB

In order to estimate when a 'large' damaging event will occur with a given precipitation amount, a logistic regression model was used. Figure 4.7 shows a logistic regression example for the events that affected the MAB and exceeded a maximum precipitation of 10 mm in 30 min (P^0=10 mm 30 min^{-1}). The model is capable of simulating the probability of total damage (D) above and below the 70th percentile as a function of 30 min precipitation (this percentile corresponds to 0.44 M Euro for the 1996-2015 series; see Table A.1, Appendix section). This result is consistent with the hypothesis that precipitation could be considered a good indicator of flood risk.
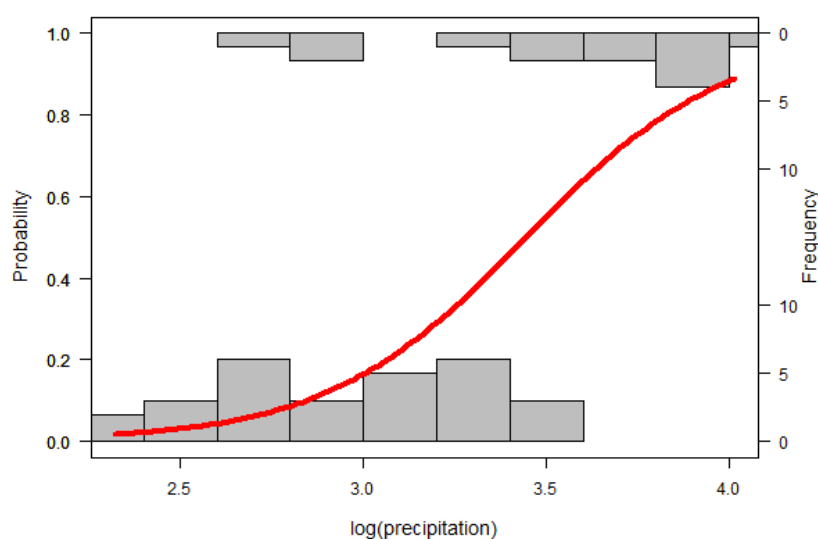
Figure 4.7: Example of a logistic regression result used to model damages (D) above the 70th percentile as a function of 30 min precipitation in units of log (mm) for the MAB. The red line indicates the best estimate and the grey bars show the frequency of the events that are above (top) and below (bottom) the 70th percentile. (P_0=10 mm 30 min^{-1})

As could be expected, this probability increases with precipitation. The regression equation of this example follows the formula 4.4:

$$\log(\frac{\pi}{1-\pi}) = -12.54 + 3.64P \tag{4.4}$$

It is important to assess whether this model can be used to separate positive and negative anomalies. The models presented in this work are not deterministic and users need to take into account the uncertainty of the forecast expressed by these probabilities. For example, users could decide to take action when a 10 % probability of an above-70th-percentile event is forecast. In this case most of the observed events are forecast, that is, the hit rate (i.e. the relative number of times a simulation event actually occurred) is close to 1, but this also implies a higher false alarm rate (i.e. the relative number of times an event had been simulated to occur but did not actually happen). On the other hand, if a higher threshold is used, we can

reduce the number of false alarms, but at the expense of a greater number of missed events. The choice of the decision threshold is a function both of the skill of the forecast and the cost / loss ratio of the user. In any case, in a forecasting system affected by uncertainties, missed events can be reduced only by increasing false alarms and vice versa. In order to validate the model, we considered the ROC diagram (see Fig. 4.8).

Figure 4.8: Relative operating characteristic (ROC) diagram for predictions for damage indicator D above the 70th percentile for the MAB using the logistic regression of Eq. 4.4. Each value of the ROC curve indicates a set of probability forecasts by stepping a decision threshold with 1 % probability through the modelling results. The numbers inside the plot are the ROC area (RA) and the best threshold (BT), here defined as the threshold that maximises the difference between the hit rate (H) and the false alarm rate (F). (P_0=10 mm 30 min^{-1})

The area under the ROC curve (RA) is a useful measure for summarising the skill of a model. RA ranges from 0, for a forecast with no hit and only false alarms, to 1, indicating a perfect forecast. Models with an RA above 0.5 have more skill than random forecasts. Figure 4.8 shows that our model has skill: the ROC curve is well above the identity line, with an RA of 0.83. The Best Threshold (BT) in this illustrative example is 0.43. This means that if we want to maximise the H-F difference (but please note that users could define other best thresholds according to their cost / loss ratio), an above 70th percentile damaging event is to be expected when our model predicts a probability higher than 0.43, resulting in H = 0.77 (this means that 77 out of 100 events are correctly modelled) and F = 0.14 (this means that 14 out of 100 events were modelled as an 'event' when it did not actually happened). For example, in this case (BT = 0.43) a precipitation amount higher than 30 mm in 30 min is needed to expect a damaging event above the 70th percentile for damage indicator D (0.44 M Euro).

Percentile	Damage	β_0	β_1	RA
50	D	-15.43	4.99	0.89
	DPC	-15.43	4.99	0.89
	DPW	-10.77	3.48	0.83
60	D	-14.12	4.34	0.87
	DPC	-12.75	3.81	0.85
	DPW	-13.27	4.02	0.86
70	D	-12.54	3.64	0.83
	DPC	-11.25	3.20	0.81
	DPW	-11.38	3.29	0.81
80	D	-16.06	4.45	0.88
	DPC	-25.19	6.99	0.95
	DPW	-16.06	4.45	0.88
90	D	-22.39	5.89	0.93
	DPC	-18.47	4.71	0.91
	DPW	-18.47	4.71	0.91

Table 4.7: Parameters of the logistic model and RA values for the MAB level with 10 mm 30 min^{-1} maximum precipitation threshold. All the results are significant (p value < 0.05). See Table A.1 of the Appendix section for the damage thresholds definition. Number of flood cases: 38

Table 4.7 summarises the model parameters and performance considering all the percentiles and the three categories of damage used for a precipitation threshold of 10 mm 30 min^{-1}. In each case, precipitation is a significant predictor (p value < 0.05) and the models have skill and significant RA values (the significance is estimated using a Mann-Whitney U test; Mason and Graham, 2002). Similar results were obtained for the three damage categories.

Figure 4.9 shows the same example (70th percentile of D damage category) as the Figure 4.7 but using the precipitation threshold of 20 mm 30 min^{-1}. In this example, the regression equation follows the formula 4.5:

$$\log(\frac{\pi}{1 - \pi}) = -29.55 + 8.11P \tag{4.5}$$

As in the previous example the probability of a damaging event (70th) increases with 30 min precipitation. In this case the model seems to perform better than the sample using 10 mm 30 min^{-1} precipitation threshold. However, not all the models are statistically significant (see Table 4.8).

Figure 4.10 shows the ROC diagram for predictions of total damages (D) above the 70th percentile for the MAB, using a precipitation threshold of 20 mm 30 min^{-1}. The total RA (0.92) shows that our model for the MAB has skill. In this case, we would obtain the biggest difference between the hit and false rates when our model predicts a probability higher than 0.30. That is, the best threshold is 0.30, with 86 % of the events well predicted (H = 0.86) and 12 % being false alarms events (F = 0.12). In this example, a precipitation amount higher than 35 mm 30 min^{-1} is needed to expect a damaging event above the 70th percentile for damage indicator D (1.82 M Euro; see Table A.1, Appendix section).
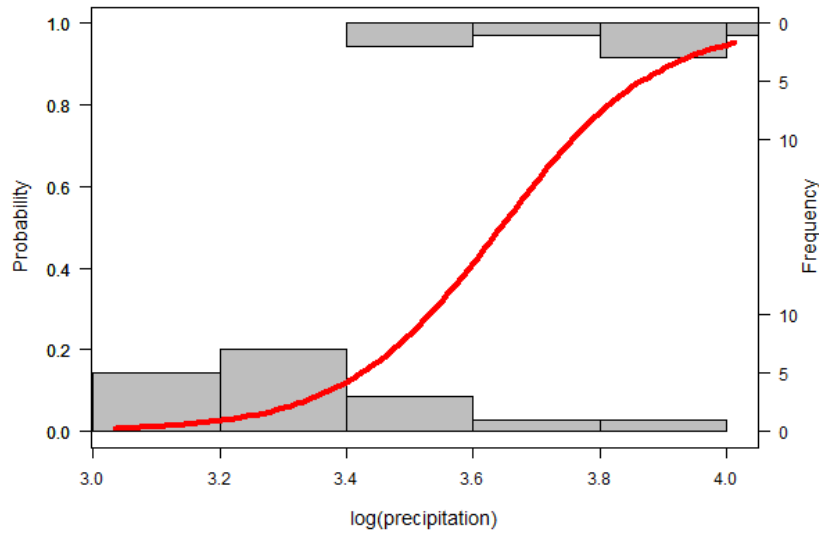
Figure 4.9: Example of a logistic regression result used to model damages (D) above the 70th percentile as a function of 30 min precipitation in units of log (mm) for the MAB. The red line indicates the best estimate and the grey bars show the frequency of the events that are above (top) and below (bottom) the 70th percentile. (P_0=20 mm 30 min^{-1})
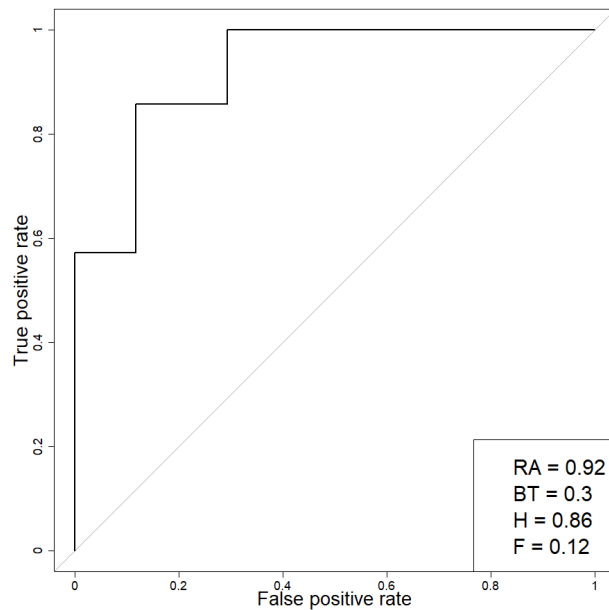
Figure 4.10: Relative operating characteristic (ROC) diagram for predictions for damage indicator D above the 70th percentile for the MAB using the logistic regression of Eq. 4.5. Each value of the ROC curve indicates a set of probability forecasts by stepping a decision threshold with 1 % probability through the modelling results. The numbers inside the plot are the ROC area (RA) and the best threshold (BT), here defined as the threshold that maximises the difference between the hit rate (H) and the false alarm rate (F). (P_0=20 mm 30 min^{-1})

Table 4.8 summarises the model parameters and performance considering all the percentiles and the three categories of damage used for a precipitation threshold of 20 mm 30 min^{-1}. In this case, precipitation is not a significant predictor (p value $<$ 0.05) in all the cases, possibly due to the reduced sample size (21 flood cases).

52

Percentile	Damage	β_0	β_1	RA
50	D	-36.11	10.59	0.92
	DPC	-36.11	10.59	0.92
	DPW	-31.20	9.14	0.89
60	D	-55.58	16.02	0.95
	DPC	-35.08	9.93	0.92
	DPW	-30.72	8.79	0.90
70	D	-29.55	8.11	0.92
	DPC	-22.43	6.11	0.87
	DPW	-29.55	8.11	0.92
80	D	-21.66	5.70	0.87
	DPC	-21.66	5.70	0.87
	DPW	-21.66	5.70	0.87
90	D	-27.17	6.92*	0.92
	DPC	-27.17	6.92*	0.92
	DPW	-27.17	6.92*	0.92

Table 4.8: Parameters of the logistic model and RA values for the MAB level with 20 mm 30 min^{-1} maximum precipitation threshold. * Indicates no significance (p value > 0.05). See Table A.1 of the Appendix section for the damage thresholds definition. Number of flood cases: 21

4.4 Conclusions

The Metropolitan Area of Barcelona (MAB) has been affected by 61 flood events between 1996 and 2015, which translates to an average of more than three episodes of flooding per year, some of them with catastrophic effects. As a result of these events, 3 people lost their lives in this region and the compensation paid by the CCS exceeded 86 M Euro during this period. Consequently, there is no doubt that flooding is one of the most important natural hazards affecting Barcelona and its metropolitan area. The majority of the damage caused by flood events is due to local events, with intense and short-lived rainfall rather than river overflow (Llasat et al., 2014a; Cortès et al., 2018). Therefore, it is assumed that precipitation is the main contributing factor for damage caused by this type of events. To corroborate this hypothesis, two main analysis have been carried out.

First of all, a correlation analysis at municipality level has been done. The results show a value of 0.23 between accumulated precipitation and total damages. However, higher significant correlations were found between precipitation and the density of damages (damages per population adjusted to each year). The correlation surpasses 0.5 when considering events that recorded more than 100 mm in 24 h. Particularly, the correlation between estimated average runoff and total damages in the event, at municipal scale, is 0.60. This study also suggested a classification of flood events in basis of different impact indicators: an extraordinary flood event would be characterised by an average daily precipitation of around 68 mm, a maximum intensity of 30 mm in 30 min and 1 M Euro in insured damages. These values would correspond to a catastrophic flood of 118.50 mm and 3 M Euro, respectively.

On the other hand, the relationship between precipitation and compensation paid by insurance companies for the entire event was studied using simple logistic regression models. To take into account the differences in vulnerability and exposure in the territory, we considered three

types of damage: total damage, damage per capita (divided by the population) and damage per unit of GDP. Linear regression has shown that 30 min precipitation is linked more closely to damages than 24 h precipitation, and the results of the logistic regression have shown that the model with 30 min precipitation has a good skill with RA values higher than 0.8 in all cases. Therefore, we have been able to confirm that 30 min rainfall is a better predictor of the probability of large damages than daily rainfall in urban areas, and this result confirms previous studies such as that of Torgersen et al. (2015), who found a significant relationship between insurance data and short-lasting rainfall when studying urban floods in Norway. In addition, Spekkers et al. (2013) showed that high claim numbers associated with private property and content damage were significantly related to maximum rainfall intensity, based on a logistic regression, with rainfall intensity for 10 min to 4 h time windows.

Overall, our results confirm the hypothesis that precipitation is a key factor in explaining the damage caused by flood events in regions in which surface water floods are the main type of flood, as is the case of the Mediterranean region of study. Also our findings align with the results of previous studies (Spekkers et al., 2013; Zhou et al., 2013; Wobus et al., 2014; Torgersen et al., 2015) and further indicate that insurance databases are a promising source for flood damage assessment at local scale (Garrote et al., 2016; Bihan et al., 2017; Zischg et al., 2018; Zhou et al., 2013).

Chapter 5

Application of the simple and multiple logistic regression model to Catalonia

Abstract

The main objective of this chapter[2] is to develop statistical models to estimate the probability of a damaging event in the Catalonia region, based on precipitation as well as considering the exposure and vulnerability of the territory. Two different logistic models were tested. Firstly, simple logistic regression with daily precipitation as the only explanatory variable and three response variables. Secondly, multiple logistic regression with 30-minute precipitation together with the proportion of urban zone and mean slope of the basin as explanatory variables and total damages as the unique response variable. The second model provided better results. Overall, results show that our model is able to simulate the probability of a damaging event as a function of precipitation. In general, highly urbanised and steeper basin will have a higher probability of a damaging event occurrence than a less urbanised and flat one. These results point out the importance of taking into account the exposure and the vulnerability of the territory in flood damage analysis.

5.1 Introduction

Most floods that have affected the region of study, north-east of Spain, are surface water floods that caused catastrophic damage (Llasat et al., 2014a, 2016b; Cortès et al., 2018). The majority of these flood events are caused by intense and short-lived rainfall rather than river overflow (Llasat et al., 2014a).

The objective of this chapter is to estimate the probability that an event producing large damage would occur in the Catalonia region given a particular precipitation amount but also taking into account the exposure and vulnerability of the territory. Therefore, the first novelty of this chapter with respect to the previous one (Chapter 4) is the change in the area of the study, which is 50 times larger than the Metropolitan Area of Barcelona (MAB) along with a

---

[2]The contents of this chapter have been partially published in Cortès et al. (2018)

much more heterogeneous region. For this reason, the river-basin-scale has been chosen for this study in order to divide the territory into different comparable units (see Figure A.1 and Table A.6, Appendix section). Furthermore, apart from the simple logistic model also developed in Chapter 4, multiple logistic regression models have been used, in order to improve the analysis by incorporating new variables in the model that provide information on the exposure and vulnerability of the territory.

In order to do this, and following the scheme of the previous chapter, first the different variables that have been taken into account in the study are represented (Section 5.3.1). Then, the possible relationships between damage caused by flood events and their drivers are analysed using two different methodologies (Section 5.3.2): simple logistic regression and multiple logistic regression. That means, different logistic regression models have been developed to determine when a damaging event will occur (i.e. exceeding different percentiles of damage) in the region of Catalonia. Finally, the Conclusions section summarises the main results obtained in this chapter and the novelties incorporated regarding to the previous one.

5.2 Methods

The main characteristics of the region of study as well as the data sources used in this chapter are explained in Chapter 3. In Section 5.3.1 of the present chapter the main variables used are represented. The river-basin-scale is the spatial resolution selected for studying the relationships between precipitation and flood damages in Catalonia by developing logistic regression models.

In the case of the simple logistic regression model, the precipitation accumulated over 24 h is the single explanatory variable of the model, while three different damage indicators have been used for the response variable: (i) total damages (D), (ii) damage per capita (DPC) and (iii) damage per unit of GDP (DPW). In the case of the multiple logistic regression model, the maximum precipitation recorded in 30 minutes together with the proportion of urban zone and the mean slope of the basin have been used as explanatory variables. The total amount of damage recorded in the basin is the only response variable for this model. Further information about the characteristics of the simple and multiple logistic regression models is described in sections 5.2.1 and 5.2.2, respectively.

5.2.1 Simple logistic regression model

The simple logistic regression model has been developed following the same methodology as in the case of the MAB (Chapter 4), however there are some differences, due mainly to the change of spatial scale, that are explained below.

Because the available data are too sparse to support our statistical assessment on a municipal scale, we assessed the precipitation-compensation link for Catalonia as a whole. That is, we sampled pairs of the response variable (i.e. the compensation series) and the 24 h precipitation per basin recorded, and pooled them into one sample for the entire region (Catalonia) to correlate them. For each event there can be more than one pair of values, depending on the

number of affected catchments. From now on we will use the expression "flood case" for each pair of values corresponding to a basin affected by a flood event.

As in the case of the MAB (Chapter 4) three categories of damages have been considered: (i) total damages (D), (ii) damage per capita (DPC) and (iii) damage per unit of GDP (DPW). After gathering together a list of all the floods that affected Catalonia between 1996 and 2015, we filtered them based on specific rainfall thresholds (P_0). The Social Impact Research Group, created within the framework of the MEDEX project (MEDiterranean EXperiment on cyclones that produce high impact weather in the Mediterranean; http://medex.aemet.uib.es) established a threshold when a maximum rainfall of over 60 mm in 24 h was recorded to indicate the expected social impact for rain events in Catalonia (Amaro et al., 2010; Jansa et al., 2014). Barbería et al. (2014) suggested that the threshold of 40 mm 24 h^{-1} is better for urban areas. Thus, both the precipitation threshold of 40 mm 24 h^{-1} and 60 mm 24 h^{-1} have been considered.

Furthermore, different spatial aggregations have been used in order to do a set of sensitivity tests (see Table 5.1): (i) basins (considering both maximum and mean precipitation of the basin), (ii) taking into account only coastal basins, and (iii) the AEMET warning areas, which has also been used in other studies like Quintana-Seguí et al. (2016). The precipitation thresholds of 40 and 60 mm in 24 h have been applied for all these spatial units. In addition, we have tested the use of maximum and mean precipitation of the basin. That means a total of 120 models developed. Given that similar results have been obtained, the basin has been the spatial resolution selected since is the most translatable to other regions.

Spatial aggregation	Maximum precipitation		Mean precipitation	
	40 mm	60 mm	40 mm	60 mm
Basins	X	X	X	X
Coastal basins	X	X		
Warming areas	X	X		

Table 5.1: Summary of the different sensitivity tests done for the simple logistic regression models developed in Catalonia (marked with "X"). Grey cells indicate the models selected and explained in the main text

The results obtained with the average precipitation of the basin, with only considering coastal basins and using the warning areas aggregation are shown in Cortès et al. (2018) (see Appendix B). Therefore, in the main text the 24 h maximum precipitation recorded in the basin has been used as the driver for flood damage in Catalonia in the simple logistic regression model, and two samples considering the precipitation thresholds of 40 mm 24 h^{-1} and 60 mm 24 h^{-1} have been considered (grey cells Table 5.1).

Figure 5.1 shows the relationship between the three categories of damages (D, DPC and DPW) and precipitation (log-transformed) in Catalonia for the 60 mm 24 h^{-1} threshold. Even if a linear regression indicates a significant link (p value < 0.05), the explanatory power of the model for D is rather low ($r^2 = 0.09$). Marginally better results are obtained for the damage indicators DPC and DPW ($r^2 = 0.14$ and $r^2 = 0.16$ respectively), underlying the importance of considering the impacts of population and wealth on damage. That is, this analysis corroborates the common experience that, given the same level of heavy precipitation, the total damage is

larger where the level of wealth is higher. As in the MAB case (Chapter 4), the significant correlation between insurance compensation and precipitation suggests that rainfall data can be used to extract information on damage in Catalonia, although the large spread of Figure 5.1 indicates that other methodology is needed instead of simple linear regression. For this reason and following the same successful methodology used in the previous chapter, we applied a logistic regression model to gauge the probability of large damaging events occurring given a certain precipitation amount. That is, our aim is not to estimate the precise amount of the monetary compensation, but to estimate when a 'large' damaging event will occur given a certain precipitation amount. As in the case of the MAB, we tested several cases for defining large damaging event: insurance compensation exceeding the 50th, 60th, 70th, 80th and 90th percentile of the total sample. This methodology is repeated for both precipitation thresholds (40 and 60 mm) and for the three damage indicators (D, DPC, DPW).

Finally, the simple logistic model is calculated following Eq. 5.1:

$$\log(\frac{\pi}{1-\pi}) = \beta_0 + \beta_1 P \tag{5.1}$$

where π is the response variable (i.e. the probability above a certain percentile) and P is the predictor (24 h precipitation in our case). The value of the β coefficient is determined using generalized linear models (GLMs). The Wald χ^2 statistic is used to assess the statistical significance of individual regression coefficients (Harrel, 2015).
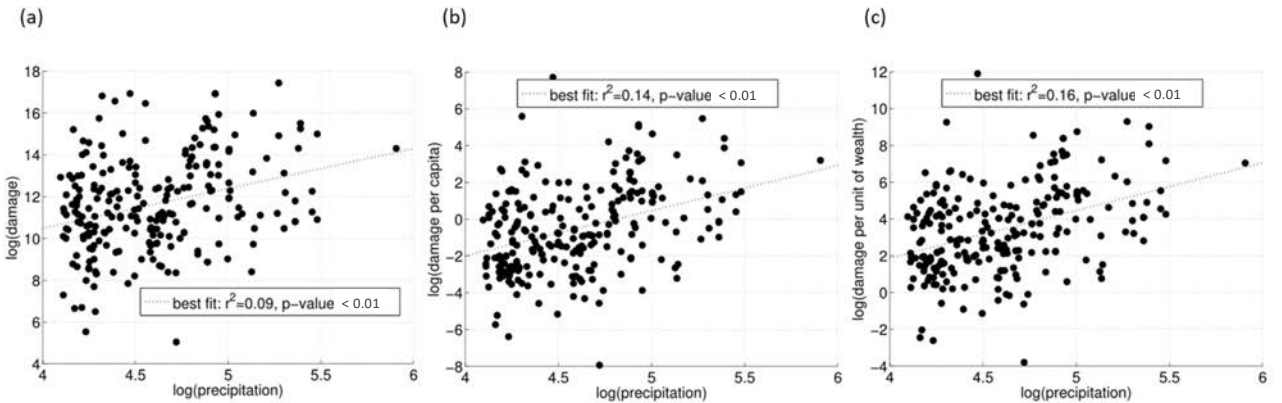
Figure 5.1: Scatter plot showing maximum precipitation in 24 h (mm) and (a) total damages (D), (b) damage per capita (DPC), and (c) damage per unit of wealth (DPW), for flood events recorded in Catalonia between 1996 and 2015 (log-transformed values; damages are given in Euro). Each point represents the insurance compensation series (D, DPC or DPW) and the maximum 24 h precipitation for each basin. The dashed line indicates the fit based on a linear regression model. (P_0=60 mm 24 h^{-1})

5.2.2 Multiple logistic regression model

In order to develop a multiple logistic regression model a variable selection process is needed to choose the explanatory variables that more information provide to the dependent (response) variable of the model. The unique dependent variable in this case is the total amount of compensation paid by CCS due to flood events in each affected basin and event. The explanatory (or independent) variables that have been taken into account in the selection process in order to built the best model are: maximum and mean 24 h precipitation recorded in the basin; maximum precipitation accumulated in 30 minutes; mean slope of the basin; proportion of urban zone; total population and GDP. Out of this group of independent variables, a selection of the greater contributors to the model has been performed. The method used was *Stepwise Regression* method (R Core Team, 2018), both backward and forward. Furthermore, this process has been validated with the estimation of two indicators of the goodness of the model for each possible combination of the explanatory variables: AIC (*Akaike Information Criterion*) and the area under the ROC curve (RA). Nine percentiles of damage have been selected in order to define a damaging event: 10th, 20th, 30th, 40th, 50th, 60th, 70th, 80th, 90th. As in the case of the simple logistic regression, the response variable has been transformed in binary variable, taking the value "1" when the specific damage percentile is exceeded and "0" if it is not.

The results of the *Stepwise Regression* method have shown that the explanatory variables that contribute the most to the model are: maximum precipitation recorded in 30 minutes, slope, GDP and proportion of urban zone of the basin. The last two mentioned variables present a high correlation (0.8) and therefore do not provide new information, reason why they do not coincide in the same model. Equation 5.2 shows the model that has obtained the best values of AIC (lower values of AIC means that the loss of information is minimised) and RA (values close to 1 means that the model is more likely to distinguish between event and non-event):

$$M1 : \log(\frac{\pi}{1 - \pi}) = \beta_0 + \beta_1 P + \beta_2 U + \beta_3 S \tag{5.2}$$

Where π is the response variable (the probability of exceeding a specific damage percentile), P is the maximum precipitation accumulated in 30 minutes, U the proportion of urban zone of the basin and S the mean slope. The regression coefficients have been estimated using Generalized Linear Models (GLMs). The Wald χ^2 statistic has been used to determine the statistical significance for each of the regression coefficients (see Cortès et al., 2018 for further information).

In the case of the multiple logistic regression model, the dataset has been divided in two samples according to the precipitation recorded in 30 minutes (> 10 mm and > 20 mm). These thresholds have been chosen based on previous studies (Cortès et al., 2017, 2018) in which it is proved that floods usually occur in Catalonia when these values are exceeded. The results of the models for both precipitation thresholds are shown in Section 5.3.2 of the present chapter.

5.2.3   Validation method

Similarly to what was done for the MAB region (Chapter 4), in order to validate both logistic regression models (simple and multiple) the ROC diagram was plotted (see Section 5.3.2). The area under the ROC curve (RA) is a useful tool for summarising the skill of a model. For further information about this method see Section 4.2.4 of Chapter 4.

5.3   Results

5.3.1   Spatial distribution

Flood events in Catalonia

Catalonia has recorded 166 flood events between 1996 and 2015. Barcelona is the most affected municipality with a total of 37 flood events registered for this period (Figure 5.2). The most affected basin was the Maresme basin with a total of 68 events (Figure 5.3).
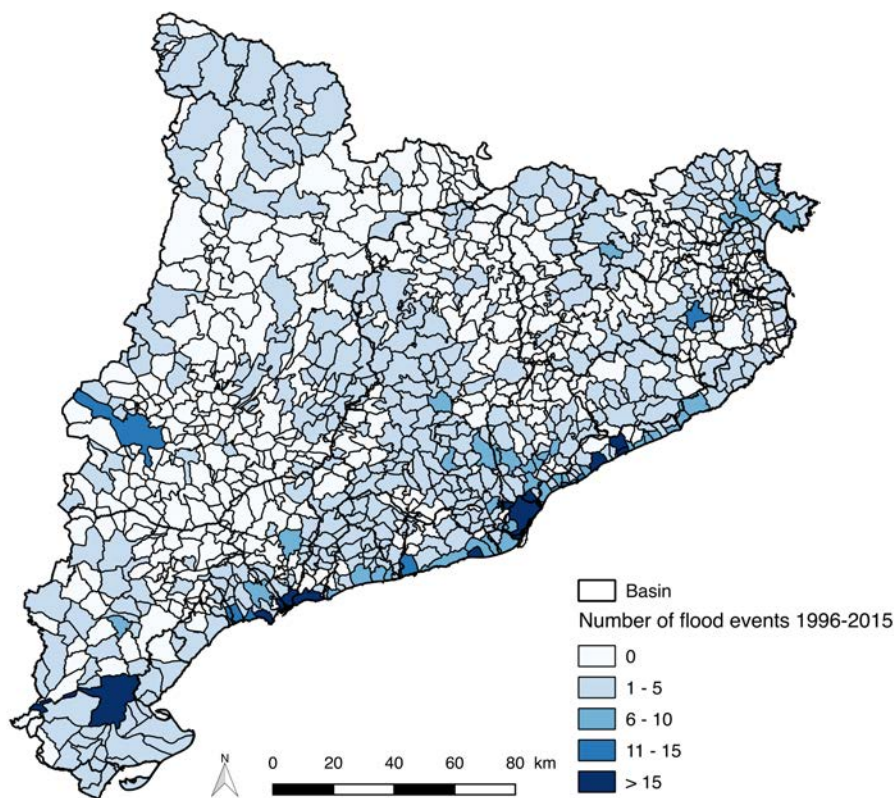
Figure 5.2: Flood events recorded in the municipalities of Catalonia for the period 1996-2015
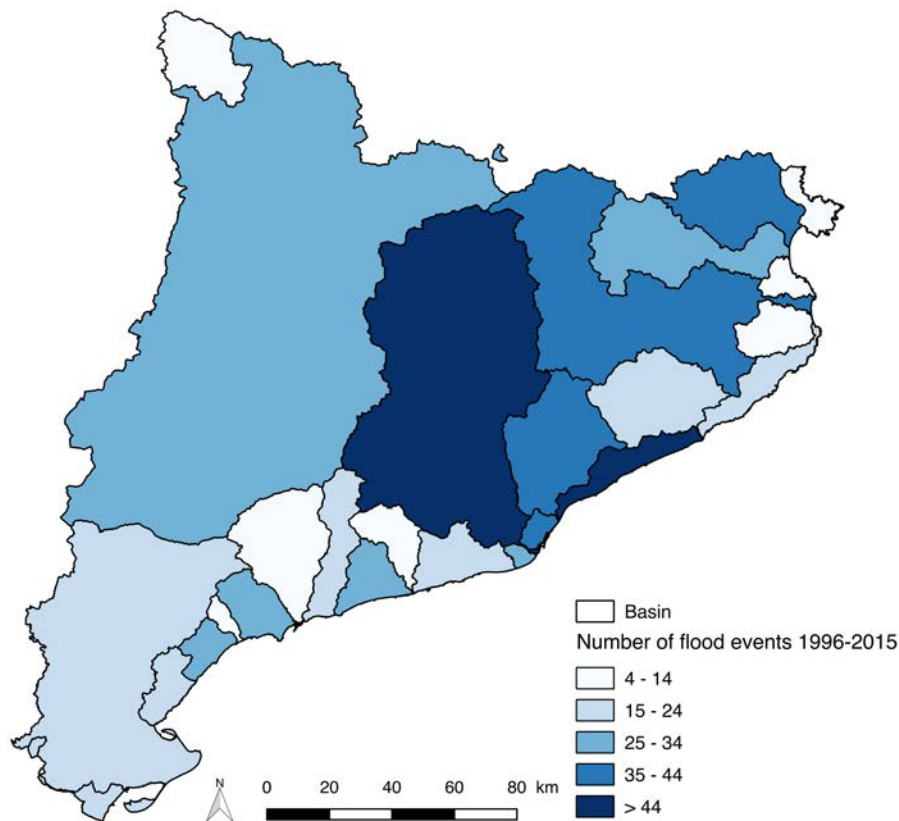
Figure 5.3: Flood events recorded in the basins of Catalonia for the period 1996-2015

Around 49 % of the events occurred during the months of July, August and September, with the latter month having the highest percentage of events (22 %). The most severe or catastrophic events occurred in autumn, with 77 % of these events taking place between September and November (Llasat et al., 2016b).

Precipitation in Catalonia

The selected weather stations (for further information see Chapter 3) with their mean annual precipitation value for the period 1996-2015 are represented in Figure 5.4. These values show a vastly wide range, with drier climates to the west of the study region with values lower than 300 mm per year and wetter climates with values close and above 1,000 mm per year in the north of the region.
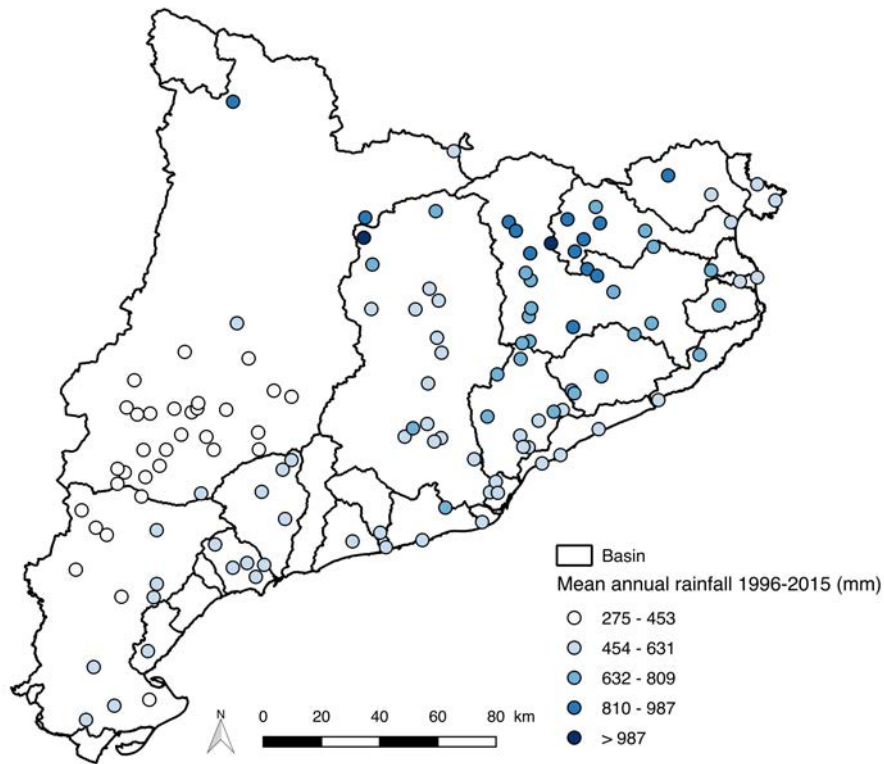
Figure 5.4: Average annual precipitation (1996-2015) for AEMET weather stations with effectiveness value > 90 %

Insurance compensation paid due to flood events in Catalonia
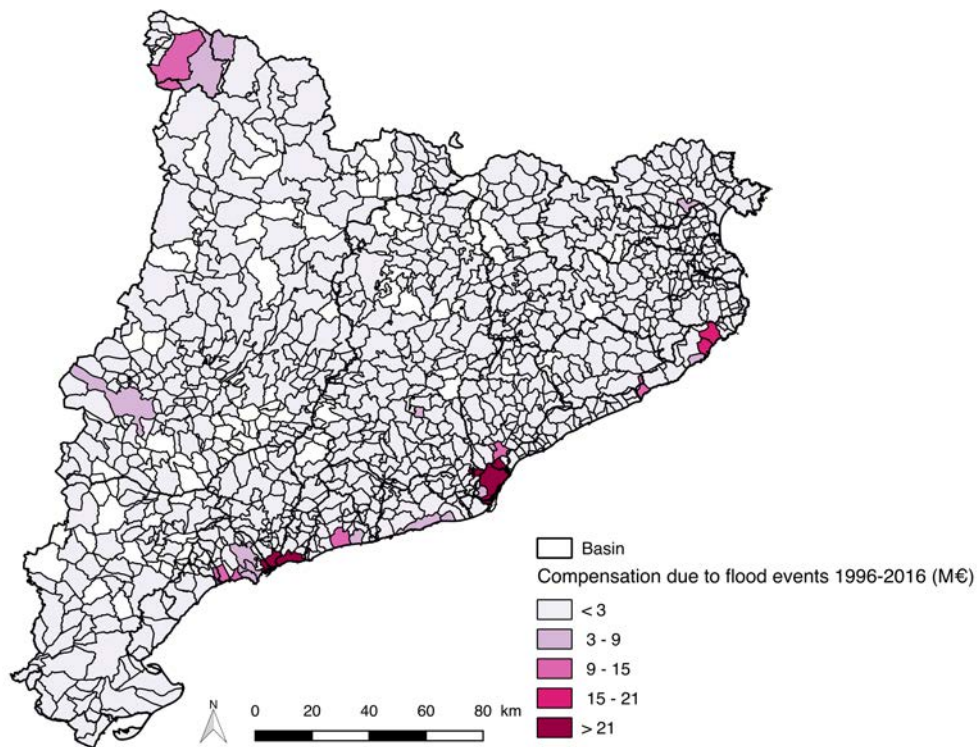
Figure 5.5: Total compensation paid by CCS due to floods for each municipality of Catalonia for the period 1996-2015

Figure 5.5 shows the compensation paid by the Insurance Compensation Consortium (CCS) due to flood events in each municipality of Catalonia for the period 1996-2015. Overall, Catalonia has received 436.40 M Euro between 1996 and 2015 in compensation for floods. Tarragona is the municipality that has received a greater amount of compensation from CCS during this period with a total value of around 26 M Euro (Figure 5.5). However, the basin that has recorded more damages is the Besòs with a total compensation amount higher than 45 M Euro according to CCS (Figure 5.6).
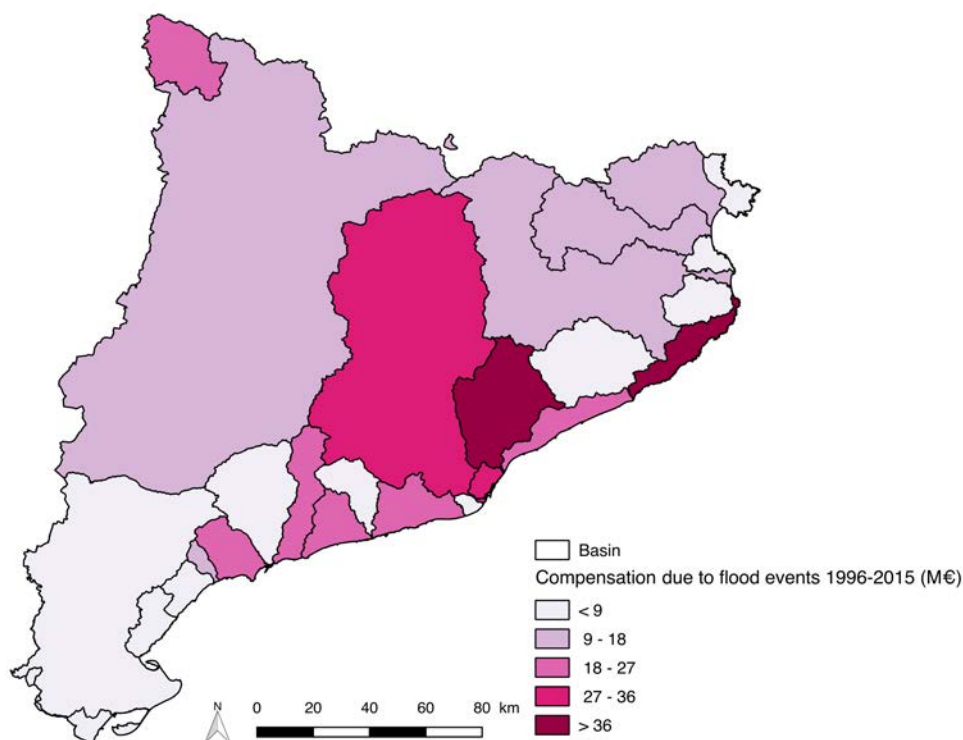
Figure 5.6: Total compensation paid by CCS due to floods for each basin of Catalonia for the period 1996-2015

Population and Gross Domestic Product in Catalonia

The average population per basin in the region of Catalonia for the period 1996-2015, is represented in Figure 5.7. Although the Barcelona catchment area is one of the smallest basins (93 km^2), it is the most populated one. Around 2 million of people (28 % of the total population of Catalonia) live in this basin, resulting in a total population density higher than 20,000 inhabitants km^{-2}.
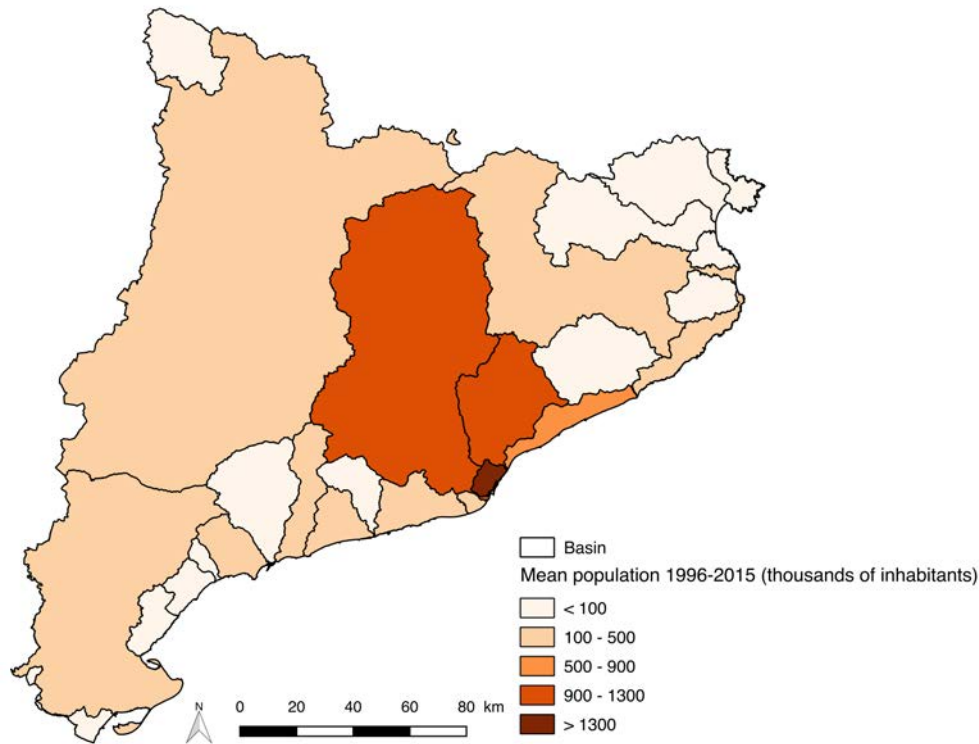
Figure 5.7: Average population per basin in Catalonia for the period 1996-2015

Figure 5.8 shows the average of the total Gross Domestic Product per basin of Catalonia for the period 1996-2015. As could be expected, the catchment area of Barcelona shows the highest GDP value, since it is also the most populated one (see Figure 5.7). The GDP of the basins of Barcelona represents the 39 % (67,773 M Euro) of the total Catalonia region.

Overall, there is a good spatial correlation among the four variables presented in this study. The basins with more recorded flood events are those that received more insurance compensation for flood damage and have higher population and GDP. For example, the Maresme Basin was affected by 41 % of the recorded events (see Figure 5.3) with damages that add up to 24.60 M Euro between 1996 and 2015 (see Figure 5.6). Coastal municipalities are the most affected by flood events and where there is the most damage (see Figures 5.2 and 5.5). This is a consequence of high vulnerability (the most vulnerable buildings and infrastructure are on the coast), exposure (population and tourism are concentrated in the coastal regions) and hazards (floods associated with local heavy rain events are frequent; Llasat et al., 2014a, 2016b).
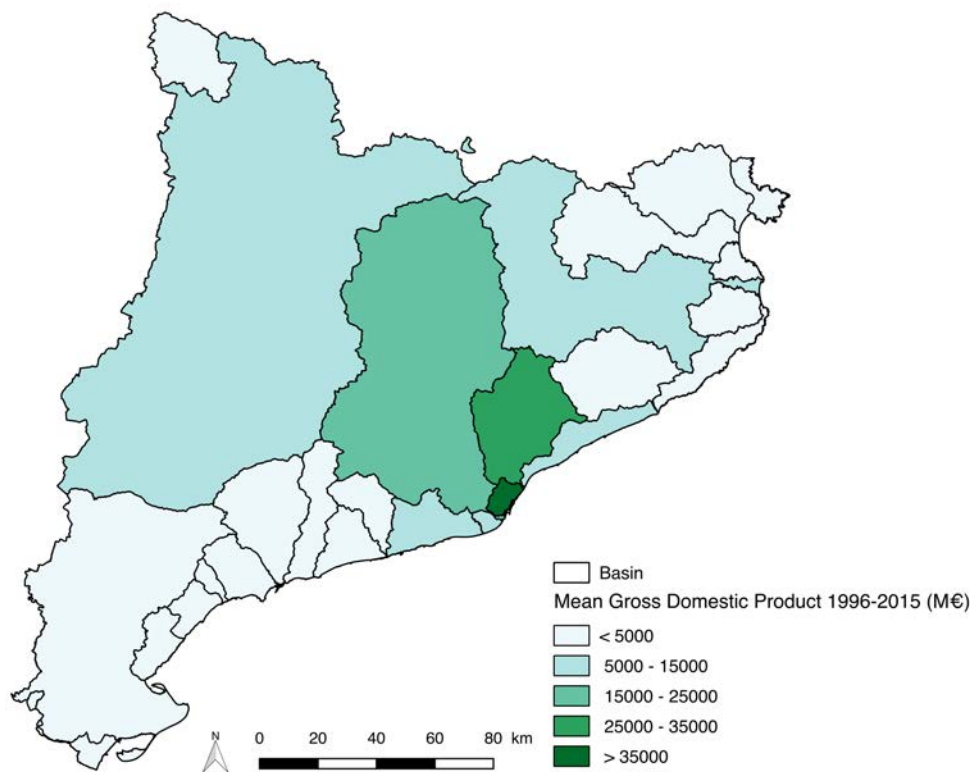
Figure 5.8: Average of the annual Gross Domestic Product in each basin of Catalonia for the period 1996-2015

5.3.2 Relationship between precipitation and flood damage

Simple logistic regression

The 166 flood events recorded in Catalonia for the period of study represent a total of 596 flood cases (i.e. pair of precipitation-damage values at a basin scale). 66 % of these flood events went beyond the 40 mm 24 h^{-1} precipitation threshold (313 flood cases) and 49 % went over the 60 mm 24 h^{-1} threshold (226 flood cases).

In order to estimate when a 'large' damaging event will occur with a given precipitation amount, a logistic regression was used. Figure 5.9 shows a logistic regression example, using the precipitation threshold of 40 mm 24 h^{-1}, that indicates that the model is able to simulate the probability of DPW above and below the 70th percentile as a function of precipitation (see Table A.2 of the Appendix section for damage percentiles). This figure illustrates that the probability of reaching above the 70th percentile for DPW increases when there is a large amount of rain. This result is consistent with the hypothesis that 24 h precipitation could be considered a good indicator for flood risk. For this example the regression equation follows the Eq. 5.3:

$$\log(\frac{\pi}{1-\pi}) = -8.01 + 1.61P \tag{5.3}$$
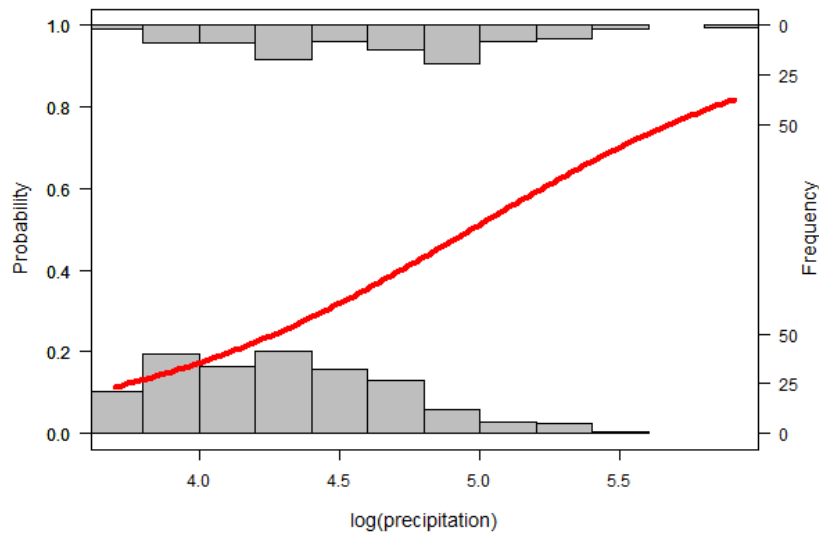
Figure 5.9: Example of logistic regression result used to model DPW damages above the 70th percentile as a function of precipitation (log-transformed precipitation given in millimetres). The red line indicates the best estimate and the grey bars show the frequency of the events that are above (top) and below (bottom) the 70th percentile. (P_0=40 mm 24 h^{-1})
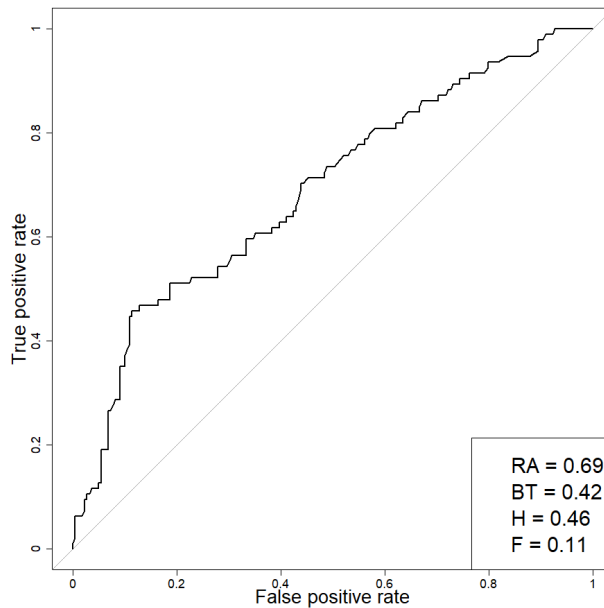
Figure 5.10: Relative operating characteristic (ROC) diagram for above 70th DPW predictions using the logistic regression of Eq. 5.3 (P_0=40 mm 24 h^{-1}). Each value of the ROC curve indicates a set of probability forecasts by stepping a decision threshold with 1 % probability through the modelling results. The numbers inside the plot are the ROC area (RA) and the best threshold (BT), here defined as the threshold that maximises the difference between the hit rate (H) and the false alarm rate (F)

In order to validate the model, we considered the area under the ROC curve (RA). Figure 5.10 shows that our model has skill: the ROC curve is well above the identity line, with an RA of 0.69. The 'best threshold' in this illustrative example is 0.42. This means that if we want to maximise the H-F difference, an above 70th percentile damaging event is to be expected

when our model predicts a probability value of 0.42, resulting in H = 0.46 (Hit rate) and F = 0.11 (False alarm rate). For example, in this case (BT = 0.42) a precipitation amount higher than 118 mm is needed to expect a damaging event above the 70th percentile for the damage indicator DPW (61.45 Euro / GDP; see Table A.2, Appendix section). Table 5.2 summarises the model parameters and performance considering all the percentiles and the three categories of damage used for the precipitation threshold of 40 mm 24 h^{-1}. In each case, precipitation is a significant predictor (p value < 0.05) and the models have skill and significant RA values. There are small differences between the damage indicators, although when the vulnerability and exposure (DPC and DPW indicators) are taken into account in the model, the results slightly improve.

Percentile	Damage	β_0	β_1	RA
50	D	-3.97	0.91	0.60
	DPC	-6.58	1.50	0.67
	DPW	-7.09	1.61	0.68
60	D	-5.68	1.20	0.64
	DPC	-7.31	1.56	0.67
	DPW	-7.49	1.60	0.68
70	D	-6.50	1.27	0.65
	DPC	-9.30	1.89	0.71
	DPW	-8.01	1.61	0.69
80	D	-9.19	1.74	0.71
	DPC	-11.62	2.27	0.76
	DPW	-10.05	1.93	0.73
90	D	-10.73	1.89	0.74
	DPC	-10.99	1.94	0.72
	DPW	-12.74	2.31	0.77

Table 5.2: Parameters of the simple logistic regression model and RA values for the basin level with 40 mm 24 h^{-1} maximum precipitation threshold. All the results are significant (p value < 0.05). See Table A.2 of the Appendix section for the damage thresholds definition. Number of flood cases: 313

The same analysis has been carried out with the precipitation threshold of 60 mm 24 h^{-1}. Table 5.3 shows the regression coefficients and RA values for this sample and for the different percentiles and damage indicators considered. The results are similar to the 40 mm 24 h^{-1} sample, with values of RA lower in some cases (see Table 5.2). Similar results were obtained for the different damage categories, with slightly larger RA considering DPW.

Equation 5.4 shows the regression coefficients values when using the percentile 70th of damage indicator DPW for the sample with 60 mm 24 h^{-1} precipitation threshold:

$$\log(\frac{\pi}{1-\pi}) = -11.39 + 2.28P \tag{5.4}$$

67

Percentile	Damage	β_0	β_1	RA
50	D	-6.42	1.40	0.63
	DPC	-8.62	1.88	0.66
	DPW	-8.34	1.82	0.66
60	D	-8.51	1.76	0.67
	DPC	-8.75	1.81	0.66
	DPW	-8.63	1.78	0.67
70	D	-8.29	1.61	0.66
	DPC	-11.98	2.40	0.72
	DPW	-11.39	2.28	0.72
80	D	-10.74	2.01	0.70
	DPC	-10.82	2.02	0.70
	DPW	-13.25	2.54	0.75
90	D	-11.56	2.00	0.72
	DPC	-12.04	2.10	0.70
	DPW	-14.93	2.70	0.77

Table 5.3: Parameters of the simple logistic regression model and RA values for the basin level with 60 mm 24 h^{-1} maximum precipitation threshold. All the results are significant (p value < 0.05). See Table A.2 of the Appendix section for the damage thresholds definition. Number of flood cases: 226

Figure 5.11 shows the logistic regression curve for the example of Eq. 5.4. As could be expected, the probability of a damaging event increases with precipitation. In this example the RA value is 0.72 (Figure 5.12), similar to the 40 mm 24 h^{-1} case, proving that this model, although with a smaller sample, has also skill. The maximum difference between hit rate and false alarm rate will be obtained when the model predicts a probability value of 0.37 (BT), with a resulting hit rate of 0.60 and false alarm rate of 0.17. In this case a precipitation amount higher than 117 mm in 24 h will be needed for a damaging event occurrence (defined with the 70th percentile of damage).
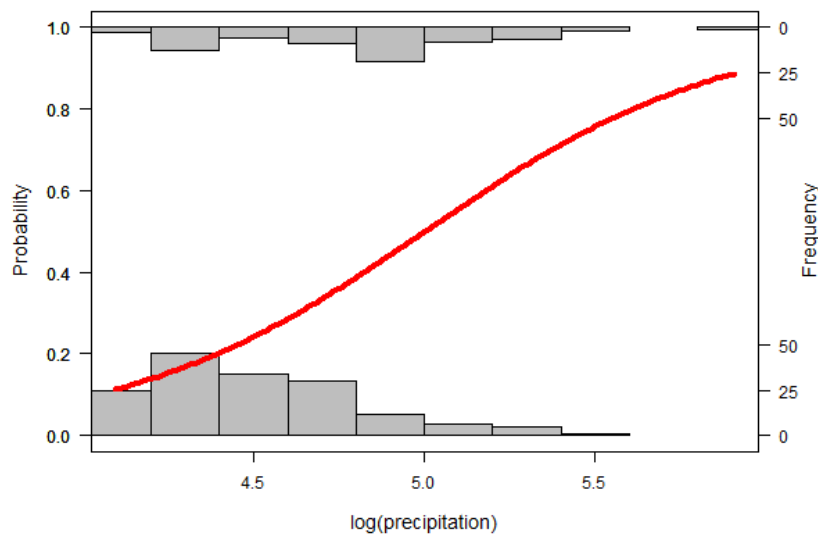
Figure 5.11: Example of logistic regression result used to model DPW damages above the 70th percentile as a function of precipitation (log-transformed precipitation given in millimetres). The red line indicates the best estimate and the grey bars show the frequency of the events that are above (top) and below (bottom) the 70th percentile. (P_0=60 mm 24 h^{-1})
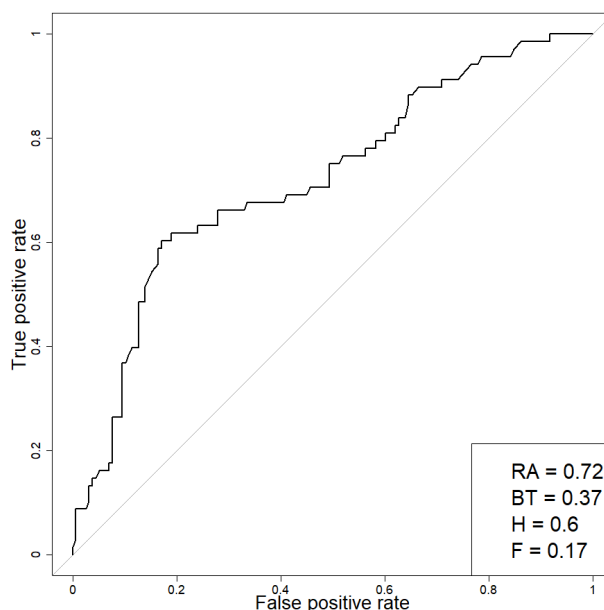
Figure 5.12: Relative operating characteristic (ROC) diagram for above 70th DPW predictions using the logistic regression of Eq. 5.4 (P_0=60 mm 24 h^{-1}). Each value of the ROC curve indicates a set of probability forecasts by stepping a decision threshold with 1 % probability through the modelling results. The numbers inside the plot are the ROC area (RA) and the best threshold (BT), here defined as the threshold that maximises the difference between the hit rate (H) and the false alarm rate (F)

Multiple logistic regression

In this section, a multiple logistic regression model has been developed in order to estimate the probability of a damaging event in Catalonia based on precipitation but also taking into account other variables related with the vulnerability and exposure of the territory. As was explained in Section 5.2.2, the variables that contribute most to this probability, and therefore those used for the development of the multiple model, are the maximum precipitation recorded in 30 minutes, the proportion of urban zone and the mean slope of the basin. The results of this methodology are presented for two different samples: flood cases that recorded a 30-minute precipitation higher than 10 mm and ones with precipitation greater than 20 mm 30 min^{-1}.

From the 596 flood cases recorded for the period of study in Catalonia, 369 registered a maximum precipitation accumulated in 30 minutes higher than 10 mm and 242 higher than 20 mm. Table 5.4 summarises the results of the multiple logistic model for each considered percentile of damages. The results displayed are those considering the best model for each of the damage percentiles, first taking into account the significance of the regression coefficients and then the highest RA value.

Percentile	β_0	β_1	β_2	β_3	RA
10	-4.69	1.82	0.32	1.25	0.73
20	-5.05	1.80	0.40	1.08	0.73
30	-5.23	1.93	-	-	0.74
40	-5.23	1.76	-	-	0.72
50	-5.73	1.78	-	-	0.72
60	-6.50	1.87	-	-	0.73
70	-6.75	2.02	0.32	-	0.74
80	-8.53	2.35	0.32	-	0.78
90	-12.00	2.83	-	-	0.82

Table 5.4: Parameters of the multiple logistic regression model and RA values with 10 mm 30 min^{-1} maximum precipitation threshold for all the percentiles of damage. β_0, β_1, β_2, and β_3 represents the regression coefficients of the logistic model (intercept, precipitation, urban zone and slope, respectively). Only the significant regression coefficients (p value < 0.05) are displayed. See Table A.3 of the Appendix section for the damage thresholds definition. Number of flood cases: 369

The results using the multiple logistic regression model show that our model is capable of simulating the probability of a damaging event based on the explanatory variables selected, being the 30-minute precipitation the most important one. The slope of the basin does not provide much information. Figure 5.13 shows the probability above and below the 70th percentile of damage (0.25 M Euro) as a function of precipitation and with the sample of the 10 mm 30 min^{-1} threshold. As could be expected, this probability increases with the 30-minute precipitation.
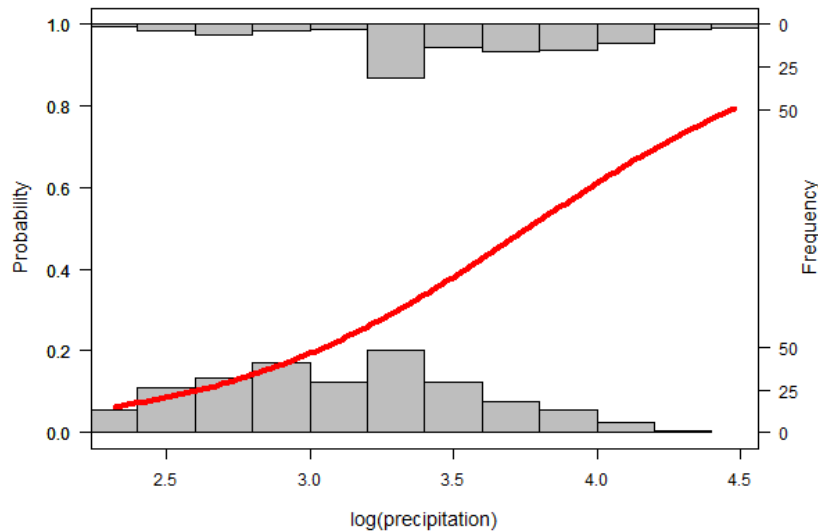
Figure 5.13: Example of logistic regression result used to model total damages above the 70th percentile as a function of precipitation (log-transformed precipitation given in millimetres). The red line indicates the best estimate and the grey bars show the frequency of the events that are above (top) and below (bottom) the 70th percentile. (P_0=10 mm 30 min^{-1})

Equation 5.5 displays the formula of the best model for the 70th percentile of damage considering the flood cases that exceeded the 10 mm 30 min^{-1} precipitation threshold, with the

coefficient regression values for the explanatory variables, precipitation (P) and proportion of urban zone (U) in this case, being both statically significant (p value < 0.05):

$$\log(\frac{\pi}{1 - \pi}) = -6.75 + 2.02P + 0.32U \tag{5.5}$$

Figure 5.14 shows the ROC diagram for the same example of Equation 5.5 and Figure 5.13. The RA value is 0.74, well above 0.5, proving tha the model has a good goodness of fit. The BT is 0.29, indicating that if the difference between the hit and the false alarm rate wants to be maximised, a probability of 0.29 is needed, resulting in H = 0.72 and F = 0.35.
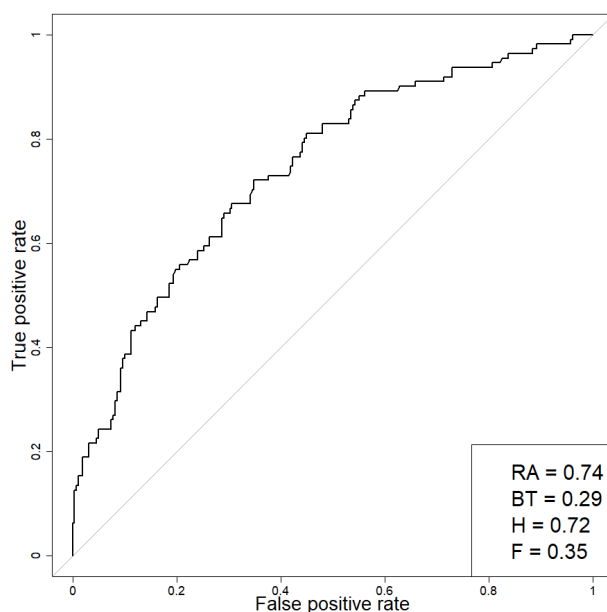
Figure 5.14: Relative operating characteristic (ROC) diagram for above 70th percentile of damage predictions using the logistic regression of Eq. 5.5 (P_0=10 mm 30 min^{-1}). Each value of the ROC curve indicates a set of probability forecasts by stepping a decision threshold with 1 % probability through the modelling results. The numbers inside the plot are the ROC area (RA) and the best threshold (BT), here defined as the threshold that maximises the difference between the hit rate (H) and the false alarm rate (F)

As can be observed in Table 5.4, all RA values are well above 0.7, indicating that the model has skill. For the lowest damage percentiles (10th and 20th percentiles) the characteristics of the basin play an important role. However, for flood events that can cause great damage (high percentiles), precipitation is the most influential variable (and in some cases also the proportion of urban zone).

Furthermore, the results show that the use of a multiple logistic regression model that takes into account other variables apart from precipitation, and also the utilisation of the 30-minute precipitation instead of the precipitation accumulated in 24 h, improve the performance of the model (higher RA values).

The same analysis has been reproduced using the flood cases that recorded a maximum precipitation in 30 minutes higher than 20 mm. As in the previous case (10 mm 30 min^{-1}), the

precipitation is statistically significant for all damage percentiles, as is the proportion of urban zone of the basin with the sole exception of the 90th percentile (see Table 5.5). The mean slope of the basin, however, only provides information to the response variable in the case of the lowest percentiles of damage (10th and 20th). All regression coefficients have positive values, showing that the probability of a damaging event increases with precipitation and in basins more urbanised and with greater slopes.

Percentile	β_0	β_1	β_2	β_3	RA
10	-10.86	3.71	0.50	1.03	0.78
20	-10.22	3.25	0.39	0.85	0.75
30	-6.63	2.38	0.30	-	0.69
40	-5.17	1.83	0.33	-	0.67
50	-6.22	2.00	0.32	-	0.67
60	-6.72	2.06	0.37	-	0.68
70	-7.37	2.15	0.44	-	0.70
80	-7.92	2.11	0.41	-	0.70
90	-12.65	2.89	-	-	0.76

Table 5.5: Parameters of the multiple logistic regression model and RA values with 20 mm 30 min^{-1} maximum precipitation threshold for all the percentiles of damage. β_0, β_1, β_2, and β_3 represents the regression coefficients of the logistic model (intercept, precipitation, urban zone and slope, respectively). Only the significant regression coefficients (p value < 0.05) are displayed. See Table A.3 of the Appendix section for the damage thresholds definition. Number of flood cases: 242

Equation 5.6 shows the formula of the best logistic model for the 70th damage percentile considering the flood cases that exceeded the 20 mm 30 min^{-1} precipitation threshold. In this example, only the precipitation (P) and the urban zone (U) are statistically significant:

$$\log(\frac{\pi}{1 - \pi}) = -7.37 + 2.15P + 0.44U \tag{5.6}$$

The curve of the logistic model for the example of Equation 5.6 is shown in Figure 5.15, indicating the probability above and below the 70th percentile of damage (0.46 M Euro) as a function of the precipitation. The validation of this model is displayed in Figure 5.16 by the ROC diagram. The RA value for this example is 0.7, proving that this model has also skill, although with a smaller sample.
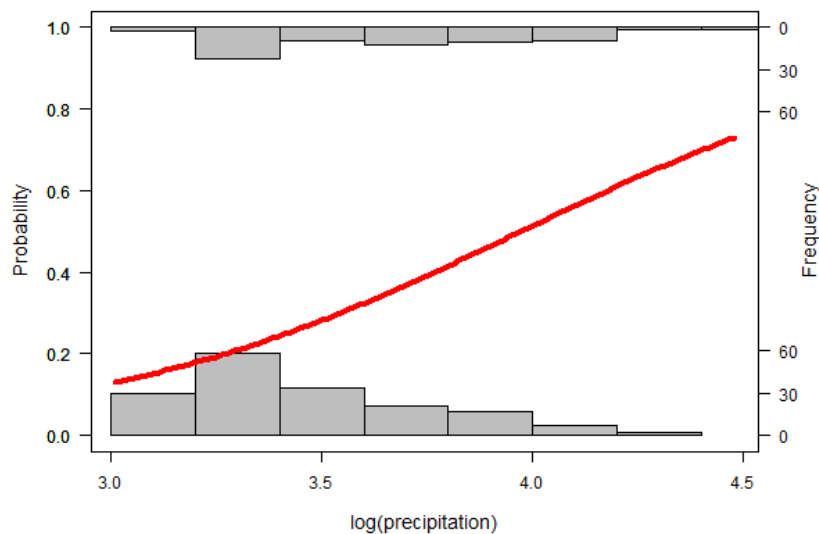
Figure 5.15: Example of logistic regression result used to model total damages above the 70th percentile as a function of precipitation (log-transformed precipitation given in millimetres). The red line indicates the best estimate and the grey bars show the frequency of the events that are above (top) and below (bottom) the 70th percentile. (P_0=20 mm 30 min^{-1})
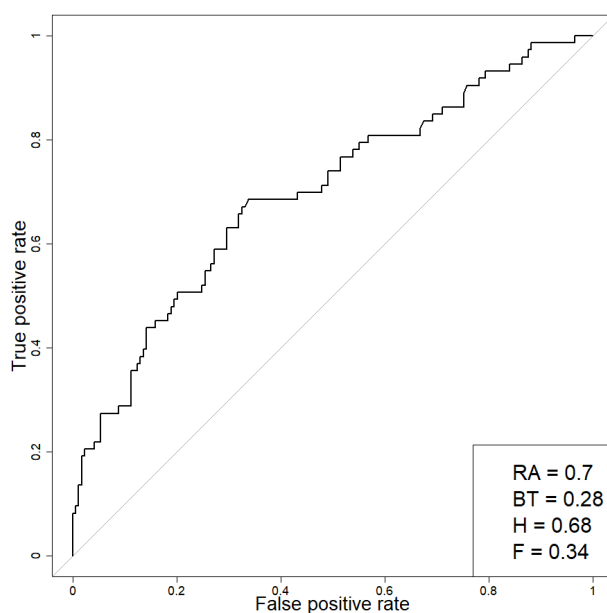
Figure 5.16: Relative operating characteristic (ROC) diagram for above 70th percentile of damage predictions using the logistic regression of Eq. 5.6 (P_0=20 mm 30 min^{-1}). Each value of the ROC curve indicates a set of probability forecasts by stepping a decision threshold with 1 % probability through the modelling results. The numbers inside the plot are the ROC area (RA) and the best threshold (BT), here defined as the threshold that maximises the difference between the hit rate (H) and the false alarm rate (F)

73

5.4   Conclusions

The Mediterranean is an area frequently affected by flood events that produce significant socioeconomic damage. Catalonia, located in the west of the Mediterranean, is affected by an average of more than 8 events per year. The majority of the damage caused by these events is due to local events, with intense and short-lived rainfall rather than river overflow (Llasat et al., 2014a). Therefore, it is assumed that precipitation is the main contributing factor for damage caused by this type of events. To corroborate this hypothesis, the relationship between precipitation and compensation paid by insurance companies was studied. This has been done by using two types of logistic regression models: simple and multiple. That is, our aim is not to estimate the precise amount of insurance compensation, but to estimate when a 'large' damaging event will occur given a particular precipitation amount.

In the case of the simple logistic regression using the precipitation recorded in 24 h, we considered three types of damage: total damage, damage per capita (divided by the population) and damage per unit of GDP, in order to take into account the differences in vulnerability and exposure in the territory. As could be expected, the logistic regression shows an increase in the probability of a damaging event occurring when precipitation increases. In order to validate the model, we considered the ROC diagram. The area under the ROC curve (RA) proved our model skill. The results show an RA above 0.6 in all percentiles of the three types of damages and thresholds of precipitation, most of them with values close or higher than 0.7. That is, our model is able to simulate the probability of a damaging event as a function of precipitation.

On the other hand, a multiple logistic regression model has been developed in order to estimate the probability of a damaging event based on precipitation 30 minutes and also considering the proportion of urban zone and the mean slope of the basin. The results show that the model has skill, obtaining better results (higher RA values) than the simple logistic regression model when using the precipitation accumulated in 24 h as a single explanatory variable. Not only the probability of a damaging event increases with the 30-minutes precipitation, but also both urban zone and slope are positively correlated with the response variable, showing that a highly urbanised and steeper basin will have a higher probability of a damaging event occurrence than a less urbanised and flat one. The Catalan basins situated between the coastal and pre-coastal mountain ranges are small but highly urbanised basins with deep slopes, and it is precisely where more flood events are recorded.

To summarise, we have developed a new model that allows us to predict the probability that a flood event causing large damage (where "large" depends on the user's criteria) will occur in Catalonia, based on precipitation, and taking into account the characteristics of the region in the model. That is, the parsimonious empirical models linking flood damages to heavy precipitation developed in this study make a substantial contribution towards developing a warning forecast system with flood management strategies. For instance, from the relationship shown between precipitation and insurance compensation it is possible to predict when damaging events will occur as a result of a certain precipitation threshold. The results were obtained by following a simple and transparent statistical methodology that can also be applied to other areas. These

links could also provide a basis to predict flood damage in future climate change scenarios as done for instance by Wobus et al. (2014) that estimated monetary damages from flooding in the United States under a 'business as usual' climate change scenario. As a word of caution it is worth noting that the complex relationships between climate variability, human activities and flood damage may limit the applicability of these findings to conditions that are very different from current ones.

Despite these limitations, this work has provided an assessment of the link between precipitation and flood damage in a Mediterranean region, and our results suggest that by exploiting the relationship between precipitation and flood damage, the model could provide satisfactory prediction of monetary compensation.

Overall, the methodological novelties included in this chapter are: (i) the significant increase in the spatial scale of the study, (ii) the change in the minimum unit of study, (iii) the development of new type of models that are able to include other explanatory variables in order to improve the variance of the response variable, (iv) the incorporation of the mean urban zone and slope of the basin in the model that allow to take into account the vulnerability and exposure of the territory.

Chapter 6

Application of the Generalized Linear Mixed Model to the western Mediterranean: Catalonia and the Valencian Community

Abstract

The aim of this chapter is to extend the study of the relationships between flood damage, precipitation and exposure to the Valencian Community. A second objective is to improve the modelling to analyse these relationships moving from simple and multiple logistic regression models to Generalized Linear Mixed models and apply them to Catalonia and the Valencian Community. The results show that mean precipitation recorded in 24 h and total population of the basin are good predictors to estimate the probability of a damaging event in both regions, obtaining better results in terms of area under the ROC curve than the previous models developed (Chapter 5). The relationships found in this chapter will be applied in Chapter 8 in order to predict the future flood damage.

6.1 Introduction

As was mentioned before, the Mediterranean region is characterised by a complex morphology of mountain chains and strong land-sea contrasts, a dense and growing human population and various environmental pressures (Cramer et al., 2018). The north-west of the Mediterranean is the area most affected by flood events (Llasat et al., 2010). In Spain, the most affected regions are Catalonia and the Valencian Community. Particularly, the Valencian Community is an area frequently affected by heavy precipitation events that cause floods with huge damages, such as the November 1987 when more than 285 M Euro were paid in insurance compensation according to the Spanish Insurance Compensation Consortium (CCS, 2018). This is the reason why it has been decided to extend the region of study considering both areas.

The main objective of this chapter is to improve the results obtained from previous ones by the use of more complex models called Generalized Linear Mixed models, which not only take into account fix predictors related to the hazard and the exposure of the territory but also allow random effects in the model.

The chapter is organised as follows. After the Methods section, in which the new model is explained in detail (Section 6.2), Section 6.3.1 presents the variables selected for the Valencian Community. The results obtained with the application of the new model for Catalonia and the Valencian Community are shown in sections 6.3.2 and 6.3.3, respectively. Finally, the Conclusions section (Section 6.4) summarises the main findings of this chapter.

6.2   Methods

The main characteristics of the regions of the study as well as the data sources used in this chapter are explained in Chapter 3. In Section 6.3.1 of the present chapter is represented the main variables used in the study at municipal and basin level for the Valencian Community. The same cartography for Catalonia region is shown in Section 5.3.1 of Chapter 5. The river-basin-scale is the spatial resolution selected for analysing the possible links between precipitation and flood damage in both regions of study. The main hypothesis of the study is that precipitation is the factor that is more related to flood damage because the most frequent type of floods are surface water flood events (see Chapters 4 and 5, and Cortès et al., 2018 for further information). In this chapter, the rainfall recorded in 24 h has been used to estimate the precipitation. Although 30-min precipitation provides better results, as has been shown previously, since the final objective of this thesis is to assess flood damage for future projections and these are given in 24 h data, the analysis has been done for this time resolution. Furthermore, and following the previous chapter (Chapter 5), only the flood cases that recorded a precipitation threshold higher than 40 mm 24 h^{-1} were selected in order to consider the potential extreme precipitation events.

6.2.1   Generalized Linear Mixed Model

Generalized Linear Mixed Models (or GLMMs) are a powerful class of statistical models that combine the characteristics of linear mixed models (models that include both fixed and random predictor variables) and generalized linear models (which handle non-normal data by using link functions and exponential family [e.g. Poisson or binomial] distributions). Thus, GLMMs are the best tool for analysing non-normal data that involve random effects (Bolker et al., 2009). That is the case of the data used in this study, which are of binary type (event or non event) and there are random effects related to space and time: each of the basins can be affected by different flood events for the whole time period and moreover, each event can affect different basins at the same time. This implies high correlations within the observations, not guaranteeing the independence requirement of the Generalized Linear Models (GLM). Figure 6.1 summarises the process followed in order to choose the best model for our type of data.
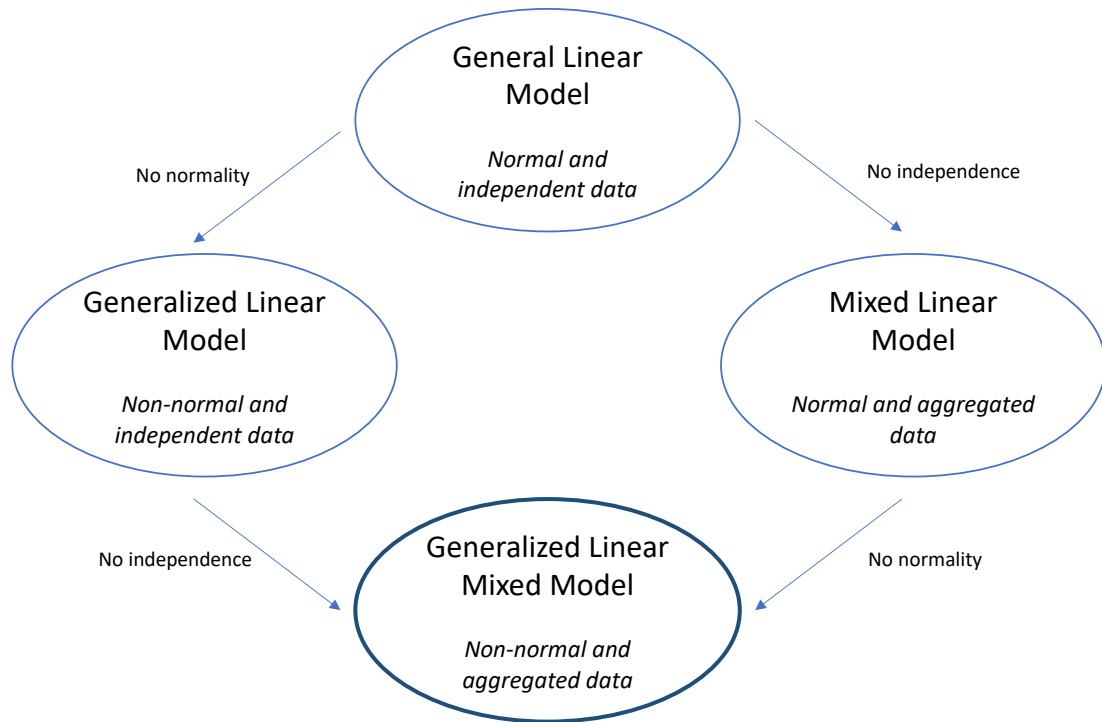
Figure 6.1: Scheme of the selection process of the type of model

The generalized linear mixed model follows the equation 8.1:

$$\log(\frac{\pi}{1-\pi}) = \beta_0 + \beta_1 P + \beta_2 R + b_i + b_j \tag{6.1}$$

Where π is the response variable (the probability to exceed a specific threshold of damage), P and R are the predictors (precipitation recorded in 24 h and total population of the basin in our case), and b_i and b_j are the random effects related to the basins and the events. The value of the β coefficient is determined using Generalized Linear Models (GLMs). The Wald χ^2 statistic is used to assess the statistical significance of individual regression coefficients (Harrell Jr, 2015).

The same methodology from chapters 4 and 5 has been applied in order to assess the probability of exceeding different thresholds of damage estimated using the percentiles of the series of damages per basin (10th, 20th, 30th, 40th, 50th, 60th, 70th, 80th, 90th).

Another possibility is to estimate the damage threshold using the average of total compensation paid by CCS for catastrophic flood events, regarding to the impact category of the INUNGAMA and FLOODHYMEX databases (for further information about the databases and the impact classification of the flood events see Chapters 4 and Cortès et al., 2017). This method is more restrictive than those used in previous chapters and flood cases that exceed

this specific damage threshold will be defined as a "big flood case". The damage threshold is obtained by dividing the mean compensation paid by CCS for these catastrophic events (14.8 M Euro for Catalonia and 43.6 M Euro for the Valencian Community) by the number of basins that have been affected by each event (flood cases). The results for these models are shown in sections 6.3.2 and 6.3.3.

6.2.2 Explanatory variables selection

To select the independent variables that maximise the variance explained by the model, different models have been developed and compared to each other by using two common indicators to assess the goodness of fit: *Aikake Information Criterion* (AIC), proposed by Akaike (1974), and *Bayes Information Criterion* (BIC), put forward by Schwarz et al. (1978). The latter penalises model complexity more heavily and also takes into account the sample size. A lower AIC or BIC value indicates a better fit. AIC and BIC estimators follows the equations 6.2 and 6.3, respectively.

$$AIC = 2K - 2\ln(L) \tag{6.2}$$

$$BIC = K\ln(n) - 2\ln(L) \tag{6.3}$$

where L is the value of the likelihood, n is the number of recorded measurements, and k is the number of estimated parameters.

The explanatory (or independent) variables that have been taken into account in the selection process in order to build the best model are: maximum and mean 24 h precipitation recorded in the basin; mean slope of the basin; proportion of urban zone; total population; Gross Domestic Product (GDP).

The AIC and BIC values for each of the models are shown in Tables 6.1 and 6.2 for Catalonia and the Valencian Community, respectively. As can be observed in both regions of study the model with better results for forecasting flood damages (in this case the probability of exceeding the 70th percentile of damage) in terms of AIC and BIC values is the one with the mean precipitation accumulated in 24 h and the total population of the basin as explanatory variables, both of them being statistically significant (p value < 0.05 with Wald Test). Therefore, these two variables will be the ones used in the GLMM in order to predict the probability of a damaging event.

Explanatory variables	AIC	BIC
Px24h	334.8	349.7
P24h	188.5	201.2
Px24h + R	325.8	344.5
P24h + R	**181.8**	**197.7**
Px24h + U*	331.1	349.8
P24h + U*	188.7	204.6
Px24h + R + S*	327.7	350.2
P24h + R + S*	183.0	202.1
Px24h + U* + S*	334.9	357.4
P24h + U + S*	191.9	211.0

Table 6.1: Example of the AIC and BIC values for the different models using the 70th percentile of damage to define a damaging event in Catalonia. The explanatory variables are: maximum precipitation recorded in 24 h (Px24h), mean precipitation recorded in 24 h (P24h), total population (R), proportion of urban zone (U) and mean slope of the basin (S). The best model is shown in bold. *p value > 0.05 with Wald Test

Explanatory variables	AIC	BIC
Px24h	113.5	125.2
P24h	75.2	84.3
Px24h + R	107.2	121.8
P24h + R	**65.6**	**77.0**
Px24h + U*	115.4	130.0
P24h + U*	77.0	88.3
Px24h + R* + S*	106.6	124.1
P24h + R + S	65.9	79.6
Px24h + U* + S	108.7	126.2
P24h + U* + S*	76.7	90.3

Table 6.2: Example of the AIC and BIC values for the different models using the 70th percentile of damage to define a damaging event in the Valencian Community. The explanatory variables are: maximum precipitation recorded in 24 h (Px24h), mean precipitation recorded in 24 h (P24h), total population (R), proportion of urban zone (U) and mean slope of the basin (S). The best model is shown in bold. *p value > 0.05 with Wald Test

6.2.3 Validation method

The ROC diagram and more specifically the area under the ROC curve (RA), was the method used in order to validate the Generalized Linear Mixed Models. The same methodology was used in Chapters 4 and 5. For further information about this method see Section 4.2.4 of Chapter 4.

6.3 Results

6.3.1 Spatial distribution

Flood events in the Valencian Community

For the 1996-2015 period the Valencian Community has recorded a total of 69 flood events, most of them produced on September (23 %) and October (17 %) months. València, capital

of this region, is the municipality that has registered the highest number of flood events for this period, with 17 events (Figure 6.2). However, the basin most affected by floods has been Marina Alta with a total of 32 flood events for the same period (Figure 6.3).
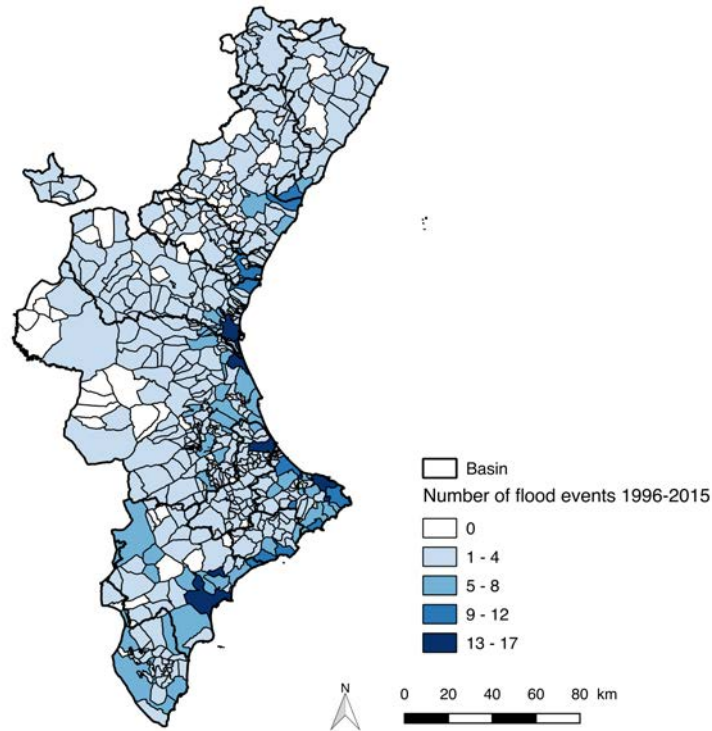
Figure 6.2: Flood events recorded in the municipalities of the Valencian Community for the period 1996-2015
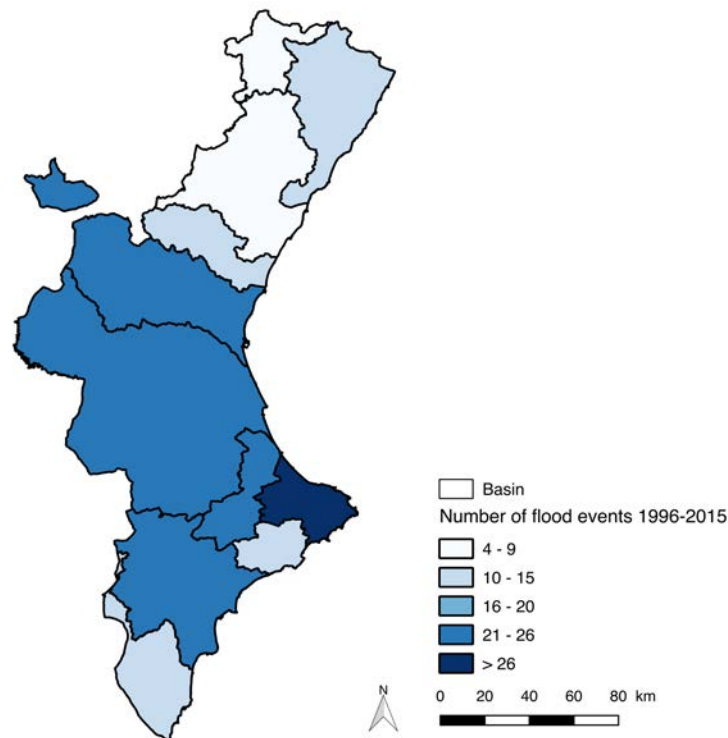
Figure 6.3: Flood events recorded in the basins of the Valencian Community for the period 1996-2015

Precipitation in the Valencian Community

The average annual precipitation for the selected weather stations (for further information see Chapter 3) is represented in Figure 6.4. As could be expected, the areas that recorded greater amounts of precipitation per year (i.e. higher than 724 mm) coincide with those that have been affected by more flood events (Figures 6.2 and 6.3). The region presents a broad range of annual precipitation values, with drier climates mainly in the south and inland of the territory with values around 300 mm per year (and even less) and wetter climates mostly located in the central coast with annual precipitation higher than 700 mm.
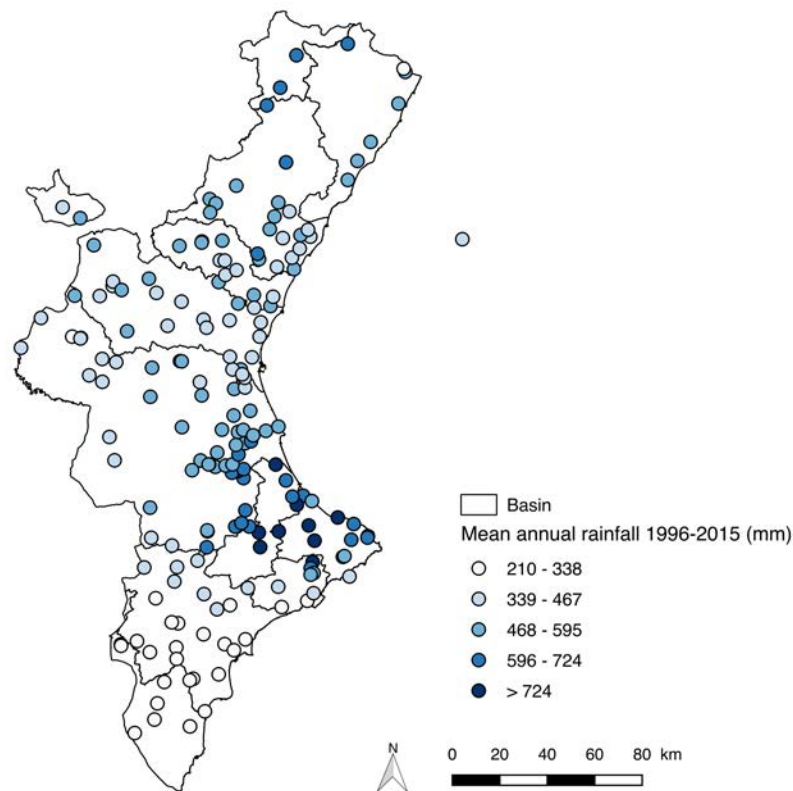
Figure 6.4: Average annual precipitation (1996-2015) for AEMET weather stations with effectiveness value > 90 %

Insurance compensation paid due to flood events in the Valencian Community

The Insurance Compensation Consortium (CCS) has paid a total of 713.75 M Euro in compensation due to flood events in the Valencian Community for the 1996-2015 period. Alacant is the municipality that has received the highest amount of compensation for this period, with a total quantity of around 40 M Euro (Figure 6.5). Nonetheless, 30 % of the total compensation (221.66 M Euro) have been paid in the Jucar basin (Figure 6.6).
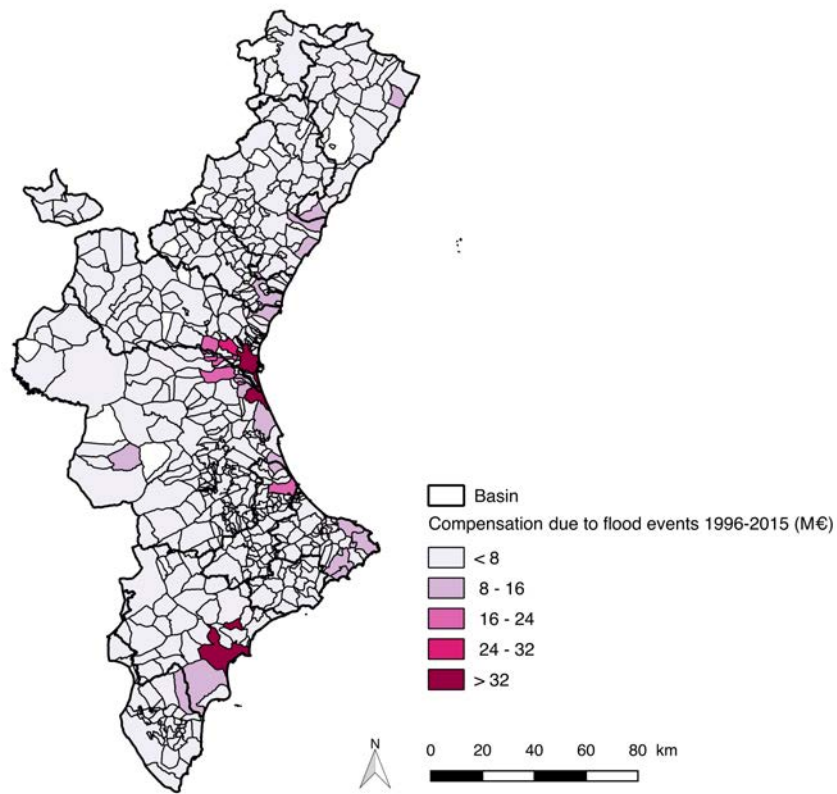
Figure 6.5: Total compensation paid by CCS due to floods for each municipality of the Valencian Community for the period 1996-2015
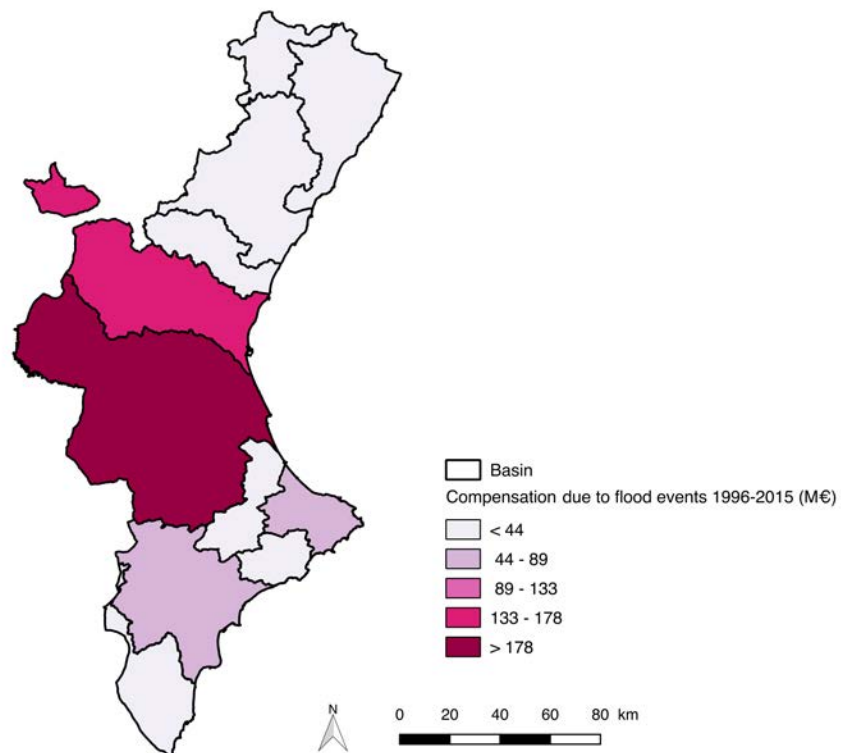
Figure 6.6: Total compensation paid by CCS due to floods for each basin of the Valencian Community for the period 1996-2015

Population in the Valencian Community
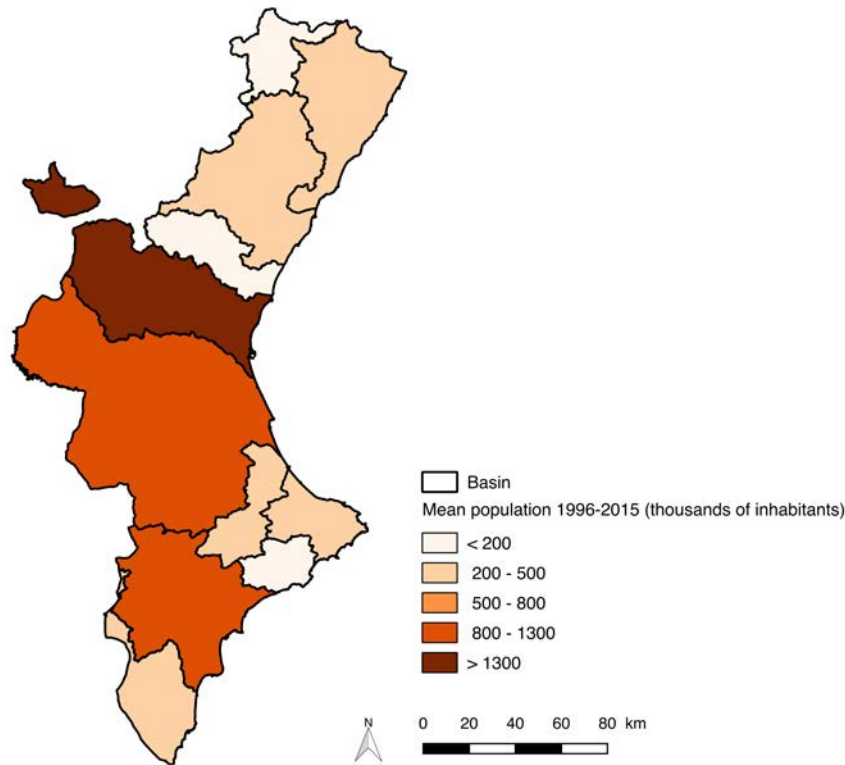
Figure 6.7: Average population in each basin of the Valencian Community for the period 1996-2015

The average population in each of the basins of the Valencian Community for the period 1996-2015 is represented in Figure 8.8. As can be observed, Turia is the most populated basin, with more than 1.3 million people living (29 % of the total population of the region) and, in addition, the one with the highest population density (more than 400 inhabitants km^{-2}).

6.3.2 Relationship between precipitation and flood damage in Catalonia

The Generalized Linear Mixed Model has been applied to all the flood events that have affected Catalonia basins within 1996-2015, which results in a total of 596 flood cases, 177 of which recorded an average precipitation in the basin higher than 40 mm (the sample used in the study). The formula considering the 70th percentile of damage is shown as an example in Equation 6.4:

$$\log(\frac{\pi}{1-\pi}) = -20.92 + 2.98\log(P) + 0.57\log(R) + b_i + b_j \tag{6.4}$$

Where π is the probability of exceeding the 70th percentile of damage (in this case), P the mean precipitation accumulated in the basin in 24 h, R the total population of the basin and b_i and b_j are the random effects related to the basin and the flood event.

Both precipitation and population are statistically significant, meaning that they are useful

variables to explain the probability of exceeding the 70th percentile of damage (0.38 M Euro). Similar results were obtained for all the percentiles of damage used (Table 6.3). In all cases both predictors present positive values proving that the probability of a damaging event increases not only with precipitation recorded in 24 h but also with the population of the basin. This can be observed in the examples in Figure 6.8, which show the effect of each explanatory variable in the case of probability exceeding the 70th percentile of damage. The solid line indicates the best estimate while the shaded blue bands show the 95 % confidence interval. For both variables, this probability increases rapidly. However, in the case of population a break point can be observed around 0.5 million people, above which the rate of increase is much lower.

Percentile	β_0	β_1	β_2	RA
10	-14.74	3.05	0.94	0.98
20	-12.98	-	0.72	0.94
30	-14.73	2.16	0.64	0.95
40	-24.87	3.12	1.11	0.97
50	-18.46	2.17	0.81	0.96
60	-17.74	2.10	0.69	0.95
70	-20.92	2.98	0.57	0.95
80	-27.22	4.19	0.54	0.96
90	-21.46	3.28	-	0.95

Table 6.3: Parameters of the Generalized Linear Mixed Model and RA values for all the percentiles of damage for Catalonia. β_0, β_1 and β_2 represent the regression coefficients of the model (intercept, precipitation and population, respectively). Only the significant regression coefficients (p value < 0.05) are displayed. See Table A.4 of the Appendix section for the damage thresholds definition
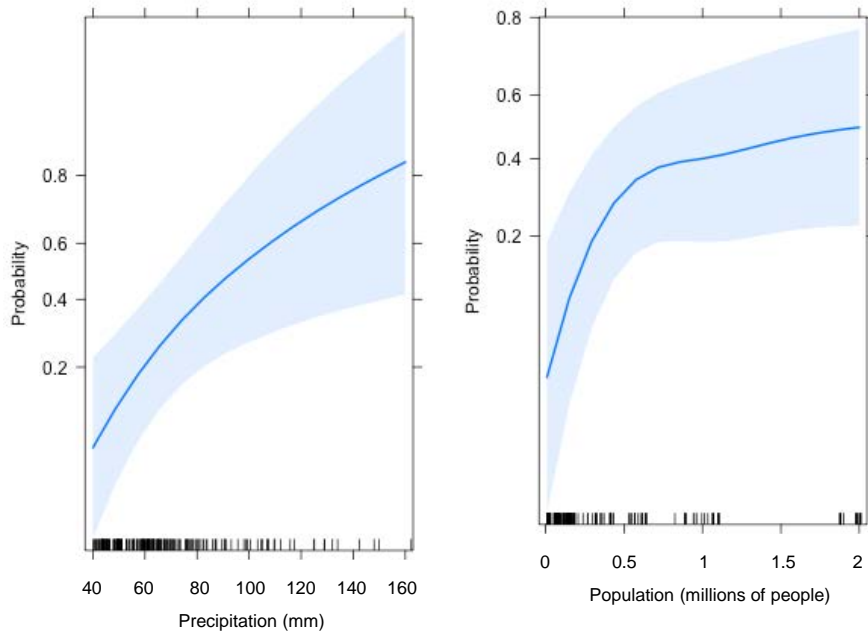
Figure 6.8: Effect of the explanatory variables (left: mean precipitation recorded in 24 h; right: total population of the basin) in the probability of exceeding the 70th percentile of damage in Catalonia. The solid lines indicate the best estimates while the shaded blue bands indicate the 95 % confidence interval. The black marks at the bottom of each graph represent the values of the independent variable for each flood case

Figure 6.9 shows the ROC diagram for the example shown in Equation 6.4. The RA value (0.95) indicates that our model has good fit to simulate the probability of a damaging event (defined as the 70th percentile of damage in this case). In this example, if the user wants to maximise the difference between the hit rate (0.94) and the false alarm rate (0.17), a probability value of 0.22 is needed (BT). The RA indicator for the different damage percentiles used is presented in Table 6.3 with values close to 1 for all the cases, indicating that the model has a good performance in all the examples. These results show that the incorporation of random effects in the model improves its performance, in respect of the generalized linear model or specifically the multiple logistic regression model used in the previous chapter (see results in Chapter 5).
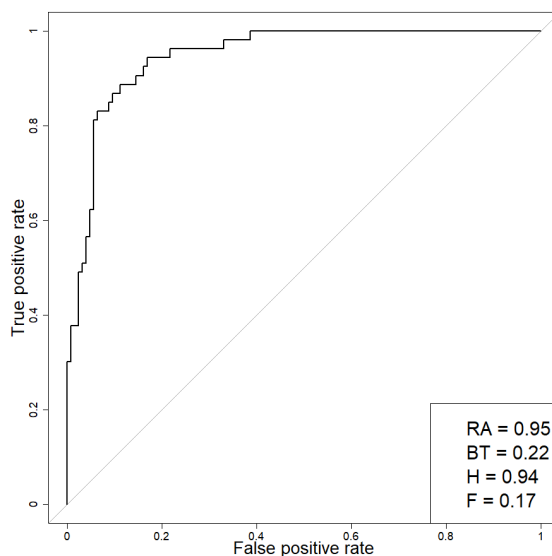
Figure 6.9: Relative operating characteristic (ROC) diagram for above 70th percentile of damage predictions using the Eq. 6.4 for Catalonia (P_0=40 mm 24 h^{-1}). Each value of the ROC curve indicates a set of probability forecasts by stepping a decision threshold with 1 % probability through the modelling results. The numbers inside the plot are the ROC area (RA) and the best threshold (BT), here defined as the threshold that maximises the difference between the hit rate (H) and the false alarm rate (F)

Application of the model for big flood cases

The same methodology has been applied to big flood cases (more information in Section 6.2.1). The model that simulates the probability of a big flood case in Catalonia follows the Equation 6.5:

$$\log(\frac{\pi}{1-\pi}) = -26.62 + 3.73\log(P) + 0.54\log(R) + b_i + b_j \tag{6.5}$$

For this example all the regression coefficients are statistically significant (p value < 0.05 with Wald Test) and both explanatory variables have positive values indicating that the probability of having a big case in Catalonia increases with precipitation and population. Figure 6.10 shows the effect of both explanatory variables in this probability. Although the confidence interval is quite wide indicating the existence of large variance in the prediction, the model performs well with a RA value of 0.96, as can be observed in the ROC diagram displayed in Figure 6.11. If it is absolutely essential to correctly classify every big flood case, we could choose a lower probability threshold, in order to reduce the risk of not predicting events with huge damages. This is the case of the present example, since the best RA value is achieved when the best threshold is low (BT=0.04), implying a high hit rate (H=0.95), however resulting in more false positives, and thus, increasing the false alarm rate (F=0.21). Therefore, the probability threshold depends on the risk that the user is willing to assume.
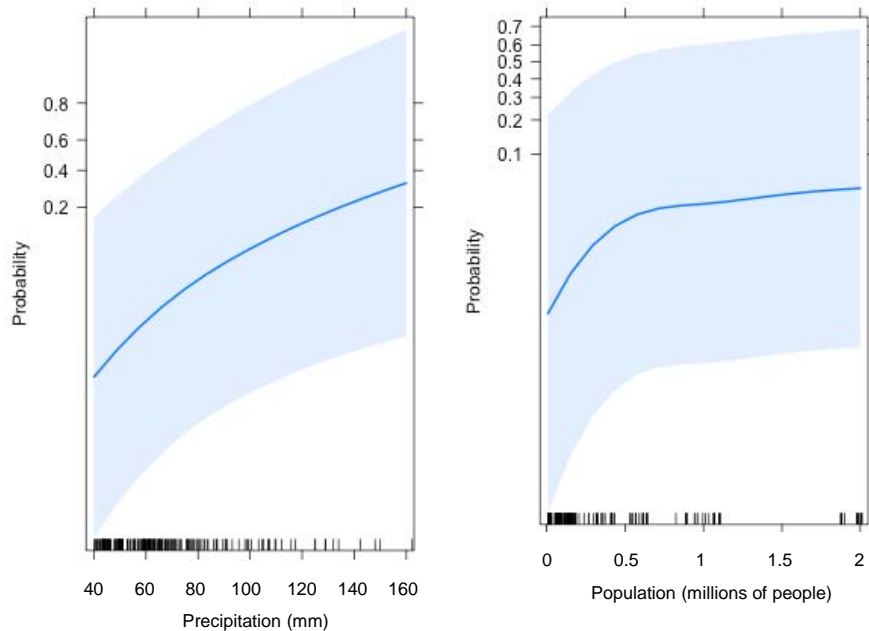
Figure 6.10: Effect of the explanatory variables (left: mean precipitation recorded in 24 h; right: total population of the basin) in the probability of occurrence a big flood case in Catalonia. The solid lines indicate the best estimates while the shaded blue bands indicate the 95 % confidence interval. The black marks at the bottom of each graph represent the values of the independent variable for each flood case
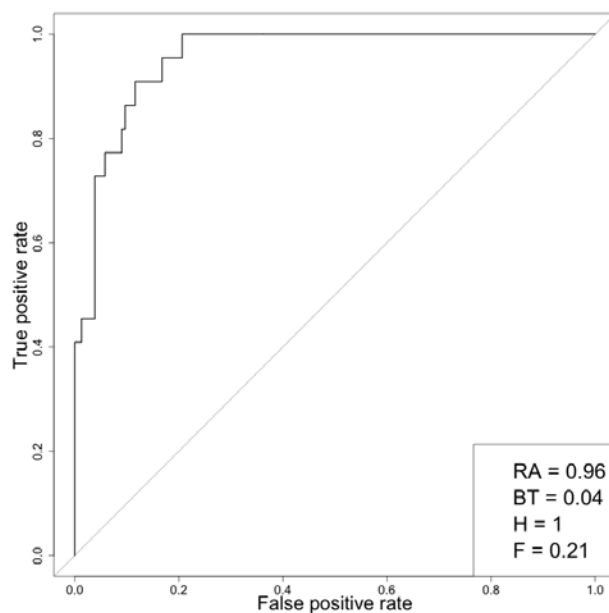
Figure 6.11: Relative operating characteristic (ROC) diagram for the big flood cases in Catalonia (P_0=40 mm 24 h^{-1}) using the Eq. 6.5. Each value of the ROC curve indicates a set of probability forecasts by stepping a decision threshold with 1 % probability through the modelling results. The numbers inside the plot are the ROC area (RA) and the best threshold (BT), here defined as the threshold that maximises the difference between the hit rate (H) and the false alarm rate (F)

This type of models also allow to show the relationship between the response variable and the predictors ones for each of the basins, since this variable is introduced in the model as a random effect. Figure 6.12 shows the linear relationship between mean precipitation and the probability of a big flood case (specific threshold of damage) for each basin of Catalonia. Most of them do not contain enough observations to get to a conclusion, however different behaviour can be found with this analysis. For example, from these results we could assume that basins like 700 and 774 (Maresme and Barcelona basins, respectively), belonging to high urbanised basins, have a linear slope steeper than other basins as 1001 or 1002 (La Muga and Fluvià, respectively), which are more rural, less urbanised (see Table A.6 and Figure A.1, Appendix section). From that we could conclude, but always taking into account that the sample is not large enough, that in urban basins the probability of big case occurrence increases more rapidly with precipitation than in rural basins. This would make sense since it would mean that the more urbanised basins have less infiltration rate and therefore less capacity to retain water.
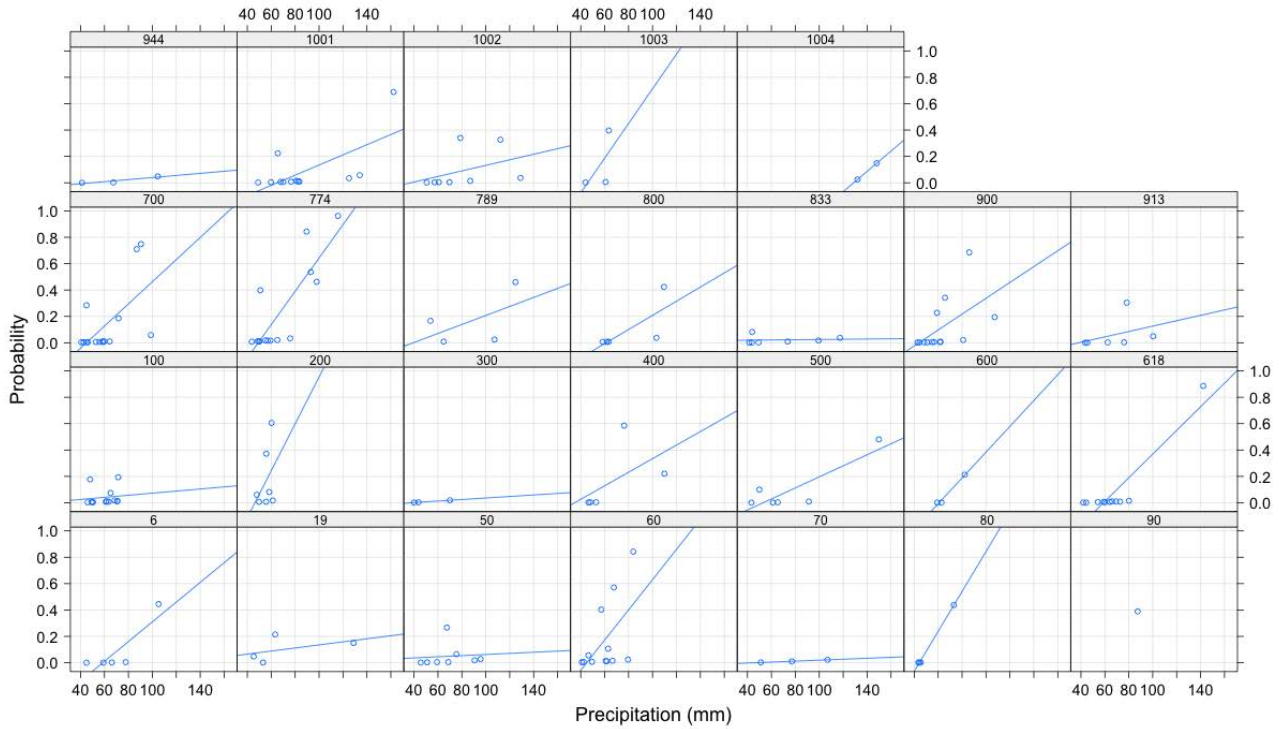
Figure 6.12: Relationship between mean precipitation accumulated in 24 h and the probability of big flood case in each basin of Catalonia. The headers indicate basins' code (see Table A.6 and Figure A.1, Appendix section)

6.3.3 Relationship between precipitation and flood damage in the Valencian Community

The same analysis has been carried out for the Valencian Community region, which was affected by 69 flood events between 1996 and 2015, resulting in 171 flood cases (72 if we only take into account the cases where the mean precipitation accumulated in 24 h in the basin exceeded the threshold of 40 mm 24 h^{-1}). As an example, the model follows Equation 6.6 when the damaging event is defined using the 70th percentile of damage:

$$\log(\frac{\pi}{1 - \pi}) = -40.96 + 2.33 \log(P) + 2.32 \log(R) + b_i + b_j \tag{6.6}$$

As in the case of Catalonia (Section 6.3.2) both mean precipitation accumulated in 24 h (P) and total population of the basin (R) are statistically significant and have positive regression coefficients. That is also the case for all the damage percentiles used, as can be observed in Table 6.4. That means that both explanatory variables are good predictors for estimating the probability of a damaging event as well as this probability increases with them. Figure 6.13 corroborates these results, showing the effect of precipitation (left graph) and population (right graph) on the probability of exceeding the 70th percentile of damage. In both cases this relationship is described by a concave curve, indicating that the increase in the probability per unit of increase of the predictor is larger when considering lower predictor values.

Percentile	β_0	β_1	β_2	RA
10	-183.57	34.47	4.95	1.00
20	-188.88	32.58	5.53	1.00
30	-43.83	4.59	1.99	1.00
40	-42.40	3.14	2.31	0.96
50	-42.85	3.06	2.32	0.90
60	-60.63	4.46	3.16	0.95
70	-40.96	2.33	2.32	0.90
80	-49.60	3.80	2.41	0.89
90	-50.97	4.05	2.34	0.94

Table 6.4: Parameters of the Generalized Linear Mixed Model and RA values for all the percentiles of damage for the Valencian Community. β_0, β_1 and β_2 represent the regression coefficients of the model (intercept, precipitation and population, respectively). Only the significant regression coefficients (p value < 0.05) are displayed. See Table A.5 of the Appendix section for the damage thresholds definition
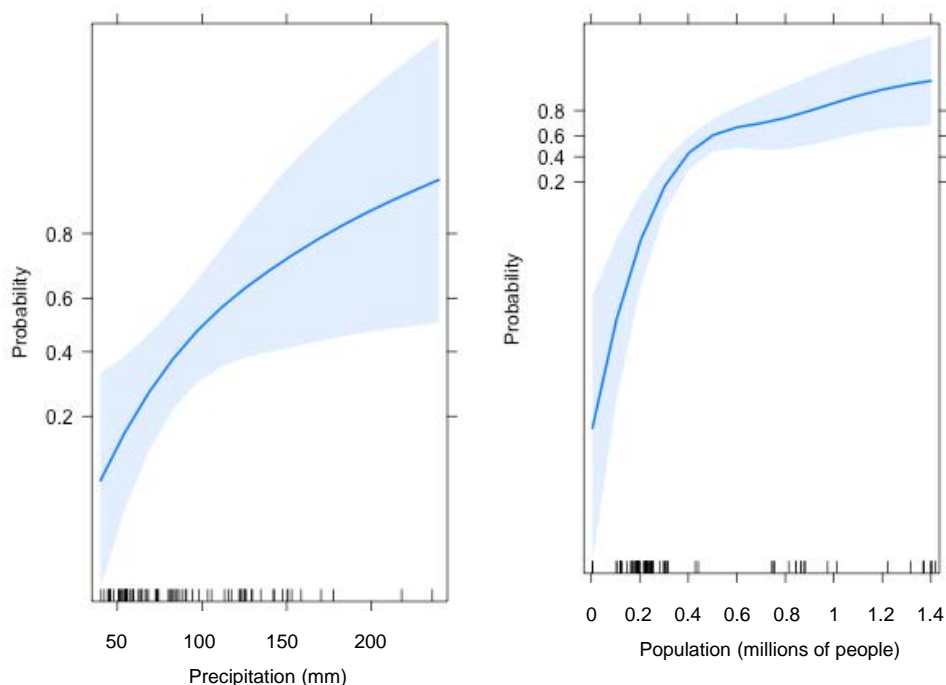
Figure 6.13: Effect of the explanatory variables (left: mean precipitation recorded in 24 h; right: total population of the basin) in the probability of exceeding the 70th percentile of damage in the Valencian Community. The solid lines indicate the best estimates while the shaded blue bands indicate the 95 % confidence interval. The small black bars at the bottom of the graphs represent the values of the independent variable for each flood case

The shaded blue bands of Figure 6.13 show the confidence level of the prediction at 95 %. In this case, these bands are narrower than in the Catalonia case (see Figure 6.8), showing that the model estimation is more precise for the Valencian Community region. Figure 6.14 displays the ROC diagram for the example of Equation 6.6, demonstrating that the model has a significant goodness of fit with a RA value of 0.9. As shown in Table 6.4, the model has a good performance for all the damage percentiles, with RA values close to 1 in all cases. Lower percentiles of damage (10, 20 and 30th) have RA values equal to 1, meaning that the model is able to totally differentiate between event and non-event for these damage thresholds. This

could be due to the low values of these percentiles (0.05, 0.21 and 0.36 M Euro, respectively; see Table A.5, Appendix section).
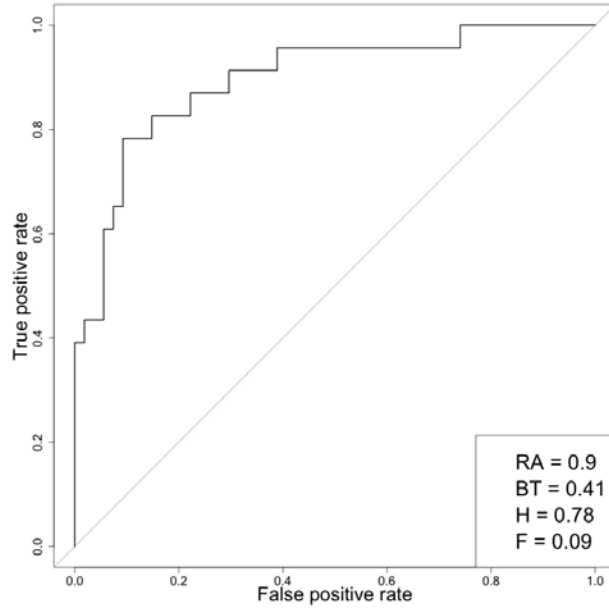
Figure 6.14: Relative operating characteristic (ROC) diagram for above 70th percentile of damage predictions using the Eq. 6.6 for the Valencian Community (P_0=40 mm 24 h^{-1}). Each value of the ROC curve indicates a set of probability forecasts by stepping a decision threshold with 1 % probability through the modelling results. The numbers inside the plot are the ROC area (RA) and the best threshold (BT), here defined as the threshold that maximises the difference between the hit rate (H) and the false alarm rate (F)

Application of the model for big flood cases

The catastrophic flood events in the Valencian Community (16 % of total events) cause in average 43.6 M Euro in insurance damage according to CCS. The same methodology has been applied for knowing when a big flood case (regarding to the impact classification based on FLOODHYMEX database) will occur in the region based on the mean precipitation accumulated in 24 h and the total population of the basin. The formula of the model follows the Equation 6.7:

$$\log(\frac{\pi}{1-\pi}) = -46.88 + 3.97 \log(P) + 1.86 \log(R) + b_i + b_j \tag{6.7}$$

As could be expected, the probability of a big flood case increases with precipitation and population, being both significant explanatory variables. Figure 6.15 corroborates this positive relationship showing the effect of both explanatory variables in this probability. The ROC diagram for this model is presented in Figure 6.16 demonstrating that the model has skill, with a RA value of 0.92. The maximum difference between hit rate and false alarm rate will be obtained when the model predicts a probability of 0.31 (BT), with a resulting hit rate of 0.83 and false alarm rate of 0.10.
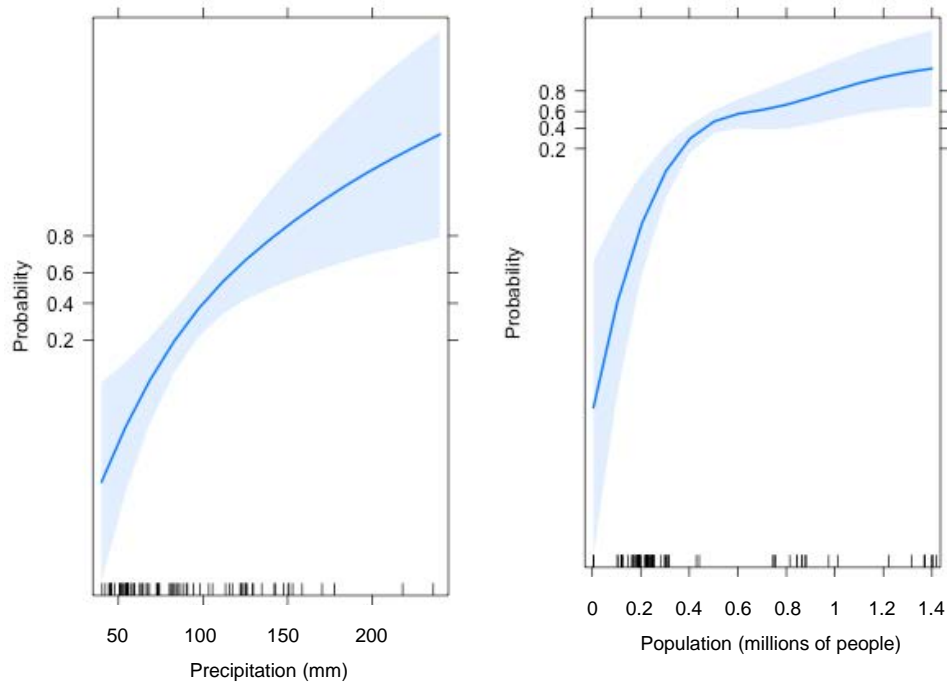
Figure 6.15: Effect of the explanatory variables (left: mean precipitation recorded in 24 h; right: total population of the basin) in the probability of occurrence a big flood case in the Valencian Community. The solid lines indicate the best estimates while the shaded blue bands indicate the 95 % confidence interval. The small black bars at the bottom of the graphs represent the values of the independent variable for each flood case
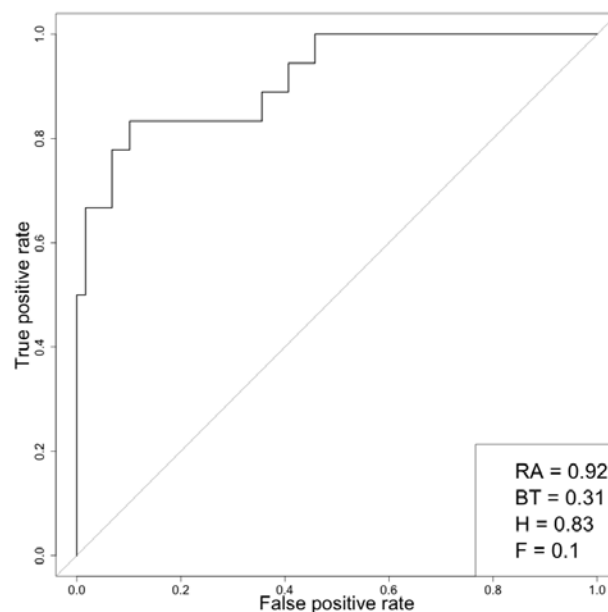
Figure 6.16: Relative operating characteristic (ROC) diagram for the big flood cases in the Valencian Community using the Eq. 6.7 (P_0=40 mm 24 h^{-1}). Each value of the ROC curve indicates a set of probability forecasts by stepping a decision threshold with 1 % probability through the modelling results. The numbers inside the plot are the ROC area (RA) and the best threshold (BT), here defined as the threshold that maximises the difference between the hit rate (H) and the false alarm rate (F)

Figure 6.17 shows the linear relationship between the precipitation and the probability of big flood case occurrence. The basins that have higher number of observations present similar slopes, being the ones of basins 128 and 130 slightly steeper (Júcar and Túria basins, respectively), where more population live (see Table A.7 and Figure A.2, Appendix section).
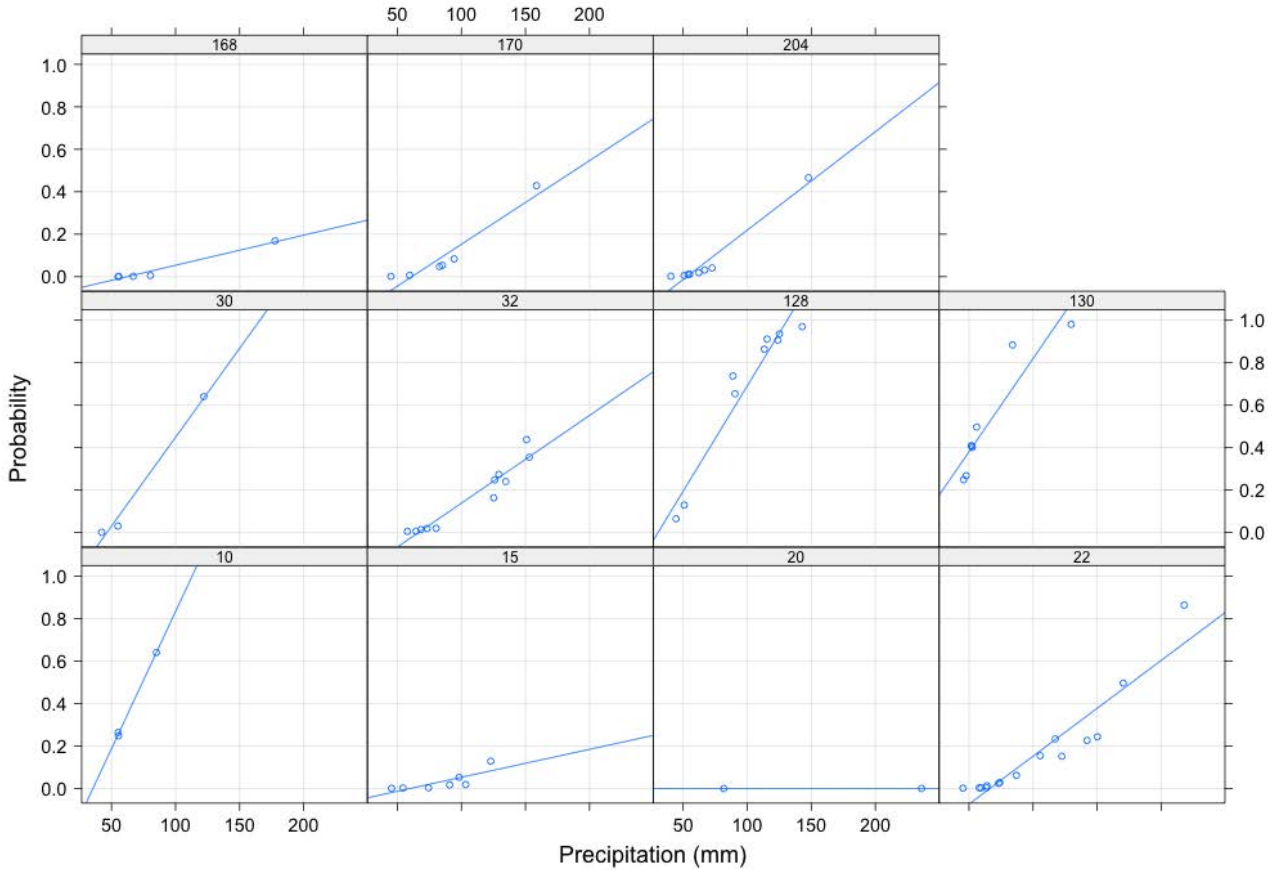
Figure 6.17: Relationship between mean precipitation accumulated in 24 h and the probability of big flood case in each basin of the Valencian Community. The headers indicate basins' code (see Table A.7 and Figure A.2, Appendix section)

6.4 Conclusions

The NW Mediterranean region experiences heavy precipitation every year and flash floods that occasionally produce catastrophic damages (Llasat et al., 2013). Both of the western Mediterranean regions covered in this chapter (Catalonia and the Valencian Community) are prone to these events, most of them caused by local heavy precipitation events (Llasat et al., 2016b).

In this chapter, the relationship between heavy precipitation and flood damage for both regions has been analysed. Generalized Linear Mixed Models have been used in order to estimate the probability of damaging events taking into account both hazard and exposure. In order to select the explanatory variables that more contribute in explaining the variance of the response variable (probability of exceeding a specific damage threshold), a selection process has been carried out. The best model for both regions was the one with the mean precipitation

accumulated in 24 h and the total population of the basin as independent variables.

The results show that the probability of a damaging event increases with precipitation and population of the basin. For both regions of study the RA values indicate that our model has a good performance, with values close to 1 in all cases. These results improve those obtained by using both simple and multiple logistic model in the case of Catalonia (see Chapter 5 and Cortès et al., 2018), demonstrating that the incorporation of random effects in the model improves its performance, since, in general, better RA values are achieved when applying GLMMs. In this chapter, apart from using different percentiles of damage for defining damaging event, a model with a specific damage threshold has also been developed for each region. This threshold allows to define a big flood case based on the mean insurance compensation received for the catastrophic flood events. The results using this model also show a good performance (RA value of 0.96 and 0.92 for Catalonia and the Valencian Community, respectively), being able to distinguish between big flood case and non big flood case, given a precipitation and population values. Furthermore, the incorporation of the basins as random effects in the model has allowed to study the relationship between precipitation and probability of having a big flood case independently per each basin. This analysis has permitted to describe a different general behaviour within basins: in the more urbanised basins this probability increases faster with precipitation than in the less urbanised ones, pointing out the importance of having high permeable surfaces in order to be able to retain the water more efficiently.

To summarise, the main novelties introduced in this chapter are the incorporation of the Valencian Community region, an area heavily affected by flood events that produce huge damages, and the improvement of the model that allows to predict when a damaging event will occur based on the precipitation recorded and the population of the basin.

The results obtained in this chapter are of great importance for analysing the flood risk and understanding the relationships between flood damage and their causes. The same methodology and relationships found will be applied in order to predict the future probability of a damaging event taking into account the future precipitation climate change projections as well as different population scenarios (see Chapter 8).

Chapter 7

Future projections of precipitation extremes in the Iberian Peninsula

Abstract

In this chapter[3], an assessment of projected changes in precipitation extremes considering the RCP 8.5 scenario and an ensemble of seven regional climate models is done. After a synthesis of state-of-the-art of the extreme precipitation projections, the climate simulations performed under the umbrella of the EURO-CORDEX project with a spatial resolution of 0.11 degree both in latitude and longitude, have been applied to the Iberian Peninsula. Different climate indices are calculated in order to estimate the changes in precipitation assuming global warming scenarios of 1.5, 2 and 3 °C above preindustrial levels. The results show a general decrease of the total annual precipitation and an increase in the length dry spell in most of the Peninsula which becomes greater with higher global warming levels and during summer months. This will probably exacerbate water scarcity and droughts impacts, which are already a problem in the area. However, a likely increase in heavy precipitation events with global warming especially during winter months can be found in the north and north-east of the Iberian Peninsula. That points out the need of improving flood management strategies in order to deal with a possible increase of the impacts caused by rainfall-related flood events.

7.1 Introduction

As has been told in previous chapters, the extreme precipitation events cause huge economic and human damage in different parts of the world, such as the Mediterranean area, where the risk of flooding is the most important natural hazard (Llasat et al., 2013). For this reason, a great concern exists about the impact that climate change could have on these extreme episodes. Although there are a large number of studies that have found a projected decrease in the mean annual precipitation in the Mediterranean (Jacob et al., 2014; Cramer et al., 2018; Sillmann et al., 2013; Rajczak and Schär, 2017), there are also many others that have observed an

---

[3]The contents of this chapter have been partially published in Turco et al. (2018a)

increase in extreme precipitation events with global warming (Drobinski et al., 2018; Colmet-Daage et al., 2018; Tramblay and Somot, 2018; Cramer et al., 2018), mostly during winter months (Kjellström et al., 2018; Vautard et al., 2014; Rajczak and Schär, 2017; Jacob et al., 2014).

Different methods exist to study the changes in the precipitation extremes. For instance, the climate indices are applied in a considerable number of studies (usually the ones developed by the Expert Team on Climate Change Detection and Indices -ETCCDI-, Karl et al., 1999; Peterson et al., 2001), both at global (Donat et al., 2016; Betts et al., 2018; Sillmann et al., 2013) and at regional scale (for example for Europe: Rajczak and Schär, 2017; Vautard et al., 2014).

Most of the methods use a future fixed period of years to assess the changes in the precipitation extremes due to climate change, such as for the last 30 years (2071-2100) of the 21st century (e.g. Colmet-Daage et al., 2018). However, many authors study this change related to the increase in the global temperature (Vautard et al., 2014; Betts et al., 2018; Kjellström et al., 2018). The Paris Agreement of the United Nations Framework Convention on Climate Change (UNFCCC), signed in December 2015, aims to *hold the increase in the global average temperature to below 2 °C above preindustrial levels and to pursue efforts to limit the temperature increase to 1.5 °C....* From this conference came the commitment of the IPCC to prepare a special report (Masson-Delmotte et al., 2018) which quantifies the impacts with a global warming of 1.5 °C with respect to preindustrial conditions (https://www.ipcc.ch/sr15/). One of the main results of the report is the increase of the human and economic impact of the climatic risks with a warming of 1.5 °C. Therefore, scientists are urged to quantify socioeconomic impacts for different warning thresholds. For instance, recent research efforts have significantly boosted our knowledge on the risks at 1.5 and 2 °C of warming, focusing relevant climate change impacts as for instance on economy (Burke et al., 2018), agriculture (Schleussner et al., 2016), the study of forest fires (Turco et al., 2018b), power generation (Tobin et al., 2018) and ecosystems (Guiot and Cramer, 2016).

Previous works consistently indicate that flood risk is expected to increase in the future in most world regions, with largest increase in Asia, America and Europe (Alfieri et al., 2017). Donnelly et al. (2017) showed that for most of Europe, the impacts of climate change on mean, low and high runoff and mean snowpack in Europe increase with increased warming level, however they do not provide an assessment of change in extremes. Vautard et al. (2014) observed an increase in average precipitation in northern Europe and a decrease in the central and southern parts, but with a general increase of the extreme precipitation events in most Europe with a warming of 2 °C, especially during winter months. King and Karoly (2017) analysed changes in the highest 1-day precipitation and indicated that there are signs that the heaviest rainfall events will likely intensify at 2 °C warming compared to 1.5 °C principally in the northern half of Europe. This larger and more robust change with 2 °C was also confirmed by Kjellström et al. (2018), that indicated that the changes in precipitation include increases in the north and decreases in the south of Europe. The precipitation decrease plays an important

role in the projected increase in future drought conditions in these areas. Global drought assessments coincide to identify the Mediterranean region as a hotspot for future drought increases (Lehner et al., 2017; Naumann et al., 2018; Park et al., 2018). However, a detailed local-scale study analysing both precipitation and runoff changes, considering both the upper tail extremes and the drought conditions, remain to be done.

The Iberian Peninsula, located on the south-west edge of Europe, is an ideal case study when it comes to the relationship between global warming and the projections of precipitations in the future. Reasons are as follows. Firstly, precipitation plays a major role on natural hazards and water resources (Garrote et al., 2007; Llasat et al., 2009), thus leading to one of the most vulnerable countries to water scarcity, droughts and floods in Europe (Kristensen, 2010). Secondly, its complex orography and particular location - at the transition area between extra-tropical and subtropical influence (Giorgi and Lionello, 2008) - leads to a great variety of climates with both Atlantic and Mediterranean influences. Due to this strong variability, this region represents a challenging area when it comes to downscaling studies (see e.g. Jiménez-Guerrero et al., 2013; Turco et al., 2017).

Taking these points into account, the aim of this chapter is to analyse the change in the precipitation extremes using an ensemble of state-of-the-art regional climate projections (RCM) in the Iberian Peninsula at 1.5, 2 and 3 °C of mean global warming. Due to the seasonal differences found in previous studies at Europe (Jacob et al., 2014; Vautard et al., 2014; Kjellström et al., 2018; Rajczak and Schär, 2017) and Mediterranean level (Colmet-Daage et al., 2018; Cramer et al., 2018), the analysis is carried out both at annual and seasonal scale. The Iberian Peninsula as a whole has been chosen as a framework to contextualise the projections of the actual study area of the thesis (Catalonia and the Valencian Community).

7.2 Data and methods

7.2.1 Precipitation data

The Representative Concentration Pathways (RCPs) are a set of climate projections developed by the scientific community in order to facilitate future assessment of climate change. Their main purpose is to provide information on possible development trajectories for the main forcing agents of climate change (Van Vuuren et al., 2011). In total, a set of four pathways were produced that lead to radiative forcing levels of 8.5, 6, 4.5 and 2.6 W m^{-2}, by the end of the 21st century. In this study, daily historical simulations from 1976 to 2005 and climate projections assuming the RCP 8.5 scenario (8.5 W m^{-2}) from the Fifth Assessment Report of the Intergovernmental Panel on Climate Change (Pachauri et al., 2014) from 2006 to 2100 are calculated using an ensemble of seven regional climate simulations. The simulations were performed under the umbrella of the EURO-CORDEX project (Jacob et al., 2014), covering Europe with a spatial resolution of 0.11 degrees both in latitude and longitude (around 12 km). Tramblay et al. (2013) observed an improvement in the representation of precipitation and its extremes at this resolution compared with previous simulations at 25 and 50 km resolution.

These projections consist of high-resolution downscaling of General Circulation Models (GCMs) from the CMIP5 (5th Coupled Model Intercomparison Project; Taylor et al., 2012), which contain tens of realisations of future climates (Alfieri et al., 2018). Their outputs are used to provide boundary conditions for higher-resolution regional climate models (RCMs). Overall, the seven climate projections used in this study are combinations of three different GCMs which were then downscaled with four RCMs, as shown in Table 7.1.

Model	Institute	GCM	RCM	1.5 °C	2 °C	3 °C
1	KNMI	EC-EARTH	RACMO22E	2017–2046	2032–2061	2055–2084
2	SMHI	HadGEM2-ES	RCA4	2011–2040	2023–2052	2041–2070
3	SMHI	EC-EARTH	RCA4	2014–2043	2028–2057	2053–2082
4	MPI-CSC	MPI-ESM-LR	REMO2009	2017–2046	2031–2060	2054–2083
5	CLMcom	MPI-ESM-LR	CCLM4-8-17	2017–2046	2031–2060	2054–2083
6	SMHI	MPI-ESM-LR	RCA4	2017–2046	2031–2060	2054–2083
7	CLMcom	EC-EARTH	CCLM4-8-17	2014–2043	2028–2057	2053–2082

Table 7.1: EURO-CORDEX climate models used, their characteristics and the periods of each simulation for the three warming levels considered in this study

7.2.2 Estimation of warming thresholds

In this study, the changes in the extremes of precipitation assuming a global warming projections of 1.5, 2 and 3 °C above preindustrial levels (1881-1910) are analysed (Vautard et al., 2014). For each simulation, the year when a 20-year running mean of global average temperature exceeds 1.5, 2 and 3 °C in the RCP8.5 is identified and then a 30-year time window applied for each warming period and model. Therefore, for each simulation we have 3 periods of 30 years, described in Table 7.1, as well as the reference period 1976-2005. This method is based on the guidelines of the HELIX project (Betts et al., 2018), also applied in others studies such as Alfieri et al. (2018). As can be observed in Table 7.1, the simulations show a certain agreement with warming periods from 2011-2040 to 2017-2046 for 1.5 °C, from 2023-2052 to 2032-2061 for 2 °C and from 2041-2070 to 2055-2084 for 3 °C.

7.2.3 Precipitation extremes indices

Several extreme precipitation indices from the Expert Team on Climate Change Detection and Indices (ETCCDI, Karl et al., 1999; Peterson et al., 2001) have been selected in order to analyse the future change in the precipitation extremes. Table 7.2 summarises the indices used.

These indices are estimated for each of the future warming periods as well as for the reference period 1976-2005 and both at annual and seasonal level. Then, the relative change of each warming period with respect to the reference one is calculated and represented. The seasons considered are: DJF (December, January, February) months for winter, MAM (March, April, May) for spring, JJA (June, July, August) for summer and SON (September, October, November) for autumn. Furthermore, the season including July, August and September (JAS) has additionally been included into the study with the purpose of checking whether there is

an increase in the convective precipitation during these months, as observed in Llasat et al. (2016b).

Index	Name/description
PRCPTOT	Annual total precipitation in wet days
CDD	Maximum length of dry spell
CWD	Maximum length of wet spell
SDII	Simple precipitation intensity index
Rx1day	Annual maximum 1-day precipitation
Rx5day	Annual maximum consecutive 5-day precipitation
R10mm	Annual count of days with precipitation > 10 mm
R20mm	Annual count of days with precipitation > 20 mm
R40mm	Annual count of days with precipitation > 40 mm
R60mm	Annual count of days with precipitation > 60 mm

Table 7.2: Description of the ETCCDI extreme precipitation indices used in the study

7.2.4 Ensemble robustness

In this study an ensemble map of the 7 models of the change of each index and period with respect to the reference period will be shown. A method to analyse the robustness of the ensemble has been applied, following the one developed in Tebaldi et al. (2011), where both the agreement in the sign of the change and the statistical significance of each model are considered. This method allows to distinguish if the changes, related to the reference period, are due to the natural variability or there is a climate change sign. The method uses the following steps, for each grid point: 1) tests for significant change in each of the models individually with a t-test comparing the mean of the reference (1976-2005) and the future period (the three warming periods), 2a) if less than half of the models (50 %) show a significant change then the mean change will be shown in colour in the ensemble map, 2b) if more than 50 % of the models show significant change then test for agreement in sign will be done by the following criteria, 3a) if less than 66 % of the significant models agree on the sign then the grid point will be painted as white, 3b) if more than 66 % agree on the sign the colour will be accompanied by an asterisk.

7.3 Results

Figure 7.1 shows the changes in the PRCPTOT index with respect to the reference period 1976-2005 at annual and seasonal scale for a warming of 1.5 °C, 2 °C and 3 °C above preindustrial conditions (1880-1910) for the entire Iberian Peninsula. A significant trend and an agreement within the models in the decrease of the total annual precipitation can be found in the south and centre of the Iberian Peninsula, mostly for greater warming level (3 °C). Furthermore, this negative trend is also observable at mountain areas (Cantabrian Mountains and the Pyrenees). This decrease is mainly due to summer months (JJA), when a more pronounced and widespread reduction of precipitation is produced for the whole Iberian Peninsula with the increase of 3 °C of the global temperature. This behaviour, but less general, is also observed during the JAS months. In the case of Catalonia, no significant changes are observed in most models.

However, it is possible to detect a significant trend, and with an agreement in the sign within simulations, of a decrease between 10 and 20 % in the total annual precipitation in the Pyrenees when the period of greatest global warming (3 °C) is considered. Actually, studies such as Lemus-Canovas et al. (2019) have already observed a statistically significant negative trend in the annual precipitation recorded between 1960 and 2010 in some parts of this mountain range. For the Valencian Community, a general and significant decrease is expected for the whole year, with the exception of the autumn months.

The annual increase in the length of dry spell (CDD) is a general and marked change with agreement between models for the whole Iberian Peninsula, especially with the warming periods of 2 and 3 °C (Figure 7.2). This increment is observed in the north and east of the Peninsula (and therefore, in the regions of study) mainly in summer months (JJA and JAS), however, during spring months (MAM) is more evident in the centre and south of the area.

In contrast to the CDD index, the maximum length of wet spell (CWD) drops with global warming (Figure 7.3), especially in the south, centre and west of the Iberian Peninsula. The months of spring (MAM) and summer (JJA) are those that contribute most to this decrease. Models also agree with this decrease in some parts of the Pyrenees, but predominantly for the highest warming period (3 °C). The annual reduction is around 10-20 % where an agreement between models is produced (shown with an asterisk), although this value can exceed the 30 % during summer months. In the Valencian Community this decrease is more pronounced than in Catalonia region, exceeding the 20 % of reduction during summer months when the highest warming period is considered.

The simple precipitation intensity index (SDII) shows an increment in most of the Iberian Peninsula except for some areas of the north and south (Figure 7.4). The agreement between models in this increase is observed especially for the greater warming period (3 °C), with an annual value higher than 10 % in some parts of Catalonia and Aragon. Most models agree with the increment in the precipitation intensity during winter months (DJF), however a decrease around 20-30 % is found in most of the north, south and west of the Peninsula during autumn months (SON). While in Catalonia a general increase is expected, mainly during the months of winter and spring, although with the exception of the Pyrenees, in the Valencian Community there is no a clear signal. However, decreases in the SDII index are expected in the south of this region in almost all seasons of the year, with the exception of the spring months.

Figure 7.5 represents the change in the maximum daily precipitation index (Rx1day). The results show no significant change with respect to the reference period in most of the Iberian Peninsula at annual scale, and only a significant increase around 10-20 % is found in the Llobregat basin (Catalonia), probably related to autumn and winter months. The seasonal analysis does not show any significant positive change, however a reduction in the maximum 1-day precipitation can be found in some parts of the south, south-east and north-west of the Peninsula from June to September. In contrast to Catalonia, a general decrease in this index can be found in the Valencian Community mainly during summer months with reductions higher than 20 %.

The maximum precipitation recorded in 5 consecutive days (Rx5day, Figure 7.6) shows a pattern similar to the maximum daily one (Figure 7.5), with barely agreement between models at annual scale. Only some parts of Catalonia and Aragon indicate an increase in this index, in contrast to the south and south-east (the Valencian Community) of the Iberian Peninsula where a decrease is found. However, if the seasonal change is considered, a significant reduction around 10-40 % with respect to the reference period is detected in the south, south-east and north-west of the Peninsula from March to September.

A robust negative change with global warming can be found in the number of days with precipitation higher than 10 mm (R10mm), as shown in Figure 7.7. This trend is clearly detected in the south and west of the Peninsula and in the northern mountain areas. On the contrary, a statistically significant increase in this index with respect to the reference period with an agreement higher of 66 % between models can be found in the Ebro and Duero basins during winter months (DJF). On the other hand, the decrease in daily precipitation exceeding 10 mm is very evident for summer months (JJA and JAS) reaching more than 40 % compared to the reference period in some parts of the south-east and north-west of the Peninsula. Both regions of study show a general decrease in this index, however some increases can be found in Catalonia during winter months.

The number of days with daily precipitation above 20 mm (R20mm) shows a pattern similar to the 10 mm (Figure 7.7), with a pronounced and statistically significant decrease around 20-30 % in this index in the south of the Peninsula for the greater warming period (3 °C), but not as general as the previous index for the rest of the area (see Figure 7.8). During winter months a more intensive and widespread increment of these events are observed in Duero, Ebro and Catalan basins, although not being statistically significant in most areas. On the contrary, an evident decrease of this index is found in the east, south-east and north-west of the Peninsula with reduction values higher than 40 % when the 3 °C warming period is considered. In the case of the Valencian Community, a general decrease in this index is found in all the seasons, however increases are expected in Catalonia from December to February.

The same pattern previously observed in the R10mm and R20mm indices (Figures 7.7 and 7.8, respectively) is also maintained when the number of days exceeding precipitations higher than 40 mm (Figure 7.9) is analysed, although with a greater domain of the increase of these events in most of the northern half of the Iberian Peninsula. This increment happens mainly during autumn and winter months, being statistically significant in some parts of Catalonia when an increase in the global temperature of 3 °C above preindustrial conditions is considered. On the other hand, an annual reduction of these events can be found in the south of the Peninsula, especially for the higher warming periods (2 and 3 °C). In contrast to Catalonia, a general decrease in this index is observed in the Valencian Community for almost all seasons of the year.

The R60mm index (Figure 7.10) shows a great variability both at annual and seasonal scale, only with a statistically significant increase in some parts of Catalonia and decrease in Andalusia when the greater warming period (3 °C) is taken into account. A pattern of an

increment of the events with daily precipitation exceeding 60 mm in the centre and north of the Peninsula and a reduction in the south of the area and north mountain areas (Cantabrian Mountains and the Pyrenees) can be found. This variability and differences between models increase when the analysis is done at seasonal scale.
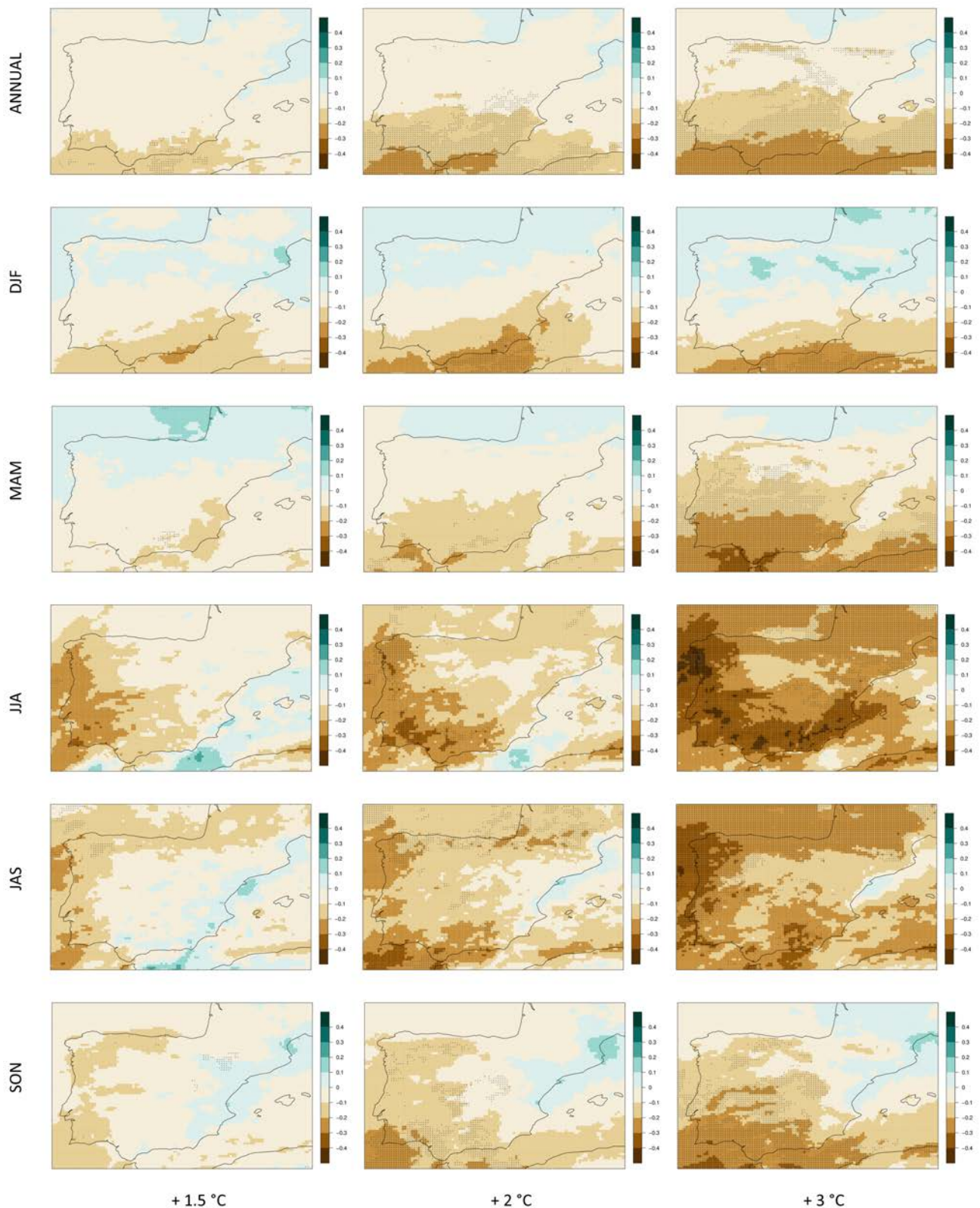
Figure 7.1: Ensemble mean of the relative change of total precipitation (PRCPTOT) for 1.5, 2 and 3 °C global warming (columns) at annual and seasonal scale (rows). Asterisks indicate areas where at least 50 % of the simulations show a statistically significant change and more than 66 % agree on the direction of the change. Coloured areas (without asterisk) indicate that changes are small compared to natural variations, and white regions (if any) indicate that no agreement between the simulations is found (similar to Tebaldi et al., 2011)
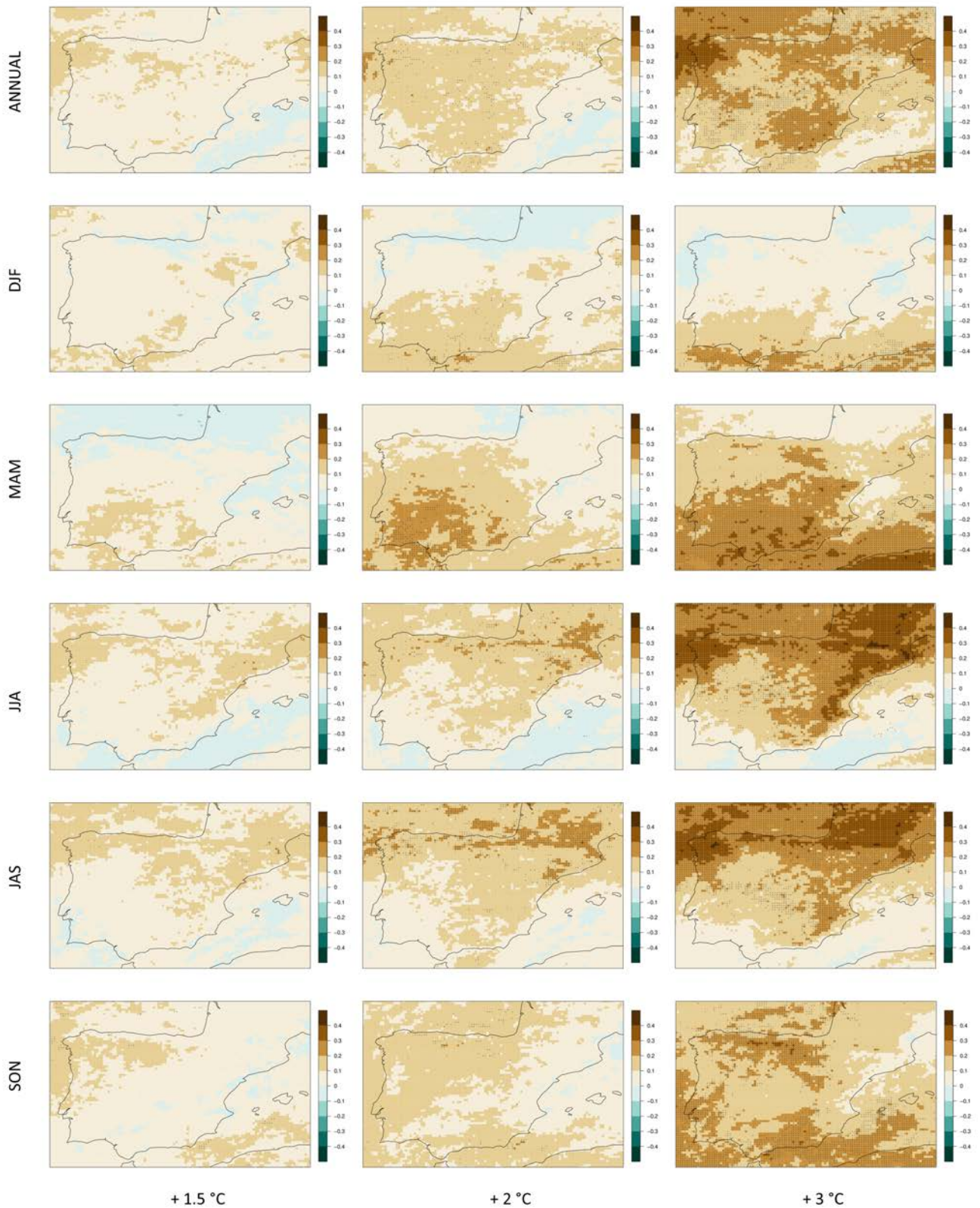
Figure 7.2: Ensemble mean of the relative change of maximum length of dry spell (CDD) for 1.5, 2 and 3 °C global warming (columns) at annual and seasonal scale (rows). Asterisks indicate areas where at least 50 % of the simulations show a statistically significant change and more than 66 % agree on the direction of the change. Coloured areas (without asterisk) indicate that changes are small compared to natural variations, and white regions (if any) indicate that no agreement between the simulations is found (similar to Tebaldi et al., 2011)
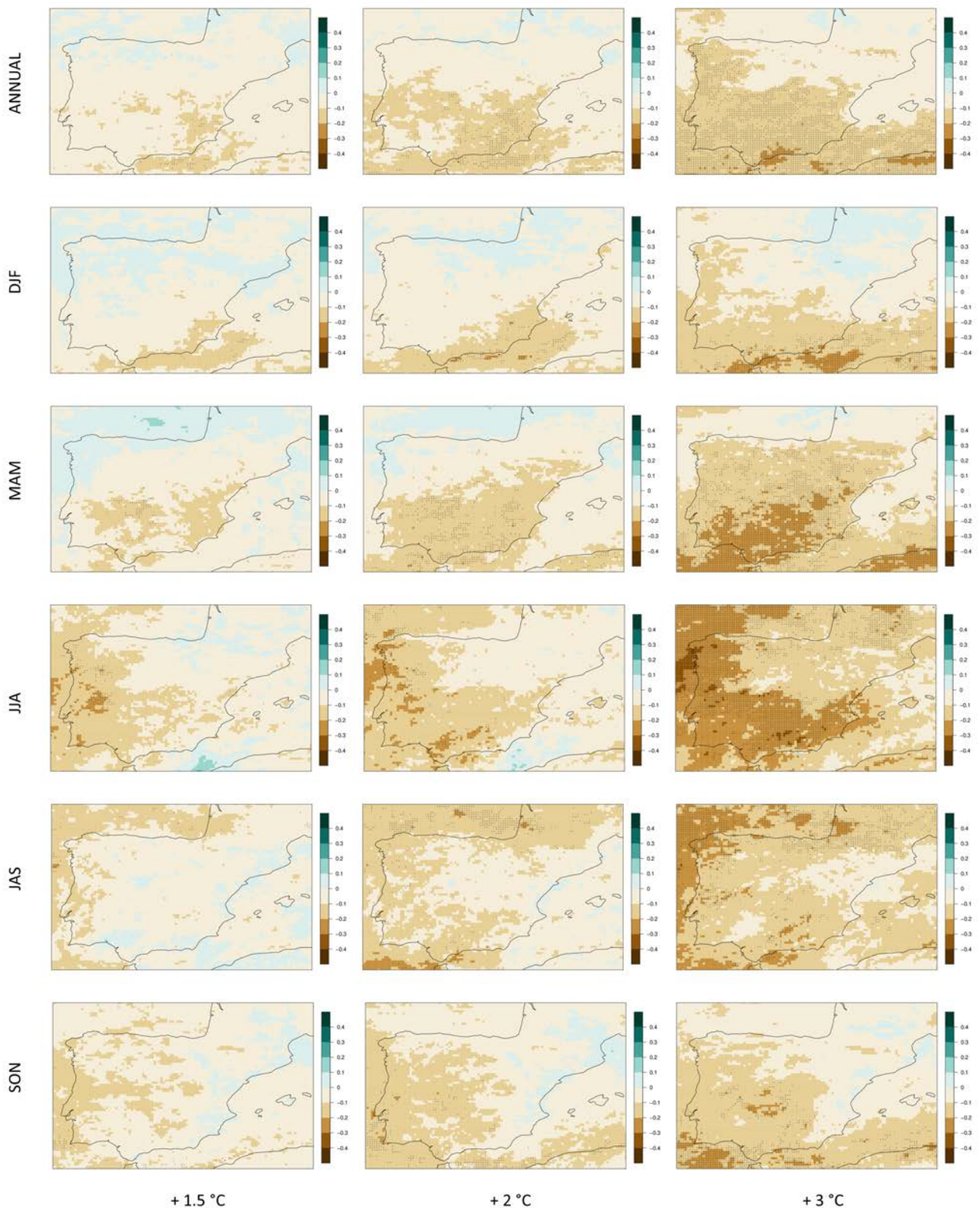
Figure 7.3: Ensemble mean of the relative change of maximum length of wet spell (CWD) for 1.5, 2 and 3 °C global warming (columns) at annual and seasonal scale (rows). Asterisks indicate areas where at least 50 % of the simulations show a statistically significant change and more than 66 % agree on the direction of the change. Coloured areas (without asterisk) indicate that changes are small compared to natural variations, and white regions (if any) indicate that no agreement between the simulations is found (similar to Tebaldi et al., 2011)
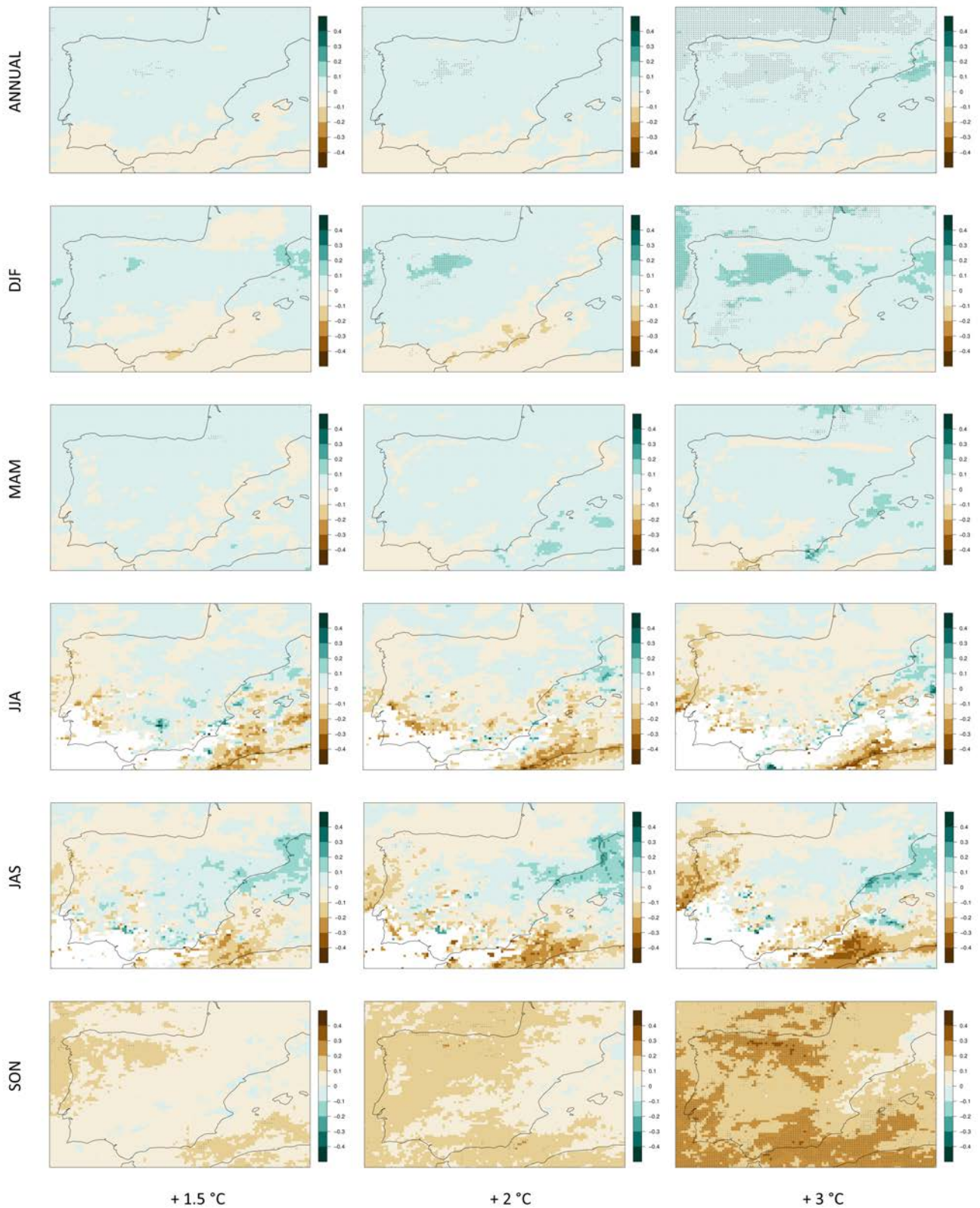
Figure 7.4: Ensemble mean of the relative change of simple precipitation intensity index (SDII) for 1.5, 2 and 3 °C global warming (columns) at annual and seasonal scale (rows). Asterisks indicate areas where at least 50 % of the simulations show a statistically significant change and more than 66 % agree on the direction of the change. Coloured areas (without asterisk) indicate that changes are small compared to natural variations, and white regions (if any) indicate that no agreement between the simulations is found (similar to Tebaldi et al., 2011)
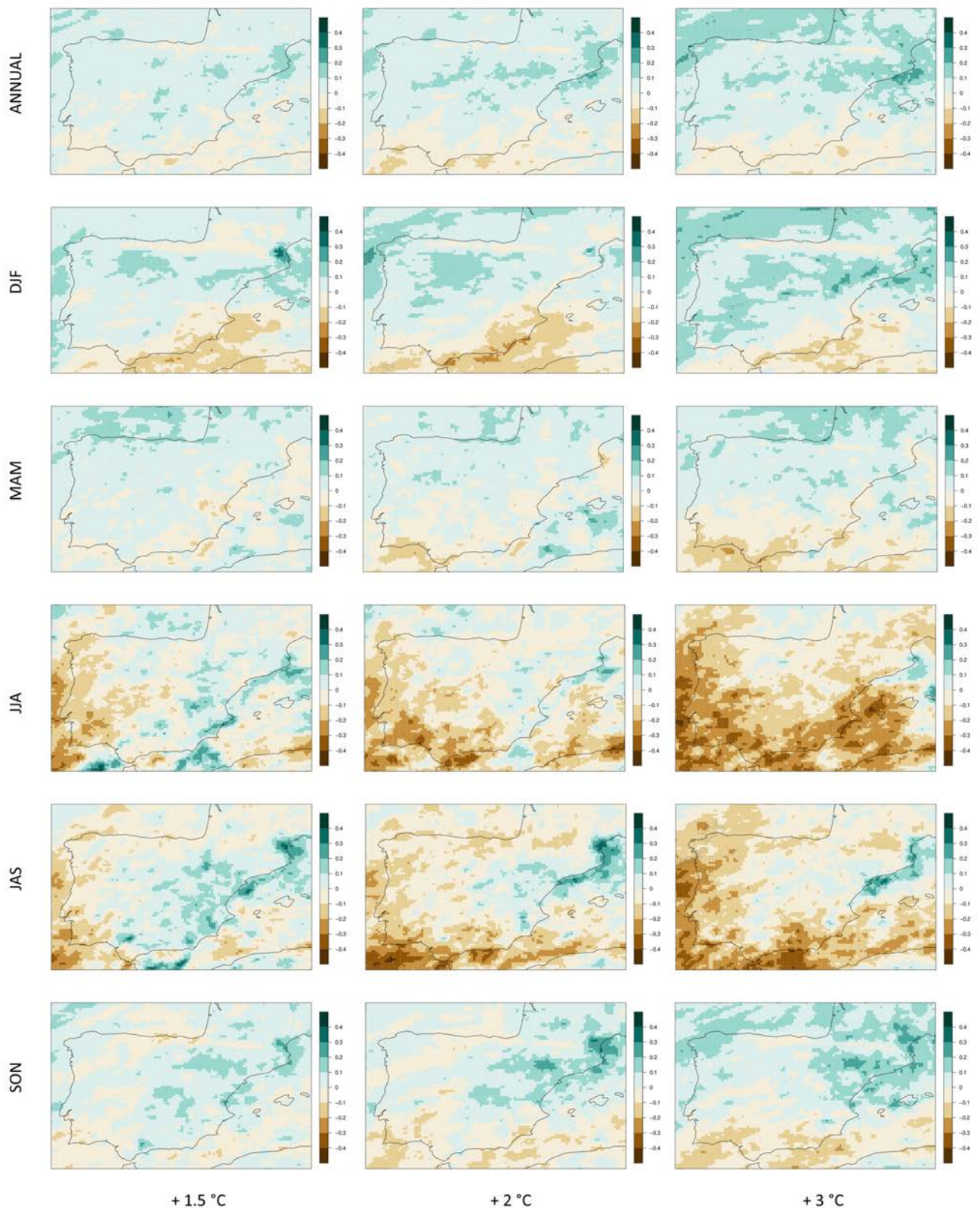
Figure 7.5: Ensemble mean of the relative change of maximum 1-day precipitation (Rx1day) for 1.5, 2 and 3 °C global warming (columns) at annual and seasonal scale (rows). Asterisks indicate areas where at least 50 % of the simulations show a statistically significant change and more than 66 % agree on the direction of the change. Coloured areas (without asterisk) indicate that changes are small compared to natural variations, and white regions (if any) indicate that no agreement between the simulations is found (similar to Tebaldi et al., 2011)
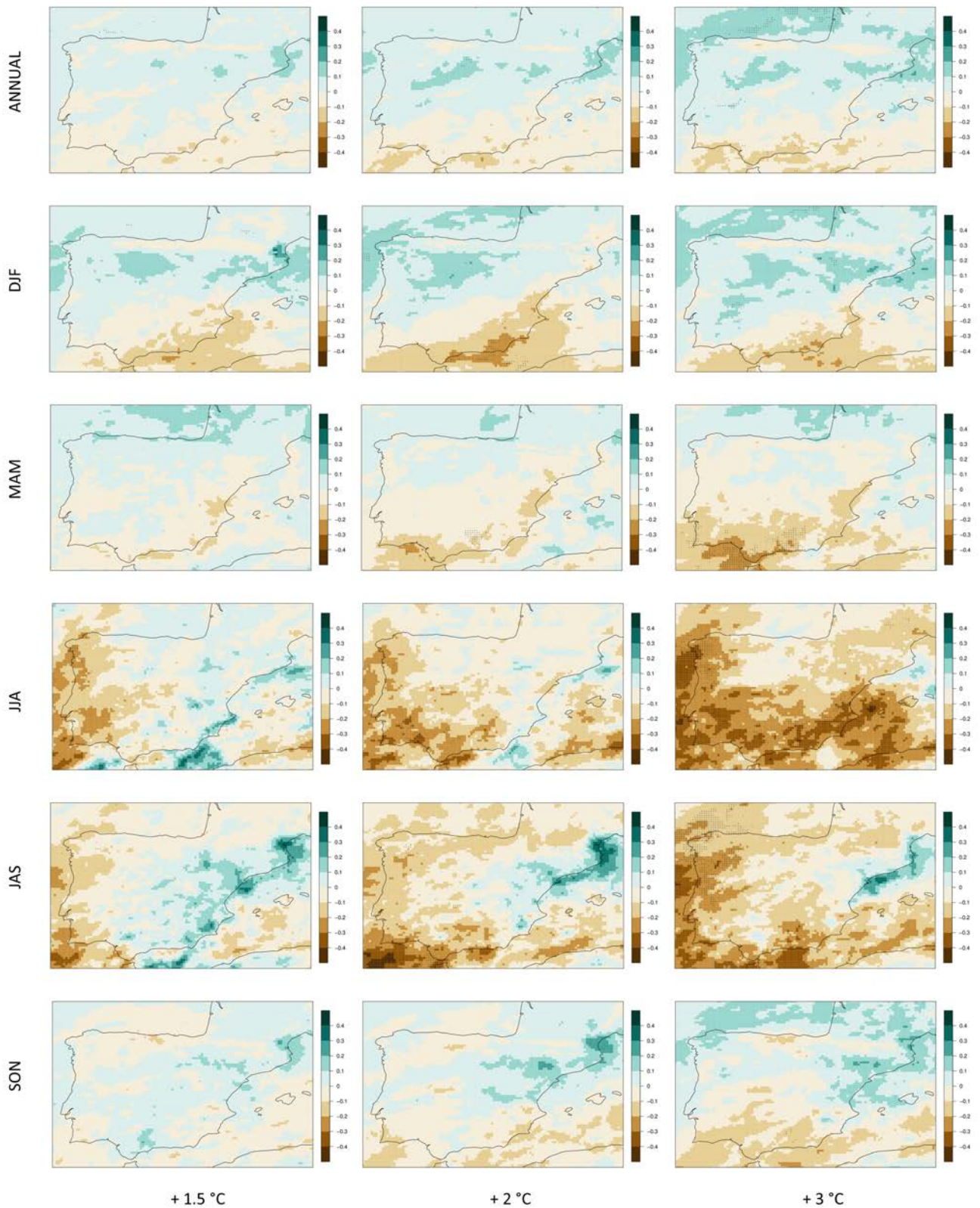
Figure 7.6: Ensemble mean of the relative change of maximum consecutive 5-day precipitation (Rx5day) for 1.5, 2 and 3 °C global warming (columns) at annual and seasonal scale (rows). Asterisks indicate areas where at least 50 % of the simulations show a statistically significant change and more than 66 % agree on the direction of the change. Coloured areas (without asterisk) indicate that changes are small compared to natural variations, and white regions (if any) indicate that no agreement between the simulations is found (similar to Tebaldi et al., 2011)
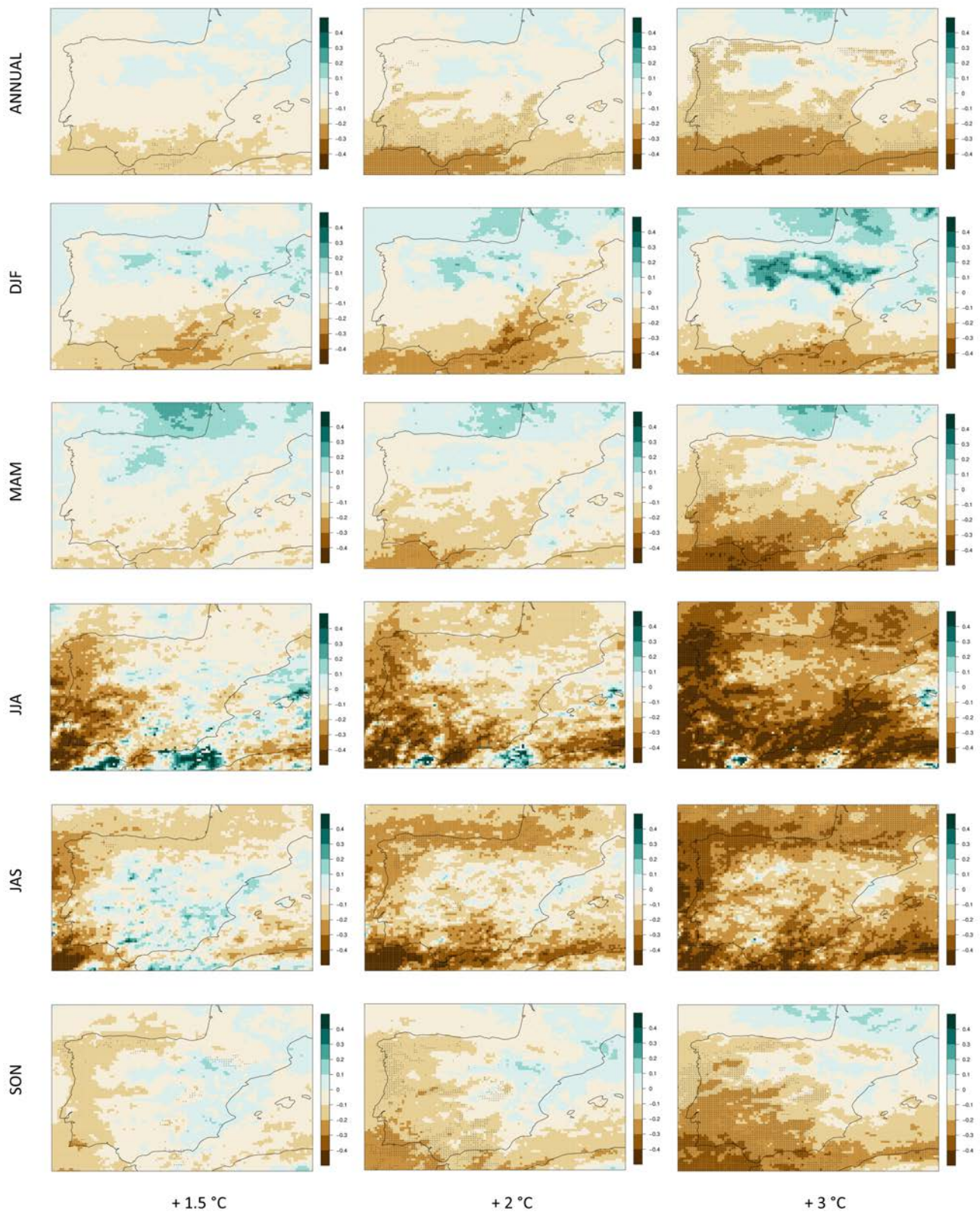
Figure 7.7: Ensemble mean of the relative change of the number of days with precipitation > 10 mm (R10mm) for 1.5, 2 and 3 °C global warming (columns) at annual and seasonal scale (rows). Asterisks indicate areas where at least 50 % of the simulations show a statistically significant change and more than 66 % agree on the direction of the change. Coloured areas (without asterisk) indicate that changes are small compared to natural variations, and white regions (if any) indicate that no agreement between the simulations is found (similar to Tebaldi et al., 2011)

111
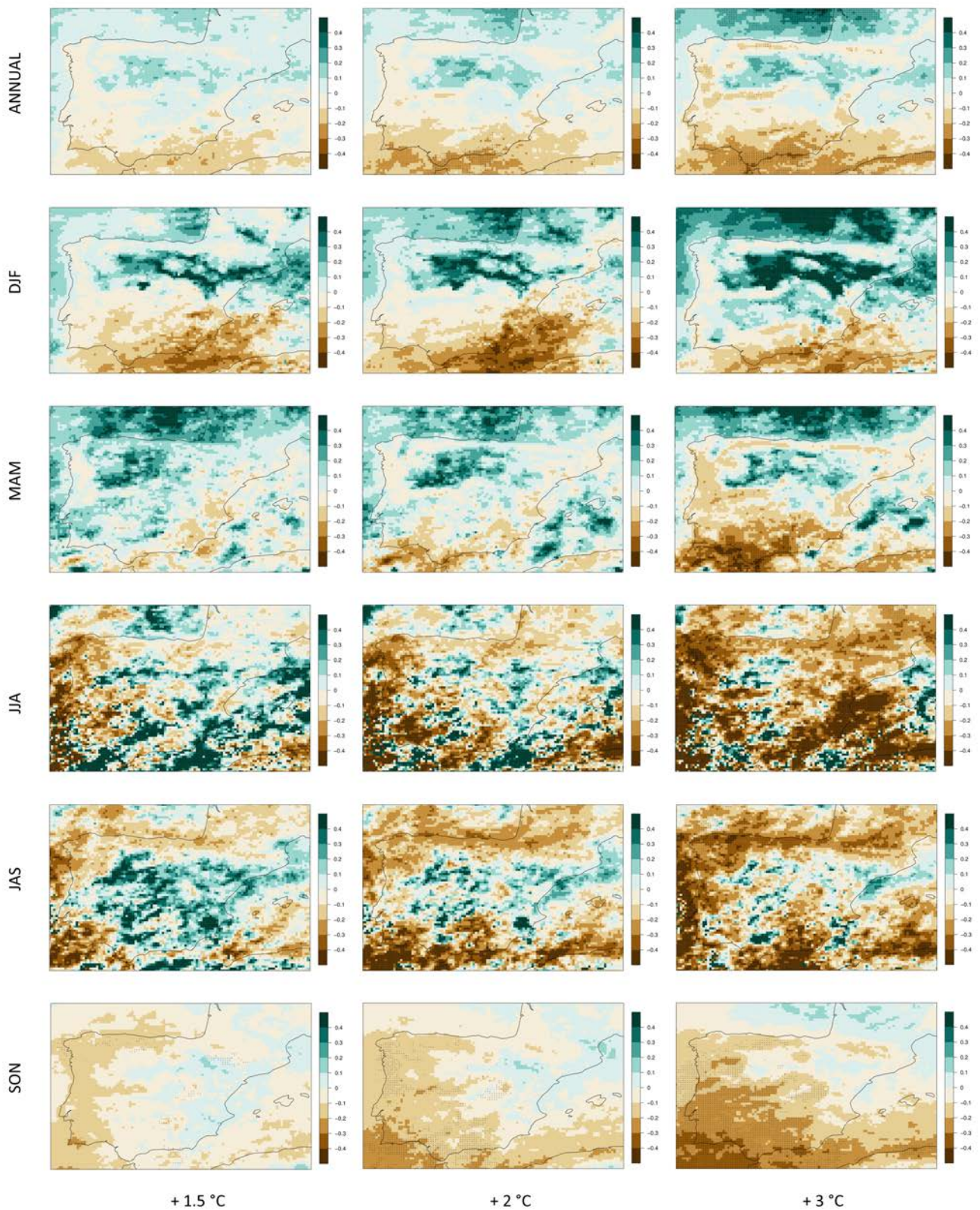
Figure 7.8: Ensemble mean of the relative change of the number of days with precipitation > 20 mm (R20mm) for 1.5, 2 and 3 °C global warming (columns) at annual and seasonal scale (rows). Asterisks indicate areas where at least 50 % of the simulations show a statistically significant change and more than 66 % agree on the direction of the change. Coloured areas (without asterisk) indicate that changes are small compared to natural variations, and white regions (if any) indicate that no agreement between the simulations is found (similar to Tebaldi et al., 2011)
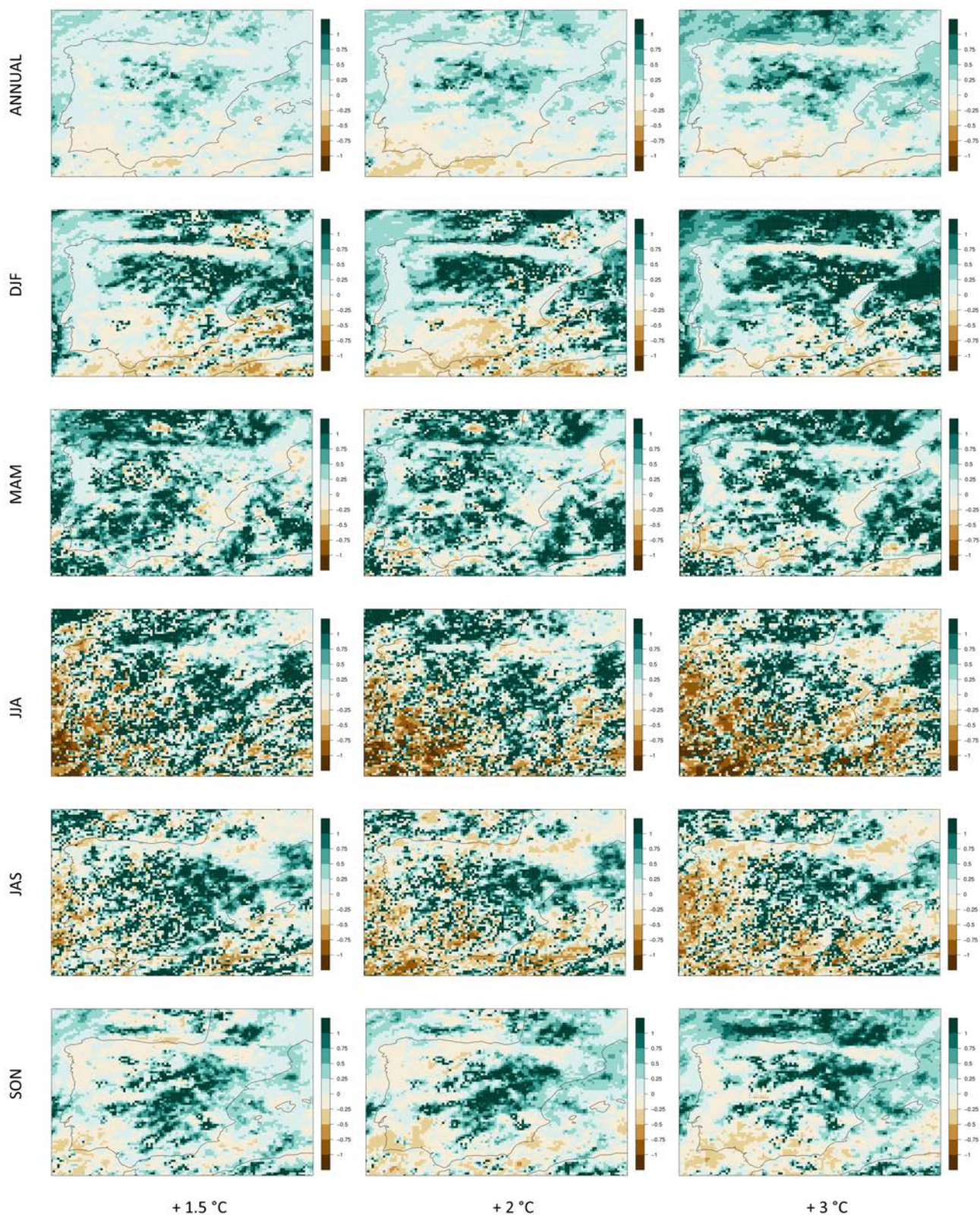
Figure 7.9: Ensemble mean of the relative change of the number of days with precipitation > 40 mm (R40mm) for 1.5, 2 and 3 °C global warming (columns) at annual and seasonal scale (rows). Asterisks indicate areas where at least 50 % of the simulations show a statistically significant change and more than 66 % agree on the direction of the change. Coloured areas (without asterisk) indicate that changes are small compared to natural variations, and white regions (if any) indicate that no agreement between the simulations is found (similar to Tebaldi et al., 2011)
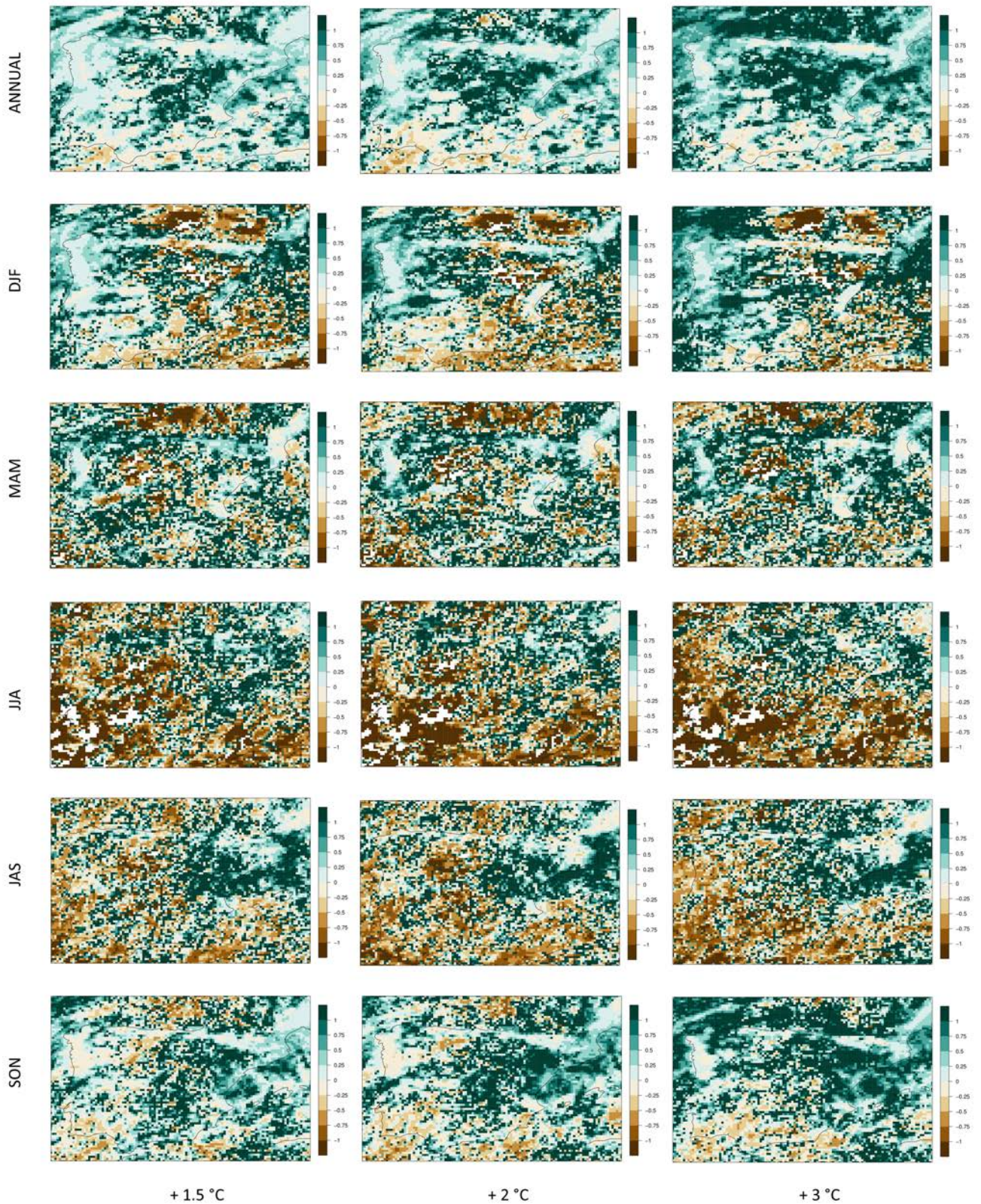
Figure 7.10: Ensemble mean of the relative change of the number of days with precipitation > 60 mm (R60mm) for 1.5, 2 and 3 °C global warming (columns) at annual and seasonal scale (rows). Asterisks indicate areas where at least 50 % of the simulations show a statistically significant change and more than 66 % agree on the direction of the change. Coloured areas (without asterisk) indicate that changes are small compared to natural variations, and white regions (if any) indicate that no agreement between the simulations is found (similar to Tebaldi et al., 2011)

7.4 Discussion and conclusions

In this chapter, the precipitation extremes in the Iberian Peninsula for a global warming at 1.5, 2 y 3 °C above preindustrial conditions are analysed.

Results show a general decrease of the total annual precipitation in most of the Peninsula, especially in the central and southern parts, which becomes greater with higher levels of global warming and during summer months. This, together with the expected increase in the length dry spell (CDD), will probably exacerbate water scarcity, which is already a problem in the area. Garrote et al. (2007) pointed out that the decreased water availability and increased drought, will have to satisfy an increased demand, as the higher mean annual temperature will increase evapotranspiration in irrigated areas. This pattern is also observable in other studies of the Mediterranean region (Jacob et al., 2014; Cramer et al., 2018; Sillmann et al., 2013; Rajczak and Schär, 2017; Turco et al., 2017). For example, Kjellström et al. (2018) found an increase in mean precipitation in the north of Europe, but a reduction in the south, especially during summer months. In addition, they found a likely decrease in the mean precipitation with global warming in mountain regions, such as the Pyrenees and Cantabrian Mountains.

On the other hand, many researchers have observed a likely increase in the extreme precipitation events in Europe and Mediterranean region with increasing global temperature (e.g. Drobinski et al., 2018). This is reflected in our study by the maximum precipitation recorded in 1 day (Figure 7.5), which shows an increase with global warming in the north and north-east of the Iberian Peninsula, with the exception of the mountain areas, especially during winter and autumn months. This pattern is repeated in the case of the maximum precipitation accumulated in 5 consecutive days (Figure 7.6), also an indicator of extreme precipitation events, although these changes are not statistically significant in most cases. In Colmet-Daage et al. (2018) an expected increase in the extreme precipitation events in 3 western Mediterranean basins (one of them belonging to Catalonia, *La Muga*) was also observed for the end of the 21st century. This trend was also found at European level in other studies, especially for winter and autumn months (Vautard et al., 2014; Rajczak and Schär, 2017; Jacob et al., 2014). However, summer and spring months show an evident reduction of these events, also observed in the number of days with daily precipitation higher than 10 mm in our case (Figure 7.7). When analysing the number of days exceeding the 20 (Figure 7.8) and 40 mm (Figure 7.9), a pronounced reduction is found in the south and in the north mountains of the Peninsula, although an increase can be detected in the centre and north of the area. Tramblay and Somot (2018) also pointed out an increment of the extreme precipitation events in the Internal Basins of Catalonia, as well as a reduction of those in the east and south of the Peninsula.

In the regions of study (Catalonia and the Valencian Community) a different behaviour has been observed. In Catalonia, a general decrease in the annual precipitation can be found mainly during summer months, being more evident in the Pyrenees. However, increases in extreme precipitation events are expected from September to May. In contrast, in the Valencian Community both annual and extreme precipitation is expected to decrease especially during spring and summer seasons, although some increases in extreme precipitation events can be

found in autumn and winter months, mainly in the north of this region.

In summary, with global warming a general decrease in the annual precipitation and a pronounced increase in the number of days without rainfall in the Iberian Peninsula is projected, especially during spring and summer months. Nevertheless, an increase of the extreme precipitation events has been found, mainly in autumn and winter months and in the north and north-east of the Peninsula.

Chapter 8

Impact of climate change on the probability of damaging flood events

Abstract

The main objective of this chapter is to estimate the changes in the probability of damaging flood events in Catalonia and the Valencian Community with a global warming of 1.5, 2 and 3 °C above preindustrial levels and taking into account different socioeconomic scenarios. The results show a general increase in the probability of a damaging event for most of the cases and in both regions of study, with larger increments when higher warming is considered. Furthermore, this increase is higher when both climate and population change are included. When population is considered, all the warming periods and climate models show a clearly higher increase in the probability of a damaging event, which is statistically significant for most of the cases. Nevertheless, when mean precipitation accumulated in 24 h is used as the sole independent variable of the damage model, not all the climate models show an increase in the probability of damaging events.

Our findings highlight the need for limiting the global warming as much as possible, as well as the importance of including variables that consider change in both climate and socioeconomic conditions in flood damage analysis.

8.1   Introduction

In the last few years, much research has focused on the study of climate change in the Mediterranean region, an area that is identified as being one of the most vulnerable to climate change according to the Fifth Assessment Report of the Intergovernmental Panel on Climate Change (Pachauri et al., 2014). Some studies have found an increase in precipitation extremes with global warming projections in the Mediterranean region (Colmet-Daage et al., 2018; Drobinski et al., 2018), although a general decrease in the annual precipitation is projected (Jacob et al., 2014; Cramer et al., 2018; Sillmann et al., 2013; Rajczak and Schär, 2017). As a result, flood risk associated with extreme precipitation events is expected to increase due to climate change,

but also due to non-climatic factors such as increasingly sealed surfaces in urban areas and ill-conceived storm-water management systems (Cramer et al., 2018).

Taking into account the above-mentioned points, the aim of this last chapter of the thesis is to estimate the future flood damage considering both climate and socioeconomic expected changes. For this purpose, the changes in the probability of a damaging event with respect to the reference period (1976-2005) with global warming of 1.5, 2 and 3 °C above preindustrial levels and considering different socioeconomic scenarios have been assessed. This has been done using the relationships between insurance data, precipitation and population resulted from the previously developed present climate model (see Chapter 6). Therefore, this last chapter of the thesis brings together all the findings obtained in the previous ones: the models developed in Chapters 4, 5 and especially 6 and the data from daily precipitation projections treated in Chapter 7.

8.2   Methods

The main characteristics of the region of the study as well as the data sources used in this chapter are explained in Chapter 3. The river-basin-scale is the spatial resolution chosen, in order to follow the same resolution of the previous analyses. The methodology and results of this chapter are divided into three parts: (i) future daily precipitation projections, (ii) population scenarios, and (iii) future probability of damaging events.

8.2.1   Treatment of daily precipitation projections

In this chapter, the changes in daily precipitation data from the 7 EURO-CORDEX simulations used in Chapter 7 have been used assuming global warming scenarios of 1.5, 2 and 3 °C above preindustrial levels (1881-1910) (Vautard et al., 2014). Further information about these data and the methodology followed can be found in Chapters 3 and 7.

To select the precipitation data to be used in the analysis, we first aggregate all of the time-series to the river-basin level, calculating the mean of the grid cells belonging to each of the basin polygons. Then, a bias correction has been applied in order to smooth the differences between the observations and the simulations. To this end, the common period 1996-2005 has been selected. The data from the simulations come from the historical data series of each climate model, while the data from the observations are the daily precipitation data from the AEMET weather stations with an effectiveness higher than 90 %. Both datasets are aggregated to the river-basin-scale, using the mean value. Once the two pairs of comparable series are available for each climate model, the differences between them are estimated by applying a quantile mapping bias correction method, specifically with a non-parametric quantile mapping using the robust empirical quantiles method (Gudmundsson et al., 2012). This method estimates the values of the quantile-quantile relation of observed and modelled time series for regularly spaced quantiles using local linear least square regression. In order to check the suitability of the method chosen, the differences between the observations and simulations for the period

1996-2005 have been compared with and without the correction applied. This has been done for the cases that recorded a mean precipitation in the basin higher than 40 mm, being this the same threshold used in the model for the present climate (Chapter 6).

Figure 8.1 shows the Catalonia example of the comparison between the simulations and observed precipitation for the common period 1996-2005 for the flood cases that exceeded the 40 mm 24 h^{-1} precipitation threshold without (top panel) and with (bottom) the correction applied. As can be observed, the differences between both databases are clearly reduced when using the corrected data, proving the aptitude of the method. In the case of Segre basin, that is basin 300 (see Table A.6 and Figure A.1 of the Appendix section), climate models M3, M4, M6 and M7 present events with mean precipitation exceeding the 40 mm 24 h^{-1} threshold, although there are no observations. The lack of observations could be due to the averaging of the data recorded in the basin, considering its large extension; the biggest of the region with a total surface around 10,150 km^2. Actually, basins with higher mean precipitation values are mainly the smallest ones (for example basins 833 and 1004 belonging to Calafell-Torredembarra and La Senia, respectively).
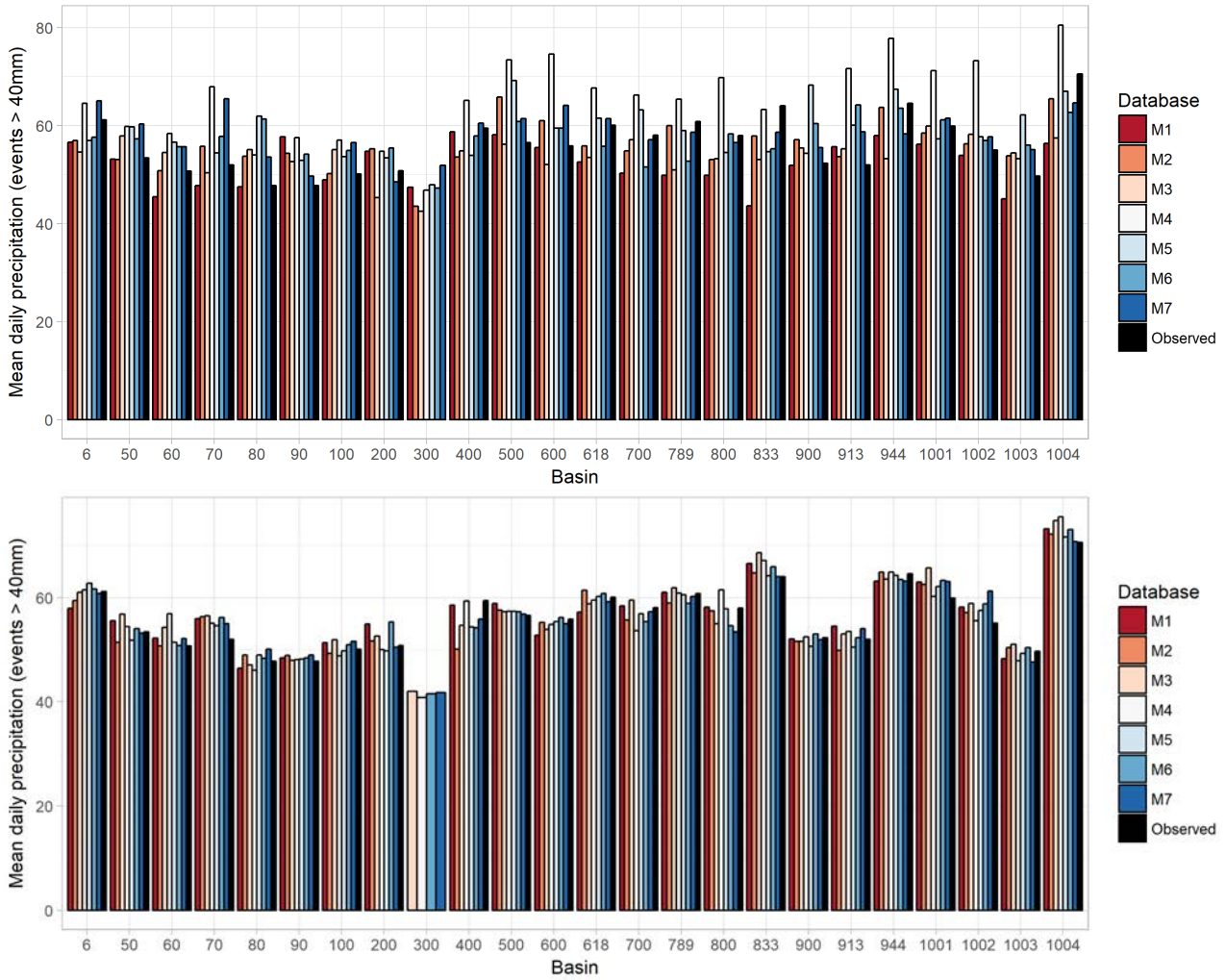
Figure 8.1: Comparison of the observed vs climate models resulted mean precipitation values for the basins of Catalonia (cases with average daily precipitation exceeding 40 mm only). Top panel excludes the correction for the common period 1996-2015 while the bottom panel includes it. M1 to M7 refer to the 7 EURO-CORDEX simulations used (see Chapter 7). The numbers on the x-axis indicate the code of each basin (see Table A.6 and Figure A.1, Appendix section)

The same methodology has been applied for the Valencian Community. In this case, all the basins and climate models have recorded a mean precipitation value higher than 40 mm 24 h^{-1} during the 1996-2005 period. The homogenisation achieved with the bias correction process is clearly reflected in the bottom panel of Figure 8.2.
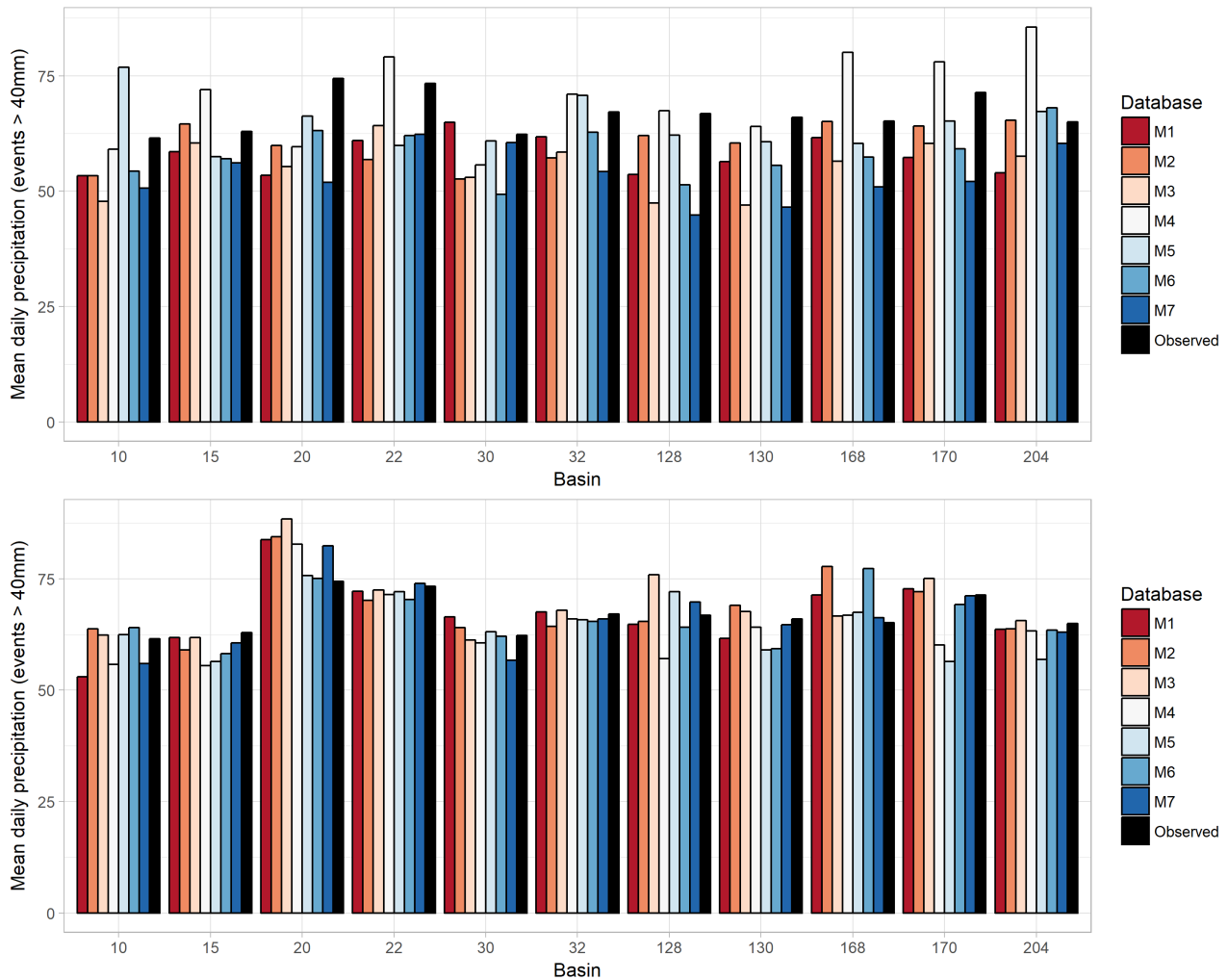
Figure 8.2: Comparison of the observed vs climate models resulted mean precipitation values for the basins of the Valencian Community (cases with average daily precipitation exceeding 40 mm only). Top panel excludes the correction for the common period 1996-2015 while the bottom panel includes it. M1 to M7 refer to the 7 EURO-CORDEX simulations used (see Chapter 7). The numbers on the x-axis indicate the code of each basin (see Table A.7 and Figure A.2, Appendix section)

The same bias correction method has been applied for the three future periods (1.5 °C, 2 °C and 3 °C), using specific correction per basin and climate model. Finally, only the cases that recorded a mean precipitation in the basin higher than 40 mm 24 h^{-1} were selected, in order to use the same data as those that were introduced to build the precipitation-damage model for the present climate (Chapter 6).

8.2.2 Treatment of population projections

The Shared Socioeconomic Pathways (SSPs), together with the 2UP model (Van Huijstee et al., 2018), have been used to obtain the total population of each of the basins of the study for the future projections. The main objective of the 2UP model is to disaggregate the scenario-based projected national-level urban population to 30 arcseconds data and simulate urban expansion for 194 countries and territories (for more information see Chapter 3). The Shared Socioeconomic Pathways (SSPs) describe plausible alternative changes in aspects of society such

as demographic, economic, technological, social, governance and environmental factors (O'Neill et al., 2017). The SSPs are based on five narratives describing alternative socio-economic developments, including sustainable development (SSP1), middle-of-the-road development (SSP2), regional rivalry (SSP3), inequality (SSP4) and fossil-fueled development (SSP5) (Riahi et al., 2017).

In order to incorporate the population data in the damage model, three main processes have been applied: (i) temporal downscaling from 10 years resolution to yearly; (ii) river-basin-level aggregation; and (iii) bias correction.

For the temporal downscaling, simple linear regression has been applied in order to obtain yearly population data for each of the SSPs. The 2UP model estimates the population every 10 years, from 2010 to 2080. However, most of the EURO-CORDEX future daily precipitation simulations reach and overpass the year 2080 (all of them except the Model 2) while using the 30-year window for the warming period of 3 °C (see Table 7.1, Chapter 7). For these years (2081-2084), the same population change coefficient for the last ten years period (2070-2080) has been applied.

After obtaining the yearly population data for all SSPs, the data were aggregated to the river-basin-level by summation. Therefore, each basin will have 5 different yearly population series (corresponding to each SSP) from 2010 to 2084 (the last year of the precipitation simulations).

Finally, a bias correction process is also required for the population data. The year 2010 has been chosen for carrying out the comparison between the population data from the observations and those from the 2UP model. Figures 8.3 and 8.4 show the 2010 population aggregated at basin and region level for Catalonia and the Valencian Community, respectively. As can be observed in both cases, differences between the projections are negligible, though there exists a significant disagreement with the observations. For this reason a scaling bias correction method has been used to correct the population projection data. This means that the ratio for each basin and SSP between the observed and simulated population for the 2010 year has been applied to the future population projections.
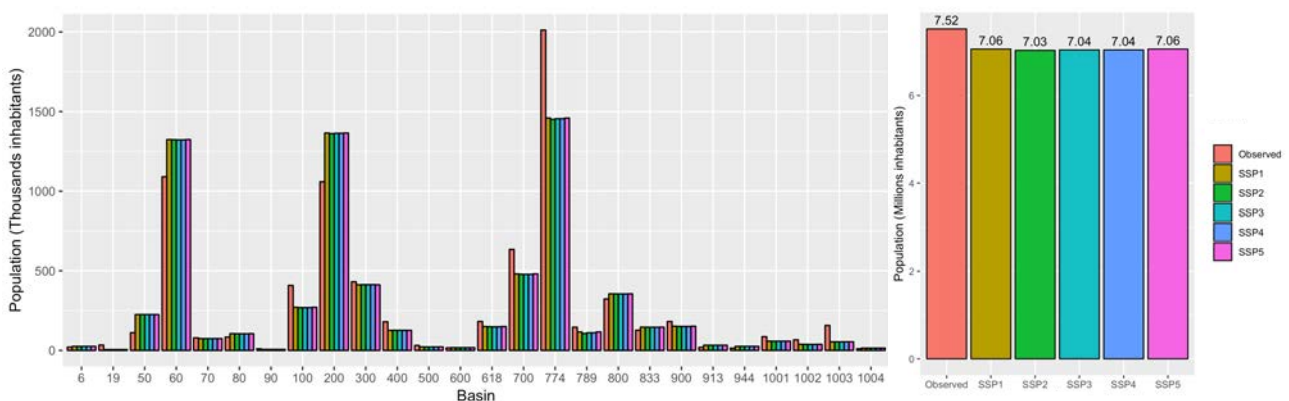
Figure 8.3: Population (year 2010) for each basin of Catalonia (left) and for the whole region (right) for the observed and simulated population (SSPs). The numbers on the x-axis indicate basins' code (see Table A.6 and Figure A.1, Appendix section)
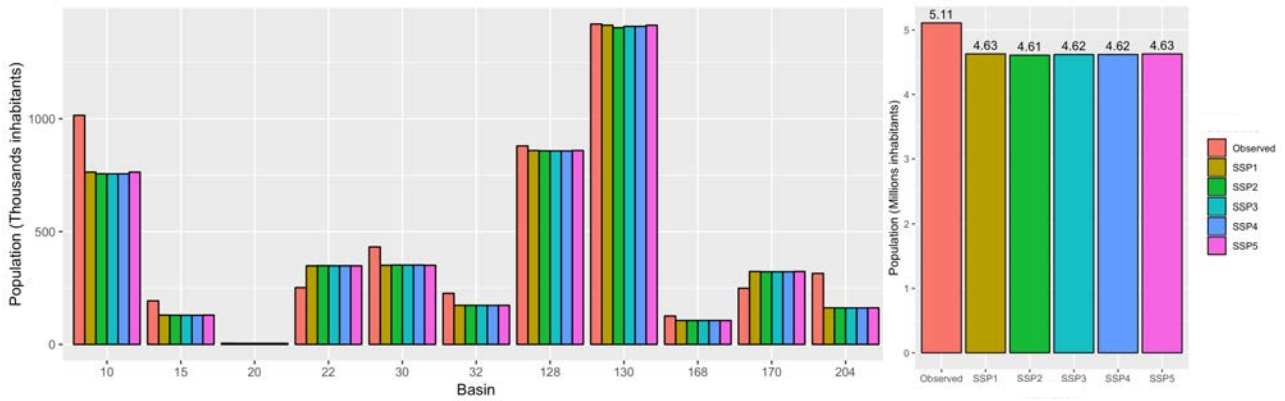
Figure 8.4: Population (year 2010) for each basin of the Valencian Community (left) and for the whole region (right) for the observed and simulated population (SPPs). The numbers on the x-axis indicate basins' code (see Table A.7 and Figure A.2, Appendix section)

Therefore, after these processes, each basin has a yearly population series corrected from 2010 to 2084 for the 5 SSP.

8.2.3 Modelling damaging events: Generalized Linear Mixed Model

Once both future precipitation and population data have been corrected, the same model developed in Chapter 6 can be applied for both regions of study in order to estimate the probability of a damaging event in the future. The Generalized Linear Mixed Model (GLMM) follows the equation 8.1:

$$\log(\frac{\pi}{1-\pi}) = \beta_0 + \beta_1 P + \beta_2 R + b_i + b_j \tag{8.1}$$

Where π is the response variable (the probability to exceed a specific threshold of damage), P and R are the predictors (mean precipitation recorded in 24 h and total population of the basin in our case), and b_i and b_j are the random effects related to the basins and the events. The value of the β coefficient is determined using Generalized Linear Models (GLMs). The Wald χ^2 statistic is used to assess the statistical significance of individual regression coefficients (Harrell Jr, 2015).

As has been explained in sections 8.2.1 and 8.2.2, 7 climate models for future daily precipitation and 5 socioeconomic scenarios for total population have been used. As a result, a total of 35 different models have been developed for each of the regions of study.

Furthermore, the results using the model with the precipitation recorded in 24 h as sole independent variable have also been estimated in order to observe the differences in the probability of a damaging event when the exposure of the territory (i.e. population) is taken into account.

8.3   Results

8.3.1   Extreme precipitation projections

Figures 8.5 and 8.6 show the change (in %) of the mean 24 h precipitation, averaged across all basins, in the future simulations compared to the reference period (1976-2005), when taking into account the cases that overpassed the 40 mm 24 h^{-1} precipitation threshold for the different climate models and warming periods (global warming at 1.5, 2 and 3 °C). In the case of Catalonia (Figure 8.5), most of the climate models and warming periods show an increase of the mean daily precipitation with the exception of Model 3 (EC-EARTH-RCA4, see Chapter 7), which projects a decrease for the 2 °C global warming level. Most of the climate models (4 out of 7) indicate greater precipitation values when the highest warming level is taken into account (3 °C), agreeing with several studies that point to an increase of precipitation extremes with global warming (Drobinski et al., 2018; Colmet-Daage et al., 2018; Tramblay and Somot, 2018; Cramer et al., 2018).
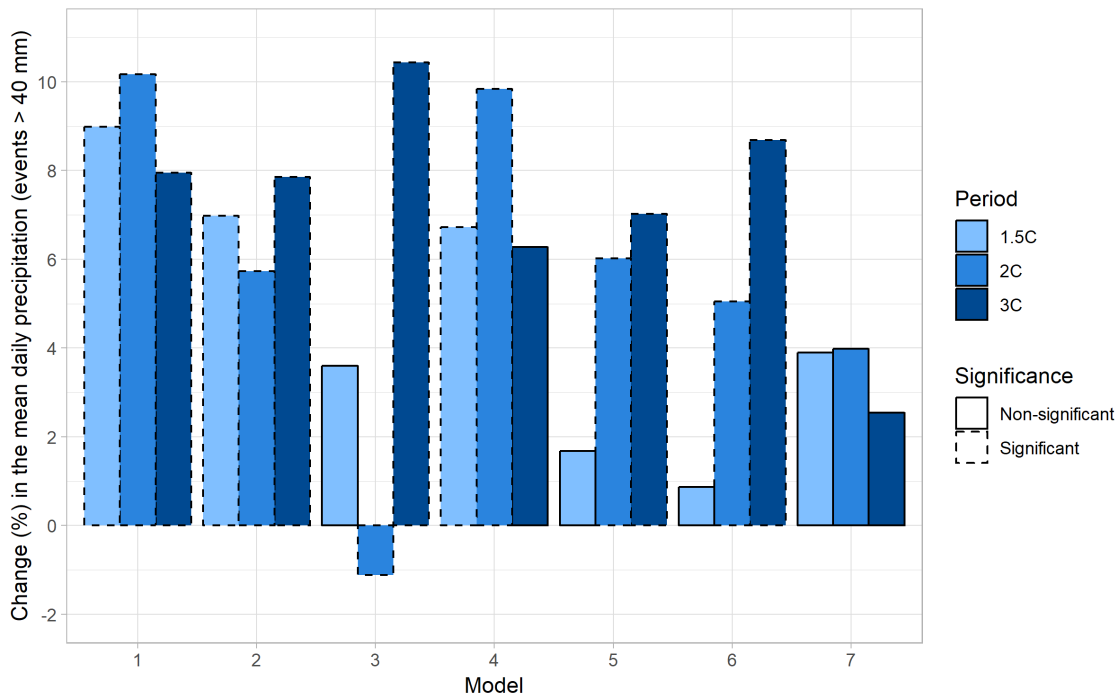
Figure 8.5: Change in the mean daily precipitation compared to the reference period (1976-2005) for cases exceeding the 40 mm 24 h^{-1} threshold for the 7 climate models and the 3 levels of warming in Catalonia. Dashed hatchings around bars indicate significant changes (p value < 0.05; Mann-Whitney Test) with respect to the reference period

In the case of the Valencian Community region, the change in the mean daily precipitation at basin scale for the future periods is lower (Figure 8.6). However, apart from one case which is non-significant (3 °C, Model 5: MPI-ESM-LR-CCLM4-8-17), all the climate models and periods show an increase of the mean precipitation of the basin when the events with daily precipitation exceeding the 40 mm are taken into account. In this case, there is no clear pattern of larger increases in extreme precipitation with higher warming levels.
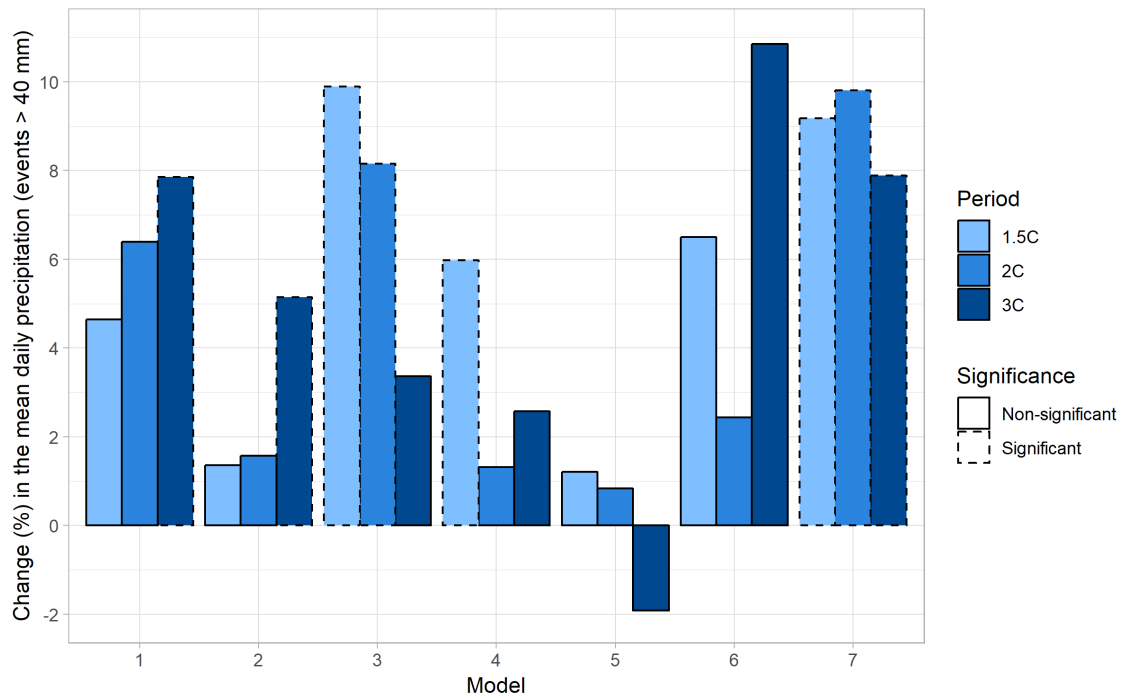
Figure 8.6: Change in the mean daily precipitation compared to the reference period (1976-2005) for cases exceeding the 40 mm 24 h^{-1} threshold for the 7 climate models and the 3 levels of warming in the Valencian Community. Dashed hatchings around bars indicate significant changes (p value < 0.05; Mann-Whitney Test) with respect to the reference period

The greater positive changes in precipitation values in the case of Catalonia was expected if we take into account the results showed in Chapter 7. The east of the Iberian Peninsula (where the Valencian Community is placed) presents a greater decrease in both annual precipitation and in the number of days with daily precipitation higher than 40 mm in comparison to the north-east part (Catalonia). Nevertheless, from these results can be concluded that heavy daily precipitation is likely to increase with global warming in both regions of study.

8.3.2 Population projections

Figures 8.7 and 8.8 show the projections in the population per region of study (Catalonia and the Valencian Community, respectively) after applying the treatment processes explained in Section 8.2.2.

For both regions, the largest increase in population is in SSP5, with population growth around 50 % for Catalonia and 62 % for the Valencian Community by the end of the 21st century with respect to 2010. SSP5 is defined by the push for economic and social development coupled with the exploitation of abundant fossil fuel resources and the adoption of resource and energy intensive lifestyles around the world (O'Neill et al., 2017). Though fertility declines rapidly in developing countries, fertility levels in high income countries are relatively high. For this reason, despite being the scenario that projects the second lowest population by the end of the 21st century in terms of global population (Samir and Lutz, 2017), in our region of study it projects the highest increase (high income economy).

On the other hand, SPP3 depicts the largest decrease in the total population in Catalonia and the Valencian Community, with a reduction of 25 % and 30 %, respectively. In this scenario a low population growth is expected in industrialised countries, while high increases can be found in developing countries (O'Neill et al., 2017). This explains the difference between the results found in studies such as Samir and Lutz (2017) in which the highest global population expected growth is found for this scenario.
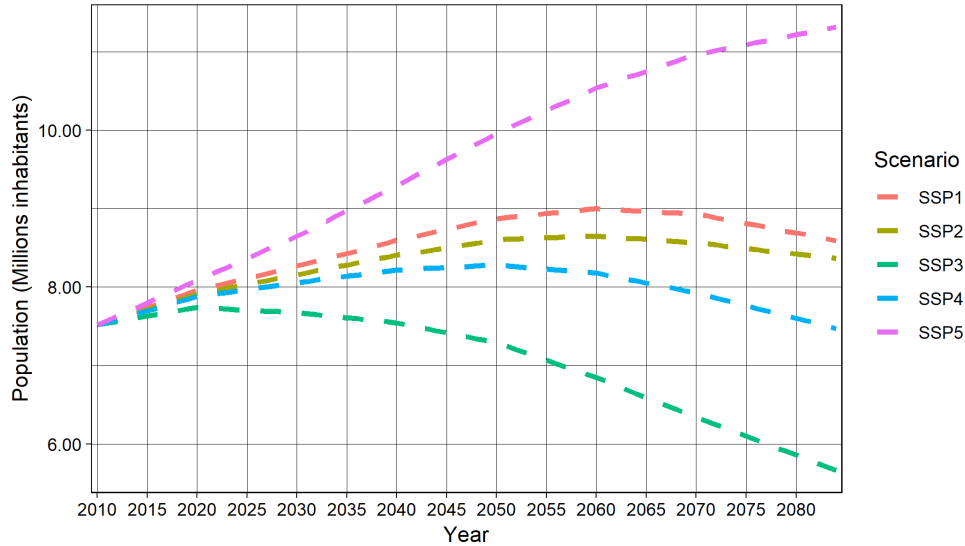
Figure 8.7: Future population projections for the different SSP's in Catalonia
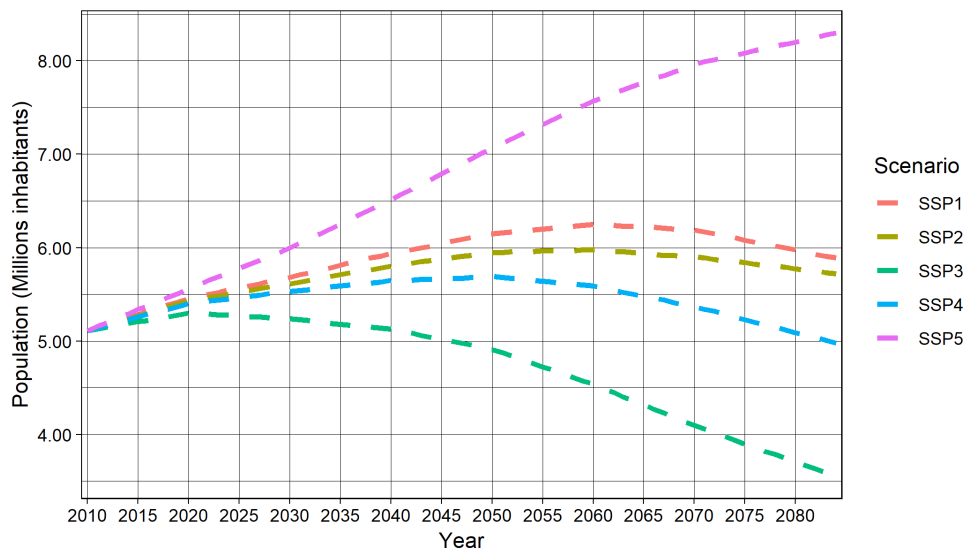
Figure 8.8: Future population projections for the different SSP's in the Valencian Community

SSP5 assumes a society that keeps relying heavily on fossil fuels. This implies that we may expect high emissions, and therefore the combination with RCP8.5 (the only RCP used in the thesis) is very plausible. For this reason, the main results of this study will focus on the RCP8.5/SSP5 combination. However, some analysis will also be performed considering all the SSPs in order to show the differences between the socioeconomic projections.

8.3.3 Future probability of damaging events

Finally, the changes in the probability of damaging events for both regions have been assessed when considering a global warming of 1.5, 2 and 3 °C.

Catalonia

Figure 8.9 shows the change in the probability of a damaging event for Catalonia, for three damage percentiles (50, 60 and 70th) and taking into account the mean precipitation recorded in 24 h and the population considering the SSP5 socioeconomic scenario. As can be observed, this probability increases with respect to the reference period (1976-2005) for all the climate models and warming periods. The increase is higher when greater warming is considered in most of the cases (the increase is usually larger with 3 °C than with 1.5 and 2 °C), which emphasises the importance of restricting global warming as much as possible. Furthermore, the increase in probability is greater for higher percentiles of damage.
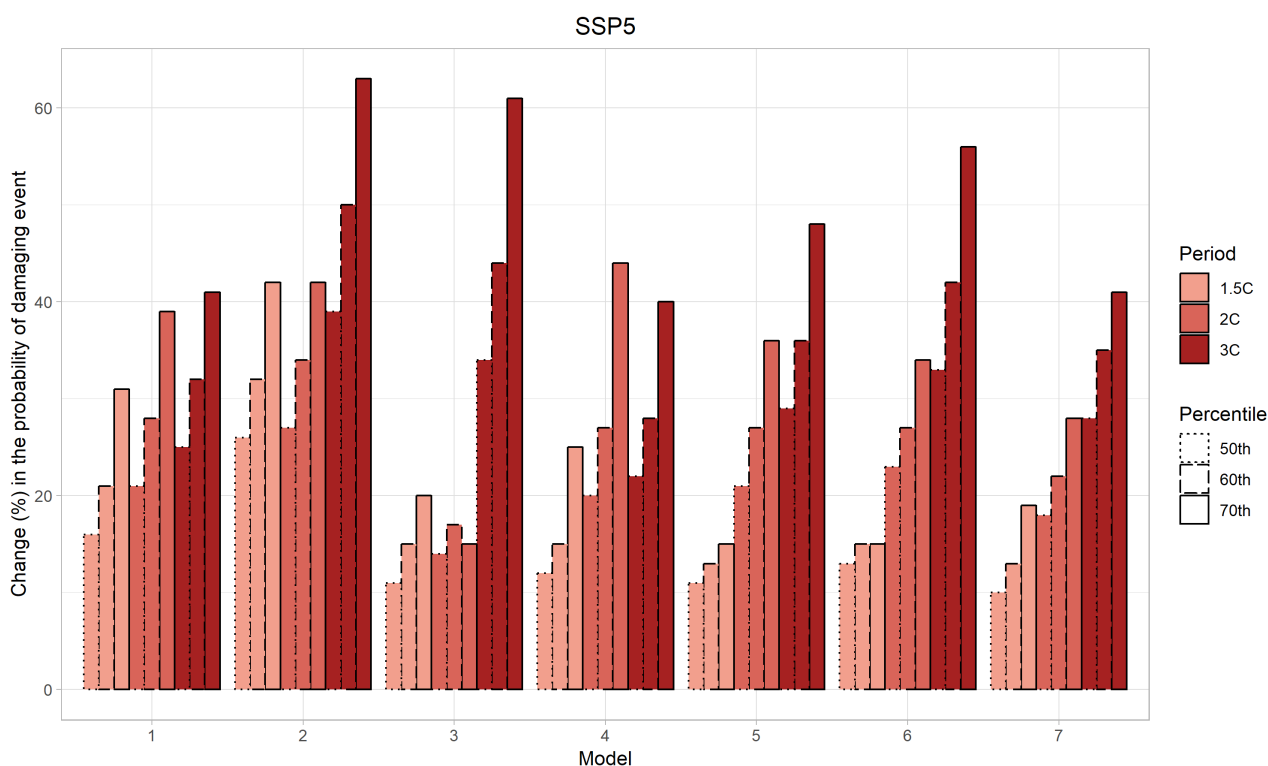
Figure 8.9: Change in the probability of a damaging event in Catalonia with respect to the reference period (1976-2005) for the 50, 60 and 70th damage percentiles and for all climate models when using the SSP5 socioeconomic scenario. Different hatchings around bars show the different percentiles of damage

The results presented above show the change in probability of damaging events due to both climate change and increasing exposure (i.e. increasing population), both of which have been shown to have a significant relationship with flood damage in Chapter 6. In Table 8.1, the change in the probability of damaging events is shown for the 70th damage percentile, when keeping population constant at today's levels (left) versus using the SSP5 population data (right). The results show that the increase in probability is higher when both climate and

population change are included. When population is considered, all the periods and climate models clearly show a higher increase in the probability of a damaging event, which is statistically significant for all cases. Nevertheless, when mean precipitation accumulated in 24 h is used as the sole independent variable of the model, not all the climate models show an increase in the probability of damaging events. These results point out the importance of including variables that represent change in both the climate and socioeconomic conditions.

Model	Precipitation			Precipitation + population		
	1.5 °C	2 °C	3 °C	1.5 °C	2 °C	3 °C
1	13 %	15 %	12 %	31 %	39 %	41 %
2	11 %	10 %	12 %	42 %	42 %	63 %
3	6 %	-2 %	17 %	20 %	15 %	61 %
4	11 %	16 %	9 %	25 %	44 %	40 %
5	3 %	10 %	10 %	15 %	36 %	48 %
6	1 %	8 %	14 %	15 %	34 %	56 %
7	6 %	5 %	4 %	19 %	28 %	41 %

Table 8.1: Change in the probability of a damaging event in Catalonia for the 70th damage percentile and the three warming periods with the mean 24 h precipitation as explanatory variable (left) and mean 24 h precipitation and population (SSP5) as explanatory variables (right). The gray cells show statically significant (p value < 0.05) increases (light) and decreases (dark) in relation to the reference period (1976-2005)

Finally, in order to see the differences between the socioeconomic scenarios (SSPs), the probability of exceeding the 70th percentile of damage in Catalonia for all the periods, climate models and SSPs are plotted in Figure 8.10. Results show an increase in the probability of a damaging event in almost all cases, pointing out that even with lower exposure than in the SSP5 scenario, increases in flood damage are evident. The only exception is for Model 3 in combination with the 2 °C warming period and the SSP3 scenario; this SSP shows a marked reduction trend in population (see Figure 8.7). The largest increases in probability are found under SSP5, since this has the largest increase in population.
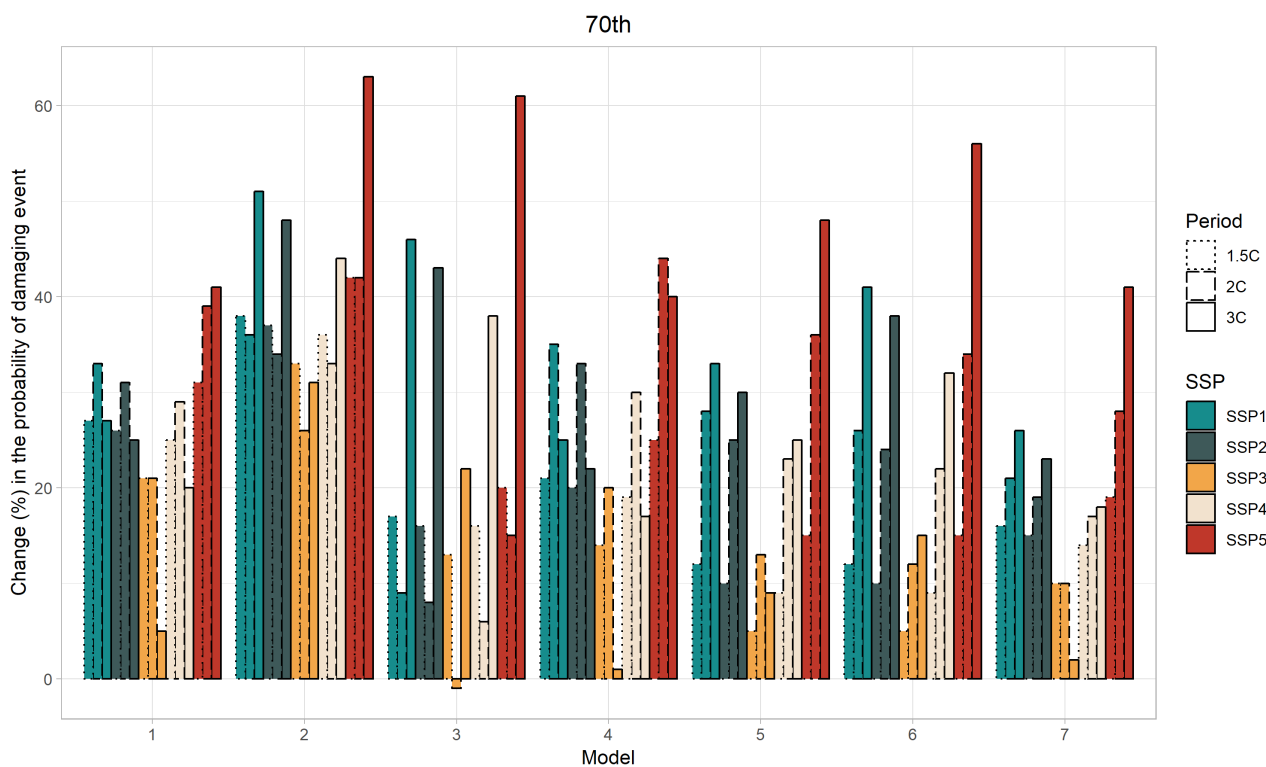
Figure 8.10: Change with respect to the reference period (1976-2005) of exceeding the 70th percentile of damage in Catalonia for all the climate models, warming periods and socioeconomic scenarios (SSP). Different hatchings around bars show different warming levels

The Valencian Community

The same analysis has been carried out for the Valencian Community, based on the relationships found for the present climate for this region (see Chapter 6). Figure 8.11 shows the change in the probability of a damaging event (defined by 3 percentiles of damage) based on the precipitation recorded in 24 h and the population (SSP5 scenario). As can be observed, all climate models and periods show an increase in this probability with respect to the reference period. Therefore, an increase in the probability of a damaging event occurrence is likely to happen with global warming and with the expected growth of the population, becoming higher when greater warming is considered. Actually, with a global temperature of 3 °C above preindustrial conditions, the change in probability is considerably higher than the other two warming periods (1.5 °C and 2 °C) in most cases, becoming twice as high in some of them. Furthermore, this probability becomes larger for higher percentiles of damages.
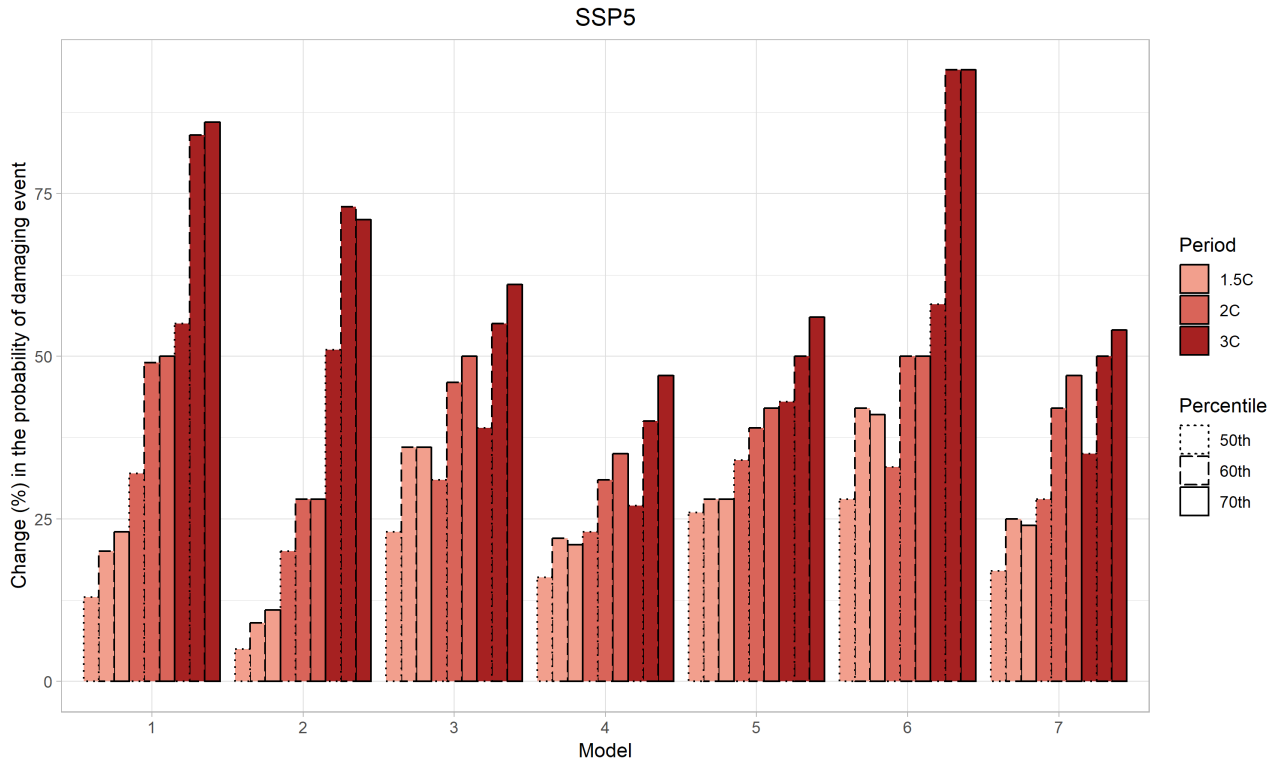
Figure 8.11: Change in the probability of a damaging event in the Valencian Community with respect to the reference period (1976-2005) for the 50, 60 and 70th damage percentiles and for all climate models when using the SSP5 socioeconomic scenario. Different hatchings around bars show the different percentiles of damage

The change in the probability of a damaging event when considering the 70th percentile of damage is shown in Table 8.2. When population is considered constant at today's levels (left), the range of values goes from -4 to 26 %, but only the positive and highest ones are statistically significant. However, when the change in population according to SSP5 is also taken into account (right), all values become positive, greater and most of them statistically significant, highlighting the importance of considering the population while analysing flood damages.

Model	Precipitation			Precipitation + population		
	1.5 °C	2 °C	3 °C	1.5 °C	2 °C	3 °C
1	12 %	12 %	16 %	23 %	50 %	86 %
2	4 %	2 %	8 %	11 %	28 %	71 %
3	13 %	19 %	14 %	36 %	50 %	61 %
4	2 %	1 %	3 %	21 %	35 %	47 %
5	-4 %	-2 %	-4 %	28 %	42 %	56 %
6	16 %	7 %	26 %	41 %	50 %	94 %
7	10 %	20 %	9 %	24 %	47 %	54 %

Table 8.2: Change in the probability of a damaging event in the Valencian Community for the 70th damage percentile and the three warming periods with the mean 24 h precipitation as explanatory variable (left) and mean 24 h precipitation and population (SSP5) as explanatory variables (right). The gray cells show statically significant (p value < 0.05) increases (light) and decreases (dark) in relation to the reference period (1976-2005)

The probability of exceeding the 70th percentile of damage for the Valencian Community for all the periods, climate models and SSPs is shown in Figure 8.12. Although most of the

cases show an increase in the probability of a damaging event, this increase is not as clear as that of the Catalonia region. When the SSP3 socioeconomic scenario is taken into account, substantial decreases can be found in most climate models. As in the case of Catalonia, the largest increases are found under the SSP5 scenario, when higher population growth rates are expected (see Figure 8.8). These results once again underline the importance of considering socioeconomic changes in flood risk analysis.
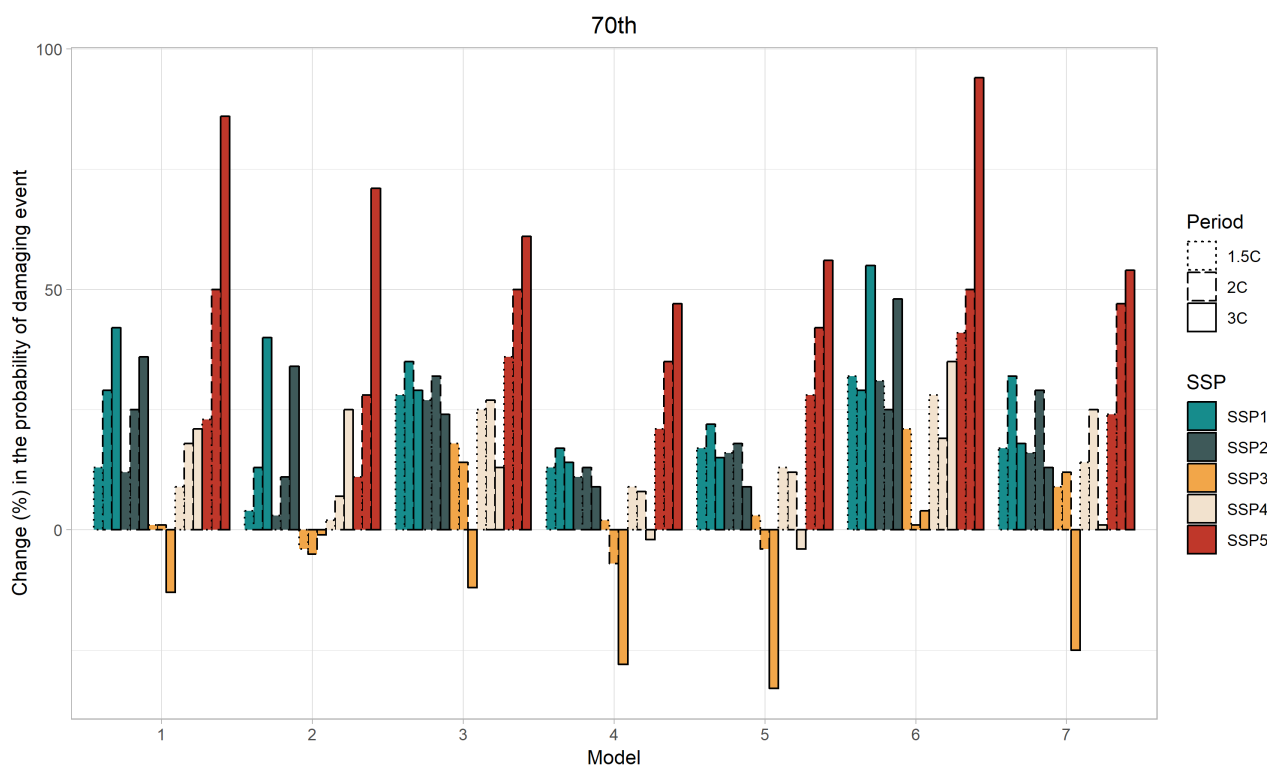
Figure 8.12: Change with respect to the reference period (1976-2005) of exceeding the 70th percentile of damage in the Valencian Community for all the climate models, warming periods and socioeconomic scenarios (SSP). Different hatchings around bars show different warming levels

8.4 Conclusions

The main contribution of this last chapter of the thesis is the assessment of the probability of future damaging events in two Western Mediterranean regions (Catalonia and the Valencian Community) considering both climatic factors and changes in exposure according to different socioeconomic scenarios.

The relationships found in the models developed for the present climate (Chapter 6) are of great importance for analysing the flood risk and understanding the links between flood damage and their causes. From these links, the future probability of flood damage can be assessed taking into account the changes in daily precipitation based on climate change projections as well as the expected changes in the population according to different socioeconomic scenarios. In this chapter, the changes in the probability of a damaging event with global warming of 1.5, 2 and 3 °C above preindustrial levels have been estimated. Our results have shown that this probability increases with respect to the reference period (1976-2005) for most climate models

and warming periods in both regions when considering the RCP8.5/SSP5 combination, being higher in the case of Catalonia. Furthermore, a remarkable result found in both areas is that this change is usually larger when greater warming is considered. That points out the importance of restricting the expected global warming increase as lower as possible. The only reductions in the probability of a damaging event is found when considering the SSP3 (and in some cases the SSP4 for the Valencian Community), since this scenario shows a marked decrease in the population by the end of 21st century in both areas. Furthermore, in both regions the results show that the increase in probability is higher when both climate and population change are included, highlighting the importance of also considering variables that take into account the exposure of the territory in flood damage analysis.

Overall, results show a general and marked increase in the probability of a damaging event with global warming with respect to the reference period when considering the RCP 8.5 climate change scenario and the SSP5 socioeconomic scenario. Other studies such as Wobus et al. (2014) also show an increase in monetary damages from flooding in nearly all regions of the United States and a total increase in damages by the end of the 21st century of approximately 30 %, although without taking into account other factors involved such as changes in demographics or infrastructure. In the Mediterranean area other authors also found an increase in flood risk associated with extreme precipitation events due to climate change (Cramer et al., 2018; Alfieri et al., 2015a), however the projections in flood hazards in Europe vary a lot regionally (Kundzewicz et al., 2017). Most of the studies of future flood projections refer to river floods (Alfieri et al., 2015a; Roudier et al., 2016; Rojas et al., 2012), without taking into account other types of floods. Therefore, this thesis ends with a substantial contribution towards assessing the future flood damage caused by other types of flood events, such as those caused by heavy precipitation episodes (surface water floods), as well as accounting for changes in population.

Chapter 9

Conclusions and future research lines

9.1 Conclusions

The overall objective of this thesis was to analyse flood damages in two Mediterranean regions frequently affected by intense precipitation events and to estimate their changes when future climate change projections and different socioeconomic scenarios are considered. To achieve this goal, the following specific aims were identified:

1. **Identify the flood events that have affected the regions of study (Catalonia and the Valencian Community).**

2. **Estimate the relationship between precipitation and flood damage for the present climate.**

3. **Analyse changes in precipitation extremes considering different climate change projections.**

4. **Assess the changes in the exposure of the regions of study.**

5. **Estimate flood damage variations due to global warming and considering different climate projections and socioeconomic scenarios.**

In this chapter we aim to summarise our central findings and the original contributions to the field.

Section 9.2 presents the main results referred to these specific goals, whilst Section 9.3 reports the overall conclusions. Finally Section 9.4 discusses some areas of study where we could be involved in the near future.

9.2   Results of this thesis

9.2.1   Identify the flood events that have affected the regions of study (Catalonia and the Valencian Community)

The north-west Mediterranean region experiences heavy precipitation every year and floods that occasionally produce catastrophic damages (Llasat et al., 2013). Both western Mediterranean regions covered in this thesis (Catalonia and the Valencian Community) are prone to these events, most of them caused by local heavy precipitation events (Llasat et al., 2016b). Therefore, the majority of floods that affect the region of study are surface water floods, which can be regarded as coming under the most general definition of rainfall-related floods.

The identification of each flood event and the collection and estimation of all the information regarding these events become crucial for the latter analysis of the links between flood damage and their causes. For the period of study, 1996-2015, Catalonia has recorded 166 flood events and received a total of 436.40 M Euro in compensation due to these events. That results in an average of 8.3 flood events and 21.82 M Euro per year. 13 of the flood events recorded caused catastrophic impacts, 87 extraordinary and 66 ordinary impacts. The basin most affected by floods was the Maresme with a total of 68 events. Besòs basin was the one that registered more damages with a total compensation amount higher than 45 M Euro according to CCS.

For the same period, the Valencian Community was affected by 69 events causing 713.75 M Euro in compensation. Therefore, this region recorded an average of 3.5 flood events and received 35.69 M Euro per year from CCS due to floods. 11 of the total flood events were catastrophic, 26 extraordinary and 32 ordinary. The most affected basin was Marina Alta with a total of 32 flood events for the same period. Nevertheless, 30 % of the total compensation (221.66 M Euro) were paid in the Jucar basin.

In both regions, more than 20 % of the flood events occurred in September, followed by August in the case of Catalonia (14 %) and October in the case of the Valencian Community (17 %). Coastal municipalities were the most affected by flood events and where most damage took place, since is where more population, infrastructure and assets are found and where local heavy precipitation events take place frequently.

9.2.2   Estimate the relationship between precipitation and flood damage for the present climate

We have tested several regression models to gauge the probability of large damaging events occurring given a certain precipitation amount and taking into account other variables related to the exposure of the territory. To do this, we analysed the relationship between these variables and flood damage estimates from insurance datasets in the region of study. Since there is not a standard definition of a large damaging event, we tested several cases, corresponding to insurance compensation exceeding different percentiles of the total damage sample.

Firstly, a correlation analysis at municipality level has been done in the Metropolitan Area of

Barcelona, showing that runoff has an important role in flood damage produced in urban zones with values of correlation close to 0.6. Then, the simple logistic regression models applied have confirmed that 30-min precipitation is a better predictor of the probability of large damages than daily precipitation in urban areas, with values under the ROC curve (RA) higher than 0.8 in all cases when sub-daily precipitation is used.

In the case of the whole Catalonia region, two types of logistic regression models have been tested to study the relationship between precipitation and compensation paid by insurance companies: simple and multiple logistic regression models. Better results have been obtained when using multiple logistic regression models with 30-min precipitation, proportion of urban zone and slope as explanatory variables. The probability of a damaging event increases with the 30-minutes precipitation data, but also both urban zone and slope are positively correlated with the response variable, showing that a highly urbanised and steeper basin will have a higher probability of a damaging event occurrence than a less urbanised and flat one, as expected. These results highlight the importance of including variables that also consider the exposure and vulnerability of the territory in flood damage analysis.

Finally, we have applied Generalized Linear Mixed models to estimate the probability of damaging events in Catalonia and the Valencian Community, taking into account both hazard and exposure. The best model for both regions was the one with the mean precipitation accumulated in 24 h and the total population of the basin as independent variables. Results have shown that the probability of a damaging event increases with precipitation and population of the basin. For both regions of study, the RA values indicate that our model has a good performance, with values close to 1 in all cases. These results improve those obtained by using both simple and multiple logistic regression models in the case of Catalonia, demonstrating that the incorporation of random effects in the model improves its performance, since, in general, better RA values are achieved when applying GLMMs.

Overall, our results have confirmed the hypothesis that precipitation is a key factor in explaining the damage caused by flood events in regions in which surface water floods are the main type of flood, as is the case in both Mediterranean regions of study. Furthermore, the results point out the need of incorporating variables such as population that give information about the exposure of the territory.

9.2.3 Analyse changes in precipitation extremes considering different climate change projections

We have analysed the precipitation extremes in the Iberian Peninsula for a global warming at 1.5, 2 and 3 °C above preindustrial conditions, using a subset of the ETCCDI (Expert Team on Climate Change Detection and Indices) precipitation indices and an ensemble of 7 EURO-CORDEX simulations assuming the RCP 8.5 scenario. We have presented an ensemble map of the 7 models showing the change of each precipitation index and warming level with respect to the reference period (1976-2005) per year and season.

Results have shown a general decrease of the total annual precipitation in most of the

Iberian Peninsula, especially in the central and southern parts. The decrease becomes larger with higher levels of global warming and especially during summer months. This, together with the expected increase in the length dry spell (CDD), could potentially exacerbate water scarcity, which is already a problem in the area. However, a likely increase in extreme precipitation with global warming, specially during the months of autumn and winter, have been found in the north and north-east half of the Iberian Peninsula. For instance, our results have shown projected increases in the number of days with daily precipitation exceeding 40 mm in the centre, north and north-west of the region. This is also in line with other studies on projections of extreme precipitation in the region (Drobinski et al., 2018; Colmet-Daage et al., 2018; Tramblay and Somot, 2018; Cramer et al., 2018), which show a likely increase in the extreme precipitation events in Europe and the Mediterranean area with increasing global temperature, mostly during the winter months (Kjellström et al., 2018; Vautard et al., 2014; Rajczak and Schär, 2017; Jacob et al., 2014).

In Catalonia, a general decrease in the annual precipitation is expected mainly during summer months, being more pronounced in the Pyrenees. However, increases in extreme precipitation events have been found from September to May, observed in the maximum 1-day and consecutive 5-day precipitation indices as well as in the number of days with precipitation exceeding 40 mm. This pattern is also observable in other studies of the region. For instance, the Third Report on Climate Change in Catalonia (TICC, 2016) points towards a general reduction of the total annual precipitation with global warming while Barrera-Escoda et al. (2014) show an increase of the frequency of heavy precipitation events (>200 mm in 24 h) during the 2021-2050 period.

In contrast, in the Valencian Community both annual and extreme precipitation are expected to decrease especially during spring and summer seasons, although some increases in extreme precipitation have been found in autumn and winter months, mainly in the north part of this region.

9.2.4   Assess the changes in the exposure of the regions of study

We have studied changes in exposure (i.e. population) in both regions of study taking into account 5 different socioeconomic scenarios. The Shared Socioeconomic Pathways (SSPs), together with the 2UP model, have been used to estimate the total population of each of the basins of the study for the future projections. The Institute for Environmental Studies (IVM) of the Vrije Universiteit of Amsterdam collaborated in the development of the 2UP model, reason why this part of the thesis was carried out during a research stay conducted at the IVM. The SSPs are based on five narratives describing alternative socio-economic developments, including sustainable development (SSP1), middle-of-the-road development (SSP2), regional rivalry (SSP3), inequality (SSP4) and fossil-fueled development (SSP5) (Riahi et al., 2017). The 2UP model disaggregates scenario-based projected national-level urban population to 30 arcseconds data and simulates urban expansion for 194 countries and territories.

All 5 scenarios has been considered in the analyses to predict the future probability of a

damaging flood event, however, main results have been focused on the RCP8.5/SSP5 combination, since this scenario assumes a society that keeps relying heavily on fossil fuels and thus, high emissions are expected.

Most of the scenarios (3 out of 5) depicts an increase in the population by the end of the 21st century, with the highest population growth around 50 % for Catalonia and 62 % for the Valencian Community with respect to 2010 when SSP5 is considered. Therefore, this implies a substantial increase in the exposure. Only SSP3 projects a clear decrease of the population in both regions.

9.2.5 Estimate flood damage variations due to global warming and considering different climate projections and socioeconomic scenarios

We have applied the Generalized Linear Mixed models developed along this thesis (specifically in Chapter 6) to assess the future probability of damaging flood events under scenarios of climate and population change. We have assessed changes in this probability with respect to the reference period (1976-2005) for both regions when considering a global warming of 1.5, 2 and 3 °C.

Our results have shown that the probability of damaging flood events increases for most models and warming periods in both regions when considering the RCP8.5/SSP5 combination, being higher in the case of Catalonia. Furthermore, a remarkable result found in both areas is that this change is usually larger when greater warming is considered and when both climate and population change are included. In the case of Catalonia, when population is considered, all the periods and models clearly show a higher increase in the probability of a damaging event (i.e. compensation exceeding 70th percentile of damage), which is statistically significant for all cases (the range of values goes from 15 % to 63 %). In the case of the Valencian Community, when population is considered constant at today's levels, the range of values goes from -4 to 26 %, but only the largest increases are statistically significant. However, when the change in population according to SSP5 is also taken into account, all values become positive, greater and most of them statistically significant. Reductions in the probability of a damaging event can be found when considering the SSP3. This is due to the decrease in population that this scenario shows for both study areas by the end of the 21st century.

Overall, our results highlight the need for limiting the global warming as much as possible, as well as the importance of including variables that consider change in both climate and socioeconomic conditions in the analysis of flood damage. The general increase found in the probability of a damaging event should be taken into account in flood management strategies.

9.3   Overall conclusions

The framework presented here could be applied to other geographic regions. For this reason, here is a summary of the main lessons learnt from a scientific and a methodological point of view.

- **Precipitation is the most important predictor for the probability of a damaging event.** We have shown that precipitation is a key factor in explaining the damage caused by flood events in regions in which surface water floods are the main type of flood, as is the case in the Mediterranean region of study.

- **Insurance data can be used as a proxy for describing flood damage.** Our findings align with the results of previous studies and further indicate that insurance databases are a promising source of information for flood damage assessment at local and regional scale.

- **Importance of considering exposure variables in flood damage analysis.** Our results have highlighted the importance of considering variables that take into account the exposure of the territory in flood damage analysis. As has been shown in both present and future climate analyses, population is a key exposure variable to explain flood damage.

- **Generalized linear mixed models are better to study the relationship between causes of floods and their damage than logistic regression models.** We have shown that GLMMs are the best tool out of the ones tested in this thesis for analysing non-normal data that involve random effects, as is the case that concern the present study. This methodology could be applied in other regions and fields.

- **Increases in extreme precipitation events are projected.** Although total annual precipitation is expected to decrease with global warming, increases in extreme precipitation have been found in the regions of study, mainly in Catalonia and during autumn and winter seasons. This has been observed with the increase in the number of days with daily precipitation exceeding 40 mm, the maximum precipitation recorded in 1 day and the maximum consecutive 5-day precipitation indices.

- **Increase in the probability of a damaging flood event with global warming.** Our analyses have shown a general and marked increase in the probability of a damaging event with global warming when considering the RCP 8.5 climate change scenario and the SSP5 socioeconomic scenario. The SSP5 scenario assumes a society that keeps relying heavily on fossil fuels and, therefore, high emissions are expected. However, an increase in the probability of a damaging event is expected in almost all scenarios, pointing out that even with lower exposure than in the SSP5 scenario, increases in flood damage are possible.

- **The need for limiting the global warming as much as possible.** We have shown that the probability of a damaging flood event is likely to become higher when greater

warming is considered. Therefore, our results support the statement of the Paris Agreement that reports that limiting the temperature increase to 1.5 °C would "significantly reduce the risks and impacts of climate change".

9.4 Future research

The development of this PhD thesis has risen several questions that require further analysis and research. Here we list some areas of study where we could be involved in the near future.

- **Taking into account other variables.** It should be noted that flood risk analysis is very complex and needs to be treated from a holistic perspective using techniques that take into account all the factors involved, both those related to the hazard of the phenomenon and those related to exposure of the territory. In this study only precipitation and population were taken into account for the future projections, and although the results show a good performance of the model for simulating the probability of a damaging event, other variables such as soil physical conditions, preventive or adaptation measures should be considered. For instance, in Garrote et al. (2016) different simulation scenarios were defined considering the modifications to the terrain due to the construction of fluvial defence structures in the area. Future research should focus on incorporating further variables into the model to reproduce the complexity of flood risk.

- **Higher spatial resolution.** The river-basin-scale is the spatial resolution selected in this thesis. Although the results are promising, future research should be focused on working in higher spatial resolution to better reproduce the different characteristics of the territory. For instance, sub-basins could be chosen to achieve this goal.

- **Sub-daily precipitation extremes.** The future projections used in this PhD focus only on daily precipitation data, while our results as well as other studies point out the possible better relationship found between sub-daily data and insurance data in the case of surface water floods (Spekkers et al., 2013; Torgersen et al., 2015; Cortès et al., 2018). Nevertheless, the analysis of sub-daily extremes would require convection-permitting regional climate models (Tramblay and Somot, 2018), and studies such as Beranová et al. (2018) have shown that convection is not captured realistically by currently available models. Therefore, projected changes of sub-daily precipitation extremes in climate change scenarios based on RCMs need to be interpreted with caution (Beranová et al., 2018).

- **Spatial resolution of precipitation projections.** Finer spatial resolutions of precipitation projections are needed to observe the intraregional climate heterogeneities and to be able to analyse which areas will be more vulnerable to flooding.

- **Indirect and non-tangible damages.** As previously discussed in Section 2.1 of Chapter 2, indirect and non-tangible damages have an important role in the assessment of the consequences of flood events. For this reason, an effort has to be made to incorporate

these damages in flood damage analysis, as these are crucial for evaluating the full impacts caused by natural hazards (Petrucci, 2013).

Appendix A

Supplementary material

A.1 Percentiles of damage

Percentile	Damage	10 mm	20 mm
50	D	202,262.16	355,630.44
	DPC	0.06	0.11
	DPW	2.16	3.95
60	D	315,590.67	440,467.02
	DPC	0.11	0.14
	DPW	3.41	5.07
70	D	441,492.99	1,822,938.94
	DPC	0.14	0.59
	DPW	5.15	17.78
80	D	1,437,832.00	2,704,309.59
	DPC	0.47	0.85
	DPW	13.87	27.56
90	D	2,922,536.83	7,382,754.22
	DPC	0.91	2.45
	DPW	27.86	72.36

Table A.1: Damage percentiles for all the damage indicators and for the 10 mm 30 min^{-1} and 20 mm 30 min^{-1} maximum precipitation thresholds for the MAB. Damage (D) is in Euro, damage per capita (DPC) in Euro/population and damage per wealth (DPW) in Euro/GDP

Percentile	Damage	40 mm	60 mm
50	D	77,833.72	94,500.50
	DPC	0.39	0.47
	DPW	15.27	21.17
60	D	149,687.23	197,795.55
	DPC	0.65	0.91
	DPW	27.87	44.22
70	D	248,533.86	316,668.04
	DPC	1.24	1.99
	DPW	61.45	80.98
80	D	571,983.55	816,655.06
	DPC	3.16	4.17
	DPW	124.73	167.36
90	D	1,695,150.48	2,371,528.42
	DPC	7.88	12.69
	DPW	320.56	500.63

Table A.2: Damage percentiles for all the damage indicators and for the 40 mm 24 h^{-1} and 60 mm 24 h^{-1} maximum precipitation thresholds for Catalonia. Damage (D) is in Euro, damage per capita (DPC) in Euro/population and damage per wealth (DPW) in Euro/GDP

Percentile	10 mm	20 mm
10	4,581.54	10,296.69
20	14,476.20	26,514.51
30	26,672.91	42,718.20
40	41,156.86	76,824.03
50	71,921.65	158,341.36
60	148,399.54	244,628.30
70	246,944.33	462,475.61
80	493,188.97	1,019,639.01
90	1,564,323.60	2,325,633.14

Table A.3: Damage percentiles (Euro) for the 10 mm 30 min^{-1} and 20 mm 30 min^{-1} maximum precipitation thresholds for Catalonia

Percentile	40 mm
10	5,617.39
20	16,161.94
30	34,194.49
40	54,945.92
50	92,555.52
60	198,602.47
70	383,686.33
80	1,074,080.45
90	2,816,026.41

Table A.4: Damage percentiles (Euro) for the 40 mm 24 h^{-1} mean precipitation threshold for Catalonia

Percentile	40 mm
10	50,113.71
20	214,678.12
30	357,659,.37
40	525,308.11
50	912,611.25
60	2,307,346.78
70	4,815,035.78
80	9,240,004.16
90	19,696,723.69

Table A.5: Damage percentiles (Euro) for the 40 mm 24 h^{-1} mean precipitation threshold for the Valencian Community

A.2 Codes of the basins
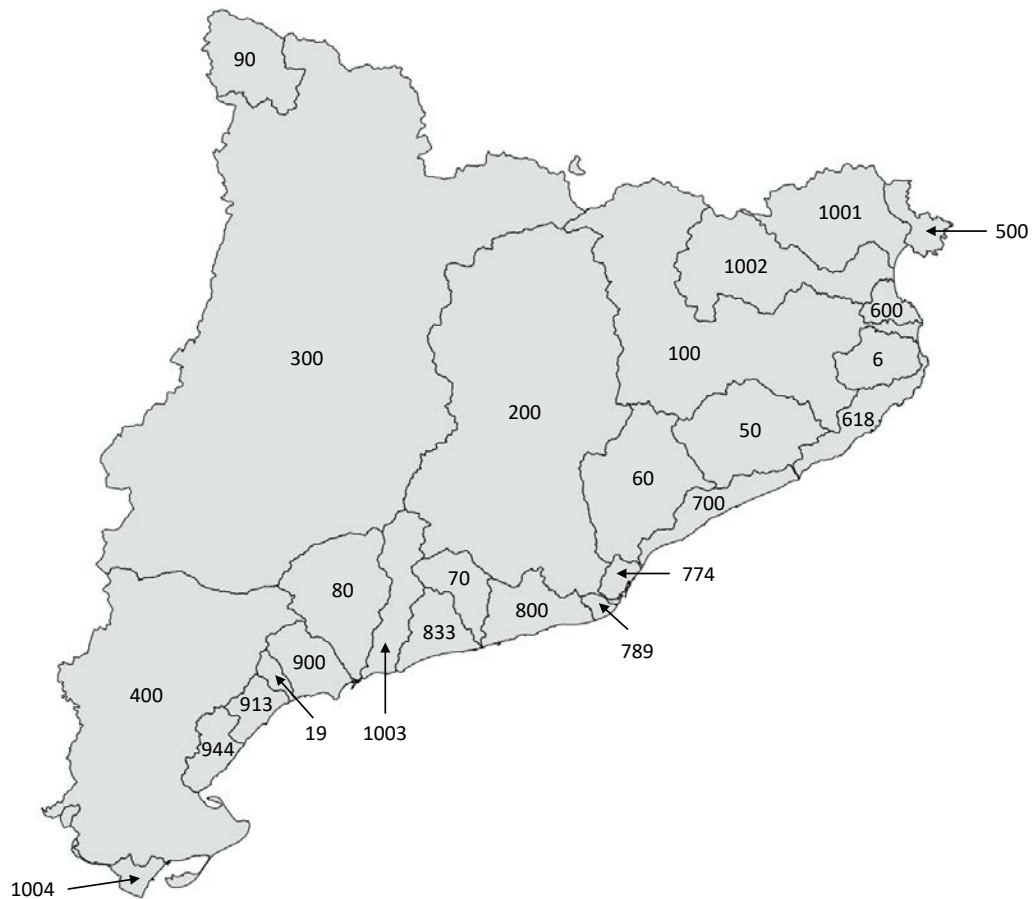
Figure A.1: Codes of the basins of Catalonia

Code	Name of the basin
6	El Daró
19	Riera de Riudecanyes
50	La Tordera
60	El Besòs
70	El Foix
80	El Francolí
90	Eth Garona
100	El Ter
200	El Llobregat
300	El Segre
400	L'Ebre
500	Rieres Costa Brava Nord
600	Rieres Costa Brava Centre
618	Rieres Costa Brava Sud
700	Rieres del Maresme
774	Torrents de l'Àrea Metropolitana de Barcelona
789	Rieres litorals Llobregat
800	Rieres del Garraf
833	Rieres Tarragona Nord
900	Rieres Tarragona Sud
913	Rieres Meridionals de Tarragona
944	Rieres litorals Ebre Nord
1001	El Tec; Rieres litorals Muga; La Muga
1002	Rieres litorals Fluvià; El Fluvià
1003	El Gaià; Rieres Tarragona Centre
1004	La Sénia; Rieres litorals Ebre Sud

Table A.6: Corresponding names of the codes of the basins of Catalonia region

Figure A.2: Codes of the basins of the Valencian Community

Code	Name of the basin
10	Vinalop-Alacant
15	Marina Baixa
20	Ebre
22	Marina Alta
30	Segura
32	Serpis
128	Jucar
168	Palancia-Los Valles
170	Mijares-Plana de Castelló
204	Cenia-Maestrazgo

Table A.7: Corresponding names of the codes of the basins of the Valencian Community region

Appendix B

Articles

CrossMark

ORIGINAL PAPER

Towards a better understanding of the evolution of the flood risk in Mediterranean urban areas: the case of Barcelona

Maria Cortès[1] · Maria Carmen Llasat[1] · Joan Gilabert[1,2] ·
Montserrat Llasat-Botija[1] · Marco Turco[1] · Raül Marcos[3] ·
Juan Pedro Martín Vide[4] · Lluís Falcón[5]

Abstract This contribution explores the evolution of the flood risk in the Metropolitan Area of Barcelona (MAB; Northeast Spain) from 1981 to 2015, and how it has been affected by changes in land use, population and precipitation. To complete this study, we analysed PRESSGAMA and INUNGAMA databases to look for all the information related to the floods and flash floods that have affected the chosen region. The "Consorcio de Compensación de Seguros", a state insurance company for extraordinary risks, provided data on economic damage. The extreme precipitation trend was analysed by the Fabra Observatory and El Prat-Airport Observatory, and daily precipitation data were provided by the State Meteorological Agency of Spain (AEMET) and the Meteorological Service of Catalonia (SMC). Population data were obtained from the Statistical Institute of Catalonia (IDESCAT). Changes in land use were estimated from the land use maps for Catalonia corresponding to 1956, 1993, 2000, 2005 and 2009. Prevention measures like rainwater tanks and improvements to the drainage system were also been considered. The specific case of Barcelona is presented, a city recognised by United Nations International Strategy for Disaster Reduction as a model city for urban resilience to floods. The evolution of flood events in the MAB does not show any significant trend for this period. We argue that the evolution in floods can be explained, at least in part, by the lack of trend in extreme precipitation indices, and also by the improvements in flood prevention measures.

Keywords Floods · Flash floods · Changes in land use · Vulnerability · Precipitation extremes · Barcelona

✉ Maria Cortès
mcortes@meteo.ub.edu

1 GAMA, Department of Applied Physics, University of Barcelona, Barcelona, Spain

2 Cartographic and Geological Institute of Catalonia, Barcelona, Spain

3 Barcelona Supercomputing Center-Centro Nacional de Supercomputación, Barcelona, Spain

4 Department of Civil and Environmental Engineering, UPC, Barcelona Tech, Barcelona, Spain

5 Urban Architect, FALCON Architecture and Urbanism, Barcelona, Spain

🌀 Springer

1 Introduction

Floods are the most dangerous natural hazard in the world, and the risk of floods would increase in a warmer climate, according to the most recent regional and global projections (IPCC 2012; Hirabayashi et al. 2013). Consequently, improving mitigation and adaptation strategies to cope with floods has become a strategic topic in national (e.g. the Spanish project HOPE, HOlistic analysis of the impact of heavy PrEcipitations and floods and their introduction in future scenarios. Application to adaptation and resilience strategies) and international (e.g. HyMeX: HYdrological cycle in the Mediterranean EXperiment) (Drobinski et al. 2014) climate programmes, and they are a priority in most government agendas (Alfieri et al. 2016).

Yet there are still many uncertainties in characterising the present and future evolution of floods. Recent reports from the IPCC (2012, 2014) still show significant uncertainty associated with future projections of extreme precipitation (Turco et al. 2017), and the uncertainties are even greater when considering floods and interaction with society in the context of increased vulnerability. The impacts are exacerbated by the increase in population and in vulnerability, especially in cities where there is already pressure from humans (Ceola et al. 2014). This is the case in the Mediterranean region, where the population is concentrated on the coast, often in areas exposed to natural hazards (Eurostat 2016).

More than 250 events causing floods, flash floods and urban floods have been recorded in Catalonia (Northeast Spain) between 1981 and 2015. The Spanish public reinsurer, the "Insurance Compensation Consortium" (CCS), has paid more than €430 million in compensation for flooding during the available period of insurance data, 1996–2015. To this amount, we must also add the loss of profits and damages to population, as well as all the compensation provided by insurance companies for damages not accepted by the CCS. The coastal zone has the highest number of episodes (70%), due to highly localised convective rainfall events (Llasat et al. 2016; Gascón et al. 2016). Approximately one-third of the episodes affected the regions of Maresme, Barcelonès and Baix Llobregat, which belong, totally or partially, to the Metropolitan Area of Barcelona (MAB). This is an area with significant exposure and vulnerability due to the high population density and concentration of infrastructures (Llasat et al. 2014a). The problem will worsen considering that 70% of the population will be concentrated in coastal cities by 2050, according to Benoit and Comeau (2005). In other words, the MAB constitutes a good example of a Mediterranean coastal region, with significant urbanisation of flood-prone areas and a high population density in an area crossed by numerous streams.

Several studies have analysed extreme climate and weather events affecting the region of Barcelona (Turco et al. 2014; Llasat et al. 2014b) and the evolution of floods in Catalonia, also considering the evolution of floods over the last six centuries (Barrera-Escoda and Llasat 2015) and over the recent period of 1981–2010 (Llasat et al. 2014a, 2016). For both periods, the extraordinary events show a positive trend, probably linked to land use changes and an increase in assets and dwellings in flood-prone areas, leading to an increased flood risk.

However, there is still little known about flood evolution in Mediterranean urban areas, combining drivers and consequences (Faccini et al. 2015). That is, the analysis of flood risk is very complex and needs to be dealt with from a holistic perspective using techniques that take into account all the factors involved, both those related to the dangerous nature of the phenomenon, those related to vulnerability and exposure and those related to the impacts (Llasat et al. 2009; Blöschl et al. 2013; Nakamura and Llasat 2017). Most studies analyse the risk of flooding from a *top-down* perspective, that is, from the nature of the

phenomenon while leaving aside other factors. According to Merz et al. (2010), the analysis of flood risk continues to be very unbalanced since, in comparison, much more attention is paid to the dangerousness of the phenomenon than to the impacts it produces. This is why progress is currently being made to incorporate impacts, exposure and vulnerability in the analysis, although limited data (e.g. availability and temporal coverage) make this challenging (Terti et al. 2015; Karagiorgos et al. 2016; Bodoque et al. 2016).

An approach that addresses the study of floods starting from impacts is called *bottom-up* (García et al. 2014) and starts on a local scale of individuals, households and communities, exploring the factors and conditions that enable them to successfully cope with hydrological extremes (Wilby and Dessai 2010). This would be the case for studies carried out in relation to the catastrophic flood episode of 2013 that affected much of Central Europe, which on the one hand analyse the hydrometeorological factors that caused the episode (Schröter et al. 2015) and on the other hand analyse the impacts produced (Thieken et al. 2016).

Merz et al. (2010) emphasised the importance of flood risk characterisation from a holistic and multidisciplinary perspective that integrates both approaches. An example of this integrated approach is the studies by Amaro et al. (2010) and Barbería et al. (2014) in which factors related to dangerousness, vulnerability and exposure are combined to develop social impact indexes. They present the challenge of identifying and improving the assessment of non-hazardous factors (non-climatic factors) and their role in the impact of flood events as indicated by Hall et al. (2014). That is, the key point of these types of analysis is to identify the key factors to be considered when improving strategies for adaptation and mitigation.

In this article, we study the evolution of the flood risk in a densely populated area, the MAB, by analysing the different factors related to the hazard, vulnerability and exposure involved, as well as the damages caused. To this end, we first analyse the evolution of flood episodes recorded in the MAB from 1981 to 2015 and the impacts caused. Then, we analyse the changes in land use, runoff, population and precipitation extremes in the MAB and their potential relationship with floods. Also, we analyse the link between damages and precipitation over 1996–2015 period, for which CCS data are available. The paper ends with some key conclusions and recommendations.

2 Region of study

Catalonia (Fig. 1a) is located in the northwest coast of the Mediterranean Sea. It covers an area of 31,895 km^2 (6.3% of Spain) and has an official population of 7,522,596 (IDESCAT 2016). The zone selected was the Metropolitan Area of Barcelona (MAB), made up of Barcelona and 35 adjacent municipalities around the city. This urban and peri-urban area has a surface of 636 km^2 and a population of 3,239,337. The larger part of the population is concentrated in the municipality of Barcelona (1,608,746 people), located between the Besòs River and the Llobregat River, the Littoral Range and the Mediterranean Sea (Fig. 1b). Although both rivers have experienced catastrophic flood events (e.g. September 1971) with return periods higher than 100 years, minor flood events occur frequently (every year) as a consequence of convective and local precipitation mainly recorded in late summer and autumn (Llasat et al. 2013; del Moral et al. 2016). Their main impacts are the consequence of drainage and runoff problems and can affect both urban and rural areas.

In the MAB, a total of 109 flood events have been registered for the 1981–2015 period, eight of them causing catastrophic impacts in the region. Most of the catastrophic flood
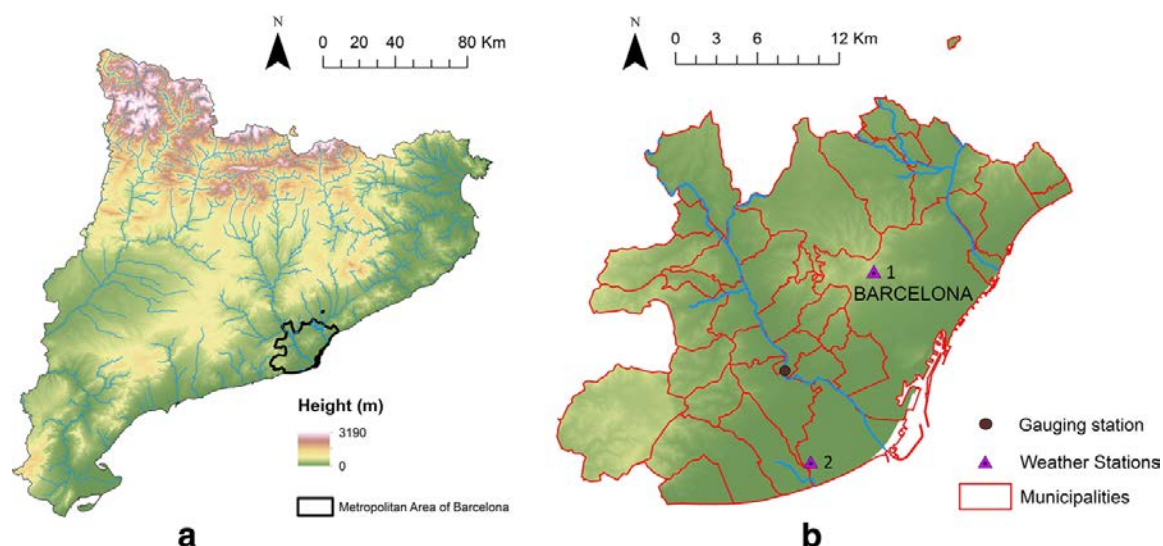
Fig. 1 a Location of Metropolitan Area of Barcelona in Catalonia; **b** map of the Metropolitan Area of Barcelona showing its municipalities, the Sant Joan Despí gauging station and the weather stations (*1* Fabra observatory; *2* International Airport of Barcelona). The Besòs River (the northern part) and the Llobregat River (the southern part) are also shown (in *blue colour*)

events that affected Barcelona occurred in the '1980s and '1990s, which led to the proposal and construction of the rainwater tanks in the city. On the other hand, due to the construction of the International Airport of Barcelona, the stream of the Llobregat River was altered (Fig. 2), and the Besòs River was channelled and modified near its mouth in order to avoid floods and built a fluvial park. A surveillance system was installed in order to warn the population in the case of possible floods.

3 Data sources

The analysis uses the INUNGAMA database, which contains more than 200 flood events for all Catalonia for the period 1981–2010 (Barnolas and Llasat 2007; Llasat et al. 2014a) and which was updated until 2015 for this study. The analysis also includes the PRESSGAMA database, which contains more than 15,000 news items on natural hazards and climate change published in the newspaper La Vanguardia (Llasat et al. 2009), and updated to cover the period 1981–2015. Information regarding the economic damage caused by floods was provided by the state insurance company "Consorcio de Compensación de Seguros", or CCS, a Spanish national reinsurance company that provides cover for losses caused by significant risks, when covered by the relevant insurance policy. These data are available on a municipal scale for the 1996–2015 period.

Changes in land cover were analysed through the Land Use Maps of Catalonia, drawn up by the Ecological and Forestry Applications Research Centre (*Centre de Recerca Ecològica I Aplicacions Forestals,* CREAF) for the available editions (1956, 1993, 2000–2002, 2005–2007 and 2009). Runoff coefficients for different land uses were taken from Chow et al. (1988). Population density since 1950 was provided by the Statistical Institute of Catalonia (*Institut d'Estadística de Catalunya,* IDESCAT). All the cartographic databases were analysed with Arc-Info GIS.

The rainfall data consist of: maps of daily expected precipitation for different return periods in Catalonia (Casas-Castillo et al. 2005); daily rainfall data from the Fabra

151
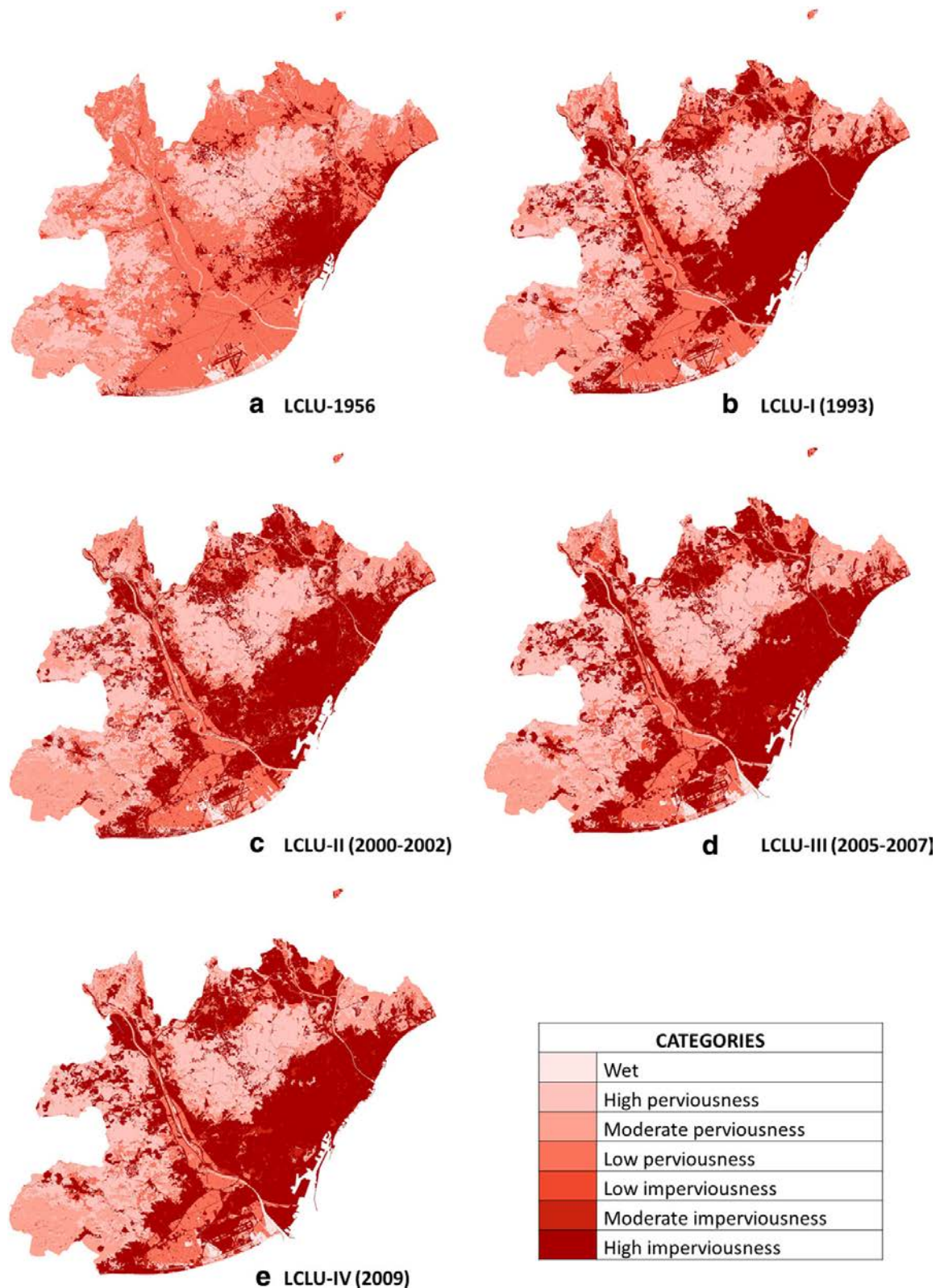
Fig. 2 Comparison between the impervious/pervious maps based on the five different LCLU maps considering 7 categories: **a** LCLU (1956); **b** LCLU-I (1993); **c** LCLU-II (200–2002); **d** LCLU-III (2005–2007); **e** LCLU-IV (2009)

Observatory (414 MASL) available since 1913, and from the International Airport of Barcelona (El Prat de Llobregat) since 1961 (4 MASL; Fig. 1); and daily precipitation fields for specific events provided by the Meteorological Service of Catalonia *(Servei*

Meteorològic de Catalunya, SMC) and the State Meteorological Agency of Spain (*Agencia Estatal de Meteorología*, AEMET). Information related to rainwater tanks was provided by the Barcelona Water Cycle (*Barcelona Cicle de l'Aigua*, BCASA).

Finally, the cartography with the fluvial network and hazard maps was provided by the Catalan Water Agency (*Agència Catalana de l'Aigua,* ACA) and also shows the flow data for the Sant Joan Despí station (Llobregat River).

4 Methodology

4.1 Flood event classification

Flood events have been classified according to their impact (Barriendos et al. 2003; Llasat et al. 2005; Barrera-Escoda et al. 2006; Llasat et al. 2014a). In order to be more specific, we have suggested some indicators, shown in Table 1. This classification allows us to

Table 1 Indicators to determine the impact of each flood event

Indicator	Definition	Catastrophic event	Extraordinary event	Ordinary event
Public buildings	City hall, hospital, school, church, emergency centres, police station, etc.	Total destruction or collapse	Partial destruction or structural damage	Flooded, habitable
Private houses	Houses with one or more floors, basements, etc.	Total destruction or collapse	Partial destruction or structural damage	Flooded, habitable
Bridges	Bridges, footbridges	Destroyed, unusable	Structural damage, unusable bridges or damage to footbridges	Usable
Hydraulic infrastructures	Mills, irrigation channels	Destroyed	Medium damage	Minor damage
Roads	Railway, highway, state road, country road, regional road, municipal road	Partially destroyed, one or more stretches of the road damaged	Flooded, closed for >12 h	Flooded, closed between 0 and 12 h or not closed
Services	Gas, electricity, telephone lines, water	Destruction and/or closure of infrastructures for >24 h	Closed between 6 and 24 h	Closed for <6 h
Productive activities	Industry, agriculture and livestock, commerce, touristic infrastructures	Interruption of production and loss of the production system	Interruption of production and loss of products	Loss of products
Cars	Cars washed away or damaged by water	20 or more washed away	Between 5 and 19 washed away	Between 1 and 4 damaged and/or washed away
Deaths	No. of people dead	10 or more	Between 5 and 9	Between 1 and 4

distinguish between three categories: (a) ordinary flood events (rivers or streams not overflowing; floods in restricted areas; minor damages, damage to hydraulic infrastructure or cars parked in the temporary flow of the torrential channel; flooded car parks, basements or ground floors; disturbances to daily activities); (b) extraordinary flood events (overflowing rivers or streams; some streets or other urban places flooded; damages or partial destruction of structures near the stream or river, damage to street furniture or cars; inconveniences in the daily life of the population); and (c) catastrophic flood events (overflowing riverbanks; extensive flooded areas; total destruction or serious damage to hydraulic infrastructures (e.g. bridges), buildings, crops, road infrastructures and private assets). In this paper, the classification was applied on four levels: first, with regard to the impact throughout Catalonia as a whole; second, according to the impact in the MAB; third, in the MAB without taking into account Barcelona; and fourth, in the Barcelona municipality.

4.2 Land cover evolution

The available maps (Table 2) have been homogenised following the characteristics of the first edition of the Land Cover and Land Use map (LCLU-I). The oldest edition of the LCLU was based on American flight photographs made in 1956 over the Barcelona Province. It was recently processed and for this reason includes 241 categories like the later editions. LCLU-1956, LCLU-III and LCLU-IV use a hierarchical legend with 5 levels of categories. In order to compare the different time editions and analyse the evolution of land use, all the maps have been homogenised in a common resolution of 2.5 m × 2.5 m and have been classified using 24 categories as used in LCLU-I.

Taking into account the heterogeneity of the region and its hydraulic features, a streamlined method has been applied to estimate the runoff, based on the application of the runoff coefficients proposed by Chow et al. (1988) for different return periods. Taking into account that the average slope in the MAB is between 2 and 7%, we considered that runoff coefficients only depend on the return period (Table 3). The 24 initial categories of the LCLU have been merged into 7 categories according to land permeability, in order to avoid the dispersal that excess categories would cause.

Each layer has been classified in a category with an assigned runoff coefficient. All this information has been aggregated on a municipal scale as the average of all the pixels. Consequently, each municipality is characterised by the previously selected return periods and a runoff coefficient, calculated using the average of all the pixels included in it. Although it only provides an approximate runoff, this approach is typical in urban public works and helps to improve estimates for running or accumulated water that can affect

Table 2 Features of the LCLU (land cover and land use maps of Catalonia) for each edition

Edition	LCLU-1956	LCLU-I	LCLU-II	LCLU-III	LCLU-IV
Year	1956	1993	2000–2002	2005–2007	2009
Orthophotos scale	1:25,000	1:25,000	1:5000	1:5000	1:2500
Resolution (pixel)	2.5 m	2.5 m	0.5 m	0.5 m	0.25 m
Working scale	1:3000	1:3000	1:1500	1:1500	1:1000
Categories	241	24	61	241	241

Table 3 Runoff coefficients for each category and return period (Chow et al. 1988)

Runoff coefficients								LCLU categories
Permeability categories	Return periods							
	2	5	10	25	50	100	500	
Lakes	0	0	0	0	0	0	0	Wetlands, beaches, water, canals and ponds, urban ponds
High perviousness	0.31	0.34	0.36	0.40	0.43	0.47	0.57	Forest (dense, not dense, riverside)
Moderate perviousness	0.33	0.36	0.38	0.42	0.45	0.49	0.58	Meadows, bushes
Low perviousness	0.35	0.38	0.41	0.44	0.48	0.51	0.6	Crops, populus and platanus plantations
Low imperviousness	0.35	0.39	0.41	0.45	0.48	0.52	0.58	Recent reforestation, burned areas, forest tracks and firebreaks
Moderate imperviousness	0.40	0.43	0.45	0.49	0.52	0.55	0.62	Vacant lots, sport and recreational areas
High imperviousness	0.74	0.78	0.82	0.87	0.91	0.96	1	Scree slopes, snowdrifts and glaciers, urban areas, roads and train tracks, mines

exposed assets and the population in general. The advantage is that it can be used in regional analysis.

Following this methodology, the return periods for rainfall have also been obtained on a municipal scale from the maps of maximum daily precipitation expected in Catalonia for different return periods (Casas-Castillo et al. 2005). The return period corresponding to the flow for each specific flood event has been calculated through GEV (generalised extreme values) with a regional value of L-coefficient of skewness (Mediero et al. 2010).

4.3 Flood and rainfall analysis

In order to analyse the flood and rainfall evolution, we carried out analysis on trend significance using the Mann–Kendall test (Mann 1945; Kendall 1975), with a threshold of significance established at 95 and 90% (p value <0.05 and p value <0.1, respectively). For flood events, we studied the annual evolution of the total number of floods as well as the floods in different categories (ordinary, extraordinary and catastrophic) for the period 1981–2015. Furthermore, a monthly and seasonal analysis was carried out.

To analyse the specific case of the city of Barcelona and the impact of the preventive measures taken in the city on flood evolution, a study was carried out for three different scenarios: MAB, Barcelona and MAB without Barcelona. For precipitation data, we used the values recorded in 24 h as well as the rainfall accumulation for the whole episode (obtained from AEMET stations). In order to analyse the data in a comparable way, we considered a subset of the "moderate and extreme" precipitation indices defined by the World Meteorological Organization (WMO 2009) CC1/CLIVAR/JCOMM Expert Team on Climate Change Detection and Indices (ETCCDI). More specifically, the chosen subsets of indices (Table 4) summarise the behaviour of precipitation, describing some standard indices such as the total precipitation (PRCPTOT) and precipitation intensity (SDII), as

Table 4 Selected ETCDDI indices

ETCCDI	Description
PRCPTOT	Total precipitation
SDII	Mean precipitation amount per rainfall day
RX1DAY	Maximum precipitation in one day
RX5DAY	Maximum accumulated precipitation in 5 days

well as two extreme indices related to critical consequences, such as the highest precipitation amount over a 1- or 5-day period (RX1DAY and RX5DAY, respectively).

The comparison between flood events and their drivers was made considering the periods 1981–1996, 1996–2015 and 1981–2015, given that CCS data are only available for the 1996–2015 period. For each of these periods, we calculated the trend in the number of total events, the trend according to flood impact categories and the trend for maximum precipitation recorded in 1 day (RX1DAY) for both the Fabra and Airport observatories. To calculate the changes in land use while taking into account the land permeability categories, the LCLU-1956 map was considered to represent the starting point. Attending that there is not any new information about land uses changes until 1993, the percentage of impervious surface in the MAB in 1981 was interpolated from LCLU-1956 and LCLU-1993 maps. The LCLU-1993 was considered as representative for the 1996 land use coverage, and the LCLU-2009 map shows 2015 coverage.

In order to carry out a more detailed analysis, we selected 10 extraordinary and 3 catastrophic flood episodes in the MAB between 1996 and 2015, considering their individual impact in each one of the 36 municipalities. Table 5 shows the episodes studied along with their start/end dates and their category (according to their impact). For each episode, the average precipitation values on a municipal level were obtained through ordinary Kriging with ArcGIS. In order to obtain the daily runoff values, the runoff coefficient on a municipal level (the average from the runoff categories for the different pixels) was multiplied by the accumulated daily precipitation. The correlation analysis was achieved using the Spearman test, and the results are discussed in Sect. 5.6.

Table 5 Flood events recorded in the MAB when CCS data is available (1996–2015)

Start date	End date	Event category
02/12/1998	04/12/1998	Extraordinary
03/09/1999	04/09/1999	Extraordinary
13/09/1999	15/09/1999	Extraordinary
10/06/2000	12/06/2000	Extraordinary
31/07/2002	02/08/2002	Extraordinary
10/08/2002	11/08/2002	Extraordinary
12/09/2002	14/09/2002	Extraordinary
08/10/2002	11/10/2002	Catastrophic
05/09/2005	09/09/2005	Catastrophic
12/09/2006	15/09/2006	Catastrophic
22/10/2009	23/10/2009	Extraordinary
30/07/2011	31/07/2011	Extraordinary
28/09/2014	01/10/2014	Extraordinary

4.4 The evolution of Societal Impact

The social impact analysis was carried out using the compensation provided for flood damages as registered in the CCS dataset. These data have the advantage that is taken directly from a municipal level, spanning the period from 1996 to 2015. However, working with a damage cost time series involves taking into account changes in living standards, as well as the different economic trends applied to insured assets (Barredo et al. 2012). Thus, we updated the currency to transfer the damage values to euros, taking the year 2015 as our reference point (*Instituto Nacional de Estadística*, INE). We considered the compensation paid by the CCS during the flooding episodes and, also, during the following 7 days after their conclusion (this is the period accepted by the CCS to report flood-related losses). The variables used were: total damages, the ratio of total damages/population density and the ratio between total damages and population. The temporal evolution of the compensations paid by CCS was also analysed, along with the correlation between damages/precipitation and damages/runoff for the 13 specific cases.

5 Results and discussion

5.1 Influence of land use changes in runoff

The comparison between the impervious/pervious maps based on LCLU maps shows how the majority of the agricultural soil (low perviousness) has been substituted by urban surfaces (high imperviousness) between the first (1956) and the last map (2009; Fig. 2). There is not so much change in this period in the area covered by forests (approximately, 25%), which mainly corresponds to the Tibidabo Mountain, with a maximum altitude of 505 m. Instead, the agricultural area has diminished around 80% between 1956 and 2009, being replaced by urban surfaces and the road network (increase of more than 225%). However, the difference between 1993 and 2009 is lower, with a decrease in the agricultural area near 47% and an increase in the urban surfaces and the road network around 20%. Consequently, the urban surfaces and impermeable soil have not increased so significantly over the last few years and have only gone from 36.5% coverage in 1993 to 43.4% in 2009.

For the 1950–2015 period, the population has increased from 1,555,236 to 3,213,775 inhabitants. The population peak in the MAB was recorded in the '1980s and afterwards began to decline until the currently situation. This changing point does not match with the general trend in Catalonia or in Spain, which recorded a maximum at the end of the first decade of the twenty-first century. The major housing price increases in the MAB, and the economic crisis are the main explanations for these turning points, as well as negative trends in population growth.

Figure 3 shows the runoff changes for a 24-h rainfall return period over 100 years for the different LCLU maps. As expected, there is an increase in average runoff for all municipalities, due to the increase in impermeable soil (a feature that can be already observed in Fig. 2). In most municipalities (67%) between 1956 and 2009, there was an increase in runoff of over 20%, with an average of 30% for the MAB. In Barcelona, the runoff increase stands at 19% for this period (without considering the improvements in sewerage systems and flood prevention infrastructures that were introduced in the '1990s). Figure 4 shows the evolution of the average runoff in the MAB and Barcelona, along with
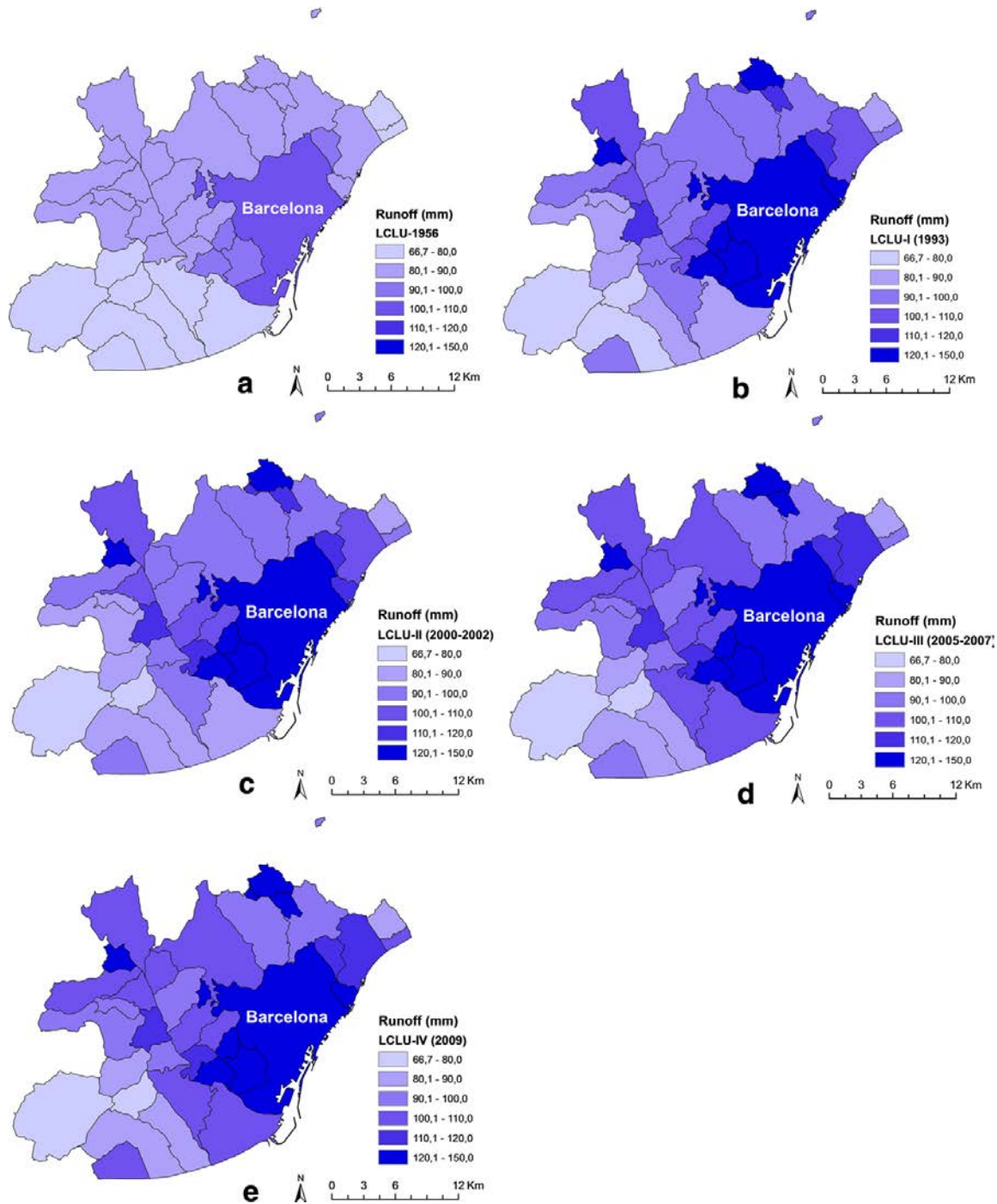
Fig. 3 Mean runoff on a municipal level for a return period showing daily precipitation over 100 years, taking into account the runoff coefficients in Table 3: **a** LCLU (1956); **b** LCLU-I (1993); **c** LCLU-II (2000–2002); **d** LCLU-III (2005–2007); **e** LCLU-IV (2009)

the installation of the first rainwater tank. This figure brings together the major changes that occurred between 1956 and 1993 due to the significant industrialisation of the region, which was the location of the majority of the textile industry in Spain during this period.

5.2 Rainfall evolution

Figure 5 and Table 6 shows the evolution of the selected ETCDDI indices for the rainfall measured in the Fabra Observatory. Although all the series show a negative trend for the
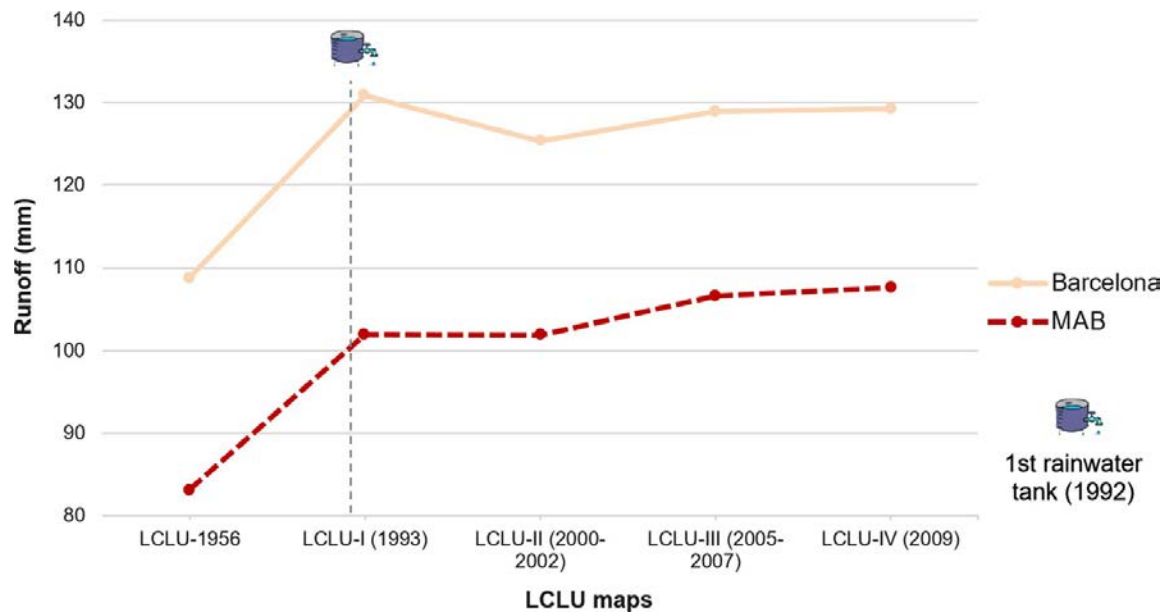
Fig. 4 The evolution of the mean runoff in the MAB and Barcelona for a return period of 100 years, based on the five different LCLU maps. The date of construction of the first rainwater tank in Barcelona is also shown

1981–2015 period, they are not statistically significant at 95 or 90%. On the other hand, the PCRPTOT, SDII and RX5DAY indices show a significant negative trend (p value <0.1) at the Airport weather station. This heterogeneity is normal for the region as shown in the last report on Climate Change in Catalonia (Martin Vide et al. 2016).

5.3 Flood evolution

MAB has been affected by 109 flood events in the period 1981–2015, concentrated in the coastal municipalities and in the Llobregat River axis (Barcelona recorded the most flood events at 73 events, followed by Castelldefels, near the Airport, with 24 events). Of the 109 events, 19 caused catastrophic impacts in Catalonia and 50% also produced catastrophic damages in the MAB. As a consequence of these floods, 11 people lost their lives: 5 deaths were caused by ordinary events; 1 by extraordinary events; and 5 by catastrophic events.

The monthly evolution of flood events shows maximum levels between August and October, with a peak in September that records 29% of the total; 26% were extraordinary events, and 13% were catastrophic events. Usually these are local flash floods and urban floods associated with heavy and short rainfall events (Llasat et al. 2016). In Barcelona, theses values decreased from 23 and 9%, respectively. This means that 68% of the events are considered ordinary events, suggesting the positive role played by rainwater tanks in reducing high-impact flood events.

Figure 6 shows the evolution of flood episodes in the MAB for the 1981–2015 period. The trends for the three categories are generally negative, although none of them are statistically significant ($p < 0.05$). On the other hand, a positive trend of total events (0.08 events/decade) was shown for September, although it is not significant at 90%. The detailed analysis of both the MAB series with and without Barcelona shows that this negative trend is a consequence of the strong weight of the Barcelona municipality. In effect, although the MAB series without Barcelona shows a positive but not a significant trend, the flood evolution in Barcelona shows a negative and significant trend (Table 7).
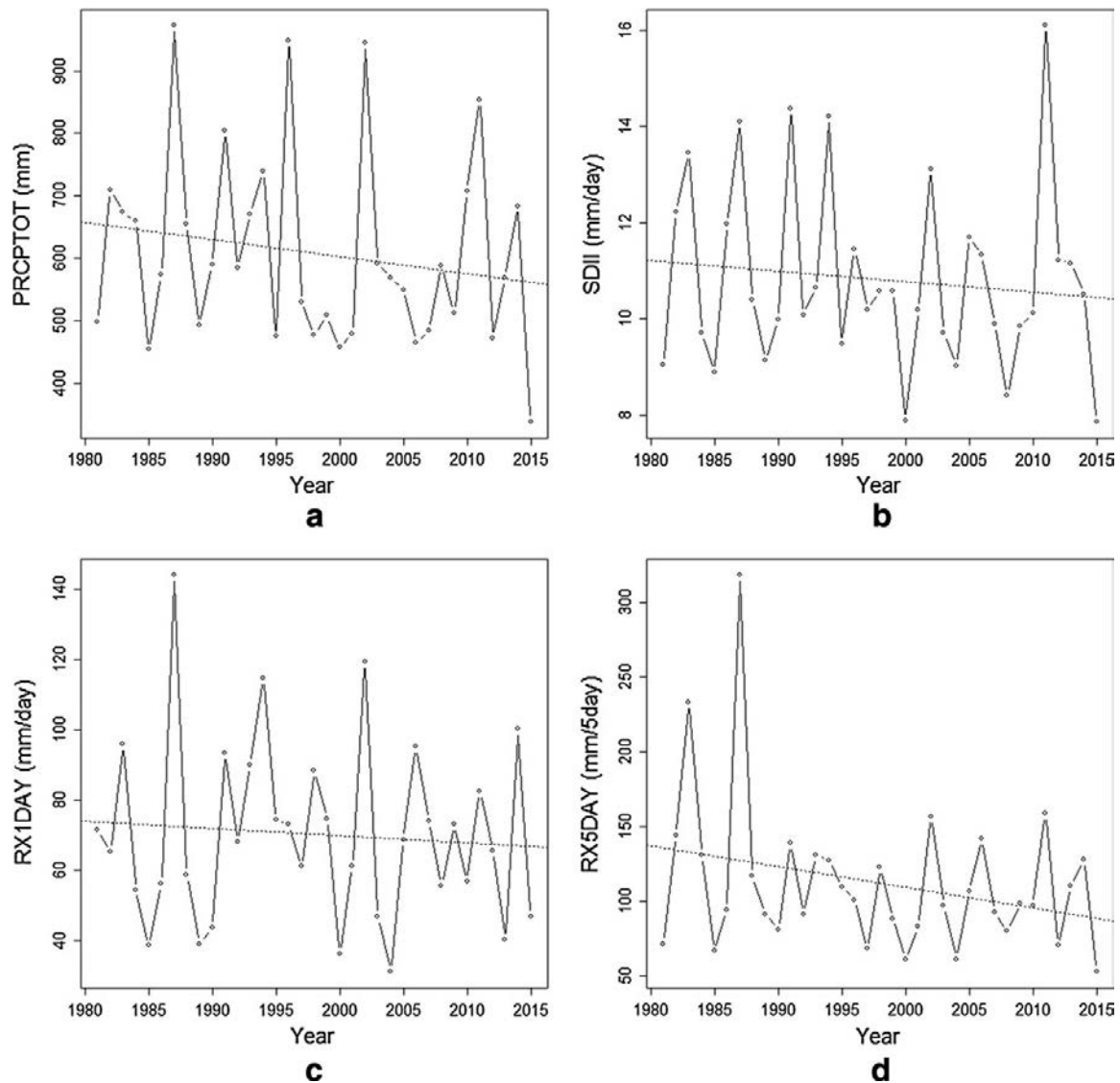
Fig. 5 Evolution of the ETCCDI indices (as given in Table 4) for the Fabra station: **a** PRCPTOT index (mm); **b** SDII (mm/day); **c** RX1DAY (mm/day); RX5DAY (mm/5 days)

This fact is consistent with the efficiency of drainage infrastructures in reducing and mitigating the flood impact of high-intensity events and the amount of precipitation in the city (Barrera-Escoda et al. 2006). The drainage network together with the rainwater tanks and the warning system for the Besòs River meant that Barcelona received acknowledgement from UNISDR (United Nations International Strategy for Disaster Reduction) as a model city for urban resilience to floods (UNISDR 2015b).

5.4 Damage evolution

Figure 7 shows the annual changes in compensation for floods paid by the CCS in the MAB between 1996 and 2015, as well as the total number of recorded flood episodes for this period. The compensation paid by the CCS shows significant variability from 1 year to another, and no trends were found. For instance, in 1999 nearly €34.8 million was paid as a consequence of two events, when the annual average is €4.3 million. In 2002, there were a total of 5 episodes, one of which was catastrophic and 3 of which were extraordinary, with a total amount of €26.6 million. The total amount paid by the CCS due to floods produced

Table 6 Trend analysis results for the ETCCDI indices for the Airport and Fabra weather stations

	PRCPTOT	SDII	RX1DAY	RX5DAY
Airport				
Trend (unit/year)	−5.44**	−0.08*	−0.60	−2.08*
Fabra				
Trend (unit/year)	−2.74	−0.02	−0.20	−1.38

* p value <0.1; ** p value <0.05
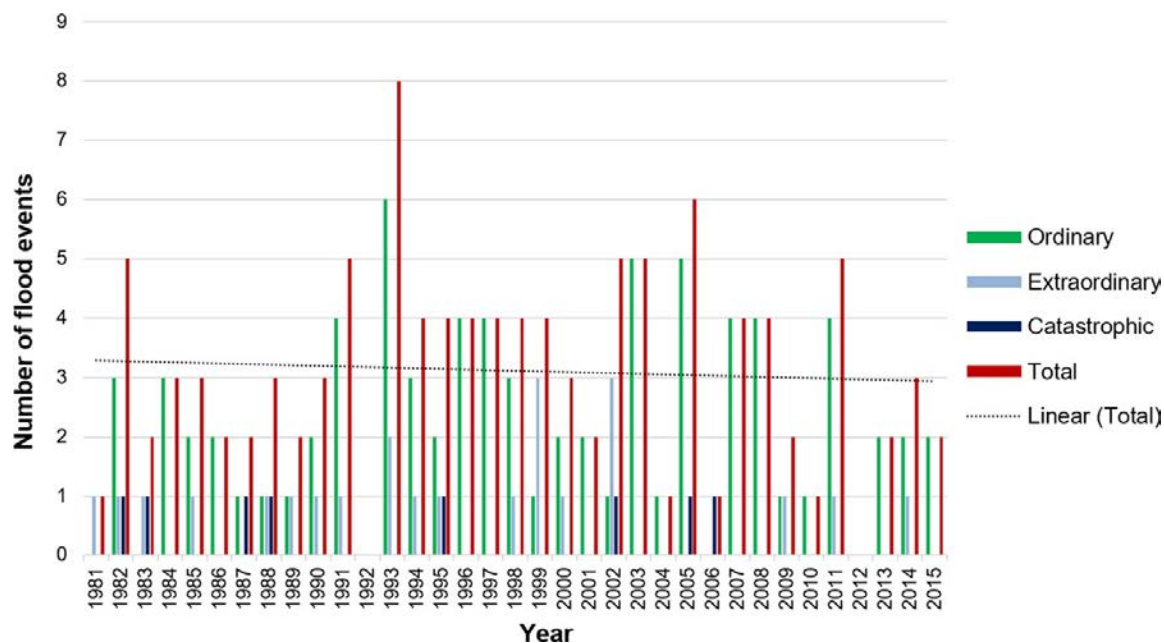
Fig. 6 Number of flood events in the MAB (1981–2015), according to their impact category

Table 7 Trend analysis result for the number of flood events in the MAB, Barcelona and the MAB without Barcelona

	Total	Ordinary	Extraordinary	Catastrophic
Metropolitan Area of Barcelona				
Trend (unit/decade)	−0.10	0.15	−0.15	−0.10
Barcelona				
Trend (unit/decade)	−0.18	0.11	−0.20**	−0.08*
Metropolitan Area of Barcelona without Barcelona				
Trend (unit/decade)	−0.13	−0.01	−0.03	−0.09

* p value <0.1; ** p value <0.05

in MAB between 1996 and 2015 is €86.3 million. The municipality of Barcelona has the maximum record with €24 million. There is a strong inter-annual variability for the number of annual news items published in *La Vanguardia,* which recorded 43 news items on floods produced in the MAB for the year 1999. During 13–14 September of 1999, an extraordinary flood event took place as a consequence of a heavy precipitation that produced more than 43 mm in 30 min, and a maximum flow of the Llobregat River (at the Sant Joan Despí gauge) of 197.3 m³/s (the average is around 20 m³/s) corresponding to a return period of
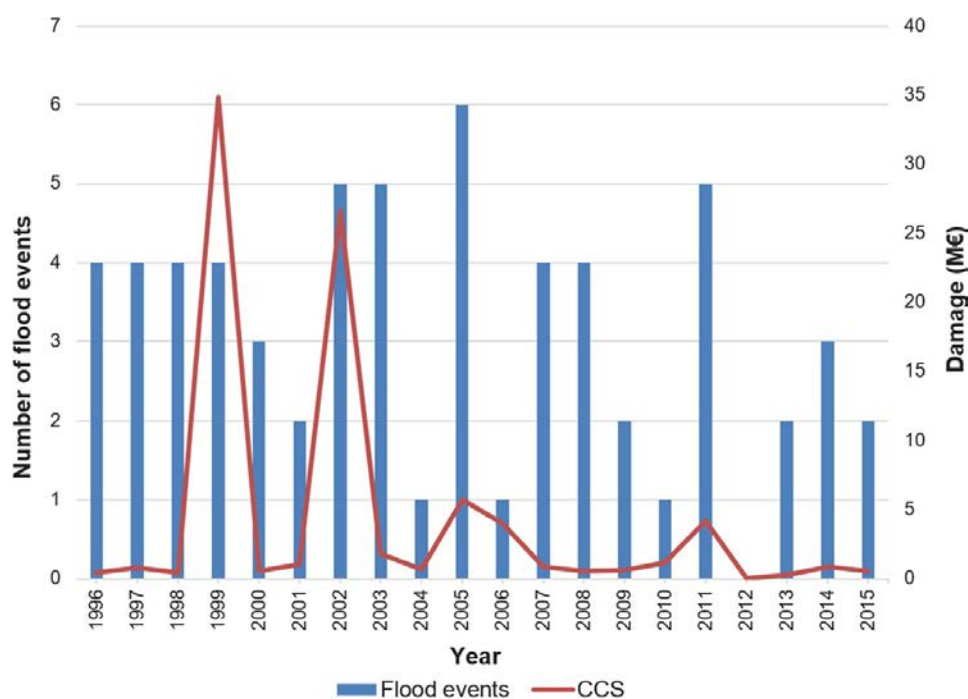
Fig. 7 Evolution of the compensation paid by CCS for floods (*line*) and the total number of flood events in the MAB

2.2 years. Despite the strong variability, a positive correlation of 0.43 (significant at 90%) was observed between the annual number of episodes and annual damages.

5.5 Floods versus land cover and rainfall

In this section, we carried out an analysis of different time periods to look for the potential relationships between flood episodes and the factors that produce them. The results obtained are shown in Table 8. There are no significant changes in either the number of flood episodes or the maximum 1-day precipitation (RX1DAY) for any period (1981–2015; 1981–1996; 1996–2015). In the 1981–1996 period, there is a positive trend in the number of flood events, although it is not statistically significant. This positive trend would be due to the increase in ordinary floods. This could be mainly related to the urban development in this period (25.81% of new impervious surfaces) and the increase in the maximum precipitation registered in a single day (Table 8). Conversely, for the 1996–2015

Table 8 Flood events, imperviousness and RX1DAY for different periods

Period	Flood evolution trend in MAB (No/decade)				Increase high imperviousness land cover MAB (%)	RX1DAY trend (mm/year)	
	TOT	ORD	EXT	CAT		Airport	Fabra
1981–1996	1.40	1.56	0.06	−0.22	25.82	1.38	1.08
1996–2015	−1.10	−0.66	−0.38	−0.05	19.56	−0.47	−0.24
1981–2015	−0.10	0.15	−0.15	−0.10	50.42	−0.60	−0.20

* *p* value <0.1; ** *p* value <0.05

Table 9 Correlation values between damage (CCS), precipitation and runoff for catastrophic flood events for the 1996–2015 period (with available CCS data)

	Total damage (millions of €)	Damage/ population density (€/inhab km^{-2})	Damage/ population (€/inhab)
Precipitation 24 h (mm)	0.19**	0.22**	**0.26****
Precipitation 24 h (mm) with $T >2$ years	0.33**	0.36**	**0.46****
Accumulated precipitation (mm)	0.23**	0.23**	**0.29****
Accumulated precipitation >100 mm (mm)	0.35**	0.40**	**0.50****
Runoff 24 h (mm)	**0.29****	0.22**	0.27**
Runoff 24 h (mm) for precipitation in 24 h with $T >2$ years	**0.57****	0.38**	0.50**
Estimated runoff (mm) for accumulated precipitation	**0.41****	0.27**	0.35**
Estimated runoff (mm) for accumulated precipitation >100 mm	**0.60****	0.44**	0.55**

The best results are in bold

* p value <0.1; ** p value <0.05

period, although there was an increase in impermeable surfaces (around 20%), there was a decrease in the number of flooding episodes, as well as in extreme precipitation. For the 1981–2015 period, the increase in impermeable surfaces was significant (more than 50%), which caused an increase in average runoff (Fig. 4). However, the results do not show any significant trends in the number of flood episodes for the 1981–2015 period. These results show the complexity of flood risk analysis, where many factors intervene simultaneously to either favour or impede flooding. In the case of Barcelona, after an unexpected heavy rainfall event recorded in September 1996, CLABSA (the company that carried out the sewer system of Barcelona, nowadays BCASA) developed a sophisticated strategy to cope with floods. This planning included building rainwater tanks and a permanent monitoring system.

5.6 Damage versus runoff and precipitation

In this section, we analysed the possible correlation between flood damage, precipitation and runoff for the extraordinary and catastrophic flood episodes that affected the MAB between 1996 and 2015. We considered the following variables: precipitation over 24 h, accumulated precipitation for the entire duration of the episode, runoff, total damage, damage relative to population density and damage relative to total population of the municipality. Correlation with damages was carried out for all the events, for the events in which precipitation in 24 h exceeded the return period of 2 years and for events in which accumulated precipitation surpassed 100 mm.

First of all, we only considered cases that caused catastrophic impacts in the MAB, before looking at all the extraordinary and catastrophic events documented in the region. Table 9 summarises the results obtained for catastrophic cases, highlighting the larger correlation values. In all cases, the correlations were significant at 95% using the Spearman

test. As it can be observed, correlations with damages are always better with runoff than with precipitation. This result may be explained by the stream's impact in flood damages and suggests the importance of the type of soil cover as a determining factor in the analysis of flood risk.

Figure 8 shows the best correlation results and the histograms for each variable (precipitation and accumulated runoff) for all of the cases (extraordinary and catastrophic) when the accumulated total rainfall was greater than 100 mm. As in catastrophic episodes, precipitation is more closely related to the density of damages (a correlation of 0.51), whereas runoff relates slightly better to total damage (0.60). This behaviour might be a consequence of the fact that the runoff already takes into account land use through the runoff coefficient. A larger population is associated with a larger impermeable surface and thus to a higher mean runoff value.

Finally, we analysed the distribution of precipitation over 24-h, 30-min rainfall intensity, accumulated precipitation and damage according to the flood category (1: extraordinary, 2: catastrophic) (Fig. 9; Table 10). As could be expected, accumulated precipitation and damages are higher for catastrophic floods than for extraordinary ones. The extraordinary episodes have a mean maximum 24-h precipitation of 68 mm, whereas catastrophic episodes have a mean maximum of 118 mm. Furthermore, 75% of the former have a maximum 24-h value higher than 55 mm. The maximum precipitation intensity values of the two categories are very high, at around 29 and 50 mm in 30 min for extraordinary and catastrophic episodes, respectively. These results confirm that the most
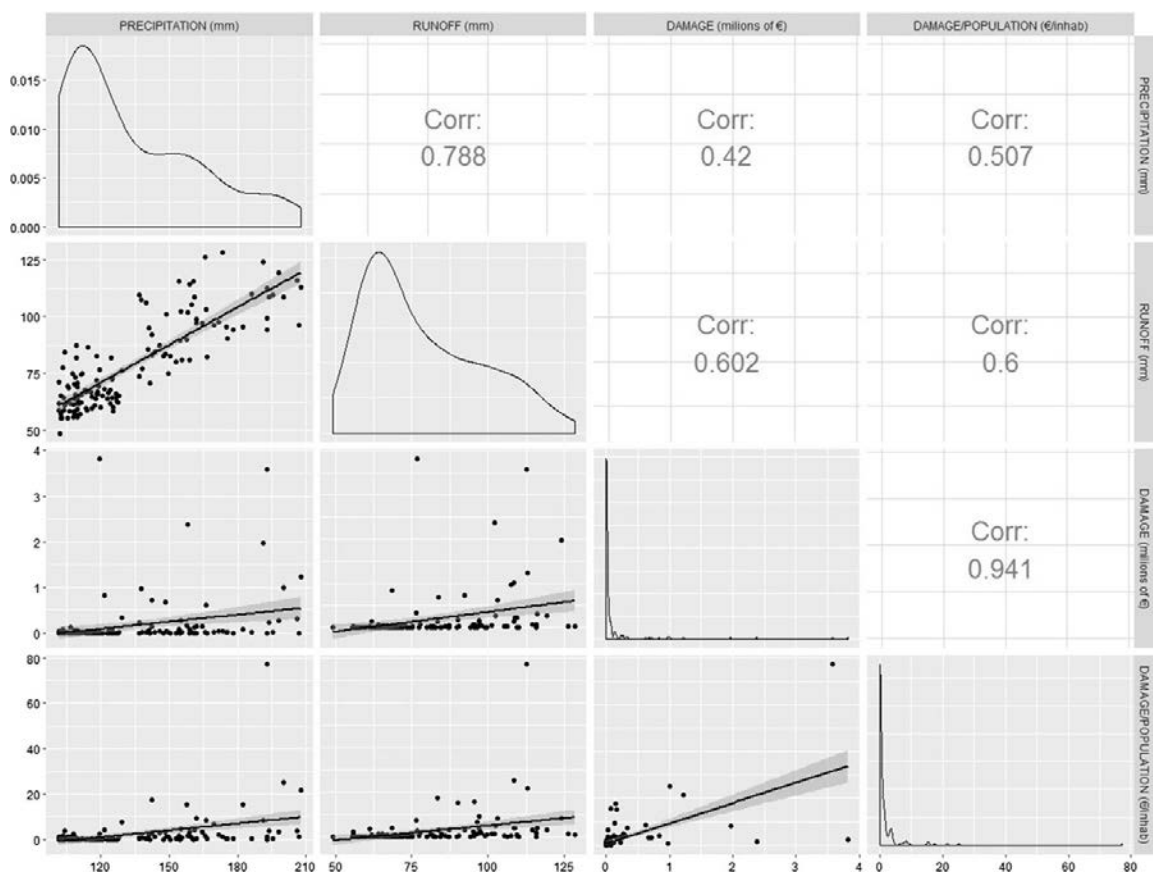
Fig. 8 Correlation results for extraordinary and catastrophic flood events where the total accumulated precipitation recorded was more than 100 mm, over the 1996–2015 period (for which CCS data are available)

Springer
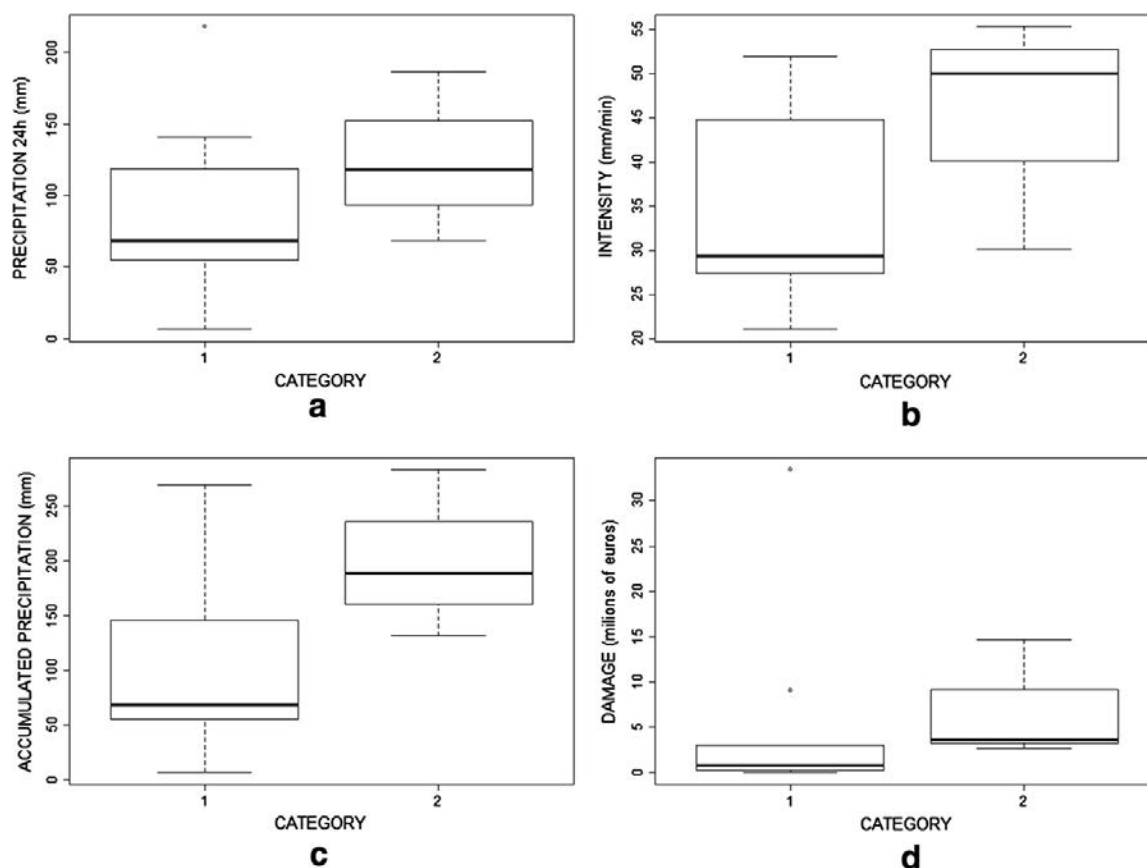
Fig. 9 Boxplots showing the distribution according to the flood category (*1* extraordinary, *2* catastrophic): **a** precipitation in 24 h; **b** precipitation in 30 min; **c** accumulated precipitation; and **d** damage

Table 10 Quartiles (*Q*1 = 25th percentile; *Q*2 = median; *Q*3 = 75th percentile) distribution for precipitation and damage variables according to flood category

	Extraordinary			Catastrophic		
	*Q*1	*Q*2	*Q*3	*Q*1	*Q*2	*Q*3
Precipitation in 24 h (mm)	56	68	115	93	118	152
Intensity (mm/min)	28	29	43	40	50	53
Accumulated precipitation (mm)	56	68	139	160	189	236
Damage (millions of €)	0.21	0.71	2.67	3.14	3.63	9.12

common type of floods in this region, flash floods, comes from intense and short precipitation events (Llasat et al. 2016).

The greatest differences in precipitation come from the total amount per episode, where the median for catastrophic floods was more than 175% larger than for extraordinary events. In fact, the latter have mean cumulative precipitation values equal to those of 24-h precipitation, indicating that the majority of episodes that produce extraordinary impacts have a duration of 1 day, as proposed in Llasat et al. (2016).

In terms of damages, catastrophic events produce median losses that exceed €3 million per episode, while in the case of extraordinary episodes these values are generally below €1 million.

6 Conclusions

The Metropolitan Area of Barcelona (MAB) has been affected by 109 flood events between 1981 and 2015, which translates to an average of more than three episodes of flooding per year, some of them with catastrophic effects. As a result of these events, 11 people lost their lives between 1981 and 2015 and the compensation paid by the CCS exceeded €86 million between 1996 and 2015. Consequently, there is no doubt that flooding is one of the most important natural hazards affecting Barcelona and its metropolitan area. The evolution of flood events (including urban floods and flash floods) shows a negative trend, although it is not significant. This result differs from the one obtained for different Mediterranean regions (Llasat et al. 2013) or Catalonia (Llasat et al. 2014a), where a positive and significant trend was found, mainly due to the increase in extraordinary events. In particular, in the case of the MAB, the analysis for the period 1981–2010 also shows a positive trend that is not significant (Llasat et al. 2016). This fact reflects the importance of period chosen when analysing trends, as well as other important points to be considered. The first is the improvement in prevention measures like constructing rainwater tanks, or the establishment of warning systems, which allows rainwater in the city to be better managed. This is the case in Barcelona, where a negative and significant trend was found, in agreement with the results for the analysis of longer periods (Barrera-Escoda et al. 2006). After the implementation of prevention measures, the seriousness of floods in this city has decreased, and nowadays, almost all events are ordinary floods. Similarly, the lack of a positive trend in precipitation extremes in this area could be another explanation (Turco and Llasat 2011; Turco et al. 2015).

Other factor to be considered is related to land use changes. Despite the fact that 80% of the land devoted to agriculture in 1956 has been transformed in urban land with impermeable surfaces, the biggest change occurred between 1956 and 1993. After this date, there was a decrease of less than 50% in the agricultural area. When land surface changes are introduced in the calculation for runoff changes over a return period of 100 years, the changes shown in the city of Barcelona are negligible and there is only an increase of 5.5% for the entire MAB.

The same behaviour was observed for the increase in population. Despite the increase in population since 1950 (by more than 206%), the last 35 years have only seen changes around 2% and, in the case of Barcelona, there has been a decrease as result of the high cost of living in the city. The correlation between accumulated precipitation and total damages is 0.23. Given that we are referring to annual values and without considering the number of insurance policies, this correlation value is quite high. But higher correlations were found between precipitation, runoff and the density of damages (damages/population adjusted to each year). The correlation surpasses 0.5 when considering events that recorded more than 100 mm in 24 h, or that have a return period of more than 2 years. Particularly, the correlation between estimated average runoff and total damages in the event, at municipal scale, is 0.60.

This study suggested a classification of flood events in basis of different impact indicators. In a preliminary analysis of the 1981–2015 period, the MAB has driven to the possibility of suggesting some thresholds. In this case, an extraordinary flood event would be characterised by an average daily precipitation of around 68 mm, a maximum intensity of 30 mm in 30 min and €1 million in damages, respectively (insured damages). These values would be for a catastrophic flood of 118, 50 mm and €3 million, respectively.

Despite this apparent success, and given that torrential rainfall may increase in the future and the MAB is one of the regions of the world with the highest number of tourists, preventive measures should still be improved, including making sure the population is more aware of the risk. This improvement in the risk awareness should be done at regional scale (informative leaflets, schools, etc.) including local interventions like exhibitions, conferences and the development of citizen science projects and tools. Although the rainwater tanks have been useful in the city of Barcelona, new infrastructures for flood defence should be avoided, with the focus on more sustainable solutions instead. For example, allow the Llobregat and Besòs rivers to have their natural and historical space; transform flood plains into permanently open and green spaces beside and inside the cities (a good solution in areas not so much urbanised); and improve new ways of channelling rainwater to these spaces; use river spaces as natural reservoirs, allowing floods to reach the coastline wherever possible, so they can fulfil their natural function in regenerating beaches and coastal ecosystems. In highly urbanised areas, it would be important to improve drainage systems taking into account the new proposals for Sustainable Urban Drainage Systems (SUDS). Between the no structural measures, the improvement in the early warning systems from a hydrometeorological point of view (rainfall and runoff) is a key issue. However, besides the sustainability criteria we cannot forget the limits imposed by the propagation of the uncertainty associated with the rainfall field in the hydrometeorological chain, the required societal consensus, the assumable costs and the own technology (Llasat and Siccardi, 2010).

The latest IPCC report (2014) points to an increased risk of flooding, but above all, of associated socio-economic impacts. According to the Hyogo and Sendai frameworks, the most recent agreements regarding natural hazards and disasters (UNISDR 2007, 2015a), and the 2015–2030 Sustainable Development Goals, prevention and resilience to floods must have a strong social and sustainable component. This can only be achieved through better empowerment and co-responsibility, not only from the population, but also from the private sector and local governments.

References

Alfieri L, Feyen L, Di Baldassarre G (2016) Increasing flood risk under climate change: a pan-European assessment of the benefits of four adaptation strategies. Clim Change 136(3–4):507–521

Amaro J, Gayà M, Aran M, Llasat MC (2010) Preliminary results of the Social Impact Research Group of MEDEX: the request database (2000–2002) of two Meteorological Services. Nat Hazards Earth Syst Sci 10(12):2643–2652. doi:10.5194/nhess-10-2643-2010

Barbería L, Amaro J, Aran M, Llasat MC (2014) The role of different factors related to social impact of heavy rain events: considerations about the intensity thresholds in densely populated areas. Nat Hazards Earth Syst Sci 14(7):1843–1852. doi:10.5194/nhess-14-1843-2014

Barnolas M, Llasat MC (2007) Metodología para el estudio de inundaciones históricas en España e implementación de un SIG en las cuencas del Ter, Segre y Llobregat. Centro de Estudios Hidrográficos (CEDEX), España

Barredo JI, Saurí D, Llasat MC (2012) Assessing trends in insured losses from floods in Spain 1971–2008. Nat Hazards Earth Syst Sci 12(5):1723–1729

Barrera-Escoda A, Llasat MC (2015) Evolving flood patterns in a Mediterranean region (1301–2012) and climatic factors—the case of Catalonia. Hydrol Earth Syst Sci 19:465–483. doi:10.5194/hess-19-465-2015

Barrera-Escoda A, Llasat MC, Barriendos M (2006) Estimation of the extreme flash flood evolution in Barcelona county from 1351 to 2005. Nat Hazards Earth Syst Sci 6:505–518

Barriendos M, Coeur D, Lang M, Llasat MC, Naulet R, Lemaitre F, Barrera A (2003) Stationarity analysis of historical flood series in france and spain (14th-20th centuries). Nat Hazards Earth Syst Sci 3:583–592

Benoit G, Comeau A (2005) A Sustainable Future for the Mediterranean: The Blue Plan's Environment and Development Outlook. Earthscan

Blöschl G, Viglione A, Montanari A (2013) Emerging Approaches to Hydrological Risk Management in a Changing World. Climate vulnerability: understanding and addressing threats to essential resources. Elsevier Inc., Academic Press, London, pp 3–10

Bodoque JM, Amérigo M, Díez-Herrero A, García JA, Cortés B, Ballesteros-Cánovas JA, Olcina J (2016) Improvement of resilience of urban areas by integrating social perception in flash-flood risk management. J Hydrol 541:665–676

Casas-Castillo C, Cunillera J, Xènia D, Herrero M, Ninyerola M, Xavier P, Redaño A, Rius A, Rodriguez R (2005) Mapes de precipitació màxima diària esperada a catalunya per a diferents períodes de retorn. Servei Meteorològic de Catalunya, Departament de Medi Ambient i Habitatge: Generalitat de Catalunya, ISBN: 84-393-6870-4

Ceola S, Laio F, Montanari A (2014) Satellite nighttime lights reveal increasing human exposure to floods worldwide. Geophys Res Lett 41(20):7184–7190

Chow VT, Maidment DR, Mays LW (1988) Applied hydrology. Mc Graw Hill, New York

Del Moral A, Llasat MC, Rigo T (2016) Identification of anomalous motion of thunderstorms using daily rainfall fields. Atmos Res 185:92–100. doi:10.1016/j.atmosres.2016.11.001

Drobinski P, Ducrocq V, Alpert P, Anagnostou E, Béranger K, Borga M, Wernli H (2014) HyMeX: a 10-year multidisciplinary program on the Mediterranean water cycle. Bull Amer Meteorol Soc 95(7):1063–1082. doi:10.1175/BAMS-D-12-00242.1

Eurostat (2016) Eurostat regional yearbook. http://ec.europa.eu/eurostat/statistics-explained/index.php/Regional_yearbook_introduction. Accessed 3 July 2017

Faccini F, Luino F, Sacchini A, Turconi L (2015) Flash flood events and urban development in Genoa (Italy): lost in translation. Engineering geology for society and territory, vol 5. Springer, Berlin, pp 797–801

García LE, Matthews JH, Rodriguez DJ, Wijnen M, DiFrancesco KN, Ray P (2014) Beyond downscaling: a bottom-up approach to climate adaptation for water resources management. AGWA report 01. World Bank Group, Washington, DC

Gascón E, Laviola S, Merino A, Miglietta MM (2016) Analysis of a localized flash-flood event over the central Mediterranean. Atmos Res 182:256–268

Hall J, Arheimer B, Borga M, Brázdil R, Claps P, Kiss A, Blösch IG (2014) Understanding flood regime changes in Europe: a state-of-the-art assessment. Hydrol Earth Syst Sci 18:2735–2772. doi:10.5194/hess-18-2735-2014

Hirabayashi Y, Mahendran R, Koirala S, Konoshima L, Yamazaki D, Watanabe S, Kim H, Kanae S (2013) Global flood risk under climate change. Nat Climate Change 3(9):816–821

Institut d'Estadística de Catalunya (IDESCAT, Statistical Institute of Catalonia) (2016) Anuari estadístic de Catalunya (Statistical Yearbook of Catalonia). http://www.idescat.cat/. Accessed 28 Feb 2017

Instituto Nacional de Estadística (INE). http://www.ine.es/. Accessed 28 Feb 2017

IPCC (2012) Managing the risks of extreme events and disasters to advance climate change adaption (SREX). Intergovernmental Panel on Climate Change. Cambridge University Press, Cambridge

IPCC (2014) Climate change 2014: impacts, adaptation, and vulnerability. IPCC Working Group II contribution to the fifth assessment report of the intergovernmental panel on climate change. http://www.ipcc.ch/report/ar5/wg2/

Karagiorgos K, Thaler T, Hübl J, Maris F, Fuchs S (2016) Multi-vulnerability analysis for flash flood risk management. Nat Hazards 82(1):63–87

Kendall MG (1975) Rank correlation methods. Oxford University Press, New York

Llasat MC, Siccardi F (2010) A reflection about the social and technological aspects in flood risk management—the case of the Italian Civil Protection. Nat Hazards Earth Syst Sci 10:109–119

Llasat MC, Barriendos M, Barrera A, Rigo T (2005) Floods in Catalonia (NE Spain) since the 14th century. Climatological and meteorological aspects from historical documentary sources and old instrumental records. Applications of palaeoflood hydrology and historical data in flood risk analysis. J Hydrol 313:32–47

Llasat MC, Llasat-Botija M, López L (2009) A press database on natural risks and its application in the study of floods in Northeastern Spain. Nat Hazards Earth Syst Sci 9:2049–2061

Llasat MC, Llasat-Botija M, Petrucci O, Pasqua AA, Rosselló J, Vinet F, Boissier L (2013) Towards a database on societal impact of Mediterranean floods in the framework of the HYMEX project. Nat Hazards Earth Syst Sci 13:1–14

Llasat MC, Marcos R, Llasat-Botija M, Gilabert J, Turco M, Quintana-Seguí P (2014a) Flash flood evolution in North-Western Mediterranean. Atmos Res 149:230–243

Llasat MC, Turco M, Quintana-Seguí P, Llasat-Botija M (2014b) The snow storm of 8 March 2010 in Catalonia (Spain): a paradigmatic wet-snow event with a high societal impact. Nat Hazards Earth Syst Sci 14:427–441. doi:10.5194/nhess-14-427-2014

Llasat MC, Marcos R, Turco M, Gilabert J, Llasat-Botija M (2016) Trends in flash flood events versus convective precipitation in the Mediterranean region: the case of Catalonia. J Hydrol 541:24–37

Mann HB (1945) Nonparametric tests against trend. Econometrica 13:245–259

Martín Vide J, (coord.) et al (2016) Tercer Informe sobre el canvi climàtic a Catalunya (Third Report in Climate Change in Catalonia). Generalitat de Catalunya-Institut d'Estudis Catalans. ISBN 9788499653174 (IEC). ISBN 9788439394488 (Generalitat de Catalunya) Barcelona, 611 p

Mediero L, Jiménez-Álvarez A, Garrote L (2010) Design flood hydrographs from the relationship between flood peak and volume. Hydrol Earth Syst Sci 14(12):2495

Merz B, Kreibich H, Schwarze R, Thieken A (2010) Review article "assessment of economic flood damage". Nat Hazards Earth Syst Sci 10:1697–1724. doi:10.5194/nhess-10-1697-2010

Nakamura I, Llasat MC (2017) Flood risk management and information—a comparative study between Japan and Spain on flood risk and warning. Nat Hazards 87:919. doi:10.1007/s11069-017-2802-x

Schröter K, Kunz M, Elmer F, Mühr B, Merz B (2015) What made the June 2013 flood in Germany an exceptional event? A hydro-meteorological evaluation. Hydrol Earth Syst Sci 19(1):309–327

Terti G, Ruin I, Anquetin S, Gourley JJ (2015) Dynamic vulnerability factors for impact-based flash flood prediction. Nat Hazards 79(3):1481–1497

Thieken AH, Bessel T, Kienzler S, Kreibich H, Müller M, Pisi S, Schröter K (2016) The flood of June 2013 in Germany: how much do we know about its impacts? Nat Hazards Earth Syst Sci Discuss (Janu) 1–57

Turco M, Llasat MC (2011) Trends in indices of daily precipitation extremes in Catalonia (NE Spain). 1951–2003. Nat Hazards Earth Syst Sci 11:3213–3226

Turco M, Marcos R, Quintana-Seguí P, Llasat MC (2014) Testing instrumental and downscaled reanalysis time series for temperature trends in NE of Spain in the last century. Reg Environ Change 14:1811. doi:10.1007/s10113-012-0363-9

Turco M, Palazzi E, von Hardenberg J, Provenzale A (2015) Observed climate change hotspots. Geophys Res Lett 42:3521–3528. doi:10.1002/2015GL063891

Turco M, Llasat MC, Herrera S, Gutiérrez JM (2017) Bias correction and downscaling of future RCM precipitation projections using a MOS-Analog technique. J Geophys Res Atmos. doi:10.1002/2016JD025724

UNISDR (United Nations International Strategy for Disaster Reduction) (2007) Hyogo framework for action 2005–2015. https://www.unisdr.org/we/coordinate/hfa. Accessed 28 Feb 2017

UNISDR (United Nations International Strategy for Disaster Reduction) (2015a) Sendai framework for disaster risk reduction 2015–2030. http://www.unisdr.org/files/43291_sendaiframeworkfordrren.pdf. Accessed 28 Feb 2017

UNISDR (United Nations International Strategy for Disaster Reduction) (2015b) Making cities resilient: My city is getting ready. http://www.unisdr.org/campaign/resilientcities. Accessed 28 Feb 2017

Wilby RL, Dessai S (2010) Robust adaptation to climate change. Weather 65(7):180–185

WMO (World Meteorological Organization) (2009) Guidelines on analysis of extremes in a changing climate in support of informed decisions for adaptation. Technical report. WCDMP 72, Geneva, Switzerland

Appendix

Natural Hazards
and Earth System
Sciences

The relationship between precipitation and insurance data for floods in a Mediterranean region (northeast Spain)

Maria Cortès[1,2], **Marco Turco**[1], **Montserrat Llasat-Botija**[1,2], **and Maria Carmen Llasat**[1,2]

[1]Department of Applied Physics, University of Barcelona, Barcelona, 08028, Spain
[2]Water Research Institute (IdRA), University of Barcelona, Barcelona, 08001, Spain

Correspondence: Maria Cortès (mcortes@meteo.ub.edu)

Abstract. Floods in the Mediterranean region are often surface water floods, in which intense precipitation is usually the main driver. Determining the link between the causes and impacts of floods can make it easier to calculate the level of flood risk. However, up until now, the limitations in quantitative observations for flood-related damages have been a major obstacle when attempting to analyse flood risk in the Mediterranean. Flood-related insurance damage claims for the last 20 years could provide a proxy for flood impact, and this information is now available in the Mediterranean region of Catalonia, in northeast Spain. This means a comprehensive analysis of the links between flood drivers and impacts is now possible. The objective of this paper is to develop and evaluate a methodology to estimate flood damages from heavy precipitation in a Mediterranean region. Results show that our model is able to simulate the probability of a damaging event as a function of precipitation. The relationship between precipitation and damage provides insights into flood risk in the Mediterranean and is also promising for supporting flood management strategies.

1 Introduction

Flooding is one of the largest natural risks in the world. Between 2005 and 2014, more than 85 000 000 people were directly affected by flood events annually, and around 6000 people were killed on average each year due to floods (UNISDR, 2015). The main factors involved in flood risk analysis are the hazard, or the likelihood of a natural phenomenon causing damage, and the vulnerability, that is, the characteristics and circumstances of a community/system

that make it susceptible to potential flood damage (UNISDR, 2009; Kundzewicz et al., 2014; Winsemius et al., 2015). Vulnerability can include factors such as exposure and other societal factors such as early warning systems, building capacity to cope with natural hazards and disaster recovery infrastructure (Jongman et al., 2014; Nakamura and Llasat, 2017).

A large number of researchers are making efforts to create methodologies that are able to analyse the impacts of floods, due to the significant consequences of this phenomenon (Messner and Meyer, 2006; García et al., 2014). Indeed, progress is being made on incorporating impact and vulnerability analysis in flood risk assessment, although the limitations of the impact data (availability and quality) make it difficult to carry out these studies (Elmer et al., 2010; Petrucci and Llasat, 2013; Jongman et al., 2014; Papagiannaki et al., 2015; Thieken et al., 2016; Kreibich et al., 2017).

Insurance data may provide a good proxy for describing flood damage (Barredo et al., 2012). Several recent works have used this kind of data to explore the causes and impacts of floods. For instance, in several European regions researchers have noted that precipitation has a significant influence on flood insurance data (see, for instance, Spekkers et al., 2013, 2015, for the Netherlands; Zhou et al., 2013, for Denmark; Sampson et al., 2014, for Ireland; Moncoulon et al., 2014, for France; Torgersen et al., 2015, for Norway). These data are very valuable for establishing causal relationships between the costs of flood damage and precipitation extremes, for developing risk maps and to use as a validation tool for damage models (Zhou et al., 2013). These studies agree on the potential of insurance data to assess the damage caused by pluvial and urban floods.

Most floods that have affected the region of study, northeast Spain, are surface water floods that caused catastrophic damage (Llasat et al., 2014, 2016a). This type of flood can be regarded as coming under the most general definition of rainfall-related floods (Bernet et al., 2017), including pluvial floods but also flooding from sewer systems, small open channels, diverted watercourses or groundwater springs (Falconer et al., 2009). River floods that affect great distances are very rare in the region, and are only related to catastrophic and extended floods (for the analysed period only the October 2000 floods were of this type). Nevertheless, these are usually absorbed by reservoirs. It is therefore expected that flood insurance data will correlate strongly with precipitation and surface water floods. However, relatively few studies exist for the Mediterranean region, being mostly limited to urban flood damage assessment (Freni et al., 2010; Papagiannaki et al., 2015; Bihan et al., 2017), while analysis of the possible links between precipitation and economic flood damages are yet to be undertaken across Mediterranean regions. This may be due to limitations in insurance data records and difficulties in estimating how heavy precipitation could affect monetary damages. In the Mediterranean region of Catalonia, in northeast Spain, 20 years of flood-related insurance damage claims are available from the Spanish public reinsurer, the Insurance Compensation Consortium (Consorcio de Compensación de Seguros, CCS), a public institution that compensates homeowners for damage caused by floods, playing a role similar to that of a reinsurance company (Barredo et al., 2012). This means an assessment of the links between precipitation and impacts is now possible. This analysis would greatly help policy makers and civil protection agencies, improving early warning systems and allowing for more efficient management strategies. Furthermore, assessing the relationship between precipitation and flood damage would provide relevant information on the underlying mechanisms of how floods evolve, as well as those particular to Mediterranean regions.

The aim of this study is to develop and evaluate a methodology to estimate surface water flood damage from heavy precipitation in the Mediterranean region of study (henceforth, "flood" refers to surface water floods). The relationship between precipitation and insurance data has been assessed, using logistic regression models, to ascertain the probability of large monetary damages in relation to heavy precipitation events. Specifically, our main goal is to answer the following research questions:

Can we predict flood damage with parsimonious precipitation–damage models?

To what extent do exposure and vulnerability (through the commonly used proxies of gross regional domestic product, GDP) and population (Pielke and Downton, 2000; Choi and Fisher, 2003; Barredo, 2009) determine the damages corresponding to precipitation events?
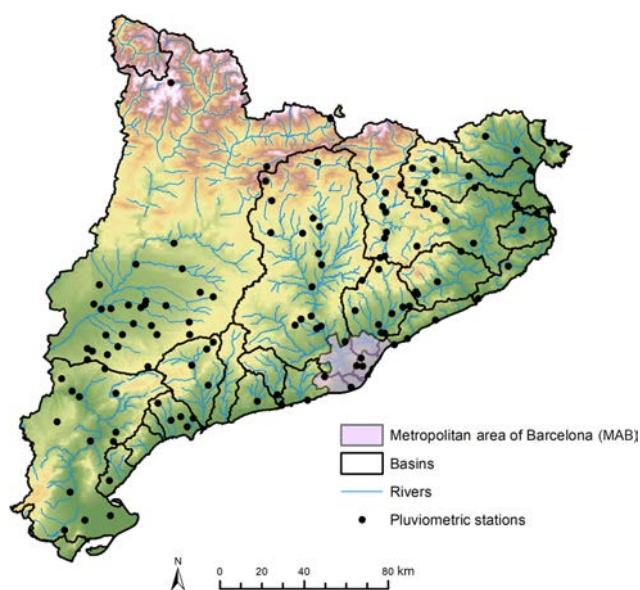
Figure 1. Map of Catalonia showing the aggregated basins, the metropolitan area of Barcelona (MAB), the main rivers and the pluviometric stations used.

Which thresholds used to define large flooding damages and heavy rainfall events determine the best applicability range?

To sum up, the results of this study can help better understand flood risk in Mediterranean areas by analysing flood causes and impacts, and can help more accurately estimate flood damage when high levels of rainfall are forecast.

The study is organised as follows. After the Introduction, the Methods section describes the study region, the observed data and the methodology used. Then, the Results section presents the regression models obtained. Finally, the Conclusions section summarises the main findings of this study.

2   Methods

2.1   Study region

The study area is Catalonia, a Spanish region of $32\,108\,\mathrm{km}^2$ in the northeast Iberian Peninsula. The region is characterised by three mountain ranges (Fig. 1): the Pyrenees in the north (maximum altitude above 3000 m a.s.l.) and parallel to the Mediterranean coast (SW–NE) between the Catalan Pre-Coastal Range (maximum altitude around 1800 m a.s.l.) and the Catalan Coastal Range (maximum altitude around 600 m a.s.l.). This marked orography is the key reason for the development of floods, both from a hydrological point of view (small torrential catchments) and due to meteorological factors (the orography forces water vapour to rise from the Mediterranean, triggering instability; Llasat et al., 2016a). The region is divided into 42 counties and 948 municipalities, with a total population of 7.5 million, most of

whom live along the coast, where more than 70 % of the flood events occur (Llasat et al., 2014), making it a very vulnerable area. From a hydrological point of view the region is divided into 31 basins, most of them with surface areas of less than 500 km^2. Some of them are located in very small municipalities for which some data needed are not available (i.e. GDP). For this reason we have aggregated some of the basins and worked with a total of 29 (see Supplement).

We also analyse the metropolitan area of Barcelona (MAB, 534.7 km^2; Fig. 1) in detail, which consists of the city of Barcelona (1 608 746 inhabitants in 101.3 km^2) and 35 municipalities. Although it represents less than 2 % of the surface area of Catalonia, it contains 48 % of the population (IDESCAT, 2016). It is affected by an average of over three flood events per year, most of which are floods due to very convective local precipitation (Cortès et al., 2017). The city of Barcelona is crossed by 20 streams that have their source in the Serra de Collserola (Catalan Coastal Range), and which are covered by part of the Barcelona drainage system, managed by the Barcelona Water Cycle (Barcelona Cicle de l'Aigua or BCASA). The United Nations International Strategy for Disaster Reduction (UNISDR) marked Barcelona as a resilient city and a model city for dealing with floods (Nakamura and Llasat, 2017), as it has a permanent surveillance and warning system running on hydraulic modelling that includes 15 rainwater tanks (13 underground and 2 open) that allow for better flood prevention. As a result, flood damages have decreased over time (Barrera-Escoda et al., 2006) while the daily rainfall threshold associated with damaging floods has increased (Barrera-Escoda and Llasat, 2015).

2.2 Data

The flood damage data were obtained from the insurance compensation for floods paid by the Spanish Insurance Compensation Consortium (CCS). The CCS compensates for damage caused to people and property by floods and other adverse weather events covered by an insurance policy. The CCS database includes more than 58 000 records of claims paid for floods in Catalonia, provided on a postal code level for the 1996–2015 period (no previous information is available with this level of detail). For flood events we use the INUNGAMA (Barnolas and Llasat, 2007; Llasat et al., 2016a) and PRESSGAMA (Llasat et al., 2009) databases, which report the flood events that have occurred in Catalonia on a municipal, district and basin level. Basic data on damaging events (i.e. event dates, duration and some hydrometeorological data) are identified using the INUNGAMA database. The PRESSGAMA database was used for the events and the description of their impacts, and to identify the worst-affected places. Population and GDP data were obtained from the Statistical Institute of Catalonia (Institut d'Estadística de Catalunya, IDESCAT). The population and GDP used correspond to the year when the flood event took place. We use daily precipitation data provided by the meteorologi-

Table 1. Summary of the data used. Precipitation refers to the number of meteorological stations considered; the number of flood events is the total sum for the period 1996–2015; the average population is the total number of inhabitants; the average GDP is in millions of euros; the damages refer to the compensation paid by the CCS for the 1996–2015 period in millions of euros.

1996–2015	Catalonia	MAB	Source
Precipitation 24 h	127	26	AEMET
Precipitation 30 min	–	14	SMC
Number of flood events	166	61	INUNGAMA/ PRESSGAMA
Population	6 854 302	3 141 703	IDESCAT
Gross domestic product	164 162.30	95 438.57	IDESCAT
No. of municipalities	948	36	IDESCAT
Damages	436.40	86.30	CCS

cal station network run by the Spanish State Meteorological Agency (Agencia Estatal de Meteorología, AEMET). To ensure temporal homogeneity, we have only considered the stations located in Catalonia with more than 90 % valid data over the 1996–2015 period (Fig. 1). For the MAB we also considered 30 min weather data obtained from the network of automatic meteorological stations belonging to the Meteorological Service of Catalonia (Servei Meteorológic de Catalunya, SMC). Table 1 summarises the data used.

Compensation paid by the CCS were adjusted to the value of the euro in 2015, following the methodology defined by the Spanish National Institute of Statistics (INE, 2007). This consists of using the exchange rate in the consumer price index (CPI) between the two years to adjust the values shown in euros. To compare this data with other variables, we first aggregated them at a municipal level. This task was made more difficult by the fact that a municipality can include different postcodes and one postcode can correspond to two municipalities. These difficulties were solved by aggregating the municipal postcodes and looking at press information. Finally, to calculate the total damages per event, we took the payments made on the day the event occurred, and the following seven days. We used this 7-day window as this is the period of time that the CCS allows insurance claims to be made. When the time difference between two events is less than 7 days, damages are associated with the first event, if the date of the claim was before the first day of the second event.

Because the available data are too sparse to support our statistical assessment on a municipal scale, we assessed the

precipitation–compensation link for Catalonia as a whole. That is, we sampled pairs of the response variable (i.e. the compensation series) and the maximum 24 h precipitation for each basin recorded, and pooled them into one sample for the entire region (Catalonia) to correlate them. For each event there can be more than one pair of values, depending on the number of affected catchments. From now on we will use the expression "flood case" for each pair of values corresponding to a basin affected by a flood event. This area is large enough to have a fairly large sample size for analysis, but small enough that the causes of flood damage are likely to be similar across the area.

The same methodology was applied for another spatial aggregation based on the AEMET warning areas (included in the Supplement), and which has also been used in other studies like Quintana-Seguí et al. (2016). Similarly as for the basins, an aggregation process was carried out (14 to 15 warning areas).

Finally, we considered three categories of damages: (i) total damages (D), (ii) damage per capita (DPC) and (iii) damage per unit of GDP (DPW). This meant the relative impacts of socioeconomic factors on damage could be estimated, while taking into account population and wealth (Zhou et al., 2017).

2.3 Modelling damage probabilities

After gathering together a list of all the floods that affected Catalonia between 1996 and 2015, we filtered them based on specific rainfall thresholds. The Social Impact Research Group, created within the framework of the MEDEX project (MEDiterranean EXperiment on cyclones that produce high-impact weather in the Mediterranean; http://medex.aemet. uib.es) has established a threshold – when a maximum rainfall of over 60 mm in 24 h was recorded – to indicate the expected social impact for rain events in Catalonia (Amaro et al., 2010; Jansà et al., 2014). Barbería et al. (2014) suggest that the threshold of 40 mm 24 h^{-1} is better for urban areas. In the main text we consider the threshold on 60 mm 24 h^{-1}, while results obtained using the lower threshold are available in the Supplement.

In the case of the MAB, the minimal unit of study is the entire MAB region, which means each flood event corresponds to a single flood case. Taking into account that applying the precipitation thresholds of 40 and 60 mm for the MAB will result in samples that are too small (36 and 23 flood cases respectively), and that the analysis would not be robust enough, we have used lower precipitation thresholds. It is worth noting that in this case we also used 30 min precipitation, which means a lower threshold might still have significant consequences. For instance, a previous study shows that with precipitation over 20 mm 30 min^{-1}, extraordinary and catastrophic flood events can occur (Cortès et al., 2017) in the region. In addition, other studies (Barrera-Escoda and Llasat, 2015) have used 20 mm 24 h^{-1} to study flood events in this

Mediterranean region. Since the sample size is still small, a 10 mm threshold was also used (results for the 20 mm threshold are, however, available in the Supplement).

Figure 2 shows the relationship between the three categories of damages considered (D, DPC and DPW) and precipitation (log-transformed) in Catalonia. Even if a linear regression indicates a significant link (p value < 0.01), the explanatory power of the model for D is rather low ($r^2 = 0.09$). Marginally better results are obtained for the damage indicators DPC and DPW ($r^2 = 0.14$ and $r^2 = 0.16$ respectively), underlying the importance of considering the impacts of population and wealth on damage. That is, this analysis corroborates the common experience that, given the same level of heavy precipitation, the total damage is larger where the level of wealth is higher.

The large spread of Fig. 2 indicates that modelling insurance compensation is a complex issue, due to the limitations in observational data and the concurrence of a variety of relevant factors. For instance, monetary data could be affected by limitations, as the value of the assets exposed and insurance coverage may change over time (Barredo et al., 2012). Unfortunately, exact data on the value and location of assets exposed are not available.

However, the significant correlation between insurance compensation and precipitation suggests that rainfall data can be used to extract information on damage in Catalonia. To do this, we applied a logistic regression model to gauge the probability of large damaging events occurring given a certain precipitation amount (an approach that is frequently used for this kind of modelling study: Kim et al., 2012; Wobus et al., 2014). That is, our aim is not to estimate the precise amount of the monetary compensation, but to estimate when a "large" damaging event will occur given a certain precipitation amount. Since there is not a standard definition of a large damaging event, we tested several cases: insurance compensation exceeding the 50th, 60th, 70th, 80th and 90th percentile of the total sample. This methodology is repeated for both thresholds (40 and 60 mm) and for the three damage indicators (D, DPC, DPW) for the basins and warning areas, meaning we made a total of 60 models.

Finally, the logistic model is calculated following Eq. (1):

$$\log\left(\frac{\pi}{1-\pi}\right) = \beta_0 + \beta_1 P, \tag{1}$$

where π is the response variable (i.e. the probability above a certain percentile) and P is the predictor (precipitation in our case). The value of the β coefficient is determined using generalised linear models (GLMs). The Wald χ^2 statistic is used to assess the statistical significance of individual regression coefficients (Harrel, 2015).

2.4 Verification method

We plotted the relative operating characteristic (ROC) diagram, a commonly used logistic prediction diagnostic, show-
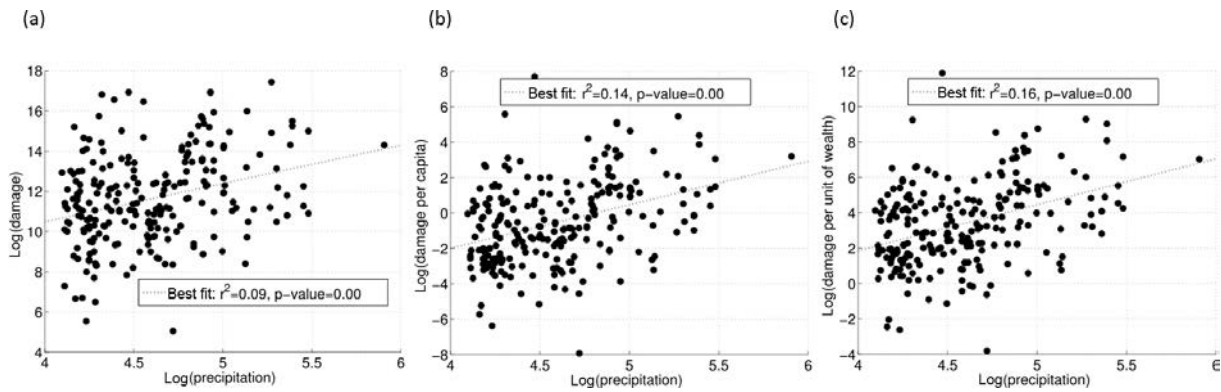
Figure 2. Scatter plot showing maximum precipitation in 24 h (mm) and **(a)** total damages (D), **(b)** damage per capita (DPC), and **(c)** damage per unit of wealth (DPW), for flood events recorded in Catalonia between 1996 and 2015 (log-transformed values; damages are given in euros). Each point represents the insurance compensation series (D, DPC or DPW) and the maximum 24 h precipitation for each basin. The dashed line indicates the fit based on a linear regression model.

Table 2. Contingency table to support Eqs. (2) and (3).

| | | Observed | |
		Yes	No
Forecasted	Yes	a	b
	No	c	d

ing the hit rate (i.e. the relative number of times a forecasted event actually occurred) against the false alarm rate (i.e. the relative number of times an event had been forecasted but did not actually happen) for different potential decision thresholds (Mason and Graham, 2002). Thus, for each insurance compensation percentile and for each precipitation threshold, we first calculated the forecast probabilities for that event, and then grouped the probability forecasts into batches (here 20 with a width of 0.05) to count the observed occurrences/non-occurrences. That is, we converted the observed and forecasted series, expressed as continuous amounts, into "exceedance" categories (yes–no statements indicating whether the data equal or exceed a selected probability). We then plotted the resulting elements on a standard contingency table (see Table 2).

The ROC diagram shows the hit rate (H) against the false alarm rate (F). These indices are defined as

$$H = \frac{a}{a+c}; \quad 0 \le H \le 1, \tag{2}$$

$$F = \frac{b}{b+d}; \quad 0 \le F \le 1. \tag{3}$$

3 Results

3.1 Damaging events and precipitation in Catalonia

The total number of flood events recorded in Catalonia for the 1996–2015 period was 166 (109 of them went beyond the 40 mm 24 h^{-1} precipitation threshold and 81 went over the 60 mm 24 h^{-1} threshold) resulting in a total number of flood cases (i.e. pair of precipitation–damage values at a basin scale) of 642 (331 for 40 mm 24 h^{-1} and 239 for 60 mm 24 h^{-1}). Coastal municipalities are the most affected by flood events and where there is the most damage. This is a consequence of high vulnerability (the most vulnerable buildings and infrastructure are on the coast), exposure (population and tourism are concentrated in the coastal regions) and hazards (floods associated with local heavy rain events are frequent; Llasat et al., 2014, 2016a). Around 49 % of the events occurred during the months of July, August and September, with the latter month having the highest percentage of events (22 %). The most severe or catastrophic events occurred in the autumn, with 77 % of these events taking place between September and November (Llasat et al., 2016a). The compensation paid by the CCS for floods during this period in Catalonia amounted to EUR 436.40 million.

Figure 3 shows the number of flood events recorded between 1996 and 2015 (Fig. 3a), the total insurance losses paid by CCS for flooding (Fig. 3b) during this period, the average population (Fig. 3c) and the GDP (Fig. 3d) in each basin. In general, there is good correlation among the four variables, as expected. The basins with more recorded flood events are those that received more insurance compensation for flood damage, with a higher population and GDP. The Maresme Basin was affected by 41 % of the recorded events (Fig. 3a) with damages that add up to EUR 24.60 million between 1996 and 2015 (Fig. 3b).
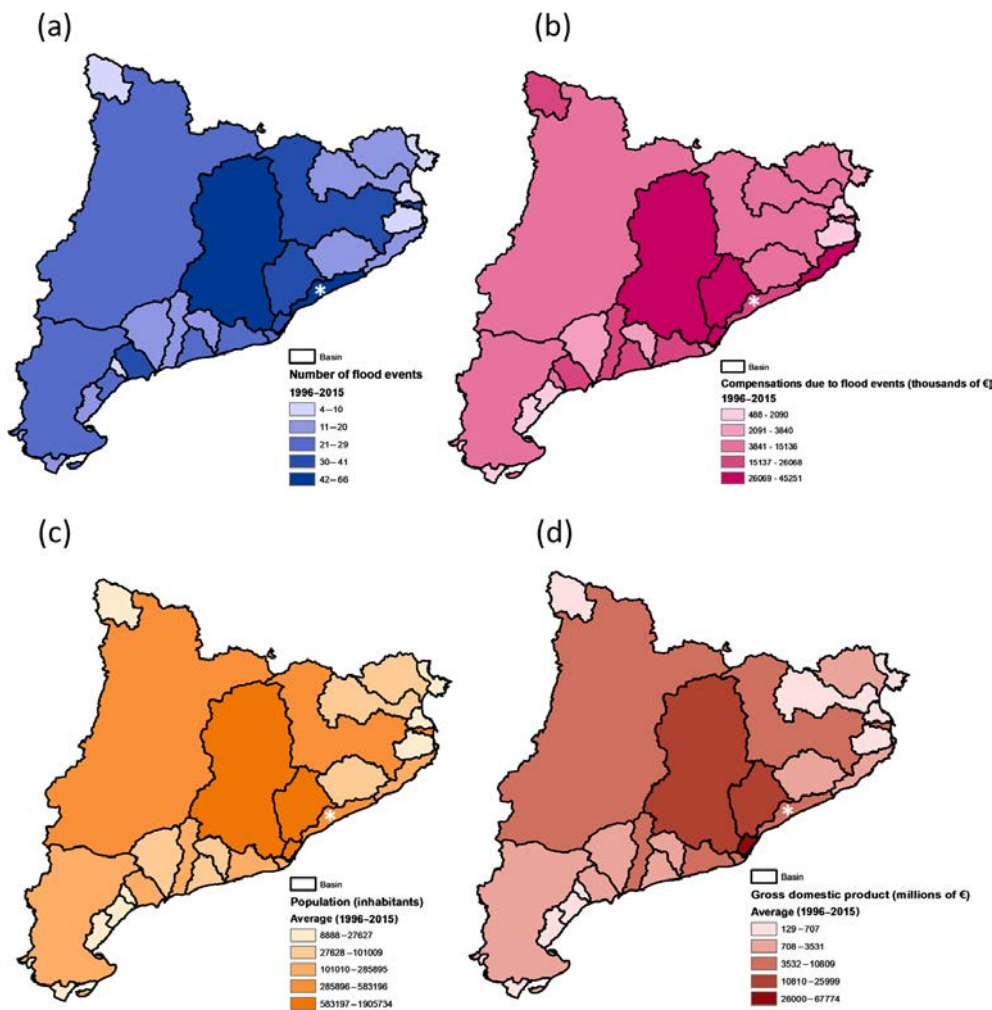
Figure 3. Basin distribution of **(a)** flood events (1996–2015), **(b)** total insurance compensation for floods made by CCS (1996–2015), **(c)** average total population, and **(d)** average GDP. Asterisk indicates Maresme Basin.

In order to estimate when a "large" damaging event will occur with a given precipitation amount, a logistic regression was used. Figure 4 shows a logistic regression example that indicates the model is able to simulate the probability of DPW above and below the 70th percentile as a function of precipitation. This figure illustrates that the probability of reaching above the 70th percentile for DPW increases when there is a large amount of rain. This result is consistent with the hypothesis that 24 h precipitation could be considered a good indicator for flood risk. For this example the regression Eq. (4) is

$$\log\left(\frac{\pi}{1-\pi}\right) = -10.5 + 2.08 \cdot P. \qquad (4)$$

Table 3 shows the values of β_0 and β_1, considering cases with a threshold of 60 mm for the different combinations of damage indicators and percentiles.

It is important to assess whether this model can be used to separate positive and negative anomalies. Our models are

not deterministic and users need to take into account the uncertainty of the forecast expressed by these probabilities. For example, users could decide to take action when a 10 % probability of an above-70th-percentile event is forecast. In this case most of the observed events are forecasted, that is, the hit rate (i.e. the relative number of times a simulation event actually occurred) is close to 1, but this also implies a higher false alarm rate (i.e. the relative number of times an event had been simulated to occur but did not actually happen). On the other hand, if a higher threshold is used, we can reduce the number of false alarms, but at the expense of a greater number of missed events. The choice of the decision threshold is a function both of the skill of the forecast and the cost / loss ratio of the user. In any case, in a forecasting system affected by uncertainties, missed events can be reduced only by increasing false alarms and vice versa. In order to validate the model, we considered the ROC diagram (see Fig. 5).

The area under the ROC curve (RA) is a useful measure for summarising the skill of a model. RA ranges from 0, for

175
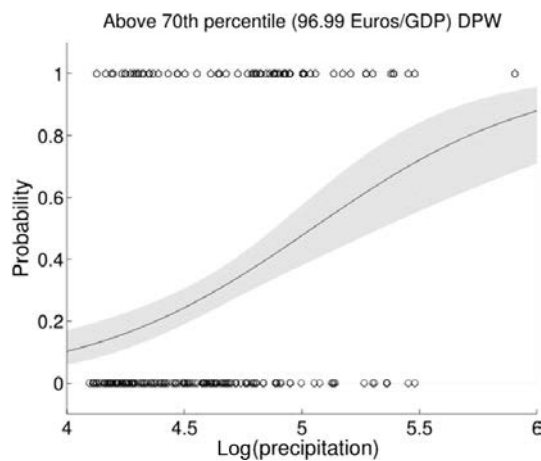
Figure 4. Example of logistic regression result used to model DPW damages above the 70th percentile as a function of precipitation (log-transformed precipitation given in millimetres). The solid line indicates the best estimate while the shaded band indicates the 95 % confidence interval. Open circles along the horizontal axis show the events that are above (top) and below (bottom) the 70th percentile.

Table 3. Parameters of the logistic model and RA values for the basin level with $60\,\text{mm}\,24\,\text{h}^{-1}$ maximum precipitation threshold. All the results are significant (p value < 0.01). Number of flood cases: 239.

Percentile	Damage	β_0	β_1	RA
50	D	-5.31	1.16	0.61
	DPC	-9.19	2.00	0.67
	DPW	-8.73	1.90	0.67
60	D	-6.89	1.41	0.64
	DPC	-8.90	1.84	0.67
	DPW	-9.58	1.99	0.68
70	D	-7.65	1.47	0.65
	DPC	-11.26	2.24	0.72
	DPW	-10.50	2.08	0.70
80	D	-10.19	1.89	0.70
	DPC	-10.44	1.94	0.70
	DPW	-11.84	2.24	0.73
90	D	-11.13	1.90	0.71
	DPC	-11.58	1.99	0.70
	DPW	-12.86	2.26	0.74

a forecast with no hit and only false alarms, to 1, indicating a perfect forecast. Models with an RA above 0.5 have more skill than random forecasts. Figure 5 shows that our model has skill: the ROC curve is well above the identity line, with an RA of 0.7. The "best threshold" in this illustrative example is 0.35. This means that if we want to maximise the $H - F$ difference (but please note that users could define other best thresholds according to their cost / loss ratio), an above-70th percentile damaging event is to be expected when our
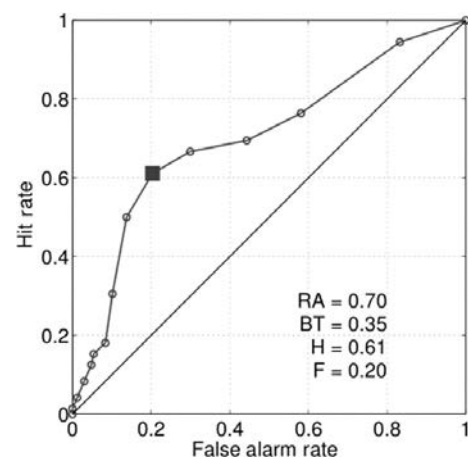
Figure 5. Relative operating characteristic (ROC) diagram for above-70th DPW predictions using the logistic regression of Eq. (1). The open dots indicate a set of probability forecasts by stepping a decision threshold with 5 % probability through the modelling results. The numbers inside the plots are the ROC area (RA) and the best threshold (BT), here defined as the threshold that maximises the difference between the hit rate (H) and the false alarm rate (F).

model predicts a probability higher then 0.35, resulting in $H = 0.61$ (this means that 61 out of 100 events are correctly modelled) and $F = 0.20$ (this means that 20 out of 100 events were modelled as an "event" when it did not actually happen). For example, in this case (BT $= 0.35$) a precipitation amount higher than 115 mm is needed to expect a damaging event above the 70th percentile for the damage indicator DPW (EUR 97 / GDP).

Table 3 summarises the model parameters and performance considering all the percentiles and the three categories of damage used. In each case, precipitation is a significant predictor (p value < 0.05) and the models have skill and significant RA values (the significance is estimated using a Mann–Whitney U test; Mason and Graham, 2002). Similar results were obtained for the damage categories, with slightly larger RA considering DPW. Finally, a number of sensitivity tests were carried out. We repeated the analysis considering (i) a precipitation threshold of 40 mm instead of 60 mm, (ii) the AEMET warning areas, (iii) only coastal regions and (iv) the basin-averaged precipitation instead of the maximum values, obtaining similar results (see Supplement).

3.2 Damaging events and precipitation in the metropolitan area of Barcelona

A total of 61 flood events were recorded in the metropolitan area of Barcelona (Fig. 1), which means an average of more than three events per year. The summer and autumn months had the highest number of flood events, with September having the most (31 %), followed by October (16 %). The insurance compensation paid by the CCS for floods

(a)

(b)
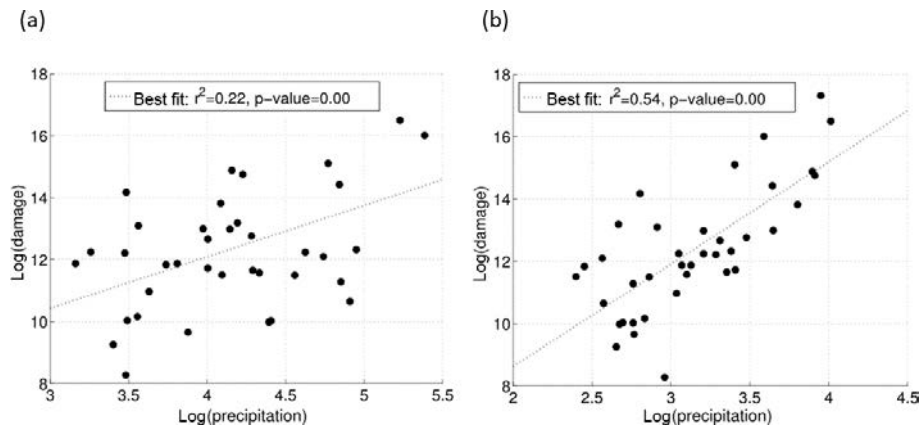
Figure 6. Scatter plot **(a)** damages (D) versus 24 h precipitation and **(b)** damages (D) versus 30 min precipitation in units of log(mm).

Table 4. Parameters of the logistic model and RA values for the MAB level with $10\,\mathrm{mm}\,30\,\mathrm{min}^{-1}$ maximum precipitation threshold. All the results are significant (p value < 0.05). Number of flood cases: 38.

Percentile	Damage	β_0	β_1	RA
50	D	−14.61	4.7	0.88
	DPC	−14.61	4.7	0.88
	DPW	−10.02	3.21	0.81
60	D	−13.34	4.06	0.85
	DPC	−13.34	4.06	0.85
	DPW	−13.72	4.18	0.86
70	D	−11.30	3.21	0.81
	DPC	−11.30	3.21	0.81
	DPW	−15.05	4.33	0.87
80	D	−16.62	4.58	0.89
	DPC	−16.62	4.58	0.89
	DPW	−16.62	4.58	0.89
90	D	−17.72	4.53	0.91
	DPC	−17.72	4.53	0.91
	DPW	−17.72	4.53	0.91

Figure 7. Example of a logistic regression result used to model damages (D) above the 70th percentile as a function of 30 min precipitation in units of log (mm) for the MAB. The solid line indicates the best estimate while the shaded band indicates the 95 % confidence interval. Open circles along the horizontal axis show the events that are above (top) and below (bottom) the percentile 70th.

amounted to EUR 86.30 million, which represents 20 % of the total compensation paid by the CCS in Catalonia. The municipality of Barcelona recorded a total of 37 events between 1996 and 2015, all due to in situ precipitation and drainage problems in the city (Llasat et al., 2016b). The city of Barcelona also receives the most compensation for floods (around EUR 19 million).

As can be seen in Fig. 6, the total damages (D) correlate more with 30 min precipitation than with 24 h precipitation, with significant results in both cases. In this particular case, similar results are obtained for the other damage categories (DPC and DPW; see Table 4).

We then repeated the logistic modelling exercise using 30 min precipitation. Figure 7 shows a logistic regression for

the events that affected the MAB. As in the basin-level aggregation, the model is capable of simulating the probability of total damage (D) above and below the 70th percentile as a function of 30 min precipitation in this case. As could be expected, this probability increases with precipitation. The same methodology was applied using a precipitation threshold of $20\,\mathrm{mm}\,30\,\mathrm{min}^{-1}$ (see Supplement) and using the 50th, 60th, 80th and 90th percentiles (Table 4). For this example, the regression equation is

$$\log\left(\frac{\pi}{1-\pi}\right) = -11.3 + 3.21 \cdot P. \tag{5}$$

Figure 8 shows the ROC diagram for predictions of total damages (D) above the 70th percentile for the MAB, using a precipitation threshold of $10\,\mathrm{mm}\,30\,\mathrm{min}^{-1}$. The total RA (0.81) shows that our model for the MAB has skill. In

177
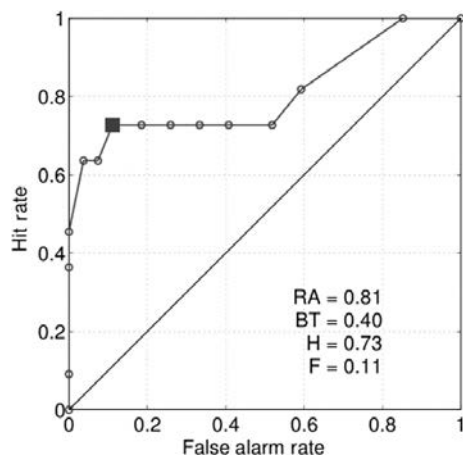
Figure 8. Relative operating characteristic (ROC) diagram for predictions for damage indicator D above the 70th percentile for the MAB using the logistic regression of Eq. (1). The open dots indicate a set of probability forecasts by stepping a decision threshold with 5 % probability through the modelling results. The numbers inside the plots are the ROC area (RA) and the best threshold (BT), here defined as the threshold that maximises the difference between the hit rate (H) and the false alarm rate (F).

this case, we would obtain the biggest difference between the hit and false rates when our model predicts a probability higher than 0.4. That is, the best threshold is 0.40, with 73 % of the events well predicted ($H = 0.73$) and only 11 % are false alarms events ($F = 0.11$). In this example, a precipitation amount higher than $30\,mm\,30\,min^{-1}$ is needed to expect a damaging event above the 70th percentile for damage indicator D (EUR 0.45 million).

Table 4 summarises the model parameters and performance considering all the percentiles and the three damage categories used for a precipitation threshold of $10\,mm\,30\,min^{-1}$ (see Supplement for results using $20\,mm\,30\,min^{-1}$ for the MAB). Similar results in terms of RA have been obtained for damage categories, whether using a 10 mm (Table 4) or a 20 mm threshold (Supplement).

4 Discussion and conclusions

The Mediterranean is an area frequently affected by flood events that produce significant socioeconomic damage. Catalonia, located in the west of the Mediterranean, is affected by an average of more than eight events per year. The majority of the damage caused by these events is due to local events, with intense and short-lived rainfall rather than river overflow (Llasat et al., 2014). Therefore, it is assumed that precipitation is the main contributing factor for damage caused by this type of event. To corroborate this hypothesis, the relationship between precipitation and compensation paid by insurance companies was studied. To take into account the differences in vulnerability and exposure in the ter-

ritory, we considered three types of damage: total damage, damage per capita (divided by the population) and damage per unit of GDP.

Although linear regression indicates a significant link (p value < 0.01), suggesting that rainfall data can be used to extract information on damages in Catalonia, the variance explained for the model is rather low ($r^2 = 0.09$ for D, $r^2 = 0.14$ for DPC and $r^2 = 0.16$ for DPW). For this reason, the relationship was assessed using logistic regression models in order to estimate the probability of large monetary damages occurring as a result of heavy precipitation events. That is, our aim is not to estimate the precise amount of insurance compensation, but to estimate when a "large" damaging event will occur given a particular precipitation amount. As could be expected, the logistic regression shows an increase in the probability of a damaging event occurring when precipitation increases. In order to validate the model, we considered the relative operating characteristic (ROC) diagram. The area under the ROC curve (RA) proved our model skill. The results show an RA above 0.6 in all percentiles of the three types of damages and thresholds of precipitation, most of them with values higher than 0.7. That is, our model is able to simulate the probability of a damaging event as a function of precipitation.

The methodology was also been applied for the metropolitan area of Barcelona (MAB) region, an urban area affected by more than three flood events per year. In this case precipitation data at subdaily scale is available. Linear regression has shown that 30 min precipitation is linked more closely with damages than 24 h precipitation, and also the logistic regression models present better results in terms of RA for the urban area considering higher-resolution data, with values higher than 0.8 in all cases. Therefore, we have been able to confirm that 30 min rainfall is a better predictor of the probability of large damages than daily rainfall in urban areas, and this result confirms previous studies such as that of Torgersen et al. (2015), who found a significant relationship between insurance data and short-lasting rainfall when studying urban floods in Norway. In addition, Spekkers et al. (2013) showed that high claim numbers associated with private property and content damage were significantly related to maximum rainfall intensity, based on a logistic regression, with rainfall intensity for 10 min to 4 h time windows.

Overall, our results confirm the hypothesis that precipitation is a key factor in explaining the damage caused by flood events in regions in which water surface floods are the main type of flood, as is the case in the Mediterranean region of study. Also our findings align with the results of previous studies (Spekkers et al., 2013; Zhou et al., 2013; Wobus et al., 2014; Torgersen et al., 2015) and further indicate that insurance databases are a promising source for flood damage assessment at local (Garrote et al., 2016; Le Bihan et al., 2017; Zischg et al., 2018; Zhou et al., 2013) and at regional

scale (Barredo et al., 2012; Kim et al., 2012; Wobus et al., 2014; Zhou et al., 2017).

To summarise, we have developed a new model that allows us to predict the probability that a flood event causing large damage (where the meaning of "large" depends on the user) will occur, based on precipitation, and taking into account the exposure and vulnerability of the region in the model. That is, the parsimonious empirical models linking flood damages to heavy precipitation developed in this study make a substantial contribution towards developing a warning forecast system with flood management strategies. For instance, from the relationship shown between precipitation and insurance compensation it is possible to predict when damaging events will occur as a result of a certain precipitation threshold.

These results were obtained by following a simple and transparent statistical methodology that can also be applied to other areas. These links could also provide a basis to predict flood damage in future climate change scenarios as done for instance by Wobus et al. (2014) that estimated monetary damages from flooding in the United States under a "business as usual" climate change scenario. As a word of caution it is worth noting that the complex relationships between climate variability, human activities and flood damage may limit the applicability of these findings to conditions that are very different from current ones. In addition, more complex analyses including more sophisticated empirical methods, and other factors such as soil physical characteristics (e.g. slope, soil characteristics, vegetation) could provide additional understanding on flood drivers and impacts. For instance, in Garrote et al. (2016) different simulation scenarios were defined considering the modifications to the terrain due to construction of fluvial defence structures in the area.

Despite these limitations, this work has provided the first assessment of the link between precipitation and flood damage in a Mediterranean region, and our results suggest that by exploiting the relationship between precipitation and flood damage, the model could provide satisfactory prediction of monetary compensation.

Data availability. The data are freely available for research purposes by contacting the corresponding author.

The Supplement related to this article is available online at https://doi.org/10.5194/nhess-18-857-2018-supplement.

Competing interests. The authors declare that they have no conflict of interest.

Special issue statement. This article is part of the special issue "Damage of natural hazards: assessment and mitigation". It is not associated with a conference.

References

Amaro, J., Gayà, M., Aran, M., and Llasat, M. C.: Preliminary results of the Social Impact Research Group of MEDEX: the request database (2000–2002) of two Meteorological Services, Nat. Hazards Earth Syst. Sci., 10, 2643–2652, https://doi.org/10.5194/nhess-10-2643-2010, 2010.

Barbería, L., Amaro, J., Aran, M., and Llasat, M. C.: The role of different factors related to social impact of heavy rain events: considerations about the intensity thresholds in densely populated areas, Nat. Hazards Earth Syst. Sci., 14, 1843–1852, https://doi.org/10.5194/nhess-14-1843-2014, 2014.

Barnolas, M. and Llasat, M. C.: A flood geodatabase and its climatological applications: the case of Catalonia for the last century, Nat. Hazards Earth Syst. Sci., 7, 271–281, https://doi.org/10.5194/nhess-7-271-2007, 2007.

Barredo, J. I.: Normalised flood losses in Europe: 1970–2006, Nat. Hazards Earth Syst. Sci., 9, 97–104, https://doi.org/10.5194/nhess-9-97-2009, 2009.

Barredo, J. I., Saurí, D., and Llasat, M. C.: Assessing trends in insured losses from floods in Spain 1971–2008, Nat. Hazards Earth Syst. Sci., 12, 1723–1729, https://doi.org/10.5194/nhess-12-1723-2012, 2012.

Barrera, A., Llasat, M. C., and Barriendos, M.: Estimation of extreme flash flood evolution in Barcelona County from 1351 to 2005, Nat. Hazards Earth Syst. Sci., 6, 505–518, https://doi.org/10.5194/nhess-6-505-2006, 2006.

Barrera-Escoda, A. and Llasat, M. C.: Evolving flood patterns in a Mediterranean region (1301–2012) and climatic factors – the case of Catalonia, Hydrol. Earth Syst. Sci., 19, 465–483, https://doi.org/10.5194/hess-19-465-2015, 2015.

Bernet, D. B., Prasuhn, V., and Weingartner, R.: Surface water floods in Switzerland: what insurance claim records tell us about the damage in space and time, Nat. Hazards Earth Syst. Sci., 17, 1659–1682, https://doi.org/10.5194/nhess-17-1659-2017, 2017.

Choi, O. and Fisher, A.: The impacts of socioeconomic development and climate change on severe weather catastrophe losses –

Nat. Hazards Earth Syst. Sci., 18, 857–868, 2018

www.nat-hazards-earth-syst-sci.net/18/857/2018/

179

Mid-Atlantic region (MAR) and the US, Clim. Change, 58, 149–170, 2003.

Cortès, M., Llasat, M. C., Gilabert, J., Llasat-Botija, M., Turco, M., Marcos, R., Martín Vide, J. P. and Falcón, L.: Towards a better understanding of the evolution of the flood risk in Mediterranean urban areas: the case of Barcelona, Nat. Hazards, 1–22, https://doi.org/10.1007/s11069-017-3014-0, 2017.

Elmer, F., Thieken, A. H., Pech, I., and Kreibich, H.: Influence of flood frequency on residential building losses, Nat. Hazards Earth Syst. Sci., 10, 2145–2159, https://doi.org/10.5194/nhess-10-2145-2010, 2010.

Falconer, R. H., Cobby, D., Smyth, P., Astle, G., Dent, J., and Golding, B.: Pluvial flooding: New approaches in flood warning, mapping and risk management, J. Flood Risk Manag., 2, 198–208, https://doi.org/10.1111/j.1753-318X.2009.01034.x, 2009.

Freni, G., La Loggia, G., and Notaro, V.: Uncertainty in urban flood damage assessment due to urban drainage modelling and depth-damage curve estimation, Water Sci. Technol., 61, 2979–2993, https://doi.org/10.2166/wst.2010.177, 2010.

García, L. E., Matthews, J. H., Rodriguez, D. J., Wijnen, M., DiFrancesco, K. N., and Ray, P.: Beyond Downscaling: A Bottom-Up Approach to Climate Adaptation for Water Resources Management, AGWA Report 01, Washington DC, World Bank Group, 2014.

Garrote, J., Alvarenga, F. M., and Díez-Herrero, A.: Quantification of flash flood economic risk using ultra-detailed stage-damage functions and 2-D hydraulic models, J. Hydrol., 541, 611–625, https://doi.org/10.1016/j.jhydrol.2016.02.006, 2016.

Harrell Jr, F. E.: Regression modeling strategies: with applications to linear models, logistic and ordinal regression, and survival analysis, Springer International Publishing, 2015.

Institut d'Estadística de Catalunya (IDESCAT, Statistical Institute of Catalonia), Anuari estadístic de Catalunya (Statistical Yearbook of Catalonia), available at: http://www.idescat.cat/, last access: 1 June 2017, 2016.

Instituto Nacional de Estadística – INE: Índice de Precios de Consumo, Base 2006 – Metodología, Metodología, 1–74, 2007.

Jansà, A., Alpert, P., Arbogast, P., Buzzi, A., Ivancan-Picek, B., Kotroni, V., Llasat, M. C., Ramis, C., Richard, E., Romero, R., and Speranza, A.: MEDEX: a general overview, Nat. Hazards Earth Syst. Sci., 14, 1965–1984, https://doi.org/10.5194/nhess-14-1965-2014, 2014.

Jongman, B., Hochrainer-stigler, S., Feyen, L., Aerts, J. C. J. H., Mechler, R., Botzen, W. J. W., Bouwer, L. M., Pflug, G., Rojas, R., and Ward, P. J.: Increasing stress on disaster-risk finance due to large floods, Nat. Clim. Change, 4, 1–5, https://doi.org/10.1038/NCLIMATE2124, 2014.

Kim, Y.-O., Seo, S. B., and Jang, O.-J.: Flood risk assessment using regional regression analysis, Nat. Hazards, 63, 1203–1217, https://doi.org/10.1007/s11069-012-0221-6, 2012.

Kreibich, H., Di Baldassarre, G., Vorogushyn, S., Aerts, J. C. J. H., Apel, H., Aronica, G. T., Arnbjerg-Nielsen, K., Bouwer, L. M., Bubeck, P., Caloiero, T., Chinh, D. T., Cortès, M., Gain, A. K., Giampá, V., Kuhlicke, C., Kundzewicz, Z. W., Llasat, M. C., Mård, J., Matczak, P., Mazzoleni, M., Molinari, D., Dung, N. V., Petrucci, O., Schröter, K., Slager, K., Thieken, A. H., Ward, P. J., and Merz, B.: Adaptation to flood risk: Results of international paired flood event studies, Earth's Future, 5, 953–965, https://doi.org/10.1002/2017EF000606, 2017.

Kundzewicz, Z. W., Kanae, S., Seneviratne, S. I., Handmer, J., Nicholls, N., Peduzzi, P., Mechler, R., Bouwer, L. M., Arnell, N., Mach, K., Muir-Wood, R., Brakenridge, G. R., Kron, W., Benito, G., Honda, Y., Takahashi, K., and Sherstyukov, B.: Flood risk and climate change: global and regional perspectives, Hydrol. Sci. J., 59, 1–28, https://doi.org/10.1080/02626667.2013.857411, 2014.

Le Bihan, G., Payrastre, O., Gaume, E., Moncoulon, D., and Pons, F.: The challenge of forecasting impacts of flash floods: test of a simplified hydraulic approach and validation based on insurance claim data, Hydrol. Earth Syst. Sci., 21, 5911–5928, https://doi.org/10.5194/hess-21-5911-2017, 2017.

Llasat, M. C., Llasat-Botija, M., and López, L.: A press database on natural risks and its application in the study of floods in Northeastern Spain, Nat. Hazards Earth Syst. Sci., 9, 2049–2061, https://doi.org/10.5194/nhess-9-2049-2009, 2009.

Llasat, M. C., Marcos, R., Llasat-Botija, M., Gilabert, J., Turco, M., and Quintana-Seguí, P.: Flash flood evolution in North-Western Mediterranean, Atmos. Res., 149, 230–243, https://doi.org/10.1016/j.atmosres.2014.05.024, 2014.

Llasat, M. C., Marcos, R., Turco, M., Gilabert, J., and Llasat-Botija, M.: Trends in flash flood events versus convective precipitation in the Mediterranean region: The case of Catalonia, J. Hydrol., 541, 24–37, https://doi.org/10.1016/j.jhydrol.2016.05.040, 2016a.

Llasat, M. C., Cortès, M., Falcón, Ll., Gilabert, J., Llasat-Botja, M., Marcos, R., Martín-Vide, J. P., and Turco, M.: A multifactorial analysis of flood variability in the Metropolitan Area of Barcelona, ICUR2016 Proceedings, ISBN:978-989-95094-1-2, 2016b.

Mason, S. J. and Graham, N. E.: Areas beneath the relative operating characteristics (ROC) and relative operating levels (ROL) curves: Statistical significance and interpretation, Q. J. R. Meteorol. Soc., 128, 2145–2166, https://doi.org/10.1256/003590002320603584, 2002.

Messner, F. and Meyer, V.: Flood damage, vulnerability and risk perception – challenges for flood damage research, in Flood Risk Management Hazards Vulnerability and Mitigation Measures, Vol. UFZ Discus, 149–167, 2006.

Moncoulon, D., Labat, D., Ardon, J., Leblois, E., Onfroy, T., Poulard, C., Aji, S., Rémy, A., and Quantin, A.: Analysis of the French insurance market exposure to floods: a stochastic model combining river overflow and surface runoff, Nat. Hazards Earth Syst. Sci., 14, 2469–2485, https://doi.org/10.5194/nhess-14-2469-2014, 2014.

Nakamura, I. and Llasat, M. C.: Policy and systems of flood risk management: a comparative study between Japan and Spain, Nat. Hazards, 87, 919–943, https://doi.org/10.1007/s11069-017-2802-x, 2017.

Papagiannaki, K., Lagouvardos, K., Kotroni, V., and Bezes, A.: Flash flood occurrence and relation to the rainfall hazard in a highly urbanized area, Nat. Hazards Earth Syst. Sci., 15, 1859–1871, https://doi.org/10.5194/nhess-15-1859-2015, 2015.

Petrucci, O. and Llasat, M. C.: Impact of disasters in mediterranean regions: An overview in the framework of the HYMEX project, in: Landslide Science and Practice: Social and Economic Impact and Policies, 7, 137–143, 2013.

Pielke Jr., R. A. and Downton, M. W.: Precipitation and damaging floods: Trends in the United States, 1932–97, J. Climate, 13, 3625–3637, https://doi.org/10.1175/1520-0442(2000)013<3625:PADFTI>2.0.CO;2, 2000.

www.nat-hazards-earth-syst-sci.net/18/857/2018/

Nat. Hazards Earth Syst. Sci., 18, 857–868, 2018

Quintana-Seguí, P., Peral, C., Turco, M., Llasat, M. C., and Martin, E.: Meteorological analysis systems in North-East Spain, Validation of SAFRAN and SPAN, J. Environ. Info., 27, 116–130, https://doi.org/10.3808/jei.201600335, 2016.

Sampson, C. C., Fewtrell, T. J., O'Loughlin, F., Pappenberger, F., Bates, P. B., Freer, J. E., and Cloke, H. L.: The impact of uncertain precipitation data on insurance loss estimates using a flood catastrophe model, Hydrol. Earth Syst. Sci., 18, 2305–2324, https://doi.org/10.5194/hess-18-2305-2014, 2014.

Spekkers, M. H., Kok, M., Clemens, F. H. L. R. and Ten Veldhuis, J. A. E.: A statistical analysis of insurance damage claims related to rainfall extremes, Hydrol. Earth Syst. Sci., 17(3), 913–922, https://doi.org/10.5194/hess-17-913-2013, 2013.

Spekkers, M. H., Clemens, F. H. L. R., and ten Veldhuis, J. A. E.: On the occurrence of rainstorm damage based on home insurance and weather data, Nat. Hazards Earth Syst. Sci., 15, 261–272, https://doi.org/10.5194/nhess-15-261-2015, 2015.

Thieken, A. H., Bessel, T., Kienzler, S., Kreibich, H., Müller, M., Pisi, S., and Schröter, K.: The flood of June 2013 in Germany: how much do we know about its impacts?, Nat. Hazards Earth Syst. Sci., 16, 1519–1540, https://doi.org/10.5194/nhess-16-1519-2016, 2016.

Torgersen, G., Bjerkholt, J. T., Kvaal, K., and Lindholm, O. G.: Correlation between extreme rainfall and insurance claims due to urban flooding – Case study Fredrikstad, Norway, J. Urban Environ. Eng., 9, 127–138, https://doi.org/10.4090/juee.2015.v9n2.127138, 2015.

UNISDR, International Strategy for Disaster Reduction (ISDR): Terminology on Disaster Risk Reduction, Geneva, Switzerland, last access: 10 May 2017, available at: https://www.unisdr.org/we/inform/publications/7817, 2009.

UNISDR, International Strategy for Disaster Reduction (ISDR): Making Development Sustainable: The Future of Disaster Risk Management, Global Assessment Report on Disaster Risk Reduction, Geneva, Switzerland, last access: 10 May 2017, available at: https://www.unisdr.org/we/inform/publications/42809, 2015.

Winsemius, H. C., Aerts, J. C. J. H., van Beek, L. P. H., Bierkens, M. F. P., Bouwman, A., Jongman, B., Kwadijk, J. C. J., Ligtvoet, W., Lucas, P. L., van Vuuren, D. P., and Ward, P. J.: Global drivers of future river flood risk, Nat. Clim. Change, 1–5, https://doi.org/10.1038/nclimate2893, 2015.

Wobus, C., Lawson, M., Jones, R., Smith, J., and Martinich, J.: Estimating monetary damages from flooding in the United States under a changing climate, J. Flood Risk Manag., 7, 217–229, https://doi.org/10.1111/jfr3.12043, 2014.

Zhou, Q., Panduro, T. E., Thorsen, B. J., and Arnbjerg-Nielsen, K.: Verification of flood damage modelling using insurance data, Water Sci. Technol., 68, 425–432, https://doi.org/10.2166/wst.2013.268, 2013.

Zhou, Q., Leng, G., and Feng, L.: Predictability of state-level flood damage in the conterminous United States: the role of hazard, exposure and vulnerability, Sci. Rep., 7, 5354, https://doi.org/10.1038/s41598-017-05773-4, 2017.

Zischg, A. P., Mosimann, M., Bernet, D. B., and Röthlisberger, V.: Validation of 2D flood models with insurance claims, J. Hydrol., 557, 350–361, https://doi.org/10.1016/j.jhydrol.2017.12.042, 2018.

Nat. Hazards Earth Syst. Sci., 18, 857–868, 2018

www.nat-hazards-earth-syst-sci.net/18/857/2018/

181
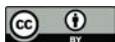
Natural Hazards
and Earth System
Sciences

Open Access

EGU

Supplement of

The relationship between precipitation and insurance data for floods in a Mediterranean region (northeast Spain)

Maria Cortès et al.

Correspondence to: Maria Cortès (mcortes@meteo.ub.edu)

SUPPLEMENTARY MATERIAL

TABLES

Table S1: Basin aggregation

BASINS

ALL BASINS		JOIN	
CODE	BASIN NAME	CODE	BASIN NAME
001	Tec, el	1001 (001; 002; 030)	El Tec; Rieres litorals Muga; La Muga
002	Rieres litorals Muga	1002 (003; 040)	Rieres litorals Fluvià; El Fluvià
003	Rieres litorals Fluvià	006	El Daró
006	Daró, el	1003 (015; 852)	El Gaià; Rieres Tarragona Centre
015	Gaià, el	019	Riera de Riudecanyes
019	Riera de Riudecanyes	1004 (025; 970)	La Sénia; Rieres litorals Ebre Sud
025	Sénia, la	050	Tordera, la
030	Muga, la	060	Besòs, el
040	Fluvià, el	070	Foix, el
050	Tordera, la	080	Francolí, el
060	Besòs, el	090	Garona, eth
070	Foix, el	100	Ter, el
080	Francolí, el	200	Llobregat, el
090	Garona, eth	300	Segre, el
100	Ter, el	400	Ebre, l'
200	Llobregat, el	500	Rieres Costa Brava Nord
300	Segre, el	600	Rieres Costa Brava Centre
400	Ebre, l'	618	Rieres Costa Brava Sud
500	Rieres Costa Brava Nord	700	Rieres del Maresme
600	Rieres Costa Brava Centre	774	Torrents de l' Àrea Metropolitana de Barcelona
618	Rieres Costa Brava Sud	789	Rieres litorals Llobregat
700	Rieres del Maresme	800	Rieres del Garraf
774	Torrents de l' Àrea Metropolitana de Barcelona	833	Rieres Tarragona Nord
789	Rieres litorals Llobregat	900	Rieres Tarragona Sud
800	Rieres del Garraf	913	Rieres Meridionals de Tarragona
833	Rieres Tarragona Nord	944	Rieres litorals Ebre Nord
852	Rieres Tarragona Centre		
900	Rieres Tarragona Sud		
913	Rieres Meridionals de Tarragona		
944	Rieres litorals Ebre Nord		
970	Rieres litorals Ebre Sud		

Table S2: Warning zones aggregation

WARNING ZONE

ALL WARNING ZONE		JOIN	
CODE	WARNING ZONE NAME	CODE	WARNING ZONE NAME
694304	Litoral sur de Tarragona	694304	Litoral sur de Tarragona
694302	Cadena prelitorial de Tarragona	694302	Cadena prelitorial de Tarragona
694301	Depresión central de Tarragona	694301	Depresión central de Tarragona
694303	Litoral norte de Tarragona	694303	Litoral norte de Tarragona
690804	Prelitoral de Barcelona	690804	Prelitoral de Barcelona
692503	Depresión central de Lleida	692503	Depresión central de Lleida
690803	Prelitoral de Barcelona	690803	Prelitoral de Barcelona
690802	Depresión central de Barcelona	690802	Depresión central de Barcelona
691704	Litoral sur de Girona	691704	Litoral sur de Girona
691702	Prelitoral de Girona	691702	Prelitoral de Girona
691703	Ampurdán	691703	Ampurdán
690801	Prepirineo de Barcelona	690000 (690801; 691701)	Prepirineo de Barcelona, pirineo de Lleida y Llivia
692502	Pirineo de Lleida	692502	Pirineo de Lleida
691701	Pirineo de Girona y Llivia	692501	Valle de Arán
692501	Valle de Arán		

Table S3: Parameters of the logistic model and RA values for the basin level with 40 mm/24 h maximum precipitation threshold. Number of flood cases: 331

PERCENTILE	DAMAGE	β_0	β_1	RA
50	D	-3.62	0.83	0.60
	DPC	-6.83	1.56	0.67
	DPW	-7.16	1.63	0.68
60	D	-5.11	1.06	0.63
	DPC	-7.79	1.67	0.69
	DPW	-8.68	1.87	0.71
70	D	-6.06	1.17	0.65
	DPC	-9.05	1.84	0.71
	DPW	-8.88	1.80	0.71
80	D	-9.19	1.73	0.72
	DPC	-10.73	2.07	0.74
	DPW	-9.74	1.85	0.73
90	D	-10.47	1.82	0.74
	DPC	-11.48	2.03	0.74
	DPW	-13.76	2.52	0.80

Table S4: Parameters of the logistic model and RA values for the basin level (without taking into account mountain basins: basin 090, 100, 200 and 300, according to Table 1 in supplementary material) with 40 mm/24 h maximum precipitation threshold. Number of flood cases: 247.

PERCENTILE	DAMAGE	β_0	β_1	RA
50	D	-3.95	0.91	0.6
	DPC	-6.53	1.51	0.65
	DPW	-7.13	1.65	0.66
60	D	-6.71	1.45	0.66
	DPC	-7.39	1.6	0.66
	DPW	-7.87	1.71	0.67
70	D	-7.37	1.49	0.66
	DPC	-10.31	2.15	0.72
	DPW	-8.88	1.83	0.70
80	D	-10.26	2.01	0.73
	DPC	-12.43	2.49	0.76
	DPW	-10.46	2.05	0.73
90	D	-10.62	1.89	0.72
	DPC	-10.83	1.94	0.72
	DPW	-13.45	2.5	0.79

Table S5: Parameters of the logistic model and RA values for the basin level (without taking into account mountain basins: basin 090, 100, 200 and 300, according to Table 1 in supplementary material) with 60 mm/24 h maximum precipitation threshold. Number of flood cases: 171.

PERCENTILE	DAMAGE	β_0	β_1	RA
50	D	-6.51	1.44	0.63
	DPC	-9.19	2.03	0.66
	DPW	-11.08	2.45	0.69
60	D	-10.06	2.13	0.69
	DPC	-10.28	2.17	0.67
	DPW	-10.25	2.16	0.68
70	D	-10.94	2.21	0.69
	DPC	-13.54	2.78	0.73
	DPW	-11.07	2.24	0.7
80	D	-11.15	2.13	0.7
	DPC	-10.3	1.95	0.69
	DPW	-10.65	2.02	0.7
90	D	-12.37	2.21	0.71
	DPC	-10.9	1.9	0.68
	DPW	-13.52	2.45	0.73

Table S6: Parameters of the logistic model and RA values for the basin level with 40 mm/24 h average precipitation threshold. Number of flood cases: 177.

PERCENTILE	DAMAGE	β_0	β_1	RA
50	D	-5.38	1.29	0.61
	DPC	-10.32	2.48	0.68
	DPW	-10.16	2.44	0.68
60	D	-5.89	1.31	0.61
	DPC	-10.70	2.46	0.69
	DPW	-9.48	2.17	0.68
70	D	-8.25	1.76	0.66
	DPC	-13.10	2.90	0.73
	DPW	-9.78	2.12	0.68
80	D	-11.75	2.44	0.73
	DPC	-11.86	2.46	0.71
	DPW	-9.96	2.02	0.67
90	D	-12.22	2.35	0.72
	DPC	-13.13	2.56	0.73
	DPW	-14.99	2.98	0.77

Table S7: Parameters of the logistic model and RA values for the basin level with 60 mm/24 h average precipitation threshold. Number of flood cases: 100. * Indicates no significance (p-value>0.05).

PERCENTILE	DAMAGE	β_0	β_1	RA
50	D	-6.02*	1.37*	0.61*
	DPC	-14.99	3.42	0.72
	DPW	-13.70	3.13	0.71
60	D	-7.95	1.71	0.64
	DPC	-17.43	3.87	0.75
	DPW	-16.95	3.76	0.75
70	D	-11.76	2.47	0.69
	DPC	-13.61	2.89	0.72
	DPW	-13.44	2.85	0.70
80	D	-9.04*	1.73*	0.64
	DPC	-15.51	3.17	0.73
	DPW	13.68	2.77	0.71
90	D	-10.20*	1.80*	0.67
	DPC	-15.75	3.02	0.74
	DPW	-12.99	2.42	0.69

Table S8: Parameters of the logistic model and RA values for the warning zone level with 40 mm/24 h maximum precipitation threshold. Number of flood cases: 243.

PERCENTILE	DAMAGE	β_0	β_1	RA
50	D	-2.73	0.62	0.6
	DPC	-6.79	1.53	0.7
	DPW	-6.81	1.54	0.7
60	D	-4.05	0.82	0.63
	DPC	-7.54	1.59	0.71
	DPW	-7.21	1.52	0.71
70	D	-4.82	0.89	0.63
	DPC	-8.25	1.64	0.73
	DPW	-9	1.8	0.74
80	D	-7.35	1.31	0.7
	DPC	-9.67	1.81	0.76
	DPW	-10.65	2.03	0.78
90	D	-8.92	1.46	0.73
	DPC	-11.04	1.9	0.79
	DPW	-11.62	2.02	0.81

Table S9: Parameters of the logistic model and RA values for the warning zone level with 60 mm/24 h maximum precipitation threshold. Number of flood cases: 180. * Indicates no significance (p-value>0.05).

PERCENTILE	DAMAGE	β_0	β_1	RA
50	D	-2.13*	0.46*	0.58*
	DPC	-6.54	1.41	0.66
	DPW	-6.52	1.41	0.67
60	D	-2.08*	0.36*	0.55*
	DPC	-7.07	1.43	0.68
	DPW	-6.94	1.4	0.67
70	D	-3.64*	0.6*	0.58*
	DPC	-8.06	1.54	0.7
	DPW	-10.04	1.96	0.75
80	D	-3.9*	0.54*	0.56*
	DPC	-10.04	1.83	0.75
	DPW	-10.01	1.82	0.74
90	D	-8.44	1.32	0.71
	DPC	-10.61	1.76	0.75
	DPW	-10.57	1.75	0.75

Table S10: Parameters of the logistic model and RA values for the MAB level with 20 mm/30 min maximum precipitation threshold. Number of flood cases: 21. * Indicates no significance (p-value>0.05).

PERCENTILE	DAMAGE	β_0	β_1	RA
50	D	-42.27	12.28	0.94
	DPC	-42.27	12.28	0.94
	DPW	-34.04	9.81	0.91
60	D	-75.09	11.66	0.95
	DPC	-26.47	11.66	0.95
	DPW	-33.68	11.66	0.95
70	D	-27.89	7.23	0.92
	DPC	-27.89	7.23	0.92
	DPW	-27.89	7.23	0.92
80	D	-16.25	4.05*	0.82
	DPC	-16.25	4.05*	0.82
	DPW	-16.25	4.05*	0.82
90	D	-6759.73	1727.74*	1*
	DPC	-6759.73	1727.74*	1*
	DPW	-6759.73	1727.74*	1*

Table S11: Damage percentiles for all the damage indicators, precipitation indicators and levels. Damage (D) is in euros, damage per capita (DPC) in euros/population and damage per wealth (DPW) in euros/GDP.

PERCENTILE	DAMAGE	BASINS		WARNING ZONES		MAB	
		40 mm/24h	60 mm/24h	40 mm/24h	60 mm/24h	10 mm/30min	20 mm/30min
50	D	76534	91732	180148	228677	191222	332437
	DPC	0.40	0.48	0.33	0.54	0.06	0.11
	DPW	20	27	15	26	2	4
60	D	142642	177573	288708	342690	253197	439954
	DPC	0.66	0.96	0.61	0.82	0.09	0.14
	DPW	36	57	31	48	3	5
70	D	244098	280868	465357	601829	446198	1754684
	DPC	1.25	1.97	1.12	1.60	0.14	0.56
	DPW	71	97	60	94	5	19
80	D	512063	798412	800506	1203333	1394559	2992793
	DPC	3.15	4.14	2.38	2.76	0.45	0.93
	DPW	141	200	132	164	13	29
90	D	1670401	2377659	2504096	3191660	3414333	10680483
	DPC	7.97	13.15	5.28	6.35	1.07	3.57
	DPW	380	591	301	417	35	103

FIGURES
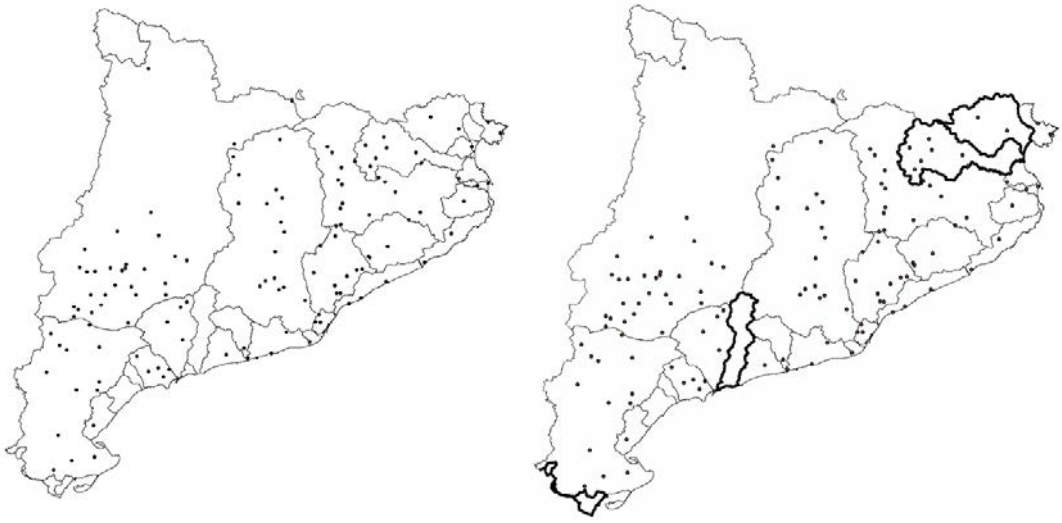
Figure S1. Basins aggregation
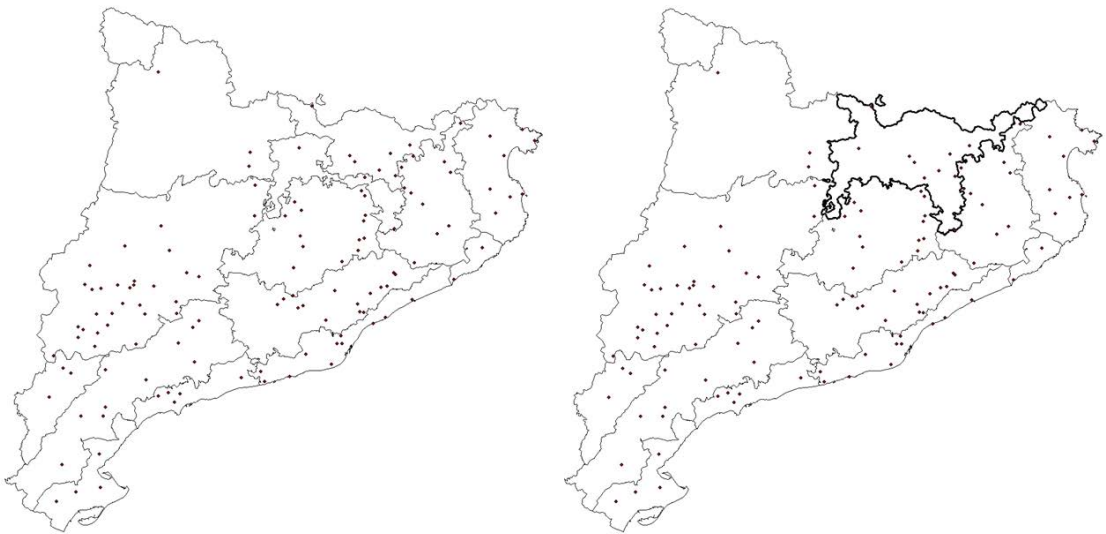
Figure S2. Warning zones aggregation
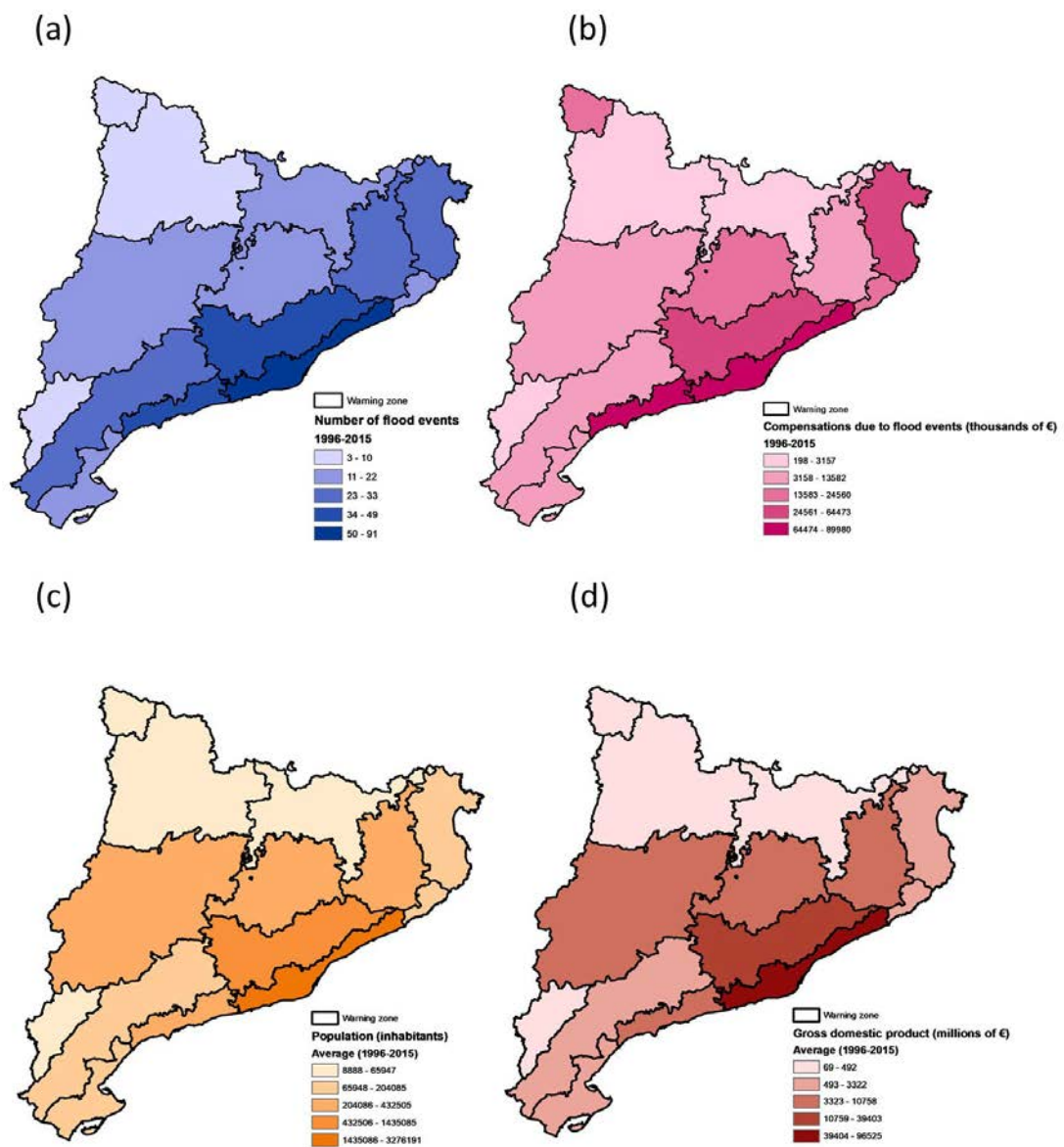
Figure S3. (a) Warning zone distribution of flood events (1996-2015); (b) total insurance compensations for floods made by CCS (1996-2015); (c) average total population; and (d) average gross domestic product.
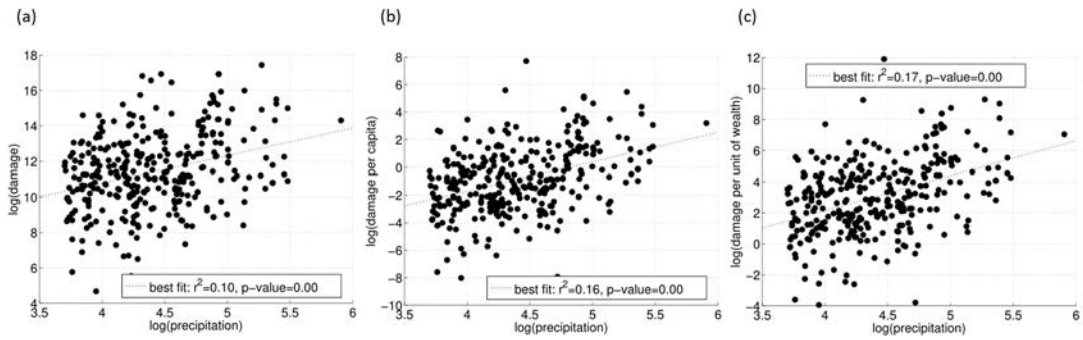
Figure S4: Scatter plot showing maximum precipitation in 24 h (mm) and (a) total damages (D); (b) damage per capita (DPC); and (c) damage per unit of wealth (DPW), for flood events recorded in Catalonia between 1996 and 2015 (log-transformed values; damage are given in euros). Each point represents the compensation series (D, DPC or DPW) and the maximum 24 h precipitation for each basin. The dashed line indicates the fit based on a linear regression model. (P_0=40 mm/24 h).
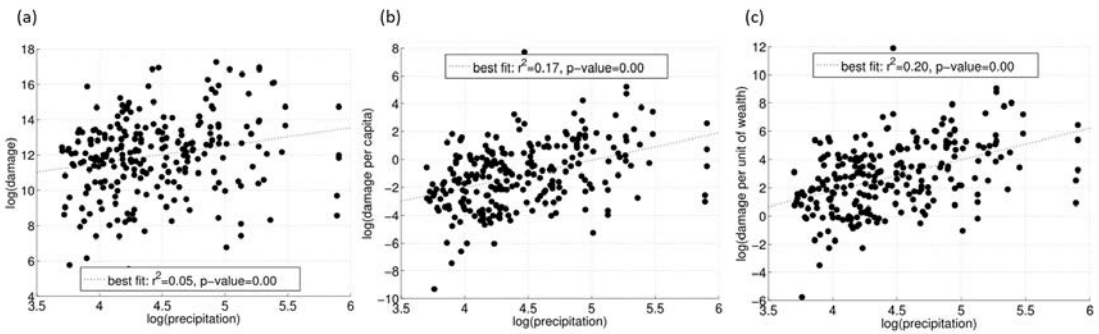
Figure S5: Scatter plot showing maximum precipitation in 24 h (mm) and (a) total damages (D); (b) damage per capita (DPC); and (c) damage per unit of wealth (DPW), for flood events recorded in Catalonia between 1996 and 2015 (log-transformed values; damage are given in euros). Each point represents the compensation series (D, DPC or DPW) and the maximum 24 h precipitation for each warning zone. The dashed line indicates the fit based on a linear regression model. (P_0=40 mm/24 h).
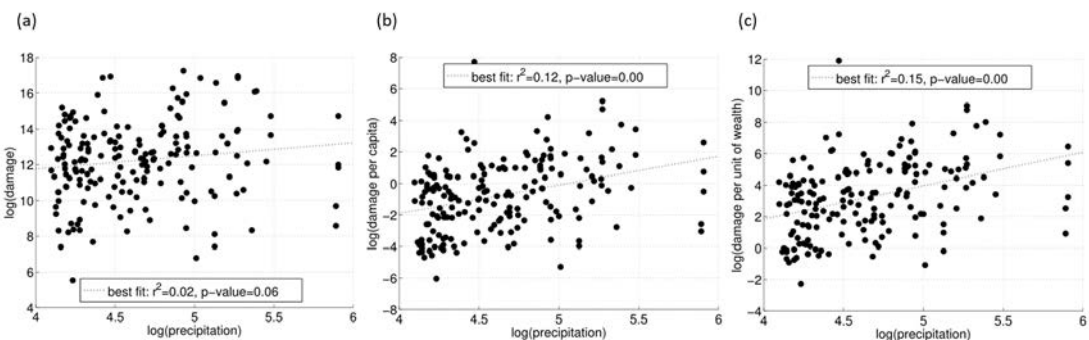
Figure S6: Scatter plot showing maximum precipitation in 24 h (mm) and (a) total damages (D); (b) damage per capita (DPC); and (c) damage per unit of wealth (DPW), for flood events recorded in Catalonia between 1996 and 2015 (log-transformed values; damage are given in euros). Each point represents the compensation series (D, DPC or DPW) and the maximum 24 h precipitation for each warning zone. The dashed line indicates the fit based on a linear regression model. (P_0=60 mm/24 h).

191
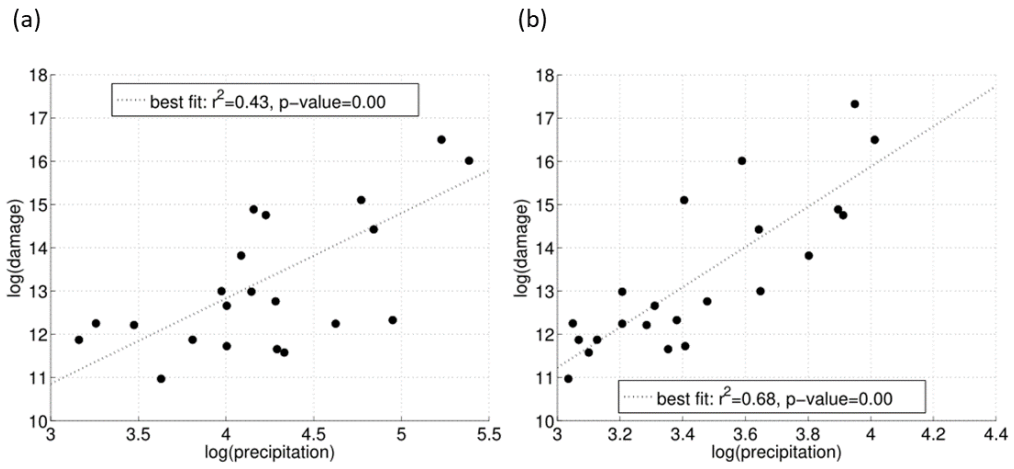
Figure S7: scatter plot (a) damages (D) versus 24 h precipitation (P$_0$=20 mm/24 h) and (b) damages (D) versus 30 minute precipitation (P$_0$=20 mm/30 min) for the MAB (unit: log(mm)).
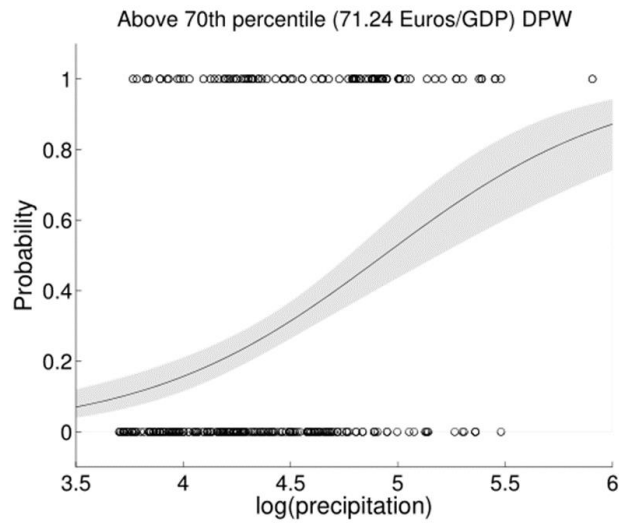
Figure S8: Example of logistic regression result to model DPW damages above the 70th percentile as a function of precipitation (log-transformed of the precipitation given in mm) for basin level. The solid line indicates the best estimate while the shaded band indicates the 95% confidence interval. Open circles along the horizontal axis show the events that are above (top) and below (bottom) the 70th percentile. (P$_0$=40 mm/24 h).
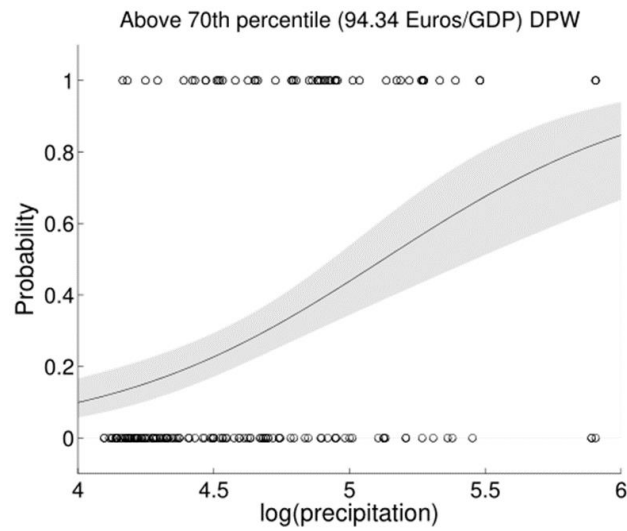
Figure S9: Example of logistic regression result to model DPW damages above the 70th percentile as a function of precipitation (log-transformed of the precipitation given in mm) for warning zone level. The solid line indicates the best estimate while the shaded band indicates the 95% confidence interval. Open circles along the horizontal axis show the events that are above (top) and below (bottom) the 70th percentile. (P_0=60 mm/24 h).
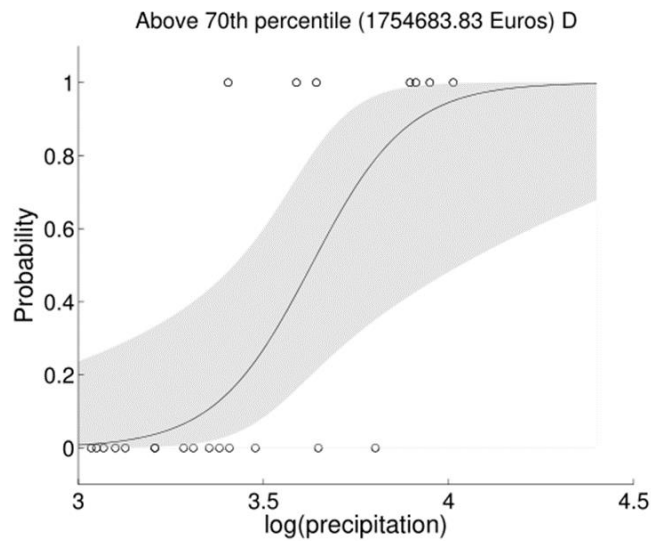
Figure S10: Example of logistic regression result to model D damages above the 70th percentile as a function of precipitation (log-transformed of the precipitation given in mm) for the MAB. The solid line indicates the best estimate while the shaded band indicates the 95% confidence interval. Open circles along the horizontal axis show the events that are above (top) and below (bottom) the 70th percentile. (P_0=20 mm/30 min).
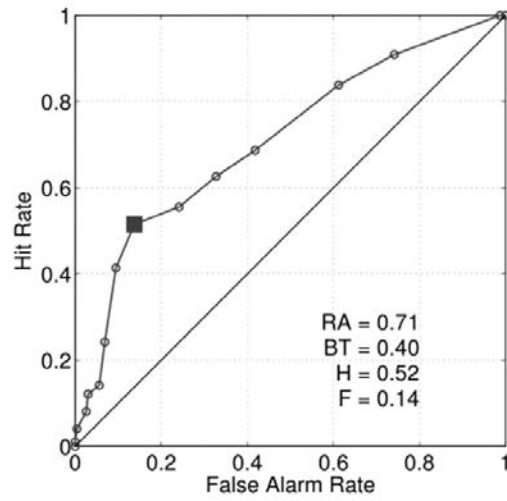
Figure S11: Relative operating characteristic (ROC) diagram for above 70th DPW predictions for basin level using the logistic regression of Eq. (1) (P_0=40 mm/24 h). The open dots indicate a set of probability forecasts by stepping a decision threshold with 5% probability through the modelling results. The numbers inside the plots are the ROC Area (RA) and the Best Threshold (BT), here defined as the threshold that maximise the difference between the hit rate (H) and the false alarm rate (F).
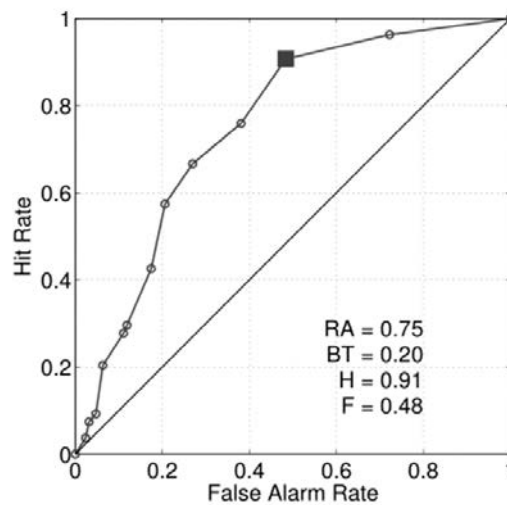
Figure S12: Relative operating characteristic (ROC) diagram for above 70th DPW predictions for the warning zones using the logistic regression of Eq. (1) (P_0=60 mm/24 h). The open dots indicate a set of probability forecasts by stepping a decision threshold with 5% probability through the modelling results. The numbers inside the plots are the ROC Area (RA) and the Best Threshold (BT), here defined as the threshold that maximise the difference between the hit rate (H) and the false alarm rate (F).
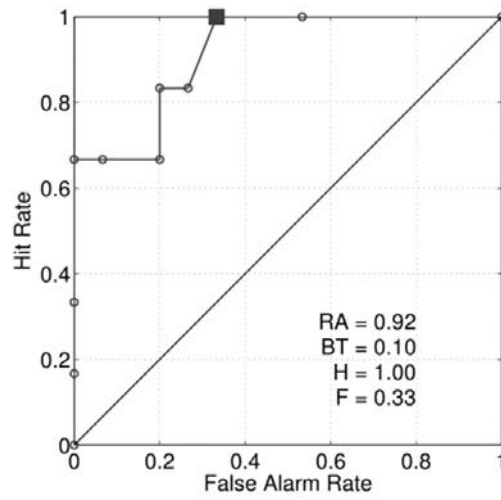
Figure S13: Relative operating characteristic (ROC) diagram for above 70th D predictions for the MAB using the logistic regression of Eq. (1) (P₀=20 mm/30 min). The open dots indicate a set of probability forecasts by stepping a decision threshold with 5% probability through the modelling results. The numbers inside the plots are the ROC Area (RA) and the Best Threshold (BT), here defined as the threshold that maximise the difference between the hit rate (H) and the false alarm rate (F).

References

ACA (2018). Agència Catalana de l'Aigua. `http://aca.gencat.cat/ca/inici`.

Akaike, H. (1974). A new look at the statistical model identification. *IEEE transactions on automatic control*, 19(6):716–723.

Alfieri, L., Bisselink, B., Dottori, F., Naumann, G., de Roo, A., Salamon, P., Wyser, K., and Feyen, L. (2017). Global projections of river flood risk in a warmer world. *Earth's Future*, 5(2):171–182.

Alfieri, L., Burek, P., Feyen, L., and Forzieri, G. (2015a). Global warming increases the frequency of river floods in Europe. *Hydrology and Earth System Sciences*, 19(5):2247–2260.

Alfieri, L., Dottori, F., Betts, R., Salamon, P., and Feyen, L. (2018). Multi-model projections of river flood risk in Europe under global warming. *Climate*, 6(1):6.

Alfieri, L., Feyen, L., Dottori, F., and Bianchi, A. (2015b). Ensemble flood risk assessment in Europe under high end climate scenarios. *Global Environmental Change*, 35:199–212.

Altava-Ortiz, V., Barrera-Escoda, A., Amaro, J., Cunillera, J., Prohom, M., and Sairouni, A. (2016). Generació d'escenaris climàtics futurs regionalitzats a molt alta resolució (1 km) per a l'Àrea Metropolitana de Barcelona (Projecte ESAMB). Technical report, Servei Meteorològic de Catalunya (SMC).

Amaro, J., Gayaà, M., Aran, M., and Llasat, M. C. (2010). Preliminary results of the Social Impact Research Group of MEDEX: The request database (2000-2002) of two Meteorological Services. *Natural Hazards and Earth System Science*, 10(12):2643–2652.

André, C., Monfort, D., Bouzit, M., and Vinchon, C. (2013). Contribution of insurance data to cost assessment of coastal flood damage to residential buildings: insights gained from Johanna (2008) and Xynthia (2010) storm events. *Natural Hazards and Earth System Sciences*, 13(8):2003–2012.

Balbi, S., Giupponi, C., Olschewski, R., and Mojtahed, V. (2015). The Total Cost of Water-Related Disasters. *Review of Economics/Jahrbuch für Wirtschaftswissenschaften*, 66(2):225–249.

Balica, S. F., Wright, N. G., and van der Meulen, F. (2012). A flood vulnerability index for coastal cities and its use in assessing climate change impacts. *Natural hazards*, 64(1):73–105.

Barbería, L., Amaro, J., Aran, M., and Llasat, M. C. (2014). The role of different factors related to social impact of heavy rain events: considerations about the intensity thresholds in densely populated areas. *Natural Hazards and Earth System Science*, 14(7):1843–1852.

Barnolas, M. and Llasat, M. (2007). Metodologıa para el estudio de inundaciones históricas en Espana e implementación de un SIG en las cuencas del Ter, Segre y Llobregat. *CEH-CEDEX, Monografıas M-90, Ministerio de Fomento, Madrid*.

Barredo, J. I. (2009). Normalised flood losses in Europe: 1970−2006. *Natural Hazards and Earth System Science*, 9(1):97–104.

Barredo, J. I., Saurí, D., and Llasat, M. C. (2012). Assessing trends in insured losses from floods in Spain 1971−2008. *Natural Hazards and Earth System Science*, 12(5):1723–1729.

Barrera, A., Llasat, M., and Barriendos, M. (2006). Estimation of extreme flash flood evolution in Barcelona County from 1351 to 2005. *Natural Hazards and Earth System Science*, 6(4):505–518.

Barrera-Escoda, A., Gonçalves, M., Guerreiro, D., Cunillera, J., and Baldasano, J. (2014). Projections of temperature and precipitation extremes in the North Western Mediterranean Basin by dynamical downscaling of climate scenarios at high resolution (1971–2050). *Climatic change*, 122(4):567–582.

Barrera-Escoda, A. and Llasat Botija, M. d. C. (2015). Evolving flood patterns in a Mediterranean region (1301-2012) and climatic factors-the case of Catalonia. *Hydrology and Earth System Sciences, 2015, vol. 19, num. 1, p. 465-483*.

Barriendos, M., Coeur, D., Lang, M., Llasat, M. C., Naulet, R., Lemaitre, F., and Barrera, a. (2003). Stationarity analysis of historical flood series in France and Spain (14th−20th centuries). *Natural Hazards and Earth System Science*, 3(6):583–592.

Barriendos Valve, M., Ruiz Bellet, J. L., Tuset Mestre, J., Mazón Bueso, J., Balasch Solanes, J. C., Pino González, D., and Ayala, J. L. (2014). The" Prediflood" database of historical floods in Catalonia (NE Iberian Peninsula) AD 1035–2013, and its potential applications in flood analysis. *Hydrology and Earth system sciences*, 18:4807–4823.

Benoit, G. and Comeau, A. (2005). *A sustainable future for the Mediterranean: the Blue Plan's environment and development outlook*. Earthscan.

Beranová, R., Kyselỳ, J., and Hanel, M. (2018). Characteristics of sub-daily precipitation extremes in observed data and regional climate model simulations. *Theoretical and applied climatology*, 132(1-2):515–527.

Bernet, D. B., Prasuhn, V., and Weingartner, R. (2017). Surface water floods in Switzerland: what insurance claim records tell us about the damage in space and time. *Natural Hazards and Earth System Science*, 17(9):1659–1682.

Betts, R., Alfieri, L., Bradshaw, C., Caesar, J., Feyen, L., Friedlingstein, P., Gohar, L., Koutroulis, A., Lewis, K., Morfopoulos, Catherine Papadimitriou, L., Richardson, K. J., Tsanis, I., and Wyser, K. (2018). Changes in climate extremes, fresh water availability and vulnerability to food insecurity projected at 1.5 °C and 2 °C global warming with a higher-resolution global climate model. *Earth's Future.*

Bihan, G. L., Payrastre, O., Gaume, E., Moncoulon, D., and Pons, F. (2017). The challenge of forecasting impacts of flash floods: test of a simplified hydraulic approach and validation based on insurance claim data. *Hydrology and Earth System Sciences*, 21(11):5911–5928.

Blöschl, G., Parajka, J., J, S., Viglione, A., and Montanari, A. (2012). Floods in Austria. In *Changes in Flood Risk in Europe.* CRC Press and IAHS Press.

Blöschl, G., Viglione, A., and Montanari, A. (2013). Emerging approaches to hydrological risk management in a changing world. In *Climate vulnerability: Understanding and Addressing Threats to Essential Resources.* Elsevier.

Bolker, B. M., Brooks, M. E., Clark, C. J., Geange, S. W., Poulsen, J. R., Stevens, M. H. H., and White, J.-S. S. (2009). Generalized linear mixed models: a practical guide for ecology and evolution. *Trends in ecology & evolution*, 24(3):127–135.

Boudou, M. (2015). *Approche multidisciplinaire pour la caractérisation inondations remarquables: enseignements tirés de neuf évènements en France (1910-2010).* PhD thesis, Université Paul Valéry-Montpellier III.

Bouwer, L. M. (2011). Have disaster losses increased due to anthropogenic climate change? *Bulletin of the American Meteorological Society*, 92(1):39–46.

Brázdil, R., Chromá, K., Řezníčková, L., Valášek, H., Dolák, L., Stachoň, Z., Soukalová, E., and Dobrovolnỳ, P. (2014). The use of taxation records in assessing historical floods in South Moravia, Czech Republic. *Hydrology and Earth System Sciences*, 18(10):3873–3889.

Brönnimann, S., Rajczak, J., Fischer, E. M., Raible, C., Rohrer, M., and Schär, C. (2018). Changing seasonality of moderate and extreme precipitation events in the Alps. *Natural Hazards and Earth System Science*, 18(7):2047–2056.

Burke, M., Davis, W. M., and Diffenbaugh, N. S. (2018). Large potential reduction in economic damages under un mitigation targets. *Nature*, 557(7706):549.

Cardell, M., Romero, R., Amengual, A., Homar, V., and Ramis, C. (2018). A quantile–quantile adjustment of the euro-cordex projections for temperatures and precipitation. *International Journal of Climatology.*

Casas-Castillo, M. C., Cunillera I grañó, J., Xènia, D., Herrero, M., Ninyerola, M., Xavier, P., Redaño, A., Rius, A., and Rodriguez, R. (2005). *Mapes de precipitació màxima diària*

esperada a Catalunya per a diferents períodes de retorn. Servei Meteorològic de Catalunya : Departament de Medi Ambient i Habitatge : Generalitat de Catalunya.

CCS (2018). Estadística de riesgos extraordinarios 1971-2017. Technical report, Consorcio de Compensación de Seguros.

Chow, V., Maidment, D., and Mays, L. (1988). *Applied hydrology.* McGraw-Hill Book Company.

Cioffi, F., Lall, U., Rus, E., and Krishnamurthy, C. K. B. (2015). Space-time structure of extreme precipitation in Europe over the last century. *International Journal of Climatology*, 35(8):1749–1760.

Colmet-Daage, A., Sanchez-Gomez, E., Ricci, S., Llovel, C., Borrell Estupina, V., Quintana-Seguí, P., Llasat Botija, M. d. C., and Servat, E. (2018). Evaluation of uncertainties in mean and extreme precipitation under climate change for northwestern Mediterranean watersheds from high-resolution Med and Euro-CORDEX ensembles. *Hydrology and Earth System Sciences, 2018, vol. 22, num. 1, p. 673-687.*

Cortès, M., Llasat, M. C., Gilabert, J., Llasat-Botija, M., Turco, M., Marcos, R., Martín Vide, J. P., and Falcón, L. (2017). Towards a better understanding of the evolution of the flood risk in Mediterranean urban areas: the case of Barcelona. *Natural Hazards*, pages 1–22.

Cortès, M., Turco, M., Llasat, M., and Llasat, Llasat, M. C. (2018). Estimación de los daños por inundaciones en el Mediterráneo español a partir de la lluvia. In *EL CLIMA: AIRE, AGUA, TIERRA Y FUEGO.* Asociación Española de Climatología.

Cortès, M., Turco, M., Llasat-Botija, M., and Llasat Botija, M. d. C. (2018). The relationship between precipitation and insurance data for floods in a Mediterranean region (northeast Spain). *Natural Hazards And Earth System Sciences, 2018, vol. 18, p. 857-868.*

Cortès, M., Turco, M., Ward, P., Sánchez-Espigares, J. A., Alfieri, L., and Llasat, M. C. (2019). Changes in flood damage with global warming in the east coast of Spain. *Natural Hazards and Earth System Sciences Discussions*, 2019:1–40.

Cramer, W., Guiot, J., Fader, M., Garrabou, J., Gattuso, J.-P., Iglesias, A., Lange, M. A., Lionello, P., Llasat, M. C., Paz, S., et al. (2018). Climate change and interconnected risks to sustainable development in the Mediterranean. *Nature Climate Change*, page 1.

CREAF (2018). Centre d'Investigació Ecològica i Aplicacions Forestals. `http://www.creaf.cat/ca`.

de Lima, M. I. P., Santo, F. E., Ramos, A. M., and Trigo, R. M. (2014). Trends and correlations in annual extreme precipitation indices for mainland Portugal, 1941−2007. *Theoretical and Applied Climatology*, 119(1-2):55–75.

Donat, M. G., Lowry, A. L., Alexander, L. V., O'Gorman, P. A., and Maher, N. (2016). More extreme precipitation in the world's dry and wet regions. *Nature Climate Change*, 6(5):508.

Donnelly, C., Greuell, W., Andersson, J., Gerten, D., Pisacane, G., Roudier, P., and Ludwig, F. (2017). Impacts of climate change on european hydrology at 1.5, 2 and 3 degrees mean global warming above preindustrial level. *Climatic Change*, 143(1-2):13–26.

Dottori, F., Martina, M. L. V., and Figueiredo, R. (2016). A methodology for flood susceptibility and vulnerability analysis in complex flood scenarios. *Journal of Flood Risk Management*.

Douglas, E. M., Vogel, R. M., and Kroll, C. N. (2000). Trends in floods and low flows in the United States: Impact of spatial correlation. *Journal of Hydrology*, 240(1-2):90–105.

Drobinski, P., Da Silva, N., Panthou, G., Bastin, S., Muller, C., Ahrens, B., Borga, M., Conte, D., Fosser, G., Giorgi, F., et al. (2018). Scaling precipitation extremes with temperature in the Mediterranean: past climate assessment and projection in anthropogenic scenarios. *Climate dynamics*, 51(3):1237–1257.

Drobinski, P., Ducrocq, V., Alpert, P., Anagnostou, E., Béranger, K., Borga, M., Braud, I., Chanzy, A., Davolio, S., Delrieu, G., et al. (2014). HyMeX: A 10-year multidisciplinary program on the Mediterranean water cycle. *Bulletin of the American Meteorological Society*, 95(7):1063–1082.

Ducrocq, V., Drobinski, P., Gualdi, S., and Raimbault, P. (2016). The water cycle in the Mediterranean. In editions, I., editor, *The Mediterranean Region under Climate Change. A scientific update*, chapter 1, pages 73–81. IRD editions.

Elmer, F., Thieken, a. H., Pech, I., and Kreibich, H. (2010). Influence of flood frequency on residential building losses. *Natural Hazards and Earth System Science*, 10(10):2145–2159.

EM-DAT (2018). CRED / UCLouvain, Brussels, Belgium. `https://www.emdat.be`.

EMA (2002). Disaster loss assessment guidelines. Technical report, Emergency Management Australia, State of Queensland and Commonwealth of Australia.

Escuder-Bueno, I., Castillo-Rodriguez, J. T., Zechner, S., Jöbstl, C., Perales-Momparler, S., and Petaccia, G. (2012). A quantitative flood risk analysis methodology for urban areas with integration of social research data. *Natural Hazards and Earth System Science*, 12(9):2843–2863.

European Comission (2007). A new EU Floods Directive 2007/60/EC. `https://eur-lex.europa.eu/eli/dir/2007/60/oj`.

Faccini, F., Luino, F., Sacchini, A., and Turconi, L. (2015). Flash flood events and urban development in Genoa (Italy): lost in translation. In *Engineering Geology for Society and Territory-Volume 5*, pages 797–801. Springer.

Falconer, R., Cobby, D., Smyth, P., Astle, G., Dent, J., and Golding, B. (2009). Pluvial flooding: new approaches in flood warning, mapping and risk management. *Journal of Flood Risk Management*, 2(3):198–208.

Field, C. B., Barros, V., Stocker, T. F., and Dahe, Q. (2012). *Managing the risks of extreme events and disasters to advance climate change adaptation: special report of the intergovernmental panel on climate change.* Cambridge University Press.

Fourrie, N., Haddouch, H., Brousseau, P., Wattrelot, E., and Fisher, C. (2016). Forecast of heavy precipitation events. In editions, I., editor, *The Mediterranean Region under Climate Change. A scientific update*, chapter 3, pages 577–585. IRD editions.

Gain, A. K., Mojtahed, V., Biscaro, C., and Balbi, S. (2015). An integrated approach of flood risk assessment in the eastern part of Dhaka City. *Natural Hazards*.

Garcia, L. E., Matthews, J. H., Rodriguez, D. J., Wijnen, M., DiFrancesco, K. N., and Ray, P. (2014). *Beyond downscaling: a bottom-up approach to climate adaptation for water resources management.* World Bank Group, Washington, DC.

Garrote, J., Alvarenga, F., and Díez-Herrero, A. (2016). Quantification of flash flood economic risk using ultra-detailed stage–damage functions and 2-D hydraulic models. *Journal of Hydrology*, 541:611–625.

Garrote, L., Martin-Carrasco, F., Flores-Montoya, F., and Iglesias, A. (2007). Linking drought indicators to policy actions in the tagus basin drought management plan. *Water resources management*, 21(5):873–882.

Gascón, E., Laviola, S., Merino, A., and Miglietta, M. (2016). Analysis of a localized flash-flood event over the central Mediterranean. *Atmospheric Research*, 182:256–268.

Gaume, E., Borga, M., Llassat, M. C., Maouche, S., Lang, M., and Diakakis, M. (2016). Mediterranean extreme floods and flash floods. In editions, I., editor, *The Mediterranean Region under Climate Change. A scientific update*, chapter 1, pages 133–144. IRD editions.

Generalitat Valenciana (2015). PATRICOVA: Plan d'Acció Territorial sobre la prevenció del Risc d'inundació a la Comunitat Valenciana. Technical report, Generalitat Valenciana.

Giorgi, F. and Lionello, P. (2008). Climate change projections for the Mediterranean region. *Global and planetary change*, 63(2-3):90–104.

Glaser, R., Riemann, D., Schönbein, J., Barriendos, M., Brázdil, R., Bertolin, C., Camuffo, D., Deutsch, M., Dobrovolnỳ, P., van Engelen, A., et al. (2010). The variability of European floods since AD 1500. *Climatic Change*, 101(1-2):235–256.

Gradeci, K., Labonnote, N., Sivertsen, E., and Time, B. (2019). The use of insurance data in the analysis of surface water flood events–a systematic review. *Journal of Hydrology*, 568:194–206.

Gudmundsson, L., Bremnes, J. B., Haugen, J. E., and Engen-Skaugen, T. (2012). Technical note: Downscaling rcm precipitation to the station scale using statistical transformations - a comparison of methods. *Hydrology and Earth System Sciences*, 16(9):3383–3390.

Guha-Sapir, D., Vos, F., Below, R., and Ponserre, S. (2012). Annual disaster statistical review 2011: the numbers and trends. Technical report, Centre for Research on the Epidemiology of Disasters (CRED).

Guiot, J. and Cramer, W. (2016). Climate change: The 2015 Paris Agreement thresholds and Mediterranean basin ecosystems. *Science*, 354(6311):465–468.

Hall, J., Arheimer, B., Borga, M., Brázdil, R., Claps, P., Kiss, A., Kjeldsen, T., Kriauciuniene, J., Kundzewicz, Z., Lang, M., et al. (2014). Understanding flood regime changes in Europe: A state of the art assessment. *Hydrology and Earth System Sciences*, 18(7):2735–2772.

Harrell Jr, F. E. (2015). *Regression modeling strategies: with applications to linear models, logistic and ordinal regression, and survival analysis*. Springer.

Hartmann, D. L., Tank, A. M. K., Rusticucci, M., Alexander, L. V., Brönnimann, S., Charabi, Y. A. R., Dentener, F. J., Dlugokencky, E. J., Easterling, D. R., Kaplan, A., Soden, B., Thorne, P., Wild, M., and Zhai, P. (2013). Observations: atmosphere and surface. In Stocker et al. (2014), chapter 2, pages 159–254.

Herget, J., Roggenkamp, T., and Krell, M. (2014). Estimation of peak discharges of historical floods. *Hydrology and Earth System Sciences*, 18(10):4029–4037.

IDESCAT (2018). Institut d'Estadística de Catalunya. `https://www.idescat.cat`.

IGN (2018). Instituto Geográfico Nacional. `http://www.ign.es`.

INE (2018). Instituto Nacional de Estadística. `https://www.ine.es`.

IPCC (2007). *Climate Change 2007: Synthesis Report. Contribution of Working Groups I, II and III to the Fourth Assessment Report of the Intergovernmental Panel on Climate Change*. IPCC, Geneva, Switzerland, 104 pp.

Jacob, D., Petersen, J., Eggert, B., Alias, A., Bøssing, O., Bouwer, L. M., Braun, A., Colette, A., Georgopoulou, E., Gobiet, A., Menut, L., Nikulin, G., Haensler, A., Kriegsmann, A., Martin, E., Meijgaard, E. V., Moseley, C., and Pfeifer, S. (2014). EURO-CORDEX: new high-resolution climate change projections for European impact research. *Regional Environmental Change*, pages 563–578.

Jansa, A., Alpert, P., Arbogast, P., Buzzi, A., Ivancan-Picek, B., Kotroni, V., Llasat, M. C., Ramis, C., Richard, E., Romero, R., and Speranza, A. (2014). MEDEX: A general overview. *Natural Hazards and Earth System Sciences*, 14(8):1965–1984.

Jiménez-Guerrero, P., Montávez, J., Domínguez, M., Romera, R., Fita, L., Fernández, J., Cabos, W., Liguori, G., and Gaertner, M. (2013). Mean fields and interannual variability in RCM simulations over Spain: the ESCENA project. *Climate Research*, 57(3):201–220.

Jongman, B., Hochrainer-Stigler, S., Feyen, L., Aerts, J. C., Mechler, R., Botzen, W. W., Bouwer, L. M., Pflug, G., Rojas, R., and Ward, P. J. (2014). Increasing stress on disaster-risk finance due to large floods. *Nature Climate Change*, 4(4):264.

Karl, T. R., Nicholls, N., and Ghazi, A. (1999). Clivar/GCOS/WMO workshop on indices and indicators for climate extremes workshop summary. In *Weather and Climate Extremes*, pages 3–7. Springer.

Kim, Y.-O., Seo, S. B., and Jang, O.-J. (2012). Flood risk assessment using regional regression analysis. *Natural hazards*, 63(2):1203–1217.

King, A. D. and Karoly, D. J. (2017). Climate extremes in Europe at 1.5 and 2 degrees of global warming. *Environmental Research Letters*, 12(11):114031.

Kirtman, B., Power, S., Adedoyin, A., Boer, G., Bojariu, R., Camilloni, I., Doblas-Reyes, F., Fiore, A., Kimoto, M., Meehl, G., Prather, M., Sarr, A., Schar, C., Sutton, R., van Oldenborgh, G., Vecchi, G., and Wang, H. (2013). Near-term climate change: projections and predictability. In Stocker et al. (2014), chapter 11.

Kjellström, E., Nikulin, G., Strandberg, G., Christensen, O. B., Jacob, D., Keuler, K., Lenderink, G., Meijgaard, E. V., Schär, C., and Somot, S. (2018). European climate change at global mean temperature increases of 1.5 and 2 °C above pre-industrial conditions as simulated by the EURO-CORDEX regional climate models. *Earth System Dynamics*, pages 459–478.

Kreibich, H., Di Baldassarre, G., Vorogushyn, S., Aerts, J. C., Apel, H., Aronica, G. T., Arnbjerg-Nielsen, K., Bouwer, L. M., Bubeck, P., Caloiero, T., et al. (2017). Adaptation to flood risk: Results of international paired flood event studies. *Earth's Future*, 5(10):953–965.

Kreibich, H., Seifert, I., Merz, B., and Thieken, A. H. (2010). Development of FLEMOcs − a new model for the estimation of flood losses in the commercial sector. *Hydrological Sciences Journal*, 55(8):1302–1314.

Kreibich, H., Thieken, A. H., Petrow, T., Müller, M., and Merz, B. (2005). Flood loss reduction of private households due to building precautionary measures - lessons learned from the Elbe flood in August 2002. *Natural Hazards and Earth System Science*, 5(1):117–126.

Kristensen, P. (2010). Water resources: Quantity and flows. *Publications Office of the European Union, State Environ. Rep*, 1:2010.

Kundzewicz, Z. W., Krysanova, V., Dankers, R., Hirabayashi, Y., Kanae, S., Hattermann, F., Huang, S., Milly, P. C., Stoffel, M., Driessen, P., et al. (2017). Differences in flood hazard projections in Europe – their causes and consequences for decision making. *Hydrological Sciences Journal*, 62(1):1–14.

Leal, M., Boavida-Portugal, I., Fragoso, M., and Ramos, C. (2019). How much does an extreme rainfall event cost? material damages and relationships between insurance, rainfall, land cover and urban flooding. *Hydrological Sciences Journal*, 64(6):673–689.

Lehner, F., Coats, S., Stocker, T. F., Pendergrass, A. G., Sanderson, B. M., Raible, C. C., and Smerdon, J. E. (2017). Projected drought risk in 1.5 °C and 2 °C warmer climates. *Geophysical Research Letters*, 44(14):7419–7428.

Lemus-Canovas, M., Lopez-Bustins, J. A., Trapero, L., and Martin-Vide, J. (2019). Combining circulation weather types and daily precipitation modelling to derive climatic precipitation regions in the Pyrenees. *Atmospheric Research*, 220:181–193.

Llasat, M. C., Barriendos, M., Barrera, A., and Rigo, T. (2005). Floods in Catalonia (NE Spain) since the 14th century. Climatological and meteorological aspects from historical documentary sources and old instrumental records. *Journal of hydrology*, 313(1-2):32–47.

Llasat, M. C., Cortès, M., Falcón, L., Gilabert, J., Llasat-Botja, M., Marcos, R., Martín-Vide, J., and Turco, M. (2016a). A multifactorial analysis of flood variability in the Metropolitan Area of Barcelona. In *ICUR2016 Proceedings*.

Llasat, M. C., Llasat-Botija, M., and López, L. (2009). A press database on natural risks and its application in the study of floods in Northeastern Spain. *Natural Hazards and Earth System Sciences*, 9(6):2049–2061.

Llasat, M. C., Llasat-Botija, M., Petrucci, O., Pasqua, a. a., Rosselló, J., Vinet, F., and Boissier, L. (2013). Towards a database on societal impact of Mediterranean floods within the framework of the HYMEX project. *Natural Hazards and Earth System Science*, 13(5):1337–1350.

Llasat, M. C., Llasat-Botija, M., Prat, M., Porcu, F., Price, C., Mugnai, A., Lagouvardos, K., Kotroni, V., Katsanos, D., Michaelides, S., et al. (2010). High-impact floods and flash floods in Mediterranean countries: the FLASH preliminary database. *Advances in Geosciences*, 23:47–55.

Llasat, M. C., Marcos, R., Llasat-Botija, M., Gilabert, J., Turco, M., and Quintana-Seguí, P. (2014a). Flash flood evolution in north-western Mediterranean. *Atmospheric Research*, 149:230–243.

Llasat, M. C., Marcos, R., Turco, M., Gilabert, J., and Llasat-Botija, M. (2016b). Trends in flash flood events versus convective precipitation in the Mediterranean region: The case of Catalonia. *Journal of Hydrology*, 541(September 2002):24–37.

Llasat, M. C., Turco, M., Quintana-Seguí, P., and Llasat-Botija, M. (2014b). The snow storm of 8 march 2010 in Catalonia (Spain): a paradigmatic wet-snow event with a high societal impact. *Natural Hazards and Earth System Sciences*, 14(2):427.

Madsen, H., Lawrence, D., Lang, M., Martinkova, M., and Kjeldsen, T. R. (2014). Review of trend analysis and climate change projections of extreme precipitation and floods in Europe. *Journal of Hydrology*, 519(PD):3634–3650.

Martín-Vide, J. and Llasat, M. (2018). The 1962 flash flood in the Rubí stream (Barcelona, Spain). *Journal of hydrology*, 566:441–454.

Mason, S. J. and Graham, N. E. (2002). Areas beneath the relative operating characteristics (ROC) and relative operating levels (ROL) curves: Statistical significance and interpretation. *Quarterly Journal of the Royal Meteorological Society*, 128(584):2145–2166.

Masson-Delmotte, V., Zhai, P., Pörtner, H.-O., Roberts, D., Skea, J., Shukla, P., Pirani, A., Moufouma-Okia, W., Péan, C., Pidcock, R., Connors, S., Matthews, J., Chen, Y., Zhou, X., Gomis, M., Lonnoy, E., Maycock, T., Tignor, M., and Waterfield, T. (2018). Ipcc, 2018: Summary for policymakers. In *Global Warming of 1.5 °C. An IPCC Special Report on the impacts of global warming of 1.5 °C above pre-industrial levels and related global greenhouse gas emission pathways, in the context of strengthening the global response to the threat of climate change, sustainable development, and efforts to eradicate poverty.* World Meteorological Organization, Geneva, Switzerland.

Mclaughlin, S. and Cooper, J. A. G. (2010). A multi-scale coastal vulnerability index: A tool for coastal managers? *Environmental Hazards*, 9(3):233–248.

Mediero, L., SantillaÂ´n, D., Garrote, L., and Granados, A. (2014). Detection and attribution of trends in magnitude, frequency and timing of floods in Spain. *Journal of Hydrology*, 517:1072–1088.

Merz, B., Kreibich, H., and Lall, U. (2013). Multi-variate flood damage assessment: A tree-based data-mining approach. *Natural Hazards and Earth System Science*, 13(1):53–64.

Merz, B., Kreibich, H., Schwarze, R., and Thieken, a. (2010). Review article "assessment of economic flood damage". *Natural Hazards and Earth System Science*, 10(8):1697–1724.

Messner, F. and Meyer, V. (2006). Flood damage, vulnerability and risk perception–challenges for flood damage research. In *Flood risk management: hazards, vulnerability and mitigation measures*, pages 149–167. Springer.

Messner, F., Penning-rowsell, E., Green, C., Tunstall, S., Veen, A. V. D., Tapsell, S., Wilson, T., Krywkow, J., Logtmeijer, C., Fernández-bilbao, A., Geurts, P., and Haase, D. (2007). Evaluating flood damages: guidance and recommendations on principles and methods principles and methods. *Flood Risk Management: Hazards, Vulnerability and Mitigation Measures*, page 189.

Moncoulon, D., Labat, D., Ardon, J., Leblois, E., Onfroy, T., Poulard, C., Aji, S., Rémy, A., and Quantin, A. (2014). Analysis of the french insurance market exposure to floods: a

stochastic model combining river overflow and surface runoff. *Natural Hazards and Earth System Sciences*, 14:p–2469.

Nakamura, I. and Llasat, M. C. (2017). Policy and systems of flood risk management: a comparative study between Japan and Spain. *Natural Hazards: Journal of the International Society for the Prevention and Mitigation of Natural Hazards*, 87(2):919–943.

Nasiri, H. and Shahmohammadi-Kalalagh, S. (2013). Flood vulnerability index as a knowledge base for flood risk assessment in urban area. *Journal of Novel Applied Sciences*, 2(8):269–272.

NATHAN (2018). Munich Re. `https://www.munichre.com/en/reinsurance/business/non-life/nathan/index.html`.

Naumann, G., Alfieri, L., Wyser, K., Mentaschi, L., Betts, R., Carrao, H., Spinoni, J., Vogt, J., and Feyen, L. (2018). Global changes in drought conditions under different levels of warming. *Geophysical Research Letters*, 45(7):3285–3296.

Neumayer, E. and Barthel, F. (2011). Normalizing economic loss from natural disasters: A global analysis. *Global Environmental Change*, 21(1):13–24.

O'Neill, B. C., Kriegler, E., Ebi, K. L., Kemp-Benedict, E., Riahi, K., Rothman, D. S., van Ruijven, B. J., van Vuuren, D. P., Birkmann, J., Kok, K., et al. (2017). The roads ahead: Narratives for shared socioeconomic pathways describing world futures in the 21st century. *Global Environmental Change*, 42:169–180.

Pachauri, R. K., Allen, M. R., Barros, V. R., Broome, J., Cramer, W., Christ, R., Church, J. A., Clarke, L., Dahe, Q., Dasgupta, P., et al. (2014). *Climate change 2014: synthesis report. Contribution of Working Groups I, II and III to the fifth assessment report of the Intergovernmental Panel on Climate Change*. IPCC.

Papagiannaki, K., Lagouvardos, K., Kotroni, V., and Bezes, a. (2015). Flash flood occurrence and relation to the rainfall hazard in a highly urbanized area. *Natural Hazards and Earth System Sciences Discussions*, 3(5):3119–3149.

Park, C.-E., Jeong, S.-J., Joshi, M., Osborn, T. J., Ho, C.-H., Piao, S., Chen, D., Liu, J., Yang, H., Park, H., et al. (2018). Keeping global warming within 1.5 °C constrains emergence of aridification. *Nature Climate Change*, 8(1):70.

Penning-Rowsell, E., Johnson, C., Tunstall, S., Tapsell, S., Morris, J., Chatterton, J., and Green, C. (2005). The benefits of flood and coastal risk management: a handbook of assessment techniques. *ISBN 1904750516*.

Peterson, T., Folland, C., Gruza, G., Hogg, W., Mokssit, A., and Plummer, N. (2001). *Report on the activities of the working group on climate change detection and related rapporteurs*. World Meteorological Organization Geneva.

Petrow, T. and Merz, B. (2009). Trends in flood magnitude, frequency and seasonality in Germany in the period 1951-2002. *Journal of Hydrology*, 371(1-4):129–141.

Petrucci, O. (2013). Brief communication "The assessment of damage caused by historical landslide events". *Natural Hazards and Earth System Sciences*, 13(3):755–761.

Petrucci, O. and Pasqua, a. a. (2009). A methodological approach to characterise Landslide Periods based on historical series of rainfall and landslide damage. *Natural Hazards and Earth System Science*, 9(5):1655–1670.

Petrucci, O., Pasqua, a. A., and Polemio, M. (2012). Flash flood occurrences since the 17th century in steep drainage basins in southern Italy. *Environmental Management*, 50(5):807–818.

Pfurtscheller, C. and Schwarze, R. (2010). Kosten des katastrophenschutzes. *Hochwasserschäden–Erfassung, Abschätzung und Vermeidung, edited by: Thieken, AH, Seifert, I., and Merz, B., München, Germany*, pages 253–262.

Pielke Jr, R. A. and Landsea, C. W. (1998). Normalized hurricane damages in the United States: 1925–95. *Weather and Forecasting*, 13(3):621–631.

Pitt, M. et al. (2008). *Learning lessons from the 2007 floods*. Cabinet Office London.

Protecció Civil de Catalunya (2017). INUNCAT: Pla d'emergències per inundacions. Technical report, Protecció Civil de Catalunya.

Przyluski, V. and Hallegatte, S. (2011). Indirect costs of natural hazards. *CONHAZ report WP02*, 2:383–398.

Quintana-Seguí, P., Peral, C., Turco, M., Llasat, M. d. C., and Martin, E. (2016). Meteorological analysis systems in North-East Spain: validation of SAFRAN and SPAN. *Journal of Environmental Informatics*.

R Core Team (2018). *R: A Language and Environment for Statistical Computing*. R Foundation for Statistical Computing, Vienna, Austria.

Rajczak, J. and Schär, C. (2017). Projections of Future Precipitation Extremes Over Europe: A Multimodel Assessment of Climate Simulations. *Journal of Geophysical Research: Atmospheres*.

Ramis, C., Homar, V., Amengual, A., Romero, R., and Alonso, S. (2013). Daily precipitation records over mainland Spain and the Balearic Islands. *Natural Hazards and Earth System Sciences*, 13(10):2483–2491.

Ramis, C., Llasat, M. C., Genovés, A., and Jansà, A. (1994). The October-1987 floods in Catalonia: Synoptic and mesoscale mechanisms. *Meteorological Applications*, 1(4):337–350.

Riahi, K., Van Vuuren, D. P., Kriegler, E., Edmonds, J., O'neill, B. C., Fujimori, S., Bauer, N., Calvin, K., Dellink, R., Fricko, O., et al. (2017). The shared socioeconomic pathways and their energy, land use, and greenhouse gas emissions implications: an overview. *Global Environmental Change*, 42:153–168.

Rojas, R., Feyen, L., Bianchi, A., and Dosio, A. (2012). Assessment of future flood hazard in Europe using a large ensemble of bias-corrected regional climate simulations. *Journal of Geophysical Research: Atmospheres*, 117(D17).

Roudier, P., Andersson, J. C., Donnelly, C., Feyen, L., Greuell, W., and Ludwig, F. (2016). Projections of future floods and hydrological droughts in europe under a +2 °C global warming. *Climatic Change*, 135(2):341–355.

Samir, K. and Lutz, W. (2017). The human core of the shared socioeconomic pathways: Population scenarios by age, sex and level of education for all countries to 2100. *Global Environmental Change*, 42:181–192.

Sampson, C. C., Fewtrell, T. J., O'Loughlin, F., Pappenberger, F., Bates, P., Freer, J. E., and Cloke, H. L. (2014). The impact of uncertain precipitation data on insurance loss estimates using a flood catastrophe model. *Hydrology and Earth System Sciences*, 18:2305–2324.

Scawthorn, C., Flores, P., Blais, N., Seligson, H., Tate, E., Chang, S., Mifflin, E., Thomas, W., Murphy, J., Jones, C., et al. (2006). HAZUS-MH flood loss estimation methodology. II. Damage and loss assessment. *Natural Hazards Review*, 7(2):72–81.

Schleussner, C.-F., Lissner, T. K., Fischer, E. M., Wohland, J., Perrette, M., Golly, A., Rogelj, J., Childers, K., Schewe, J., Frieler, K., et al. (2016). Differential climate impacts for policy-relevant limits to global warming: the case of 1.5 °C and 2 °C. *Earth system dynamics*, 7:327–351.

Schröter, K., Kreibich, H., Vogel, K., Riggelsen, C., Scherbaum, F., and Merz, B. (2014). How useful are complex flood damage models? *Water Resources Research*, 50(4):3378–3395.

Schröter, K., Kunz, M., Elmer, F., Mühr, B., and Merz, B. (2015). What made the June 2013 flood in Germany an exceptional event? A hydro-meteorological evaluation. *Hydrology and Earth System Sciences Discussions*, 11(7):8125–8166.

Schwarz, G. et al. (1978). Estimating the dimension of a model. *The annals of statistics*, 6(2):461–464.

Seneviratne, S. I., Nicholls, N., Easterling, D., Goodess, C. M., Kanae, S., Kossin, J., Luo, Y., Marengo, J., McInnes, K., Rahimi, M., et al. (2012). *Managing the Risks of Extreme Events and Disasters to Advance Climate Change Adaptation: Changes in Climate Extremes and their Impacts on the Natural Physical Environment*. Cambridge University Press, Cambridge, UK, and New York, NY, USA.

Serra-Llobet, A., Tàbara, J. D., and Sauri, D. (2013). The Tous dam disaster of 1982 and the origins of integrated flood risk management in Spain. *Natural hazards*, 65(3):1981–1998.

Sillmann, J., Kharin, V. V., Zwiers, F. W., Zhang, X., and Bronaugh, D. (2013). Climate extremes indices in the CMIP5 multimodel ensemble : Part 2 . Future climate projections. *Journal of Geophysical Research: Atmospheres*, 118(March):2473–2493.

SIOSE (2018). Sistema de Información sobre Ocupación del Suelo de España. `http://www.siose.es`.

Smith, K. and Ward, R. (1998). *Floods: physical processes and human impacts*. Wiley Chichester.

Spekkers, M. H. (2015). *On rainstorm damage to building structure and content*. PhD thesis, Technische Universiteit Delft.

Spekkers, M. H., Clemens, F. H., and Ten Veldhuis, J. A. (2015). On the occurrence of rainstorm damage based on home insurance and weather data. *Natural Hazards and Earth System Sciences*, 15(2):261–272.

Spekkers, M. H., Kok, M., Clemens, F. H., and Ten Veldhuis, J. A. (2013). A statistical analysis of insurance damage claims related to rainfall extremes. *Hydrology and Earth System Sciences*, 17(3):913–922.

Stocker, T., Qin, D., Plattner, G.-K., Tignor, M., Allen, S.K. Boschung, J., Nauels, A., Xia, Y., Bex, V., Midgley, P., and editors (2014). *Climate change 2013: the physical science basis: Working Group I contribution to the Fifth assessment report of the Intergovernmental Panel on Climate Change*. Cambridge University Press, Cambridge, United Kingdom and New York, NY, USA.

Strobl, E. (2011). The economic growth impact of hurricanes: Evidence from us coastal counties. *The review of economics and statistics*, 93(2):575–589.

Sun, X., Lall, U., Merz, B., and Dung, N. V. (2015). Hierarchical Bayesian clustering for nonstationary flood frequency analysis: Application to trends of annual maximum flow in Germany. *Water Resources Research*, 51(8):6586–6601.

Svensson, C., Kundzewicz, Z. W., and Maurer, T. (2005). Trend detection in river flow series: 2. Flood and low-flow index series. *Hydrological Sciences Journal*, 50(5):811–824.

Taylor, K. E., Stouffer, R. J., and Meehl, G. A. (2012). An overview of CMIP5 and the experiment design. *Bulletin of the American Meteorological Society*, 93(4):485–498.

Tebaldi, C., Arblaster, J. M., and Knutti, R. (2011). Mapping model agreement on future climate projections. *Geophysical Research Letters*, 38(23):1–5.

Thieken, a. H., Bessel, T., Kienzler, S., Kreibich, H., Müller, M., Pisi, S., and Schröter, K. (2016). The flood of June 2013 in Germany: how much do we know about its impacts? *Natural Hazards and Earth System Sciences Discussions*, 16(6):1–57.

Thieken, A. H., Müller, M., Kreibich, H., and Merz, B. (2005). Flood damage and influencing factors: New insights from the August 2002 flood in Germany. *Water Resources Research*, 41(12):1–16.

Thieken, A. H., Olschewski, A., and Kreibich, H. (2008). Development and evaluation of FLEMOps a new Flood Loss Estimation MOdel for the private sector. *WIT Transactions on Ecology and the Environment*, 118:315–324.

TICC (2016). *Tercer Informe sobre el Canvi Climàtic a Catalunya*. Generalitat de Catalunya and Institut d'Estudis Catalans.

Tobin, I., Greuell, W., Jerez, S., Ludwig, F., Vautard, R., van Vliet, M., and Bréon, F. (2018). Vulnerabilities and resilience of European power generation to 1.5 °C, 2 °C and 3 °C warming. *Environmental Research Letters*, 13(4):044024.

Torgersen, G., Bjerkholt, J. T., Kvaal, K., and Lindholm, O. G. (2015). Correlation between extreme rainfall and insurance claims due to urban flooding – case study Fredrikstad, Norway. *Journal of Urban and Environmental Engineering*, 9(2):127–138.

Tramblay, Y., Ruelland, D., Somot, S., Bouaicha, R., and Servat, E. (2013). High-resolution Med-CORDEX regional climate model simulations for hydrological impact studies: A first evaluation of the ALADIN-Climate model in Morocco. *Hydrology and Earth System Sciences*, 17(10):3721–3739.

Tramblay, Y. and Somot, S. (2018). Future evolution of extreme precipitation in the Mediterranean. *Climatic Change*.

Turco, M., Cortès Simó, M., Quintana Seguí, P., Jerez, S., Llasat, M. d. C., and Alfieri, L. (2018a). Changes in meteo-hydrological extremes in Spain at different levels of global warming. In *EL CLIMA: AIRE, AGUA, TIERRA Y FUEGO*. Asociación Española de Climatología.

Turco, M. and Llasat, M. C. (2011). Trends in indices of daily precipitation extremes in Catalonia (NE Spain), 1951-2003. *Natural Hazards and Earth System Science*, 11(12):3213–3226.

Turco, M., Llasat, M. C., Herrera, S., and Gutiérrez, J. M. (2017). Bias correction and downscaling of future RCM precipitation projections using a MOS-Analog technique. *Journal of Geophysical Research: Atmospheres*, 122(5):2631–2648.

Turco, M., Marcos, R., Quintana-Seguí, P., and Llasat, M. (2014). Testing instrumental and downscaled reanalysis time series for temperature trends in NE of Spain in the last century. *Regional environmental change*, 14(5):1811–1823.

Turco, M., Rosa-Cánovas, J. J., Bedia, J., Jerez, S., Montávez, J. P., Llasat, M. C., and Provenzale, A. (2018b). Exacerbated fires in Mediterranean Europe due to anthropogenic warming projected with non-stationary climate-fire models. *Nature communications*, 9(1):3821.

UNISDR (2009). International Strategy for Disaster Reduction (ISDR): Terminology on Disaster Risk Reduction. `https://www.unisdr.org/we/inform/publications/7817`.

UNISDR (2015). International Strategy for Disaster Reduction (ISDR): Making Development Sustainable: The Future of Disaster Risk Management, Global Assessment Report on Disaster Risk Reduction. `https://www.unisdr.org/we/inform/publications/42809`.

UTE (2013). Plan director de Defensa contra las Avenidas: Comarca de la Marina Baja. Alicante. Technical report, Dirección General del Agua y Confederación Hidrográfica del Júcar.

Van den Besselaar, E. J. M., Klein Tank, A. M. G., and Buishand, T. A. (2013). Trends in European precipitation extremes over 1951-2010. *International Journal of Climatology*, 33(12):2682–2689.

Van Huijstee, J., van Bemmel, B., Bouwman, A., and van Rijn, F. (2018). Towards an Urban Preview: Modelling future urban growth with 2UP. Technical report, PBL Netherlands Environmental Assessment Agency, The Hague.

Van Ootegem, L., Van Herck, K., Creten, T., Verhofstadt, E., Foresti, L., Goudenhoofdt, E., Reyniers, M., Delobbe, L., Murla Tuyls, D., and Willems, P. (2018). Exploring the potential of multivariate depth-damage and rainfall-damage models. *Journal of Flood Risk Management*, 11:S916–S929.

Van Vuuren, D. P., Edmonds, J., Kainuma, M., Riahi, K., Thomson, A., Hibbard, K., Hurtt, G. C., Kram, T., Krey, V., Lamarque, J.-F., et al. (2011). The representative concentration pathways: an overview. *Climatic change*, 109(1-2):5.

Vautard, R., Gobiet, A., Sobolowski, S., and Kjellström, E. (2014). The European climate under a °2C global warming. *Environmental Research Letters*.

Wagenaar, D., Jong, J. d., and Bouwer, L. M. (2017). Multi-variable flood damage modelling with limited data using supervised learning approaches. *Natural Hazards and Earth System Sciences*, 17(9):1683–1696.

Wilson, D., Hisdal, H., and Lawrence, D. (2010). Has streamflow changed in the Nordic countries? - Recent trends and comparisons to hydrological projections. *Journal of Hydrology*, 394(3-4):334–346.

Wobus, C., Lawson, M., Jones, R., Smith, J., and Martinich, J. (2014). Estimating monetary damages from flooding in the United States under a changing climate. *Journal of Flood Risk Management*, 7(3):217–229.

Ye, H., Fetzer, E. J., Wong, S., and Lambrigtsen, B. H. (2017). Rapid decadal convective precipitation increase over Eurasia during the last three decades of the 20th century. *Science advances*, 3(1):e1600944.

Zhou, Q., Leng, G., and Feng, L. (2017). Predictability of state-level flood damage in the conterminous United States: the role of hazard, exposure and vulnerability. *Scientific Reports*, 7(1):5354.

Zhou, Q., Panduro, T. E., Thorsen, B. J., and Arnbjerg-Nielsen, K. (2013). Verification of flood damage modelling using insurance data. *Water Science and Technology*, 68(2):425–432.

Zischg, A. P., Mosimann, M., Bernet, D. B., and Röthlisberger, V. (2018). Validation of 2D flood models with insurance claims. *Journal of Hydrology*, 557:350–361.